



# University of HUDDERSFIELD

## University of Huddersfield Repository

Smith, Oliver

A Study into the Enhancement of Solubility through Surfactants using Chromatography and Calorimetry

### Original Citation

Smith, Oliver (2021) A Study into the Enhancement of Solubility through Surfactants using Chromatography and Calorimetry. Doctoral thesis, University of Huddersfield.

This version is available at <http://eprints.hud.ac.uk/id/eprint/35623/>

The University Repository is a digital collection of the research output of the University, available on Open Access. Copyright and Moral Rights for the items on this site are retained by the individual author and/or other copyright owners. Users may access full items free of charge; copies of full text items generally can be reproduced, displayed or performed and given to third parties in any format or medium for personal research or study, educational or not-for-profit purposes without prior permission or charge, provided:

- The authors, title and full bibliographic details is credited in any copy;
- A hyperlink and/or URL is included for the original metadata page; and
- The content is not changed in any way.

For more information, including our policy and submission procedure, please contact the Repository Team at: [E.mailbox@hud.ac.uk](mailto:E.mailbox@hud.ac.uk).

<http://eprints.hud.ac.uk/>

# A Study into the Enhancement of Solubility through Surfactants using Chromatography and Calorimetry

By Oliver Smith

Academic Supervisor: Professor Laura Waters

## **Acknowledgments.**

I'd like to thank Professor Laura Waters for her patience and guidance and Mel for always believing in me.

## **Declaration.**

This work includes parts which have been published prior to the submission of my thesis in the publication: Understanding polysorbate-compound interactions within the CMC region. Journal of Chromatography A, Volume 1623, 19 July 2020, 461212. My contributions were listed as follows: Methodology, Validation, Formal analysis, Investigation, Writing - review & editing.

## Abstract

Surfactants, such as Tween 20, Tween 80, Etocas 35, Croduret 40, Crodasol HS HP, SDS and Brij 35 are routinely used within the healthcare and pharmaceutical industry to enhance solubility. This work focuses on analysing the aforementioned surfactants, with Tween 20 and Tween 80 each considered at three purity levels with four model compounds, across the critical micellar concentration (CMC) range for each surfactant in addition to determining the CMC of Tween 20, Tween 80, Etocas 35, Croduret 40 and Crodasol HS HP. Such data is of interest to investigate the influence of micelle formation upon compound-polysorbate interaction. three analytical techniques were utilised, namely spectroscopic solubility determination, micellar liquid chromatography (MLC) and isothermal titration calorimetry (ITC). In all cases it was apparent that the maximum solubility for all four compounds increased substantially at concentrations greater than the CMC and that, in most cases, a different retention profile was observed using MLC once the CMC had been exceeded. This thesis is the first to have used such techniques to investigate the behaviour of these polysorbates over a series of concentrations and three levels of polysorbate purity. The findings indicate that the solubilisation potential of polysorbates differs once the CMC has been surpassed and is dependent upon the level of purity selected, i.e. compound-surfactant interactions are partially a consequence of the presence of micelles rather than monomer as well as polysorbate purity. This thesis also investigates the micellisation process for each of the aforementioned surfactants using isothermal titration calorimetry, thus avoiding issues regarding precision found with other techniques. Furthermore, this methodology has not previously been applied to this group of surfactants. For the most commonly used non-ionics (Tween 20 and Tween 80) a further study was undertaken to consider the influence of surfactant purity on the CMC determined. Such information regarding the CMC event is useful from a formulation perspective as it can ensure that the most optimum concentration of surfactant is included within a formulation to maximise its efficacy.

# Contents

Contents .....	4
List of Figures.....	6
List of Equations .....	10
List of Tables .....	12
<b>1. Introduction.....</b>	<b>14</b>
<b>1.1 Solubility .....</b>	<b>14</b>
<b>1.2 Surfactants and Micelles .....</b>	<b>18</b>
<b>1.3 High Performance Liquid Chromatography (HPLC).....</b>	<b>26</b>
<b>1.4 Micellar Liquid Chromatography (MLC).....</b>	<b>30</b>
<b>1.4.1 An Overview of MLC .....</b>	<b>30</b>
<b>1.4.2 Recent uses of MLC.....</b>	<b>35</b>
<b>1.5 Isothermal Titration Calorimetry (ITC).....</b>	<b>39</b>
<b>1.5.1 An Overview of ITC.....</b>	<b>39</b>
<b>1.5.2 Using ITC to Determine CMC.....</b>	<b>41</b>
<b>1.6. Aims and Objectives .....</b>	<b>45</b>
<b>2. Experimental .....</b>	<b>46</b>
<b>2.1 Materials .....</b>	<b>46</b>
<b>2.2 MLC Methodology.....</b>	<b>48</b>
<b>2.3 UV Methodology .....</b>	<b>49</b>
<b>2.3.1 UV Absorption of Surfactants .....</b>	<b>49</b>
<b>2.3.2 Measuring the effect of Surfactants on the Lambda max of APIs.....</b>	<b>49</b>
<b>2.4 CMC determination using ITC Methodology .....</b>	<b>50</b>
<b>2.5 Maximum Solubility Methodology .....</b>	<b>50</b>
<b>3. Micellar Liquid Chromatography .....</b>	<b>51</b>
<b>3.1 Method Optimisation.....</b>	<b>51</b>
<b>3.2 Column Selection .....</b>	<b>54</b>
<b>3.3 MLC with Acetaminophen.....</b>	<b>55</b>
<b>3.4 MLC with Benzamide.....</b>	<b>61</b>
<b>3.5 MLC with 4-Hydroxybenzamide.....</b>	<b>65</b>
<b>3.6 MLC with Hydrocortisone.....</b>	<b>72</b>
<b>3.7 MLC Discussion .....</b>	<b>77</b>
<b>3.8 pH Testing.....</b>	<b>81</b>
<b>4. Solubility Enhancement.....</b>	<b>83</b>

4.1 Calibrations .....	83
4.2 Solubility of Acetaminophen .....	85
4.3 Solubility of Benzamide .....	89
4.4 Solubility of 4-Hydroxybenzamide .....	94
4.5 Solubility of Hydrocortisone .....	99
4.6 Solubility Discussion .....	103
5. UV .....	105
5.1 Surfactants .....	105
5.2 The effect of Surfactants on the Lambda max of APIs .....	109
6. ITC .....	112
6.1 CMC Determination of Tween 20 .....	112
6.1.1 CMC Determination of Standard Grade Tween 20 .....	112
6.1.2 CMC Determination of HP Tween 20 .....	115
6.1.3 CMC Determination of SR Tween 20 .....	117
6.2 CMC Determination of Tween 80 .....	120
6.2.1 CMC Determination of Standard Grade Tween 80 .....	120
6.2.2 CMC Determination of HP Tween 80 .....	123
6.2.3 CMC Determination of SR Tween 80 .....	126
6.3 CMC Determination of Etocas 35 .....	129
6.4 CMC Determination of Croduret 40 .....	132
6.5 CMC Determination of Crodasol HS HP .....	135
6.6 ITC Discussion .....	138
7. General Discussion .....	140
7.1 MLC .....	140
7.1.1 Impact of Surfactant Concentration on Retention Time in MLC .....	140
7.1.2 Impact of Surfactant Purity on Retention Time in MLC .....	141
7.2 Solubility Enhancement .....	142
7.2.1 The Impact of Surfactants on API Solubility .....	142
7.2.2 The Impact of Surfactant Purity on Solubility Enhancement of APIs .....	143
7.3 ITC .....	143
7.3.1 CMC Determination .....	143
7.4 Future Work .....	144
8. Conclusions .....	144
9. References .....	146

## List of Figures

<b>Figure 1.</b> The different structures that micelles can form. <sup>30</sup> .....	20
<b>Figure 2.</b> The equilibrium between a monomer and a micelle.....	21
<b>Figure 3.</b> A diagram showing how increasing surfactant concentration leads to micelle formation. ..	23
<b>Figure 4.</b> A flow chart showing how the components of a HPLC work together. <sup>37</sup> .....	28
<b>Figure 5.</b> The different modes of diffusion. Top – eddy diffusion, middle – mobile phase mass transfer, bottom – longitudinal diffusion. Where red circles represent particles of the support in the column and blue circles represent solute. ....	30
<b>Figure 6.</b> A diagram of the two equilibria that occur during MLC with soluble APIs because of the solute partitioning between the mobile phase, micellar phase, and the modified stationary phase. This example uses SDS and an octadecyl-bonded column. <sup>48</sup> .....	32
<b>Figure 7.</b> A diagram showing direct transfer of a hydrophilic API between micelles and the modified stationary phase. <sup>48</sup> .....	33
<b>Figure 8.</b> A schematic diagram of an ITC.....	40
<b>Figure 9.</b> A plot of $\mu\text{cal/second}$ against Time (mins) for SR Tween 20. ....	41
<b>Figure 10.</b> A plot of $\Delta H$ (kJoules/mol) against Surfactant Concentration (M) for SR Tween 20.....	42
<b>Figure 11.</b> A plot of the 2 <sup>nd</sup> Derivative of $\Delta H$ (Arbitrary Units) against Surfactant Concentration (M). .....	43
<b>Figure 12.</b> MLC with 4-hydroxybenzamide using a mobile phase consisting of 30 % acetonitrile with 70 % Tween 20, Tween 80, Etocas 35, Croduret 40 and Crodasol HS HP by volume. Error bars were calculated using the standard deviation from 3 repeats. ....	52
<b>Figure 13.</b> MLC with 4-hydroxybenzamide using a mobile phase consisting of 5 % acetonitrile with 95 % Tween 20 by volume, Tween 20, Etocas 35 and Croduret 40. Error bars were calculated using the standard deviation from 3 repeats. ....	53
<b>Figure 14.</b> MLC with 4-hydroxybenzamide, where the column was cleaned between each experiment and the mobile phase was Tween 20, Tween 80, Etocas 35, Croduret 40 and Crodasol HS HP. Error bars were calculated using the standard deviation from 3 repeats. ....	53
<b>Figure 15.</b> MLC with acetaminophen using: Tween 20, HP Tween 20, SR Tween 20, Tween 80, HP Tween 80, SR Tween 80, Etocas 35, Croduret 40, Crodasol HS HP, SDS and Brij 35 as the mobile phase at concentrations: $1 \times 10^{-2}$ , $1 \times 10^{-3}$ , $1 \times 10^{-4}$ , $1 \times 10^{-5}$ , $1 \times 10^{-6}$ , $1 \times 10^{-7}$ , $1 \times 10^{-8}$ M. Error bars were calculated using the standard deviation from 3 repeats.....	56
<b>Figure 16.</b> MLC with acetaminophen using: Tween 20, HP Tween 20 and SR Tween 20, as the mobile phase at concentrations: $1 \times 10^{-2}$ , $1 \times 10^{-3}$ , $1 \times 10^{-4}$ , $1 \times 10^{-5}$ , $1 \times 10^{-6}$ , $1 \times 10^{-7}$ , $1 \times 10^{-8}$ M. Error bars were calculated using the standard deviation from 3 repeats. ....	58
<b>Figure 17.</b> MLC with acetaminophen using: Tween 80, HP Tween 80 and SR Tween 80, as the mobile phase at concentrations: $1 \times 10^{-2}$ , $1 \times 10^{-3}$ , $1 \times 10^{-4}$ , $1 \times 10^{-5}$ , $1 \times 10^{-6}$ , $1 \times 10^{-7}$ , $1 \times 10^{-8}$ M. Error bars were calculated using the standard deviation from 3 repeats. ....	59
<b>Figure 18.</b> MLC with benzamide using: Tween 20, SR Tween 20, Tween 80, Etocas 35, Croduret 40, Crodasol HS HP, SDS and Brij 35 as the mobile phase at concentrations: $1 \times 10^{-2}$ , $1 \times 10^{-3}$ , $1 \times 10^{-4}$ , $1 \times 10^{-5}$ , $1 \times 10^{-6}$ , $1 \times 10^{-7}$ , $1 \times 10^{-8}$ M. Error bars were calculated using the standard deviation from 3 repeats. ....	61
<b>Figure 19.</b> MLC with benzamide using: Tween 20, HP Tween 20 and SR Tween 20, as the mobile phase at concentrations: $1 \times 10^{-2}$ , $1 \times 10^{-3}$ , $1 \times 10^{-4}$ , $1 \times 10^{-5}$ , $1 \times 10^{-6}$ , $1 \times 10^{-7}$ , $1 \times 10^{-8}$ M. Error bars were calculated using the standard deviation from 3 repeats.....	62
<b>Figure 20.</b> MLC with benzamide using: Tween 80, HP Tween 80 and SR Tween 80, as the mobile phase at concentrations: $1 \times 10^{-2}$ , $1 \times 10^{-3}$ , $1 \times 10^{-4}$ , $1 \times 10^{-5}$ , $1 \times 10^{-6}$ , $1 \times 10^{-7}$ , $1 \times 10^{-8}$ M. Error bars were calculated using the standard deviation from 3 repeats.....	64

<b>Figure 21.</b> MLC with 4-hydroxybenzamide using: Tween 20, HP Tween 20, SR Tween 20, Tween 80, HP Tween 80, SR Tween 80, Etocas 35, Croduret 40, Crodasol HS HP, SDS and Brij 35 as the mobile phase at concentrations: $1 \times 10^{-2}$ , $1 \times 10^{-3}$ , $1 \times 10^{-4}$ , $1 \times 10^{-5}$ , $1 \times 10^{-6}$ , $1 \times 10^{-7}$ , $1 \times 10^{-8}$ M. Error bars were calculated using the standard deviation from 3 repeats. ....	66
<b>Figure 22.</b> MLC with 4-hydroxybenzamide using: Tween 20, HP Tween 20 and SR Tween 20, as the mobile phase at concentrations: $1 \times 10^{-2}$ , $1 \times 10^{-3}$ , $1 \times 10^{-4}$ , $1 \times 10^{-5}$ , $1 \times 10^{-6}$ , $1 \times 10^{-7}$ , $1 \times 10^{-8}$ M. Error bars were calculated using the standard deviation from 3 repeats. ....	67
<b>Figure 23.</b> The equilibria that exists between the modified stationary phase, bulk solvent and micellar-pseudo phase.....	68
<b>Figure 24.</b> The equilibria that exists between the modified stationary phase, bulk solvent and micellar-pseudo phase for hydrophilic APIs in MLC.....	69
<b>Figure 25.</b> MLC with 4-hydroxybenzamide using: Tween 80, HP Tween 80 and SR Tween 80, as the mobile phase at concentrations: $1 \times 10^{-2}$ , $1 \times 10^{-3}$ , $1 \times 10^{-4}$ , $1 \times 10^{-5}$ , $1 \times 10^{-6}$ , $1 \times 10^{-7}$ , $1 \times 10^{-8}$ M. Error bars were calculated using the standard deviation from 3 repeats. ....	70
<b>Figure 26.</b> MLC with 4-hydroxybenzamide using: Tween 20, HP Tween 20, SR Tween 20, Tween 80, HP Tween 80, SR Tween 80, Etocas 35, Croduret 40, Crodasol HS HP, SDS and Brij 35 as the mobile phase at concentrations: $1 \times 10^{-2}$ , $1 \times 10^{-3}$ , $1 \times 10^{-4}$ , $1 \times 10^{-5}$ , $1 \times 10^{-6}$ , $1 \times 10^{-7}$ , $1 \times 10^{-8}$ M. Error bars were calculated using the standard deviation from 3 repeats. ....	73
<b>Figure 27.</b> MLC with hydrocortisone using: Tween 20, HP Tween 20 and SR Tween 20, as the mobile phase at concentrations: $1 \times 10^{-2}$ , $1 \times 10^{-3}$ , $1 \times 10^{-4}$ , $1 \times 10^{-5}$ , $1 \times 10^{-6}$ , $1 \times 10^{-7}$ , $1 \times 10^{-8}$ M. Error bars were calculated using the standard deviation from 3 repeats. ....	74
<b>Figure 28.</b> MLC with hydrocortisone using: Tween 80, HP Tween 80 and SR Tween 80, as the mobile phase at concentrations: $1 \times 10^{-2}$ , $1 \times 10^{-3}$ , $1 \times 10^{-4}$ , $1 \times 10^{-5}$ , $1 \times 10^{-6}$ , $1 \times 10^{-7}$ , $1 \times 10^{-8}$ M. Error bars were calculated using the standard deviation from 3 repeats. ....	75
<b>Figure 29.</b> Acetaminophen calibration graph with an $r^2$ value of 0.991. ....	83
<b>Figure 30.</b> Benzamide calibration graph with an $r^2$ value of 0.982.....	84
<b>Figure 31.</b> 4-hydroxybenzamide calibration graph with an $r^2$ value of 0.999.....	84
<b>Figure 32.</b> Hydrocortisone calibration graph with an $r^2$ value of 0.996.....	85
<b>Figure 33.</b> The results of the maximum solubility determination of acetaminophen in the presence of Tween 20, HP Tween 20, SR Tween 20, Tween 80, HP Tween 80, SR Tween 80, Etocas 35, Croduret 40, Crodasol HS HP, SDS, Brij 35 at surfactant concentrations of $1 \times 10^{-2}$ , $1 \times 10^{-3}$ , $1 \times 10^{-4}$ , $1 \times 10^{-5}$ , $1 \times 10^{-6}$ , $1 \times 10^{-7}$ and $1 \times 10^{-8}$ at 31°C. Error bars were calculated using the standard deviation from 3 repeats. ....	<b>Error! Bookmark not defined.</b>
<b>Figure 34.</b> Solubility determination of acetaminophen in the presence of Tween 20, HP Tween 20, SR Tween 20, at surfactant concentrations of $1 \times 10^{-2}$ , $1 \times 10^{-3}$ , $1 \times 10^{-4}$ , $1 \times 10^{-5}$ , $1 \times 10^{-6}$ , $1 \times 10^{-7}$ and $1 \times 10^{-8}$ M <sup>8</sup> at 31°C. Error bars were calculated using the standard deviation from 3 repeats. ....	87
<b>Figure 35.</b> Solubility determination of acetaminophen in the presence of Tween 80, HP Tween 80, SR Tween 80, at surfactant concentrations of $1 \times 10^{-2}$ , $1 \times 10^{-3}$ , $1 \times 10^{-4}$ , $1 \times 10^{-5}$ , $1 \times 10^{-6}$ , $1 \times 10^{-7}$ and $1 \times 10^{-8}$ M <sup>8</sup> at 31°C. Error bars were calculated using the standard deviation from 3 repeats. ....	88
<b>Figure 36.</b> Solubility determination of benzamide in the presence of Tween 20, HP Tween 20, SR Tween 20, Tween 80, HP Tween 80, SR Tween 80, Etocas 35, Croduret 40, Crodasol HS HP, SDS, Brij 35 at surfactant concentrations of $1 \times 10^{-2}$ , $1 \times 10^{-3}$ , $1 \times 10^{-4}$ , $1 \times 10^{-5}$ , $1 \times 10^{-6}$ , $1 \times 10^{-7}$ and $1 \times 10^{-8}$ M <sup>8</sup> at 31°C. Error bars were calculated using the standard deviation from 3 repeats.....	90
<b>Figure 37.</b> Solubility determination of benzamide in the presence of Tween 80, HP Tween 80, SR Tween 80, at surfactant concentrations of $1 \times 10^{-2}$ , $1 \times 10^{-3}$ , $1 \times 10^{-4}$ , $1 \times 10^{-5}$ , $1 \times 10^{-6}$ , $1 \times 10^{-7}$ and $1 \times 10^{-8}$ M <sup>8</sup> at 31°C. Error bars were calculated using the standard deviation from 3 repeats. ....	92
<b>Figure 38.</b> Solubility determination of benzamide in the presence of Tween 20, HP Tween 20, SR Tween 20, at surfactant concentrations of $1 \times 10^{-2}$ , $1 \times 10^{-3}$ , $1 \times 10^{-4}$ , $1 \times 10^{-5}$ , $1 \times 10^{-6}$ , $1 \times 10^{-7}$ and $1 \times 10^{-8}$ M <sup>8</sup> at 31°C. Error bars were calculated using the standard deviation from 3 repeats. ....	92



<b>Figure 39.</b> Solubility determination of 4-hydroxybenzamide in the presence of Tween 20, HP Tween 20, SR Tween 20, Tween 80, HP Tween 80, SR Tween 80, Etocas 35, Croduret 40, Crodasol HS HP, SDS, Brij 35 at surfactant concentrations of $1 \times 10^{-2}$ , $1 \times 10^{-3}$ , $1 \times 10^{-4}$ , $1 \times 10^{-5}$ , $1 \times 10^{-6}$ , $1 \times 10^{-7}$ and $1 \times 10^{-8}$ M at 31°C. Error bars were calculated using the standard deviation from 3 repeats. ....	95
<b>Figure 40.</b> The results of the maximum solubility determination of 4-hydroxybenzamide in the presence of Tween 80, HP Tween 80, SR Tween 80, at surfactant concentrations of $1 \times 10^{-2}$ , $1 \times 10^{-3}$ , $1 \times 10^{-4}$ , $1 \times 10^{-5}$ , $1 \times 10^{-6}$ , $1 \times 10^{-7}$ and $1 \times 10^{-8}$ M at 31°C. Error bars were calculated using the standard deviation from 3 repeats.....	97
<b>Figure 41.</b> The results of the maximum solubility determination of 4-hydroxybenzamide in the presence of Tween 20, HP Tween 20, SR Tween 20, at surfactant concentrations of $1 \times 10^{-2}$ , $1 \times 10^{-3}$ , $1 \times 10^{-4}$ , $1 \times 10^{-5}$ , $1 \times 10^{-6}$ , $1 \times 10^{-7}$ and $1 \times 10^{-8}$ M at 31°C. Error bars were calculated using the standard deviation from 3 repeats.....	97
<b>Figure 43.</b> Solubility determination of hydrocortisone in the presence of Tween 20, HP Tween 20, SR Tween 20, at surfactant concentrations of $1 \times 10^{-2}$ , $1 \times 10^{-3}$ , $1 \times 10^{-4}$ , $1 \times 10^{-5}$ , $1 \times 10^{-6}$ , $1 \times 10^{-7}$ and $1 \times 10^{-8}$ M at 31°C. Error bars were calculated using the standard deviation from 3 repeats. ....	100
<b>Figure 42.</b> Solubility determination of hydrocortisone in the presence of Tween 20, HP Tween 20, SR Tween 20, at surfactant concentrations of $1 \times 10^{-2}$ , $1 \times 10^{-3}$ , $1 \times 10^{-4}$ , $1 \times 10^{-5}$ , $1 \times 10^{-6}$ , $1 \times 10^{-7}$ and $1 \times 10^{-8}$ M at 31°C. Error bars were calculated using the standard deviation from 3 repeats. ....	100
<b>Figure 44.</b> The chromatogram of a full scan of Tween 20 at concentrations: $1 \times 10^{-2}$ , $1 \times 10^{-3}$ , $1 \times 10^{-4}$ , $1 \times 10^{-5}$ , $1 \times 10^{-6}$ , $1 \times 10^{-7}$ , $1 \times 10^{-8}$ M at 200 – 800 nm. ....	105
<b>Figure 45.</b> The chromatogram of a full scan of Tween 80 at concentrations: $1 \times 10^{-2}$ , $1 \times 10^{-3}$ , $1 \times 10^{-4}$ , $1 \times 10^{-5}$ , $1 \times 10^{-6}$ , $1 \times 10^{-7}$ , $1 \times 10^{-8}$ M at 200 – 800 nm. ....	106
<b>Figure 46.</b> The chromatogram of a full scan of Etocas 35 at concentrations: $1 \times 10^{-2}$ , $1 \times 10^{-3}$ , $1 \times 10^{-4}$ , $1 \times 10^{-5}$ , $1 \times 10^{-6}$ , $1 \times 10^{-7}$ , $1 \times 10^{-8}$ M at 200 – 800 nm. ....	106
<b>Figure 47.</b> The chromatogram of a full scan of Croduret 40 at concentrations: $1 \times 10^{-2}$ , $1 \times 10^{-3}$ , $1 \times 10^{-4}$ , $1 \times 10^{-5}$ , $1 \times 10^{-6}$ , $1 \times 10^{-7}$ , $1 \times 10^{-8}$ M at 200 – 800 nm. ....	107
<b>Figure 48.</b> The chromatogram of a full scan of Crodasol HS HP at concentrations: $1 \times 10^{-2}$ , $1 \times 10^{-3}$ , $1 \times 10^{-4}$ , $1 \times 10^{-5}$ , $1 \times 10^{-6}$ , $1 \times 10^{-7}$ , $1 \times 10^{-8}$ M at 200 – 800 nm. ....	107
<b>Figure 49.</b> The chromatogram of a full scan of SDS at concentrations: $1 \times 10^{-2}$ , $1 \times 10^{-3}$ , $1 \times 10^{-4}$ , $1 \times 10^{-5}$ , $1 \times 10^{-6}$ , $1 \times 10^{-7}$ , $1 \times 10^{-8}$ M at 200 – 800 nm. ....	108
<b>Figure 50.</b> The chromatogram of a full scan of Brij 35 at concentrations: $1 \times 10^{-2}$ , $1 \times 10^{-3}$ , $1 \times 10^{-4}$ , $1 \times 10^{-5}$ , $1 \times 10^{-6}$ , $1 \times 10^{-7}$ , $1 \times 10^{-8}$ M at 200 – 800 nm. ....	108
<b>Figure 51.</b> The chromatogram of a full scan of acetaminophen in $1 \times 10^{-4}$ M of Tween 20, Tween 80, Etocas 35 Croduret 40, Crodasol HS HP, Brij 35 and SDS.....	110
<b>Figure 52.</b> The chromatogram of a full scan of Benzamide in $1 \times 10^{-4}$ M of Tween 20, Tween 80, Etocas 35 Croduret 40, Crodasol HS HP, Brij 35 and SDS.....	110
<b>Figure 53.</b> The chromatogram of a full scan of 4-hydroxybenzamide in $1 \times 10^{-4}$ M of Tween 20, Tween 80, Etocas 35 Croduret 40, Crodasol HS HP, Brij 35 and SDS. ....	111
<b>Figure 54.</b> An example of a plot displaying $\mu\text{cal}/\text{sec}$ with time (min) for the demicellisation of Tween 20. ....	113
<b>Figure 55.</b> An example of a plot of $\Delta H$ (kJoules/mol) with surfactant concentration (M) for Tween 20. ....	113
<b>Figure 56.</b> An example of a plot of the 2 <sup>nd</sup> derivative of $\Delta H$ (Arbitrary Units) with surfactant concentration (M) for Tween 20. ....	114
<b>Figure 57.</b> An example of a plot of $\Delta H$ (kJoules/mol) with surfactant concentration (M) for HP Tween 20.....	116
<b>Figure 58.</b> An example of a plot displaying $\mu\text{cal}/\text{sec}$ with time (min) for the demicellisation of HP Tween 20.....	116

<b>Figure 59.</b> An example of a plot of the 2 <sup>nd</sup> derivative of $\Delta H$ (Arbitrary Units) with surfactant concentration (M) for HP Tween 20. ....	117
<b>Figure 60.</b> An example of a plot displaying $\mu\text{cal}/\text{sec}$ against time (min) for the demicellisation of SR Tween 20. ....	118
<b>Figure 61.</b> An example of a plot of $\Delta H$ (kJoules/mol) with surfactant concentration (M) for SR Tween 20. ....	119
<b>Figure 62.</b> An example of a plot of the 2 <sup>nd</sup> derivative of $\Delta H$ (Arbitrary Units) with surfactant concentration (M) for SR Tween 20. ....	120
<b>Figure 63.</b> An example of a plot displaying $\mu\text{cal}/\text{sec}$ against time (min) for the demicellisation of Tween 80. ....	121
<b>Figure 64.</b> An example of a plot of $\Delta H$ (kJoules/mol) with surfactant concentration (M) for Tween 80. ....	122
<b>Figure 65.</b> An example of a plot of the 2 <sup>nd</sup> derivative of $\Delta H$ (Arbitrary Units) with surfactant concentration (M) for Tween 80. ....	123
<b>Figure 66.</b> An example of a plot displaying $\mu\text{cal}/\text{sec}$ against time (min) for the demicellisation of HP Tween 80. ....	124
<b>Figure 67.</b> An example of a plot of $\Delta H$ (kJoules/mol) with surfactant concentration (M) for HP Tween 80. ....	125
<b>Figure 68.</b> An example of a plot of the 2 <sup>nd</sup> derivative of $\Delta H$ (Arbitrary Units) with surfactant concentration (M) for HP Tween 80. ....	126
<b>Figure 69.</b> An example of a plot displaying $\mu\text{cal}/\text{sec}$ against time (min) for the demicellisation of SR Tween 80. ....	127
<b>Figure 70.</b> An example of a plot of $\Delta H$ (kJoules/mol) with surfactant concentration (M) for HP Tween 80. ....	128
<b>Figure 71.</b> An example of a plot of the 2 <sup>nd</sup> derivative of $\Delta H$ (Arbitrary Units) with surfactant concentration (M) for SR Tween 80. ....	129
<b>Figure 72.</b> An example of a plot displaying $\mu\text{cal}/\text{sec}$ against time (min) for the demicellisation of Etocas 35. ....	130
<b>Figure 73.</b> An example of a plot of $\Delta H$ (kJoules/mol) with surfactant concentration (M) for Etocas 35. ....	131
<b>Figure 74.</b> An example of a plot of the 2 <sup>nd</sup> derivative of $\Delta H$ (Arbitrary Units) with surfactant concentration (M) for Etocas 35. ....	132
<b>Figure 75.</b> An example of a plot displaying $\mu\text{cal}/\text{sec}$ against time (min) for the demicellisation of Croduret 40. ....	133
<b>Figure 76.</b> An example of a plot of $\Delta H$ (kJoules/mol) with surfactant concentration (M) for Croduret 40. ....	134
<b>Figure 77.</b> An example of a plot of the 2 <sup>nd</sup> derivative of $\Delta H$ (Arbitrary Units) with surfactant concentration (M) for Croduret 40. ....	135
<b>Figure 78.</b> An example of a plot displaying $\mu\text{cal}/\text{sec}$ against time (min) for the demicellisation of Crodasol HS HP. ....	136
<b>Figure 79.</b> An example of a plot of $\Delta H$ (kJoules/mol) with surfactant concentration (M) for Crodasol HS HP. ....	137
<b>Figure 80.</b> An example of a plot of the 2 <sup>nd</sup> derivative of $\Delta H$ (Arbitrary Units) with surfactant concentration (M) for Crodasol HS HP. ....	138

## List of Equations

<b>Equation 1.</b> The Henderson-Hasselbach Equation. <sup>3</sup> .....	14
<b>Equation 2.</b> The Noyes-Whitney Equation. Where $dm/dt$ is the dissolution rate, $k$ is the dissolution rate constant, $A$ is the surface area of the dissolving solid, $C_s$ is the solubility of the solid in the dissolution medium and $C$ is the concentration of drug in the dissolution medium at time $t$ . <sup>8</sup> .....	15
<b>Equation 3.</b> The Henderson Hasselbach variation used by Völgyi. $S$ is the buffered solubility, $S_0$ is the intrinsic solubility and $pK_a$ is the negative Logarithm of the ionisation constant of the molecule. <sup>11</sup> .....	16
<b>Equation 4.</b> A mathematical description of micelle formation. Where $AN$ is the aggregate number, $S$ is the concentration of given surfactant associating to form a micelle and $S_{AN}$ is the micelle comprised of $S$ monomer. <sup>32</sup> .....	21
<b>Equation 5.</b> A mathematical description of micelle formation. Where $AN$ is the aggregate number, $S$ is the concentration of given surfactant associating to form a micelle, $m$ is the free number of surfactant molecules and $S_{AN}$ is the micelle comprised of $S$ monomer. <sup>32</sup> .....	21
<b>Equation 6.</b> The equation for expressing the equilibrium constant for micelle formation. <sup>32</sup> .....	21
<b>Equation 7.</b> Equation relating the equilibrium constant for micelle formation to the change in Gibb's free energy ( $\Delta G$ ). Where $R$ is the gas constant and $T$ is temperature in Kelvin. <sup>32</sup> .....	22
<b>Equation 8.</b> Equation relating the equilibrium constant for micelle formation to change in Gibb's free energy ( $\Delta G$ ). Where $R$ is the gas constant $S_{AN}$ is the micelle comprised of $S$ monomer, $AN$ is the aggregate number and $T$ is temperature in Kelvin. <sup>32</sup> .....	22
<b>Equation 9.</b> An equation showing that micellisation is a spontaneous exothermic process. <sup>32</sup> .....	22
<b>Equation 10.</b> An equation that allows the calculation of change in entropy ( $\Delta S$ ) with regards to micelle formation. <sup>32</sup> .....	<b>Error! Bookmark not defined.</b>
<b>Equation 11.</b> An equation for the standard free energy of solubilisation ( $\Delta G_0^S$ ), where $R$ is the universal constant of gasses, $T$ is the temperature and $P$ is the partition coefficient between the micellar and the aqueous phase.....	24
<b>Equation 12.</b> An equation for calculating the molar solubilisation capacity ( $\chi$ ), where $S_{tot}$ is the total drug solubility, $S_w$ is the water drug solubility, $C_{surf}$ is the molar concentration of surfactant in solution and CMC is the critical micelle concentration. ....	25
<b>Equation 13.</b> An equation for calculating the micelle-water partition coefficient ( $P$ ) where $S_{tot}$ is the total drug solubility and $S_w$ is the water drug solubility.....	25
<b>Equation 14.</b> An equation combining the two most common solubility descriptors ( $\chi$ and $P$ ) where $S_w$ is the water drug solubility, $C_{surf}$ is the molar concentration of surfactant in solution and CMC is the critical micelle concentration. ....	25
<b>Equation 15.</b> An equation for the molar micelle-water partition coefficient ( $PM$ ), where $\chi$ is the molar solubilisation capacity, CMC is the critical micelle concentration and $SW$ is the water drug solubility. ....	26
<b>Equation 16.</b> The equation for calculating capacity factor $k'$ . Where $t_r$ is the retention time and $t_m$ is the void time. <sup>39</sup> .....	28
<b>Equation 17.</b> An equation showing the relationship between $k'$ , $A$ (the compound that is distributed between the two phases) and Volume. <sup>39</sup> .....	28
<b>Equation 18.</b> An equation showing the relationship between $K_D$ (Distribution Constant) and $k'$ where $A$ is the compound that is distributed between the two phases. <sup>39</sup> .....	28
<b>Equation 19.</b> An equation demonstrating the relationship between free energy and $K_D$ . <sup>39</sup> .....	29
<b>Equation 20.</b> Armstrong and Nome's equation for describing the retention time in pure micellar mobile phases. Where $V_e$ represent the total volume of mobile phase needed to elute a given solute from the column. $V_s$ is the volume of the API surface on the stationary phase, $V_0$ is the column void	

volume, $\Phi$ is the phase ratio, $v$ is the partial specific volume of monomers of surfactant in the micelle. <sup>41</sup> .....	33
<b>Equation 21.</b> Arunyanart and Cline-Love's equation for describing retention time in pure micellar phases. $K_{AS}$ is the binding constant between the solute in bulk aqueous solvent and stationary sites and $K_{AM}$ is the binding constant between the solute in the aqueous phase and the monomers of surfactant in the micelle. <sup>41</sup> .....	33
<b>Equation 22.</b> An equation showing the linear relationship between SR and the octanol-water partition coefficient. <sup>45</sup> .....	34
<b>Equation 23.</b> An equation enabling the prediction of solubility. Where $C_{sx}$ = the solubility of the drug in the presence of taurocholate, $C_{so}$ = the solubility of the drug in the absence of taurocholate, and $SC_{bs}$ is the solubilisation capacity of the bile salt (taurocholate) for the drug, $M_r$ is the molecular weight of the drug. <sup>45</sup> .....	35
<b>Equation 24</b> An equation for calculating the water-micelle partition coefficient. Where $k'$ is the capacity factor, $C_M$ is the micelle concentration (total surfactant concentration – CMC) $P_{WS}$ is the solute partition coefficient between water and the stationary phase and $\Phi$ is the chromatographic phase ratio. <sup>47</sup> .....	35

## List of Tables

<b>Table 1.</b> The reported CMCs of Tween 20, Tween 80, Brij 35 and SDS using various techniques and at several temperatures.....	44
<b>Table 2.</b> The structure and properties of the surfactants used. All of the properties were obtained from PubChem <sup>87</sup> , properties currently unknown = (-) .....	47
<b>Table 3.</b> The Aq solubility, Mr, Log P, pKa and lambda max of the APIs used in the project. The values for Mr, Log P and pKa are from PubChem <sup>87</sup> and the lambda max and Aq solubility values were experimentally derived.....	48
<b>Table 4.</b> The average k' values of acetaminophen with Tween 20, HP Tween 20, SR Tween 20, Tween 80, HP Tween 80, SR Tween 80, Etocas 3, Croduret 40, Crodasol HS HP, SDS and Brij 35 at $1 \times 10^{-2}$ and $1 \times 10^{-8}$ M.....	57
<b>Table 5.</b> The average k' values of benzamide with Tween 20, HP Tween 20, SR Tween 20, Tween 80, HP Tween 80, SR Tween 80, Etocas 3, Croduret 40, Crodasol HS HP, SDS and Brij 35 at $1 \times 10^{-2}$ and $1 \times 10^{-8}$ M.....	62
<b>Table 6.</b> The average k' values of 4-hydroxybenzamide with Tween 20, HP Tween 20, SR Tween 20, Tween 80, HP Tween 80, SR Tween 80, Etocas 3, Croduret 40, Crodasol HS HP, SDS and Brij 35 at $1 \times 10^{-2}$ and $1 \times 10^{-8}$ M.....	66
<b>Table 7.</b> The average k' values of hydrocortisone with Tween 20, HP Tween 20, SR Tween 20, Tween 80, HP Tween 80, SR Tween 80, Etocas 3, Croduret 40, Crodasol HS HP, SDS and Brij 35 at $1 \times 10^{-2}$ and $1 \times 10^{-8}$ M.....	73
<b>Table 8.</b> The ranked overall change in k' values for each surfactant with each API used in this study. The ranking order is green (the greatest reduction) yellow, orange and red (smallest reduction). .....	78
<b>Table 9.</b> Ranked Log P and pKa values for the APIs used in this study. The ranking order is green (greatest value), yellow, orange and red (lowest value). Log P and pKa values obtained from PubChem. <sup>87</sup> .....	78
<b>Table 10.</b> The fatty acid composition of polysorbate 20 and polysorbate 80 the values of which are obtained from the USP – NF <sup>92</sup> . .....	79
<b>Table 11.</b> pH values for Tween 20, HP Tween 20, SR Tween 20, Tween 80, HP Tween 80, SR Tween 80, Etocas 35, Croduret 40, Crodasol HS HP, SDS and Brij 35 at concentrations: $1 \times 10^{-2}$ , $1 \times 10^{-3}$ , $1 \times 10^{-4}$ , $1 \times 10^{-5}$ , $1 \times 10^{-6}$ , $1 \times 10^{-7}$ , $1 \times 10^{-8}$ M.....	82
<b>Table 12.</b> Solubility of acetaminophen in Tween 20, HP Tween 20, SR Tween 20, Tween 80, HP Tween 80, SR Tween 80, Etocas 35, Croduret 40, Crodasol HS HP, SDS and Brij 35 at $1 \times 10^{-2}$ M. ...	86
<b>Table 13.</b> The derived values of the molar solubilisation capacity ( $\chi$ ), micelle-water partition coefficient (P) and the molar micelle-water partition coefficient ( $P_M$ ) for acetaminophen with Tween 20, HP Tween 20, SR Tween 20, Tween 80, HP Tween 80, SR Tween 80, Etocas 35, Croduret 40, Crodasol HS HP, SDS and Brij 35. Where $S_{Tot}$ is the total amount of acetaminophen solubilised, $S_w$ is the water solubility of acetaminophen (value determined experimentally), $C_{Surf}$ is the surfactant concentration and CMC is the critical micelle concentration (using the derived values for Tween 20, HP Tween 20, SR Tween 20, Tween 80 HP Tween 80, SR Tween 80, Etocas 35, Croduret 40 and Crodasol HS HP from Section 6).....	89
<b>Table 14.</b> Solubility of benzamide in Tween 20, HP Tween 20, SR Tween 20, Tween 80, HP Tween 80, SR Tween 80, Etocas 35, Croduret 40, Crodasol HS HP, SDS and Brij 35 at $1 \times 10^{-2}$ M.....	90
<b>Table 15.</b> The derived values of the molar solubilisation capacity ( $\chi$ ), micelle-water partition coefficient (P) and the molar micelle-water partition coefficient ( $P_M$ ) for benzamide with Tween 20, HP Tween 20, SR Tween 20, Tween 80, HP Tween 80, SR Tween 80, Etocas 35, Croduret 40, Crodasol HS HP, SDS and Brij 35. Where $S_{Tot}$ is the total amount of acetaminophen solubilised, $S_w$ is the water solubility of benzamide (value determined experimentally), $C_{Surf}$ is the surfactant concentration and CMC is the critical micelle concentration (using the derived values for Tween 20,	

HP Tween 20, SR Tween 20, Tween 80, HP Tween 80, SR Tween 80, Etocas 35, Croduret 40 and Crodasol HS HP from Section 6).....	94
<b>Table 16.</b> The solubility of 4-hydroxybenzamide in Tween 20, HP Tween 20, SR Tween 20, Tween 80, HP Tween 80, SR Tween 80, Etocas 35, Croduret 40, Crodasol HS HP, SDS and Brij 35 at $1 \times 10^{-2}$ M.....	95
<b>Table 17.</b> The derived values of the molar solubilisation capacity ( $\chi$ ), micelle-water partition coefficient (P) and the molar micelle-water partition coefficient ( $P_M$ ) for 4-hydroxybenzamide with Tween 20, HP Tween 20, SR Tween 20, Tween 80, HP Tween 80, SR Tween 80, Etocas 35, Croduret 40, Crodasol HS HP, SDS and Brij 35. Where $S_{Tot}$ is the total amount of acetaminophen solubilised, $S_w$ is the water solubility of 4-hydroxybenzamide (value determined experimentally), $C_{Surf}$ is the surfactant concentration and CMC is the critical micelle concentration (using the derived values for Tween 20, HP Tween 20, SR Tween 20, Tween 80 HP Tween 80, SR Tween 80, Etocas 35, Croduret 40 and Crodasol HS HP from Section 6). .....	98
<b>Table 18.</b> The literature and experimental solubility values for the aqueous solubility of acetaminophen, benzamide and hydrocortisone. The literature values are taken from PubChem <sup>101</sup> and are recorded at 25 °C, the experimental values were recorded at 31 °C.....	99
<b>Table 19.</b> The solubility of hydrocortisone in Tween 20, HP Tween 20, SR Tween 20, Tween 80, HP Tween 80, SR Tween 80 at $1 \times 10^{-2}$ M. ....	101
<b>Table 20.</b> The derived values of the molar solubilisation capacity ( $\chi$ ), micelle-water partition coefficient (P) and the molar micelle-water partition coefficient ( $P_M$ ) for hydrocortisone with Tween 20, HP Tween 20, SR Tween 20, Tween 80, HP Tween 80 and SR Tween 80. Where $S_{Tot}$ is the total amount of acetaminophen solubilised, $S_w$ is the water solubility of hydrocortisone (value determined experimentally), $C_{Surf}$ is the surfactant concentration and CMC is the critical micelle concentration (using the derived values for Tween 20, HP Tween 20, SR Tween 20, Tween 80, HP Tween 80 and SR Tween 80 from Section 6).....	102
<b>Table 21.</b> A table showing the graded solubility improvement of acetaminophen (A), benzamide (B), 4-hydroxybenzamide (4) and hydrocortisone (H) in terms of increase in mg/mL and percentage increase with Tween 20, HP Tween 20, SR Tween 20, Tween 80, HP Tween 80 and SR Tween 80 at a concentration of $1 \times 10^{-2}$ M. Where green is the greatest improvement, followed by yellow, then orange then red.....	103
<b>Table 22.</b> A table showing the graded solubility improvement of acetaminophen (A), benzamide (B), 4-hydroxybenzamide (4) and hydrocortisone (H) in terms of increase in mg/mL and percentage increase with Etocas 35, Croduret 40, Crodasol HS HP, SDS and Brij 35 at a concentration of $1 \times 10^{-2}$ M. Where green is the greatest improvement, followed by yellow, then orange then red.....	104
<b>Table 23.</b> Lambda max values in nm for acetaminophen, benzamide and 4-hydroxybenzamide in ultra-pure water, and the following surfactants at $1 \times 10^{-4}$ M: Tween 20, Tween 80, Etocas 35, Croduret 40, Crodasol HS HP, SDS and Brij 35 .....	111
<b>Table 24.</b> The derived average CMCs in mM via ITC of Tween 20, HP Tween 20, SR Tween 20, Tween 80, HP Tween 80, SR Tween 80, Etocas 35, Croduret 40 and Crodasol HS HP the error values were determined to be the standard deviation calculated from 3 repeats.....	138

# 1. Introduction

## 1.1 Solubility

Solubility is defined as the quantity of solute that dissolves in a given quantity of solvent, to form a saturated solution.<sup>1</sup> However, there are three, more specific definitions of solubility which are commonly used. These are buffered solubility, unbuffered solubility, and intrinsic solubility. Unbuffered solubility refers to the solubility of a saturated solution of the compound at the final pH of the solution. Buffered solubility is the solubility at a given pH and intrinsic solubility refers to the solubility of an ionisable compound.<sup>2</sup> It is possible to calculate the intrinsic solubility from the buffered solubility for neutral compounds using the Henderson-Hasselbach equation.<sup>3</sup>

$$\text{pH} = \text{pK}_a + \text{Log} \frac{[\text{A}^-]}{[\text{HA}]}$$

*Equation 1.* The Henderson-Hasselbach Equation.<sup>3</sup>

Solubility is a key factor in drug design, because of the impact that solubility has on bioavailability. If a drug is not suitably soluble then it will not be transported to the target site in the body and will be excreted. Therefore, when designing a drug solubility must be considered, as low bioavailability is frequently linked to poor solubility.<sup>4</sup> It is also a key factor when designing a drug where a specific concentration is required in the systemic circulation, allowing for an effective dose of the drug to remain in the system.<sup>5</sup>

There are two types of solubility that can be experimentally derived; kinetic or thermodynamic (true) solubility. In drug discovery, kinetic solubility is usually calculated due to the increased speed at which it can be derived, this is because of high throughput screening (HTS) which involves synthesising a high volume of compounds based on desired physiochemical characteristics. It is normal for hundreds of drugs to be synthesised in the course of this process.<sup>6</sup> As only small amounts of the potential drugs

might be synthesised, normally a few milligrams, there might not be enough to use to calculate thermodynamic solubility. In addition to this, thermodynamic solubility can take in excess of 24 hours to experimentally calculate, requiring an unrealistic amount of time when there are hundreds of possible drug candidates.<sup>2</sup> However, it is worth noting that kinetic solubility does not take into account the co-solvent (normally DMSO) leading to inaccuracies.

When experimentally calculating kinetic solubility, measurements are taken when the compound is dissolved and precipitation begins, as a result, this represents the maximum solubility. The values calculated this way are largely temperature dependent, and as super saturation can occur, can over predict the thermodynamic solubility.<sup>7</sup>

Thermodynamic solubility is experimentally calculated using a saturated solution with an excess of undissolved substance. It is the result of a dynamic equilibrium between the two forces of dissolution and precipitation. When a solute is added to a solvent it initially disperses, this is the process known as dissolution. Dissolution relies on the solute-solvent intermolecular forces being more energetically favourable than the solute-solute bonds. The rate of dissolution can be calculated using the Noyes-Whitney equation as shown in **Equation 2**.<sup>8</sup>

$$\frac{dm}{dt} = kA(C_s - C)$$

**Equation 2.** The Noyes-Whitney Equation. Where  $dm/dt$  is the dissolution rate in  $kg\ s^{-1}$ ,  $k$  is the dissolution rate constant,  $A$  is the surface area of the dissolving solid,  $C_s$  is the solubility of the solid in the dissolution medium and  $C$  is the concentration of drug in the dissolution medium at time  $t$ .<sup>8</sup>

Factors such as temperature, pH,  $pK_a$ , and particle size can have a large impact on whether a solute will be soluble in a given solvent. Whilst solubility and dissolution are linked, they are not the same. A compound can have a high solubility value but have a low rate of dissolution, meaning that most of a compound will dissolve but it will take a long time. Conversely, a compound can have a low solubility



but a high rate of dissolution, this would mean that only a small amount of the compound would dissolve but it would happen very quickly.

Black and Muller found, by testing a series of 50 organic compounds in varying temperatures of water, that increasing the temperature resulted in an increase in solubility, with the solubility doubling with temperature in some cases.<sup>9</sup> This fits with the theoretical model that dissolution is generally an endothermic reaction, however, there are compounds such as calcium chloride which undergo an exothermic dissolution.

Decreasing the particle size of a compound will also lead to an increase in solubility, this is supported by the published findings of Sun and Wang regarding the effect of particle size on solubility, dissolution rate, and oral bioavailability.<sup>10</sup> Decreasing the particle size results in an overall increase in the surface area of the compound, this leads to an increase in solute-solvent intermolecular forces and therefore an increase in solubility.

The majority of drugs are either slightly basic or slightly acidic, this means that changes in solubility because of an alteration of the pH of the solvent can be predicted, using a variation of the Henderson-Hasselbach equation, as used by Völgyi.<sup>11</sup>

$$\text{LogS} = \text{LogS}_0 + \text{Log}(10^{\text{pK}_a - \text{pH}} + 1)$$

**Equation 3.** The Henderson Hasselbach variation used by Völgyi. S is the buffered solubility, S<sub>0</sub> is the intrinsic solubility and pK<sub>a</sub> is the negative Logarithm of the ionisation constant of the molecule.<sup>11</sup>

Currently, there are several methods for calculating either the kinetic or the thermodynamic solubility of a compound. A commonly used method for calculating the thermodynamic solubility, known as the shake-flask method, was published by Higuchi and Connors in 1965.<sup>12</sup> For this method an excess amount of solute is added to a known volume of solvent. The amount of drug added should be enough to make a saturated solution; a solution where the maximum amount of a solute has been dissolved

under the conditions that the solution exists. The solution must then be allowed to reach equilibrium, which can take 24 hours or more. It is possible to speed up the process of equilibrium using a sonicator or vortexing the solution. After this the resulting two phases are separated, often via filtration, however, when using filtration it is important to consider adsorption of the solute on the filter because of oversaturation of the absorption sites; centrifugation is often used to overcome this issue.<sup>13</sup> HPLC is then used to calculate the concentration of solute present in the solution and from that, the solubility can be calculated. This process can often take in excess of 2 days to complete and is therefore a time-consuming process.

An alternative method for calculating the thermodynamic solubility was published by Hankinson and Thompson in 1965 and is called the synthetic method.<sup>14</sup> An adaptation of this early method as published by Yang in 2008 is now commonly used.<sup>15</sup> Yang's method involves adding a known amount of drug to a known volume of solvent, which is then stirred at a constant temperature. As the drug slowly dissolves the intensity of a laser beam which goes through the reaction vessel to a transmittance detector and is used to identify the presence of the drug, gradually increasing to a maximum value, which signifies that all of the drug has been dissolved. Once this occurs, further aliquots of the drug are added, reducing the transmittance through the solution until the further aliquots of the drug dissolve and the laser reaches its maximum intensity again, but the detector records less than the maximum value, signifying that the drug couldn't be dissolved. The total amount of the drug that was added is then used to calculate the solubility. This process, like the shake-flask method, is also time-consuming.

One method for calculating kinetic solubility is known as the nephelometric method, the determination of the kinetic solubility can be completed using turbidimetry readings. It involves creating solutions of different concentrations using a 10 millimolar stock solution, made by dissolving appropriate amounts of solute into an appropriate solvent. The stock solution is then diluted using a buffer solution to provide the desired concentrations which is then placed into a 96-well plate, with a final volume of 200  $\mu$ L and a 5 % concentration of an appropriate solvent.<sup>16</sup> The 96 sample plate is then placed into a nephelometer apparatus, which will use a laser beam and a light detector to measure the turbidity by measuring the

transmittance through the sample, a lower reading relates to greater turbidity. Finally, by plotting a graph of turbidity against concentration, the kinetic solubility can be calculated. This is accomplished by plotting the asymptotes, which then gives a coordinate for the x-axis which in turn gives the kinetic solubility. This method allows for a rapid determination of kinetic solubility and once the sample plate is placed into the nephelometer apparatus only takes a couple of minutes, further demonstrating why kinetic solubility is calculated over thermodynamic solubility in HTS.

Alternatively, a UV/Vis-spectroscopy apparatus can be used instead of the nephelometer apparatus, this has the benefit of having a wider range of wavelengths for detection to choose from for measuring turbidity. However, it is worth noting that the majority of organic molecules that contain a benzene ring will also exhibit fluorescence which can interfere with the turbidity readings.<sup>17</sup>

There are many methods for determining solubility, however, all the methods for calculating thermodynamic solubility are long and therefore time-consuming. In an industry where thousands of potential drugs are synthesised daily the need for a quicker, and therefore, more efficient method for measuring thermodynamic solubility is strongly apparent. Furthermore, once solubility has been measured it is often found to be far lower than desired thus research must then focus on ways to increase it.

A common way to increase the solubility of an active pharmaceutical ingredient (API) in a formulation is the addition of a surfactant, this allows for an increase in dosage whilst retaining the same volume.

## **1.2 Surfactants and Micelles**

A surfactant molecule consists of a head group which is either ionic, polar or non-ionic, as well as an extended non-polar organic chain (tail). Surfactants have a variety of applications in the pharmaceutical industry because of the diverse way in which they can differ structurally, which results in different physiochemical properties. Variations of the head group allow the classification of surfactants into four categories: cationic, anionic, zwitterionic and non-ionic. Surfactants enjoy widespread usage

throughout the pharmaceutical industry such as the anionic surfactant sodium dodecyl sulphate (SDS), which has been used in conjunction with other compounds as a preoperative skin cleaner because of its bacteriostatic action against gram-positive bacteria.<sup>18</sup> Zwitterionic surfactants have been observed to have excellent dermatological properties because of their mild nature.<sup>19</sup> It has also been reported that cationic surfactants, such as quaternary ammonium and pyridinium cationic surfactants exhibit bacteriostatic action against a wide range of gram-positive bacteria as well as limited activity against gram-negative bacteria.<sup>19</sup> The cationic surfactant benzalkonium chloride has been used in some parts of the world in contraception, whilst a common vaginal spermicide used in America is the non-ionic surfactant nonoxynol-9.<sup>20</sup>

Surfactants have been used as a means of enhancing the solubilities of APIs that are taken in an oral dosage form. Surfactants such as alkylsulfates, polysorbates and alcohol ethoxylates have widespread use as solubilisers for low solubility APIs such as steroids, benzimidazole and sesquiterpene lactones.<sup>21</sup> It has been reported that the solubility of some APIs can be increased by several orders of magnitude depending on the interactions between functional groups present in the surfactant nominally the head group and the API, allowing for greater concentrations to be formulated.<sup>22</sup> Some of the surfactants used in this project were supplied by Croda, these include Tween™ 20 (polysorbate 20), Tween™ 80 (polysorbate 80), Etocas 35 (polyoxyl 35 castor oil), Croduret 40 (polyoxyl 40 hydrogenated castor oil) and Crodasol HS HP (macrogol 15 hydroxystearate). Several purities of each polysorbate are commercially available; 'Standard compendial grade' (no prefix), 'High Purity' (HP) and 'Super Refined' (SR). According to the manufacturers, the HP range was developed to address the purity and control requirements of the pharmaceutical industry with the HP range having limits on peroxide value (< 2.0 meq.), 1,4 dioxane (<5 ppm) and ethylene oxide (<1 ppm), a low moisture content (< 0.2 %) and packaged under nitrogen to prevent peroxide escalation. SR polysorbates have undergone a further proprietary process that improves clarity and removes polar impurities such as peroxides, aldehydes and ketones, without altering the surfactants chemical composition, and therefore enhancing the stability of the solute and/or vehicle itself.<sup>23</sup> Polysorbates are commonly used in pharmaceutical

formulations as emulsifying agents, solubilisers in essential oils, oil-soluble vitamins and as wetting agents for oral and parenteral suspensions such as Cordarone and Kytril.<sup>24</sup> Tween 20 has been used in the cosmetics industry as a wetting agent as well as an additive in food as a solubiliser.<sup>25,26</sup> Tween 80 is widely used in the preparation of drugs, cosmetics and skin care products as a solubiliser, emulsifier and stabiliser.<sup>27,24</sup> Etocas 35 has been reported as being used in the cosmetic industry, mainly as a solubilising agent in perfume bases, as well as in hand lotions as a replacement for castor oil.<sup>24,28</sup> Croduret 40 is used as an emulsifier of fatty acids and alcohols as well as a solubiliser in oral nanoemulsion formulations.<sup>24,29</sup> Crodasol HS HP has been frequently used in preclinical testing of drugs including clotrimazole, carbamazepine and sulfathiazole.<sup>24,30</sup>

There are several different surfactants available within the pharmaceutical and chemical industry, however, regardless of choice, the mechanism of micelle formation remains largely the same. When the concentration of a surfactant exceeds the critical micelle concentration (CMC) the surfactant molecules undergo self-assembly to form a micelle. Micelles normally consist of a specific quantity of monomers; this number is known as the aggregate number (AN). A micelle is a supramolecular assembly of surfactants in aqueous phase, generally in the shape of a sphere, normally with the hydrophobic tails orientating towards the centre and the heads directing out.<sup>31</sup> However, ionic surfactants can adopt multiple micelle configurations at higher concentrations, these take the shape of

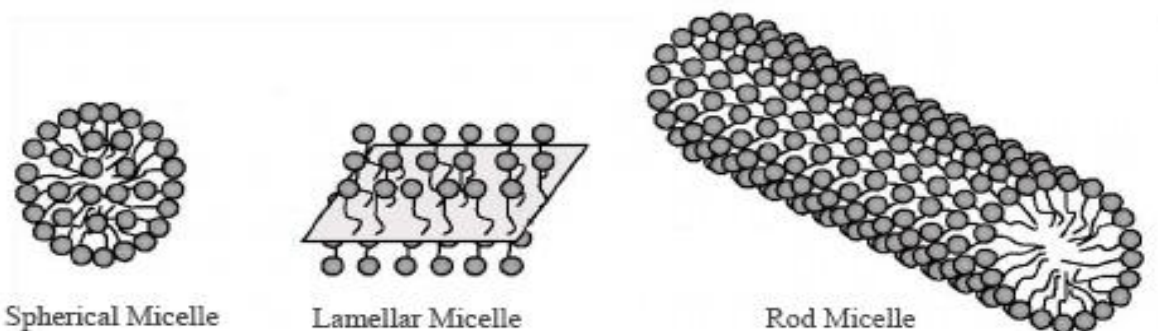


*Figure 1.* The different structures that micelles can form.<sup>30</sup>

either an elongated cylinder, a rod-like shape, lamellar or vesicular structures as shown in **Figure 1**. At high concentrations, non-ionic surfactants will also form lamellar structures.<sup>32</sup>

Micelle formation is a dynamic process, with an equilibrium being established between the monomer and micelle, as shown in **Figure 2**. Micelles have an average lifetime of  $10^{-3}$  - 1 second, with the exchange of small amounts of monomers between micelles occurring within  $10^{-8}$  -  $10^{-4}$  seconds.

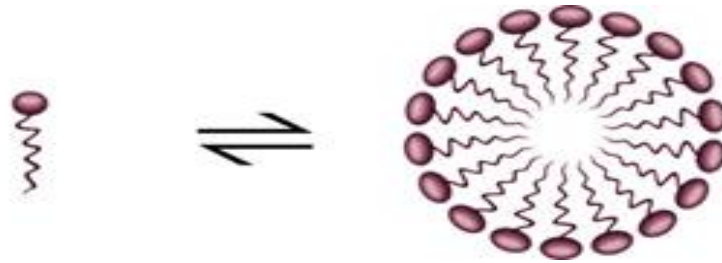
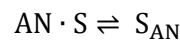
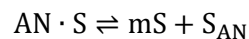


**Figure 2.** The equilibrium between a monomer and a micelle.

It can be said that micellisation is governed by four sets of interactions, those between the hydrophobic tails and water, between adjacent hydrophobic tails, between head groups and the solvation of head groups in water. Using these four interactions, it is then possible to describe the equilibrium of formation of a micelle mathematically using **Equation 4**, **Equation 5** and **Equation 6**.<sup>33</sup>



**Equation 4.** A mathematical description of micelle formation. Where AN is the aggregate number, S is the concentration of given surfactant associating to form a micelle and  $S_{AN}$  is the micelle comprised of S monomer.<sup>33</sup>



**Equation 5.** A mathematical description of micelle formation. Where AN is the aggregate number, S is the concentration of given surfactant associating to form a micelle, m is the free number of surfactant molecules and  $S_{AN}$  is the micelle comprised of S monomer.<sup>33</sup>

Using the equilibrium displayed in **Equation 5** it is then possible to create an equation for the equilibrium constant ( $K_{eq}$ ) for micelle formation as shown in **Equation 6**.

$$K_{eq} = \frac{[S_{AN}]}{[S]^{AN}}$$

**Equation 6.** The equation for expressing the equilibrium constant for micelle formation.<sup>33</sup>

This then allows for expression of changes in Gibb's free energy as shown in **Equation 7** and **Equation 8**.

$$\Delta G = -RT \ln K_{eq}$$

**Equation 7.** Equation relating the equilibrium constant for micelle formation to the change in Gibb's free energy ( $\Delta G$ ). Where R is the gas constant and T is temperature in Kelvin.<sup>33</sup>

$$\frac{\Delta G}{AN} = -\frac{RT}{AN} \ln S_{AN} + RT \ln S$$

**Equation 8.** Equation relating the equilibrium constant for micelle formation to change in Gibb's free energy ( $\Delta G$ ). Where R is the gas constant  $S_{AN}$  is the micelle comprised of S monomer, AN is the aggregate number and T is temperature in Kelvin.<sup>33</sup>

When micelles are formed with an aggregate number that is greater than 50, the first term in **Equation 8** (on the right) can be removed. CMC can also be used instead of S, as S is the concentration at which micelles form, this allows **Equation 8** to be rewritten as **Equation 9** which shows that micellisation is a spontaneous exothermic process.<sup>33</sup>

$$\Delta G \approx RT \ln CMC$$

**Equation 9.** An equation showing that micellisation is a spontaneous exothermic process.<sup>33</sup>

Surfactant molecules are commonly used because of their ability to reduce interfacial tension between two liquid phases, this enables normally immiscible liquids such as oil and water to become miscible. The reduction in surface tension is brought about by the molecule's preference to orientate itself so that its hydrophilic head is directed towards water and the hydrophobic tail is directed inwards. When the hydrophobic tail is in water it interferes with the water's intermolecular interactions, by disrupting the hydrogen bonds between water molecules. This results in a rearrangement of local water molecules

which increases the free energy. Therefore, surfactant molecules orientate themselves as previously stated, in an orientation that leads to a reduction in unfavourable interactions which is energetically favourable. As surfactants can form relatively strong intermolecular interactions with both phases, the interfacial tension is decreased.<sup>34</sup> The addition of more surfactant molecules further reduces the interfacial tension allowing for mixing between the two phases until the interface is saturated, at this point further increasing the concentration of surfactant has no effect on interfacial tension. Instead, surfactant molecules begin to aggregate and form micelles, this is shown in **Figure 3**.<sup>35</sup>

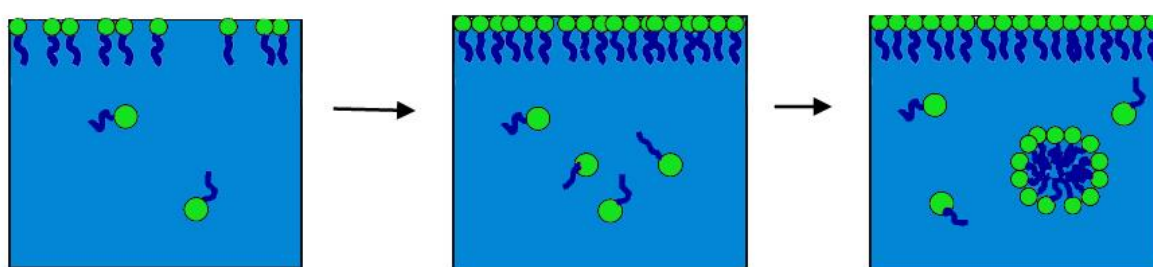


*Figure 3.* A diagram showing how increasing surfactant concentration leads to micelle formation.

This process is entropy driven, at low concentrations of surfactant, the entropy loss from the grouping of the monomers prevents the formation of micelles. However, when the concentration increases, the entropy gain from the release of water molecules that are in the solvation shells surrounding the hydrophobic tails, overcomes the negative entropy loss allowing for the formation of micelles.<sup>36</sup> The concentration of surfactant at which this occurs is the CMC. The CMC can be affected by the amount of secondary solvent present as well as temperature. In a series of experiments using conductance measurements to calculate CMC with differing temperatures, Baloch demonstrated that increasing temperature results in a decrease of the CMC.<sup>37</sup>

The mechanism by which monomers aggregate and disaggregate is a topic of debate within the scientific community. Starov reviews four theoretical models explaining how this occurs, concluding that only one model is viable. Starov suggests that small clusters of monomers of any size can aggregate with each other to form micelles, however, only single molecules can disconnect from a cluster or micelle.<sup>38</sup>



This is further supported by Cui, who determined via NMR that prior to the CMC, premicelles or clusters begin to form and increase in size, once the CMC is reached micelle formation occurs. However, premicelles continue to form after the CMC. This suggests that micelle formation is a gradual, multistep process.<sup>31</sup>

In addition to facilitating the mixing of immiscible liquids, surfactants are widely used in the pharmaceutical industry because of their ability to increase the solubility of insoluble drugs, such as glipizide and cyclosporine.<sup>39, 40, 41</sup> Micelles have an anisotropic water distribution, therefore they are said to contain a water free hydrophobic core with a graduated dispersion of water from the core outward, towards the bulk liquid of solution.<sup>39</sup> This means that the positioning of an API within a micelle will depend upon its polarity, with hydrophobic drugs favouring the core, and those with intermediate polarity being distributed intermediately among the micelle. Torchilin reviews the use of micelles as drug carriers, compared to alternatives such as soluble polymers and liposomes. It was found that micelles, as previously stated can solubilise poorly soluble drugs and increase their bioavailability, stay in the blood long enough to provide gradual systemic accumulation, and that their sizes allowed them to accumulate in areas with leaky vascularity.<sup>42</sup>

Ambrose defines micellar solubilisation as “the spontaneous dissolving of a substance by reversible interactions with the micelles of a surfactant in water, to form a thermodynamically stable isotropic solution with reduced thermodynamic activity of the solubilised material”.<sup>43</sup> This means that micellar solubilisation can be viewed, from a thermodynamic point of view, as the normal partitioning of an API between two phases; (micellar and aqueous) and that the standard free energy of solubilisation ( $\Delta G_s^0$ ) can be calculated using **Equation 10**.

$$\Delta G_s^0 = - R T \ln P$$

**Equation 10.** An equation for the standard free energy of solubilisation ( $\Delta G_s^0$ ), where R is the universal constant of gasses, T is the temperature and P is the partition coefficient between the micellar and the aqueous phase.

There are 2 main factors considered when evaluating the solubilising ability of a surfactant with a given API, these are the molar solubilisation capacity ( $\chi$ ) and the water partition coefficient (P).  $\chi$  is defined as the number of moles of the solute (API) that can be solubilised by one mole of micellar surfactant and characterises the ability of the surfactant to solubilise the drug, and can be calculated using **Equation 11**.<sup>39</sup>

$$\chi = \frac{(S_{\text{tot}} - S_{\text{w}})}{(C_{\text{surf}} - \text{CMC})}$$

**Equation 11.** An equation for calculating the molar solubilisation capacity ( $\chi$ ), where  $S_{\text{tot}}$  is the total drug solubility,  $S_{\text{w}}$  is the water drug solubility,  $C_{\text{surf}}$  is the molar concentration of surfactant in solution and CMC is the critical micelle concentration.

The other solubility descriptor, P can be described as the ratio of API concentration in the micelle to the drug concentration in water for a particular surfactant concentration. P can be mathematically calculated using **Equation 12**.<sup>39</sup>

$$P = \frac{(S_{\text{tot}} - S_{\text{w}})}{S_{\text{w}}}$$

**Equation 12.** An equation for calculating the micelle-water partition coefficient (P) where  $S_{\text{tot}}$  is the total drug solubility and  $S_{\text{w}}$  is the water drug solubility.

Combining **Equation 11** and **Equation 12** gives rise to **Equation 13**, allowing a combination of the two solubility descriptors.<sup>39</sup>

$$P = \frac{\chi(C_{\text{surf}} - \text{CMC})}{S_{\text{w}}}$$

**Equation 13.** An equation combining the two most common solubility descriptors ( $\chi$  and P) where  $S_{\text{w}}$  is the water drug solubility,  $C_{\text{surf}}$  is the molar concentration of surfactant in solution and CMC is the critical micelle concentration.

However, in **Equation 13**, P is related to the water solubility of the API in contrary to  $\chi$ . Therefore, in order to eliminate the dependence of P on the surfactant concentration, a molar micelle-water partition coefficient ( $P_{\text{M}}$ ), corresponding to the partition coefficient when  $C_{\text{surf}} = 1 \text{ M}$  can be defined as **Equation 14**.<sup>44</sup>

$$P_M = \frac{\chi(1 - CMC)}{S_W}$$

**Equation 14.** An equation for the molar micelle-water partition coefficient (PM), where  $\chi$  is the molar solubilisation capacity, CMC is the critical micelle concentration and SW is the water drug solubility.

**Equation 14** demonstrates that the lower the CMC of surfactant the greater the molar micelle-water partition coefficient. It has also been reported by Lu that surfactant with a lower CMC will produce more stable micelles because of the increased negative Gibbs free energy associated when compared with surfactants with a higher CMC, as shown by **Equation 9**.<sup>45</sup> Surfactants with a low CMC are also desirable from a pharmacological perspective, as if used intravenously, only surfactants with a low CMC will continue to exist *in vivo*, because of the dilution occurring from the large volume of blood in the body.<sup>46</sup> It has also been reported that generally, non-ionic surfactants have lower CMC values, making them preferable for pharmaceutical formulations.<sup>39</sup>

As previously stated, surfactants have a variety of uses in the pharmaceutical and chemical industry. In addition to these formulation applications they can also be used in conjunction with the analytical technique HPLC for characterising compounds.

### 1.3 High Performance Liquid Chromatography (HPLC)

The governing principle of chromatography is that molecules in a liquid (mobile phase) can interact with the surface of solids (stationary phase). If the liquid is being forced past the stationary phase either by gravity or pressure, molecules that interact with it, will move slower than those that do not, thus separation occurs. In normal phase chromatography, properties such as solubility in organic solvents, net charge and size govern to what extent the solutes will interact with the stationary phase, this interaction is adsorption. For normal phase chromatography, the mobile phase is non-polar and the stationary phase polar, this allows the mobile phase to remove polar molecules from the stationary phase. The degree of polarity of the mobile phase dictates how effective it is at separating and thus has an impact on retention time.<sup>47</sup> Reverse phase chromatography involves the use of a polar mobile phase

and a non-polar stationary phase. Generally, increasingly hydrophobic solvents remove non-polar molecules from the stationary phase with greater ease.

Increasing the amount of contact that the solute has with the stationary phase inevitably leads to a greater degree of separation, one way to do this is to increase the size of the column. However, this has its limits as anything over a metre becomes, not only expensive to run, but also difficult to use. A far more effective way to increase the contact is to reduce the particle size of the stationary phase into the range of 250  $\mu\text{m}$  to 5  $\mu\text{m}$ . Reducing particle size leads to an overall increase in the surface area allowing for a greater amount of contact between the molecule and the stationary phase. In addition to this, the amount of mobile phase needed also decreases leading to a reduced diffusion time because of the distance between stationary phase particles being smaller. However, it is worth considering that particle size cannot be reduced indefinitely and has to take into account the size of the molecule that is being analysed, as, obviously if the gaps between the stationary phase are smaller than the size of the analyte, it will stop moving through the column. Increasing the pressure can reduce retention time whilst retaining separation, essentially reducing the runtime whilst producing accurate results. However, as the space between particles decreases the back-pressure increases, therefore if the pressure is increased the stationary phase can collapse. Fortunately, certain stationary phases such as silica bonded with alkyl chains with a particle size of 5  $\mu\text{m}$  can withstand the higher pressure, a technique known as HPLC.<sup>47</sup>

HPLC apparatus has several features but nominally is composed of a few key components, a pump with a regulator to determine flow rate as well as pressure, an injector, where the sample is introduced to the system, a column where the separation occurs, and a detector. The detector is commonly a UV detector set to a specified wavelength allowing for the detection of a particular analyte. Data produced from HPLC is commonly displayed as a chromatogram, i.e. a plot of absorbance against time, resulting in a series of peaks. Each peak represents a different compound, and peak area corresponds to the amount of the compound present. A diagram showing how all of these components work together is shown in **Figure 4.**<sup>48</sup> Using retention time and void time, which is the time taken for the mobile phase to reach

the detector after being injected it is possible to calculate the capacity factor  $k'$ , which is used to compare retention times across different systems and can be calculated using **Equation 15**.<sup>49</sup>

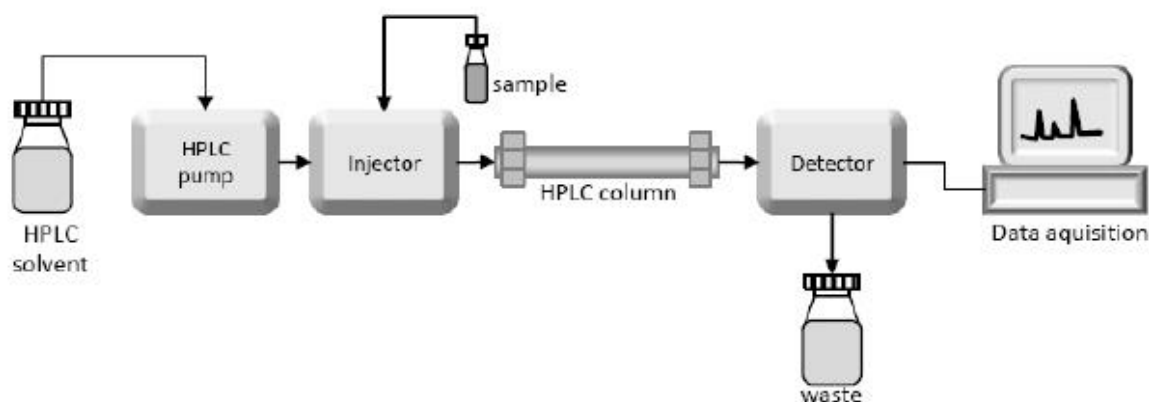


**Figure 4.** A flow chart showing how the components of a HPLC work together.<sup>37</sup>

$$k' = (t_r - t_m)/t_m$$

**Equation 15.** The equation for calculating capacity factor  $k'$ . Where  $t_r$  is the retention time in s and  $t_m$  is the void time in s.<sup>39</sup>

The capacity factor is also related to the equilibrium constant for the distribution of the compound between the mobile and the stationary phase, as shown in **Equation 16** and **Equation 17**.<sup>49</sup>

$$k' = \frac{[A]_{\text{stationary phase}} \times \text{Volume}_{\text{stationary phase}}}{[A]_{\text{mobile phase}} \times \text{Volume}_{\text{mobile phase}}}$$

**Equation 16.** An equation showing the relationship between  $k'$ ,  $[A]$  (the concentration of a compound that is distributed between the two phases) and Volume.<sup>39</sup>

$$k' = K_D \frac{\text{Volume}_{\text{stationary phase}}}{\text{Volume}_{\text{mobile phase}}}$$

**Equation 17.** An equation showing the relationship between  $K_D$  (Distribution Constant) and  $k'$  where A is the compound that is distributed between the two phases.<sup>39</sup>

As  $K_D$  increases so do the interactions between the solute and the stationary phase, thus  $k'$  also increases. The separation between two peaks, therefore, requires the solutes to have differing values of  $K_D$ , which also represents a difference in free energy as shown in **Equation 18**.<sup>49</sup>

$$\Delta G = -RT \ln K_D$$

*Equation 18.* An equation demonstrating the relationship between free energy and  $K_D$ .<sup>39</sup>

Whilst the ideal peak in a chromatogram is sharp and narrow, quite often this is not the case. The broadening of peaks is common and is because of how the solute navigates its way through the column. If an analyte is not released from the column in its entirety at the same time, broadening occurs. Peak broadening happens for several reasons including: eddy diffusion, mobile phase transfer, stagnant mobile phase mass transfer, stationary phase mass transfer and longitudinal transfer. Eddy diffusion occurs because of the presence of multiple flow paths through a column, whilst mobile phase transfer results in peak broadening because of the presence of different flow profiles within channels between particles of the column both of which are shown in **Figure 5**. Stagnant mobile phase mass transfer leads to a broadening of peaks because of differences in the rate of diffusion between the mobile phase outside the pores of the stationary phase and the mobile phase within the pores of the stationary phase. Stationary phase mass transfer can also produce broadening because of the movement of solute between the stagnant phase and the stationary phase. The final factor to consider is longitudinal diffusion, which leads to peak broadening because of the diffusion of the solute along the length of the column in the flowing mobile phase and is shown in **Figure 5**.<sup>50</sup>

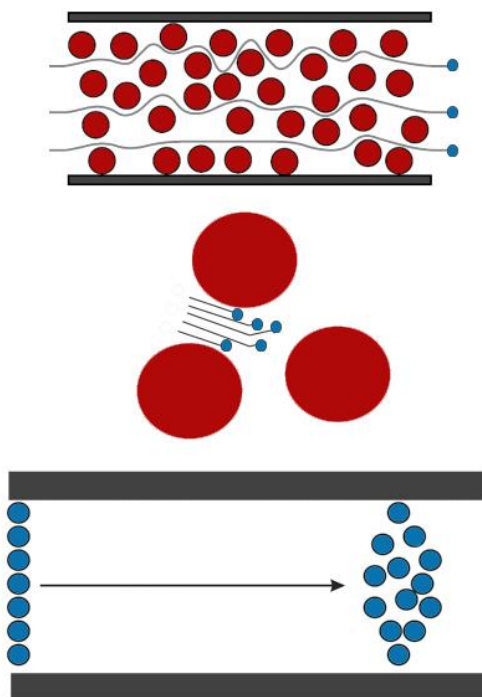


**Figure 5.** The different modes of diffusion. Top – eddy diffusion, middle – mobile phase mass transfer, bottom – longitudinal diffusion. Where red circles represent particles of the support in the column and blue circles represent solute.

HPLC can be used in conjunction with surfactants, by replacing the mobile phase with a surfactant solution. This technique is known as micellar liquid chromatography and has recently gained popularity as an analytical technique.

## 1.4 Micellar Liquid Chromatography (MLC)

### 1.4.1 An Overview of MLC

Micellar liquid chromatography (MLC) is a reversed-phase liquid chromatographic mode, where the mobile phase is an aqueous solution of surfactant.<sup>35</sup> It has gained popularity because it is environmentally friendly, with very small amounts of organic solvent being used, as well as its speed of analysis. As with all modes of reversed phase liquid chromatography, the stationary phase is non-polar, and the mobile phase is polar. The mobile phase is either purely surfactant at a concentration greater than its CMC, or a combination of an aqueous solution of surfactant at a concentration above its CMC and a polar organic solvent, commonly acetonitrile. Whilst the low toxicity, and therefore the low environmental impact of surfactants, would make the exclusion of an organic solvent from the

mobile phase attractive, it is sometimes required to achieve a practical time scale for each experiment. It has been reported that adding an organic modifier to the mobile phase can produce a variety of effects such as, changing the polarity of the mobile phase and changing the aggregate number and CMC values for the surfactant. Ultimately, the solute equilibrium is shifted away from the micellar-pseudo phase and the modified stationary phase and towards the bulk solvent. In this situation the elution power of the mobile phase increases, reducing retention times.<sup>51</sup>

Normally, in LC there is only one equilibrium to consider, that which exists between the solute partitioning between the mobile phase and the stationary phase. However, in MLC there is a secondary equilibrium to consider which is that of the solute partitioning between the bulk solvent and micelles and is shown in **Figure 6**.<sup>35</sup> The addition of a surfactant has several implications, the most noticeable being on the stationary phase. The surfactant is adsorbed onto the surface of the stationary phase, modifying it and creating a structure similar to that of an opened micelle. This has a large impact on the retention time because of the change of properties such as surface area, pore volume and polarity. The change in polarity is caused by the reduction of silanophilic interactions caused by the adsorption of surfactant monomers onto the stationary phase, causing the hydrophobicity to increase. It is also important to note that the concentration of surfactant on the stationary phase does not increase with increasing concentration of surfactant in the mobile phase and can be said to be independent of it.<sup>51</sup> One of the most widely used columns for MLC is the alkyl-bonded C18 stationary phase, normally chosen because of the large modification that occurs when used in conjunction with SDS, Brij35 or CTAB, the tail groups have hydrophobic interactions with the C18 chains, which results in the head groups of each surfactant facing away from the column surface. This causes the charged head groups to form a pseudo column surface or “modified surface”. However, it is important to note that other columns such as C8 or cyanopropyl columns are also used.<sup>52</sup>

Micelles provide alternative sites of interaction to the modified stationary phase, these being the hydrophobic core, the hydrophilic surface and the palisade layer that exists between the surface and the core. Solutes that partition in micelles experience a microenvironment that is different to that of the



bulk solvent, which can lead to a change in properties such as solubility, pH and physiochemical properties.<sup>53</sup>

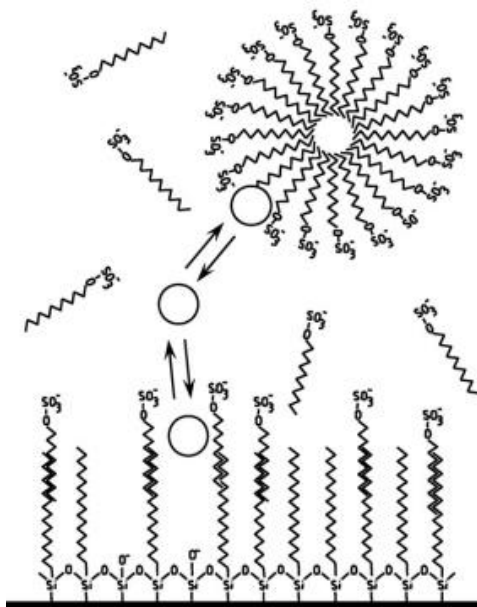


**Figure 6.** A diagram of the two equilibria that occur during MLC with soluble APIs because of the solute partitioning between the mobile phase, micellar phase, and the modified stationary phase. This example uses SDS and an octadecyl-bonded column.<sup>48</sup>

Retention times produced by MLC can be explained by considering it to be a system of three phases, the modified stationary, bulk solvent, and micellar-pseudo phase. When MLC is used for poorly water-soluble active pharmaceutical ingredients (APIs), direct transfer between micelles and modified stationary phase can also occur as shown in **Figure 7**. Following this, the partitioning equilibria can then be described by three partition coefficients;  $P_{MS}$ ,  $P_{WM}$  and  $P_{WS}$  where S is the modified stationary phase, M is the micellar-pseudo phase and W is bulk solvent. If  $P_{WS}$  increases, the retention time will as well, however, if  $P_{WM}$  increases then the retention time will decrease.

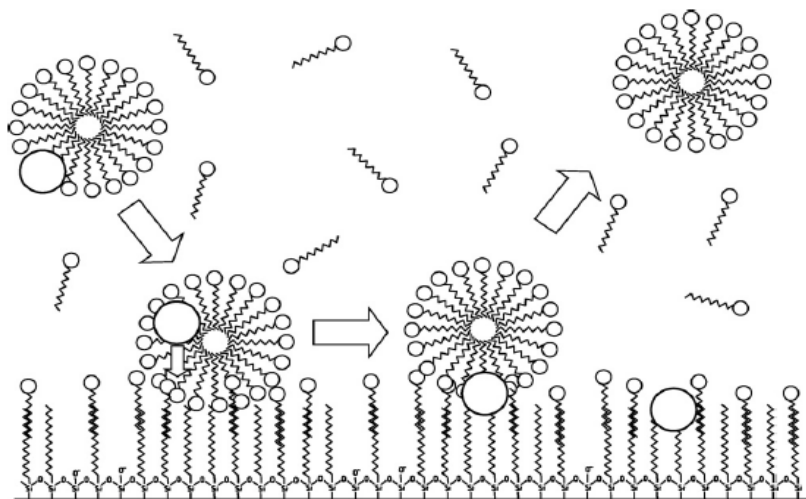


**Figure 7.** A diagram showing direct transfer of a hydrophilic API between micelles and the modified stationary phase.<sup>48</sup>

Armstrong and Nome proposed a mathematical model to describe retention time in a pure micellar phase, their model is based upon the three environments; bulk solvent, micellar-pseudo phase and the modified stationary phase, within the micellar chromatographic system (**Equation 19**).<sup>35</sup>

$$\frac{V_e - V_0}{V_s} = \frac{k'}{\Phi} = \frac{P_{WS}}{1 + v(P_{WM} - 1)[M]}$$

**Equation 19.** Armstrong and Nome's equation for describing the retention time in pure micellar mobile phases. Where  $V_e$  represent the total volume of mobile phase needed to elute a given solute from the column.  $V_s$  is the volume of the API surface on the stationary phase,  $V_0$  is the column void volume,  $\Phi$  is the phase ratio,  $v$  is the partial specific volume of monomers of surfactant in the micelle.<sup>41</sup>

Arunyanart and Cline-Love proposed an alternative model which built upon Armstrong and Nome's (**Equation 20**).<sup>35</sup>

$$\frac{1}{k'} = \frac{1}{K_{AS}} + \frac{K_{AM}}{K_{AS}} [M] = c_0 + c_1 [M]$$

**Equation 20.** Arunyanart and Cline-Love's equation for describing retention time in pure micellar phases.  $K_{AS}$  is the binding constant between the solute in bulk aqueous solvent and stationary sites and  $K_{AM}$  is the binding constant between the solute in the aqueous phase and the monomers of surfactant in the micelle.<sup>41</sup>

The nature of the interactions between the solute and micelles can have a large impact on retention times. For a neutral solute and a non-ionic or ionic surfactant the only interactions to consider are dipole-dipole, van der Waals and proton-donor/acceptor interactions. The same can be said for a charged solute

with a non-ionic surfactant.<sup>54</sup> Charged solutes will have electrostatic interactions with ionic surfactants, ionic solutes will also interact with ionic surfactants, however, only two types of interaction are possible, either attraction or repulsion. It is also important to note that steric hindrance is an important factor to take into account when considering how the solute and surfactant will interact.

Generally, retention time decreases with increasing micellar concentration. When this occurs, it can be said that the solute interacts in a binding manner with the micelles, thus, less interaction with the modified stationary phase occurs and therefore a reduction in retention time. However, it is also possible for retention time to increase. This occurs when both the solute and surfactant are ionic as repulsion is one of the possible interactions of this pairing. When this occurs, the interactions with the micelles are unfavourable, and as a result, interactions with the stationary phase increase, leading to an increase in retention time.

The amount of interaction a micelle has with a drug, whether this is binding or anti-binding can be summarised to some extent by a solubility ratio. Solubility ratios have been used to predict the solubility of a drug in the presence of a surfactant to varying degrees of success, as shown by Mithani<sup>55</sup>. A solubility ratio, SR, is the ratio between the solubilisation capacity of one phase and the solubilisation capacity of water for a given drug. A plot of Log (SR) against Log (P) indicated that a linear relationship existed between the two as shown in **Equation 21**.<sup>55</sup>

$$\text{Log (SR)} = 2.23 + 0.61 \text{ Log P } (r^2 = 0.99)$$

*Equation 21.* An equation showing the linear relationship between SR and the octanol-water partition coefficient.<sup>45</sup>

From the relationship displayed in **Equation 21**, it was then possible for Mithani to determine the solubility of a drug with an increase in SR, using **Equation 22**.<sup>55</sup> The alternative phase for Mithani's paper was sodium taurocholate, a naturally occurring bile salt found in the small intestine. The bile salt

acts as a surfactant and increases the uptake of nutrients by reducing the interfacial tension, leading to a greater surface area and therefore, a greater dissolution rate.<sup>55</sup>

$$C_{sx} = C_{so} + (SC_{bs})(Mr)([NATC])$$

**Equation 22.** An equation enabling the prediction of solubility. Where  $C_{sx}$  = the solubility of the drug in the presence of taurocholate,  $C_{so}$  = the solubility of the drug in the absence of taurocholate, and  $SC_{bs}$  is the solubilisation capacity of the bile salt (taurocholate) for the drug,  $Mr$  is the molecular weight of the drug.<sup>45</sup>

Mithani found that the model accurately predicted the solubility of griseofulvin and cyclosporine A. However, it overpredicted the solubility of phenytoin and diazepam by a factor of 1.33 and 1.62 respectively, confirming that it cannot correctly predict solubility for all APIs.

#### 1.4.2 Recent uses of MLC

MLC has previously been used to predict drug penetration of the blood-brain barrier as reported by Lu in 2009. Lu used the linear solvation energy relationship (LSER) to characterise biopartitioning micellar liquid chromatography using a monolithic column. Principal component analysis of the LSER coefficients confirmed that the system had similarities to bio-membrane transport processes, such as blood-brain barrier penetration and its ability to predict blood-brain barrier penetration.<sup>56</sup>

In 2010 Waters demonstrated that MLC could be used for the calculation of  $\text{Log } P_{WM}$ , the micellar-water partition coefficient, using **Equation 23**. Waters demonstrated that experimentally calculating  $k'$  over a range of surfactant concentrations allows for a plot of  $\frac{1}{k'}$  against  $C_M$ , which would yield a value for  $P_{WM}$  as  $P_{MW} = \text{slope/intercept}$ .<sup>57</sup>

$$\frac{1}{k'} = \left( \frac{((P_{WM} + 1)V \cdot C_M)}{P_{WS}\Phi} \right) + \left( \frac{1}{P_{WS}\Phi} \right)$$

**Equation 23** An equation for calculating the water-micelle partition coefficient. Where  $k'$  is the capacity factor,  $C_M$  is the micelle concentration (total surfactant concentration – CMC)  $P_{WS}$  is the solute partition coefficient between water and the stationary phase and  $\Phi$  is the chromatographic phase ratio.<sup>47</sup>

De Vrieze published an article in 2013 comparing MLC to immobilised artificial membrane (IAM) liquid chromatography for the purpose of predicting blood-brain barrier penetration. For the comparison, De Vrieze used 3 different surfactants, Brij35, SDC and SDS in the MLC system. Values predicted by the SDS system provided a superior correlation between predicted and experimental results, more so than that produced by the IAM LC system ( $R=0.7993$  to  $R=0.7724$ ). This was in part because of the complexity of the MLC system, i.e the existence of a second equilibrium, providing a more accurate model.<sup>58</sup>

In 2013 Waters published an article demonstrating how MLC improves upon traditional methods for predicting skin permeability. Waters demonstrated that replacing  $\text{Log } P_{\text{OW}}$  (the octanol-water partition coefficient) with the experimentally determined value  $\text{Log } P_{\text{MW}}$  (water-micelle partition coefficient) enables the realisation of a quantitative partition-permeability relationship that can withstand variation, therefore enhancing the prediction of skin permeability.<sup>59</sup>

MLC has also been used to quantify and detect melamine in swine kidneys as published by Beltrán-Martinavarró in 2014. Melamine is a cheap chemical commonly used to manufacture resins, however, it is also an illegal and toxic feed additive that boosts protein content, which can reach humans through the food chain. Its ingestion has been related to renal diseases as well as bladder cancer which in some cases can be terminal. Previous methods for its detection such as LC-MS and indirect competitive enzyme-linked immunosorbent assay (ELISA) tandem GC-MS require large amounts of toxic solvents as well as large amounts of time. The method proposed by Beltrán-Martinavarró used substantially less organic solvents, as is the nature of MLC, as well as being much quicker.<sup>60</sup>

In 2015 Ferrer proposed a method for the analysis of three catecholamines in urine. Previous methods for detecting and quantifying catecholamines involved long extraction steps and the use of an internal standard. The new method does not involve those steps as the sample can simply be diluted in a micellar solution, filtered and then directly injected. This reduces the turn-around time for analysis, as well as making it more environmentally friendly because of the reduction in organic solvents required.

In 2016 Waters published an article stating how MLC could be used to predict human intestinal absorption in the presence of bile salts. A large volume of oral drugs are absorbed in the gastrointestinal tract, therefore a method with which to predict how much of a drug will be absorbed was needed. At the time of publication, this was completed using *in vivo* methods involving animal models. However, because of factors such as ethical considerations, interspecies variability and financial cost, an alternative way in which to predict the intestinal absorption was desired. Waters proposed a quantitative partition-absorption relationship using MLC in conjunction with bile salts.<sup>61</sup>

Pitarch-Andrés published an article in 2016 outlining the use of MLC as a replacement for hydroorganic gas and reversed-phase liquid chromatography for the detection of herbicides, nominally DIU, TBA and TBT. At the time of publication, the current methods involved lengthy sample extractions such as cartridge solid-phase extraction, solid-phase microextraction and liquid/liquid extraction to name a few. Pitarch-Andrés states that MLC does not use an extraction method because of the ability of the micelles to easily solubilise hydrophobic compounds, removing the risk of column clogging. Instead, after a simple filtration, samples can be directly injected, thus greatly reducing the turnaround time, as well as reducing the amount of organic solvents used. Pitarch-Andrés concludes that MLC is a viable, efficient and a more environmentally friendly alternative to the industry standard.

MLC has also been used as a method for purifying terephthalic acid (TPA) as reported by Richardson in 2017. TPA is polymerised to give polyethylene terephthalate, the primary polymer which is used to make plastic bottles for beverages. The production of TPA results in 8 impurities which need to be removed prior to polymerisation. The current method used reversed-phase gradient HPLC and can take over an hour, whereas the method proposed by Richardson reduced this to 20 minutes and also has the benefit of being environmentally friendly because of the significantly lower volume of solvent required.<sup>62</sup>

In 2018 Shokry derived a mathematical model with an  $R^{2 \text{ PRED}}$  of 81 % for the prediction of human intestinal absorption (HIA). This was completed using water-micelle partition coefficients derived from MLC, using a unique mobile phase consisting of a mixed micellar mixture of lecithin and 6 bile salts, which is a composition similar to that found in the human intestine environment. This is considered to be the first method to use a physiological mixture of biosurfactants in the prediction of HIA.<sup>63</sup>

In addition to this, in 2019 Shokry also published a paper on her findings on the use of an aminopropyl column for the prediction of HIA using MLC. In the 2018 paper a cyanopropyl column was used as well as a mixture of bile salts in the mobile phase. For this paper the mobile phase only consisted of sodium deoxycholate. A mathematical model was also derived with a  $R^{2 \text{ PRED}}$  of 72 %.<sup>64</sup>

Al-karim *et al.* in 2019 published results on MLC with a C18 column using Tween 20 as the mobile phase, for monitoring contaminants during the various stages of terephthalic acid production. They remarked that the modified stationary phase, produced by the saturation of the C18 column with Tween 20 showed an excellent capability to separate structural isomers in a reasonable time, markedly better than the bare C18 stationary phase.<sup>65</sup>

Ramezani *et al.* designed a sustainable method for the monitoring of melamine composition in milk samples and published their findings in 2019. They experimented with using different percentage compositions of SDS and a natural deep eutectic solvent (NADES) as the mobile phase. The optimised mobile phase consisted of 4 % SDS, 4 % NADES and 4 % glacial acetic acid and was reported to elute melamine within 10 minutes without interference from coexisting proteins and endogenous species in milk.<sup>66</sup>

In 2020 Duan reviewed the use of MLC for the rapid analysis of eight sulphonamides in milk. It was reported that MLC offers the advantage of being able to inject the samples straight onto the column, due to the micelles being able to dissolve the proteins in the milk, thus eliminating the need for a complex gradient elution. As reported by others, the authors found that the MLC method offered a

preferable alternative method for rapid analysis because of the low-cost and environmentally friendly nature of the method.<sup>67</sup>

Another paper on the use of MLC for the analysis of compounds in dairy products was published by Pawar in 2020. Pawar et al. analysed dairy products, such as milk, butter and cheese for residues of mebendazole, which is an anthelmintic drug used in cattle production. It was found that an MLC method using SDS and a C18 column were able to resolve the analyte from matrix compounds in less than 8 minutes, and reported the method being reliable, sensitive, easy-to-handle, eco-friendly, safe and inexpensive.<sup>68</sup>

In summary, there have been several varied applications for MLC, this diversity is owed largely to the complex nature of a system generated by a secondary equilibrium. The usage of MLC has increased recently with it gaining a wider audience within the chemical community, enabling it to become a method of choice for a range of analytical methods and models.

When MLC appears in literature the surfactants that are used the majority of the time are either Tween 20, SDS, Brij 35 or CTAB. This is because other surfactants tend not to be characterised, with data such as aggregate number and CMC not available. Thus, providing a need for characteristic data on other surfactants to expand the number of viable surfactants for MLC. One of the techniques that can be used to determine physiochemical properties such as CMC is isothermal titration calorimetry.

## **1.5 Isothermal Titration Calorimetry (ITC)**

### **1.5.1 An Overview of ITC**

Isothermal titration calorimetry (ITC) is an analytical technique that is used to measure the heat absorbed or released during changes to the composition of a system undergoing a titration. The changes in temperature are incredibly small and thus ITC is a very sensitive technique.<sup>69</sup> The system consists of a microcalorimeter which is kept at constant pressure, inside of which are two cells, one acts as the reference cell, the other contains a solvent. Above the sample cell is a syringe that injects precise



aliquots (5 – 15  $\mu\text{L}$ ) of a sample, a diagram showing this can be seen in **Figure 8**. The microcalorimeter contains heat sensors which detect changes in temperature and plots this against time, the sensors also feed information to heaters which compensate so that the cells are corrected to the same, constant temperature. A variety of data can be obtained from one experiment such as  $\Delta G$ ,  $\Delta H$  and from these terms  $\Delta S$ , making ITC an efficient analytical tool.

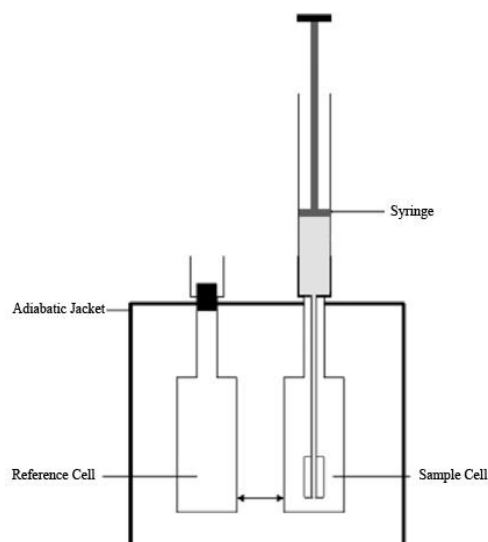


**Figure 8.** A schematic diagram of an ITC

### 1.5.2 Using ITC to Determine CMC

Determining the CMC of a surfactant consists of titrating a concentrated surfactant solution stepwise into the reaction cell via a number of injections necessary to be able to observe the CMC, the first injection is half the volume of the rest of the injections. The reaction cell is filled with either water or a buffer solution. This then produces a graph of  $\mu\text{cal}/\text{second}$  against time an example of which is shown in **Figure 9** and shows the process of demicellisation initially when the peak size is decreasing, and micellisation later, when the peak height remains constant. The red line is the programme generated baseline.

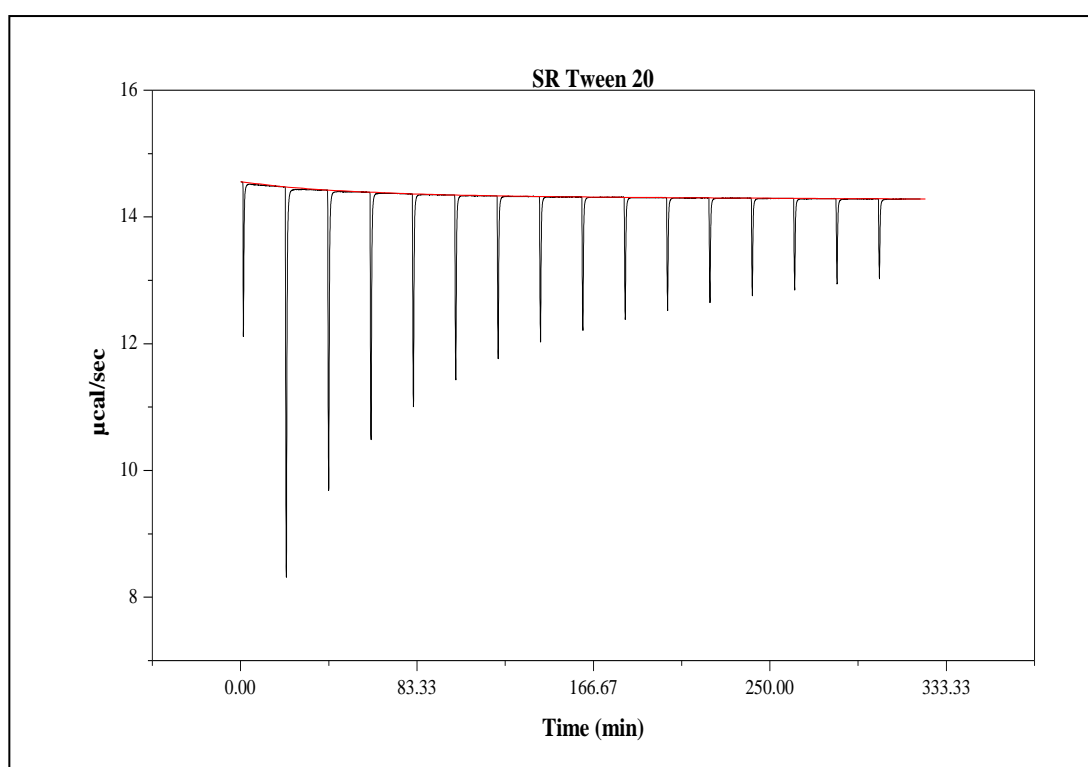


**Figure 9.** A plot of  $\mu\text{cal}/\text{second}$  against Time (mins) for SR Tween 20.

The integration of the resulting peaks and subsequent conversion of units to  $\text{kJoules}/\text{mol}$  gives  $\Delta H_{\text{obs}}$  values for each injection allowing for a graph of  $\Delta H$  against surfactant concentration to be plotted as shown in **Figure 10**.

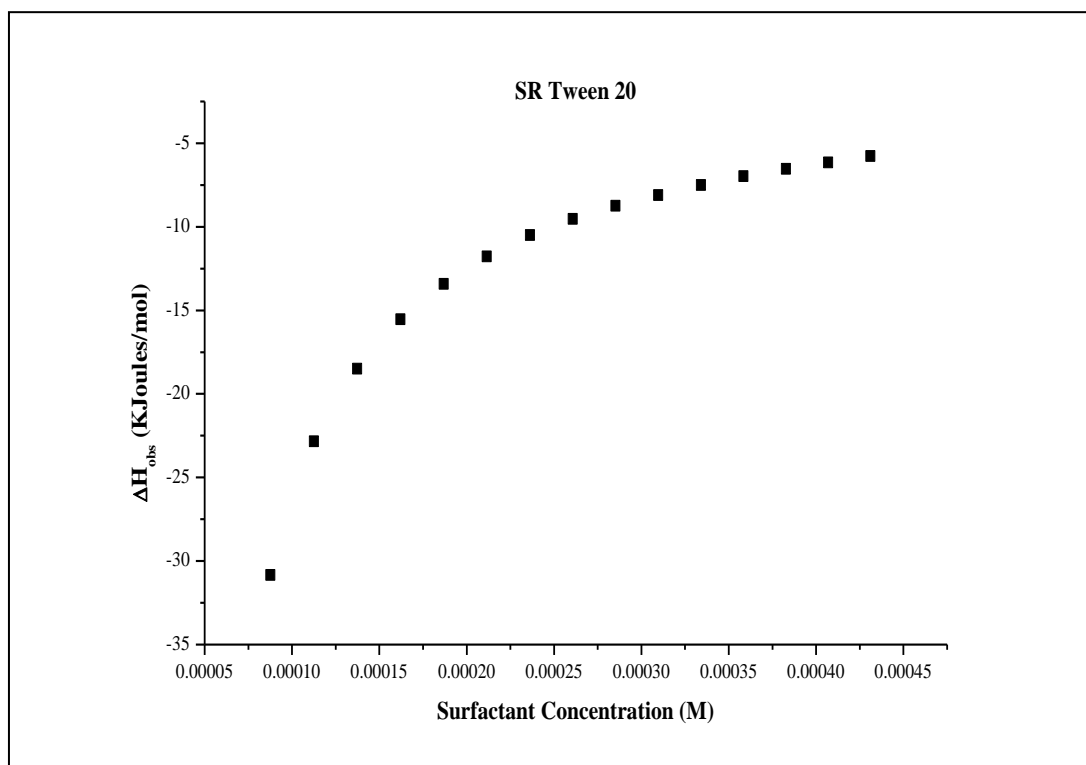


**Figure 10.** A plot of  $\Delta H$  (kJoules/mol) against Surfactant Concentration (M) for SR Tween 20.

A plot of  $\Delta H_{obs}$  against surfactant concentration allows for the calculation of CMC, as it is taken as the inflection point calculated using the derivative method.<sup>70</sup> An example of this is shown in **Figure 11** with the more obvious peak being considered the inflection point and the first minor peak the result of a compound error introduced by using the second derivative.

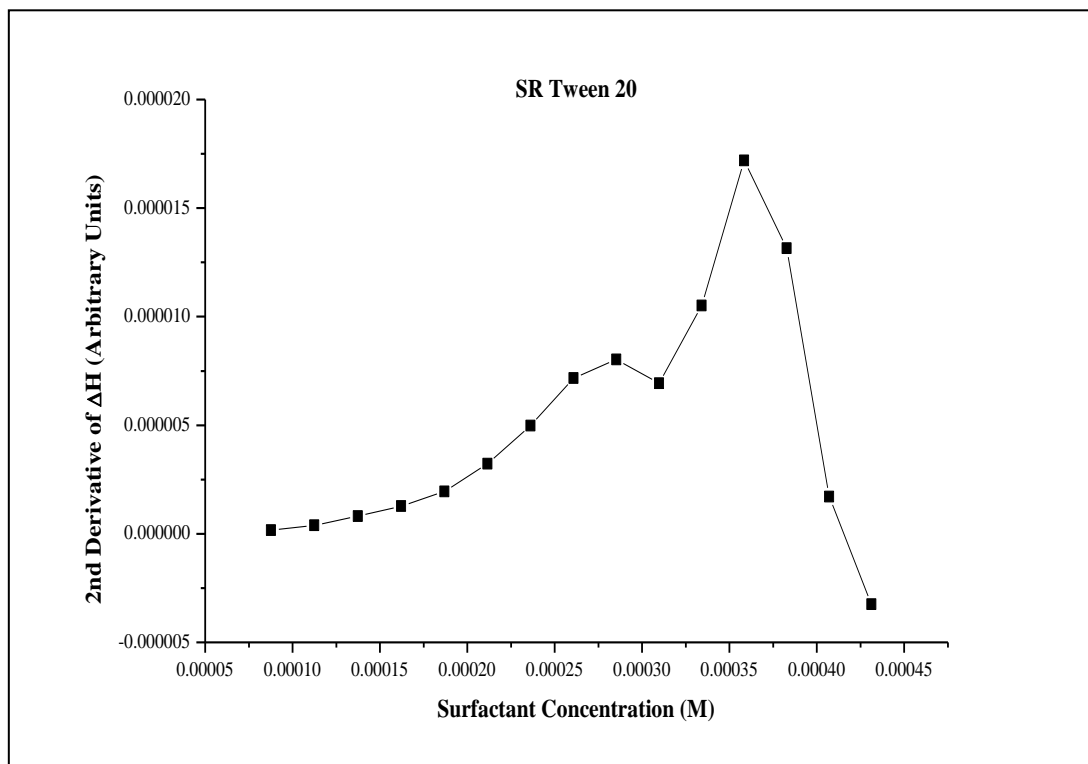


*Figure 11.* A plot of the 2<sup>nd</sup> Derivative of ΔH (Arbitrary Units) against Surfactant Concentration (M).

The CMC of surfactants is a widely debated subject with several studies reporting different values, as well as using different techniques for the derivation of the CMC. A few examples of this are shown in **Table 1**.

**Table 1.** The reported CMCs of Tween 20, Tween 80, Brij 35 and SDS using various techniques and at several temperatures.

<b>Surfactant</b>	<b>CMC Calculated (mM)</b>	<b>Method</b>	<b>Temperature</b>	<b>Reference</b>
Tween 20	0.011	Surface tension	22	71
Tween 20	0.042	Dye (eosin Y)	22	71
Tween 80	0.018	Surface Tension	22	71
Tween 80	0.028	Dye (eosin Y)	22	71
Brij 35	0.030	Surface Tension	22	71
Brij 35	0.068	Dye (eosin Y)	22	71
Tween 20	0.049	Surface Tension	28	72
Tween 20	0.049	Surface Tension	25	73
Tween 80	0.011	Surface Tension	25	73
Tween 20	0.115	Dye (pyrene)	20	74
Tween 20	0.129	Dye (pyrene)	25	74
Tween 20	0.144	Dye (pyrene)	30	74
Tween 20	0.160	Dye (pyrene)	35	74
Tween 20	0.178	Dye (pyrene)	40	74
Tween 20	0.200	Dye (pyrene)	45	74
Tween 80	0.093	Dye (pyrene)	20	74
Tween 80	0.110	Dye (pyrene)	25	74
Tween 80	0.110	Dye (pyrene)	30	74
Tween 80	0.120	Dye (pyrene)	35	74
Tween 80	0.130	Dye (pyrene)	40	74
Tween 80	0.130	Dye (pyrene)	45	74
Tween 20	0.002	Surface Tension	25	75
Tween 20	0.020	Surface Tension	5	76
Tween 20	0.017	Surface Tension	20	76
Tween 20	0.011	Surface Tension	30	76
Tween 80	0.017	Cyclic Voltammetry	25	77
Tween 20	0.975	Surface Tension	20	78
Tween 20	0.942	Surface Tension	30	78
Tween 20	0.918	Surface Tension	40	78
Tween 80	0.574	Surface Tension	20	78
Tween 80	0.441	Surface Tension	30	78
Tween 80	0.439	Surface Tension	40	78
SDS	8.000	Cyclic Voltammetry	25	77
SDS	6.500	Dye (pyrene)	25	79
SDS	5.600	Surface Tension	25	80
SDS	4.800	Electrophoresis (naphthalene)	25	80
SDS	5.000	Fluorescence (Coumarin)	25	80
SDS	5.500	Fluorescence (Rhodamine)	25	80

The sensitivity and therefore potential precision offered by ITC is superior to the above methods, theoretically allowing for a more accurate derivation of the CMC.<sup>70, 81</sup> ITC has been found to have an uncertainty of less than 1 % when used for obtaining the enthalpy of micellization.<sup>82</sup> This is contrary to surface tension which has been reported to have an uncertainty value as high as 13 % with Triton X,

methods utilising fluorescent measurements used in conjunction with dyes have been reported to exceed 13 %.<sup>83</sup>

ITC has previously been used to characterise a variety of surfactants and their respective properties of micellisation such as change in Gibbs free energy, entropy, the heat capacity of micellisation and the CMC. Boucehmal has previously used ITC to analyse the effect of adding propanediol-1,2 on pluronic F127 micellisation. He found that the CMC was lowered by the addition of propanediol-1,2 with a 3.7 % w/v addition lowering the CMC by 0.011 mM.<sup>81</sup> The effect of caffeine, diprophylline, acetaminophen and theophylline on the CMC of SDS was derived using ITC by Waters in 2012. No appreciable alteration to the CMC of SDS was detected.<sup>84</sup> The CMC of sodium deoxycholate and how it changes with the addition of 5 APIs was measured by Waters in 2014, the CMC of SDS without an API was determined to be 2.1 mM. NaDC's CMC was shown to be affected by the addition of APIs with the biggest change occurring with paracetamol.<sup>85</sup> The CMC of a several different mixtures of varying concentrations of gemini surfactants alkanediyl- $\alpha,\omega$ -bis-(dodecyldimalkanediyl- $\alpha,\omega$ -bis-(dodecyldimethylammoniumbromide) ( $C_{12}C_sC_{12}Br_2$ ,  $s = 2, 6, 10$ ) ethylammonium bromide) with SDS was determined by Wang in 2019.<sup>86</sup>

## 1.6. Aims and Objectives

The need to better understand the effect of surfactants on APIs is apparent, as this is key interaction with regards to increasing the solubilities of API's, which can lead to more efficient formulations. MLC in combination with ITC and solubility measurements will increase the understanding of surfactant API interactions, as well as provide characterisation of surfactant properties such as CMC for: Tween 20, Tween 20 HP, SR Tween 20, Tween 80, Tween 80 HP, SR Tween 80, Etocas 35, Croduret 40, Crodasol HS HP, SDS and Brij 35.

The objectives of this project were:

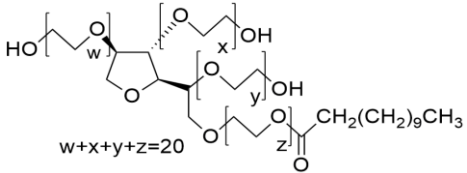
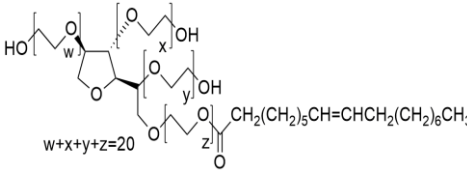
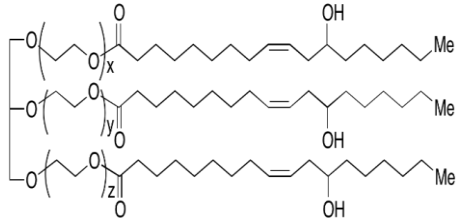
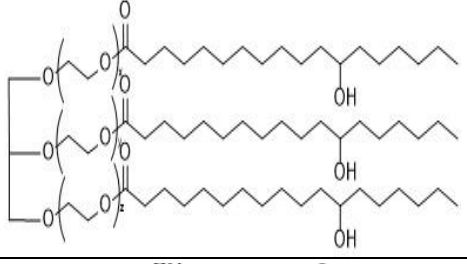
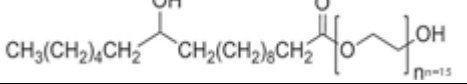
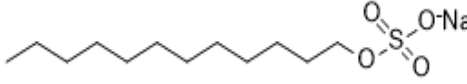
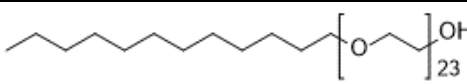
- Investigate how surfactant concentration affects retention time in MLC with Tween 20, Tween 20 HP, SR Tween 20, Tween 80, Tween 80 HP, SR Tween 80, Etocas 35, Croduret 40, Crodasol HS HP, SDS and Brij 35.
- Investigate how surfactant purity affects retention time in MLC with Tween 20, HP Tween 20, SR Tween 20, Tween 80, HP Tween 80 and SR Tween 80.
- Investigate how the solubility of API's is affected by the presence of Tween 20, Tween 20 HP, SR Tween 20, Tween 80, Tween 80 HP, SR Tween 80, Etocas 35, Croduret 40, Crodasol HS HP, SDS and Brij 35 across a concentration range.
- Investigate how the solubility enhancement of API's in the presence of surfactant is affected by surfactant purity with Tween 20, Tween 20 HP, SR Tween 20, Tween 80, Tween 80 HP and SR Tween 80.
- Experimentally derive the CMC using ITC for Tween 20, HP Tween 20, SR Tween 20, Tween 80, HP Tween 80, SR Tween 80, Etocas 35, Croduret 40 and Crodasol HS HP.

## 2. Experimental

### 2.1 Materials

The materials used in the study are summarised in **Table 2** (surfactants) and **Table 3** (APIs).

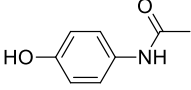
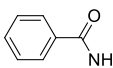
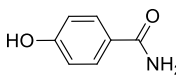
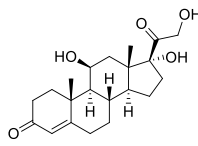
**Table 2.** The structure and properties of the surfactants used. All of the properties were obtained from PubChem<sup>87</sup>, properties currently unknown = (-)

Name	Mr (g mol <sup>-1</sup> )	Supplier	Batch Number	Structure
Polysorbate 20 (Tween 20)	1228	Croda Europe Ltd	SD05535	
Polysorbate 80 (Tween 80)	1310	Croda Europe Ltd	SD02355	
Polyoxyl 35 Castor Oil (Etocas 35)	2476	Croda Europe Ltd	SD03673	
Polyoxyl 40 Hydrogenated Castor Oil (Croduret 40)	2703	Croda Europe Ltd	SD04753	
Macrogol 15 Hydroxystearate (Crodasol HS HP)	947	Croda Europe Ltd	SD04721	
Sodium dodecyl sulfate (SDS)	288	Sigma Aldrich	07328812	
Polyoxyethylene (23) lauryl ether (Brij 35)	1200	Sigma Aldrich	23848123	

There are 3 purity grades of Tween 80 and Tween 20 that were used in this project, super refined (SR), high purity (HP) and standard grade.



**Table 3.** The Aq solubility, Mr, Log P, pKa and lambda max of the APIs used in the project. The values for Mr, Log P and pKa are from PubChem<sup>87</sup> and the lambda max and Aq solubility values were experimentally derived.

API	Solubility (mg/mL)	Mr (g mol <sup>-1</sup> )	Log P	pKa	$\lambda_{\text{max}}$ (nm)	Supplier	Batch Number	Structure
Acetaminophen	15.10	121.139	0.46	9.4	243	Sigma Aldrich	21391214	
Benzamide	14.30	151.165	0.64	13.0	227	Sigma Aldrich	20471836	
4-hydroxybenzamide	9.30	137.138	0.33	8.6	252	Sigma Aldrich	28561529	
Hydrocortisone	0.28	362.500	1.61	13.8	242	Sigma Aldrich	40192847	

The above API's were chosen for this project for a variety of reasons. Acetaminophen, benzamide and 4-hydroxybenzamide have a similar molecular structure but have different values for characteristics such as pKa and Log P, allowing for the study of how each characteristic impact retention time. Hydrocortisone was chosen as it had a higher Log P value and wasn't readily water soluble, other API's with Log P values greater than 2 were trialed but didn't produce any usable data.

## 2.2 MLC Methodology

The following methodology is for MLC with a series of API's. MLC with acetaminophen, benzamide and 4-hydroxybenzamide was completed using a C18 column (Spherisorb ODSB cartridge, 80Å, 5µm, 4.6 mm x 150 mm) with a flow rate of 1.35 mL/min at 31°C. For MLC with hydrocortisone, a C1 column was used (Spherisorb 3.0 µm C1, 4.6 mm x 50 mm) also at 31 °C with a flow rate of 3.00 mL/min. This column was selected instead of a C18 column in order to optimise the retention time separations acquired, owing to the low aqueous solubility of the compound. A stock solution of each surfactant (0.02 M 800 mL) was prepared using ultra-pure water from a Thermo Scientific Barnstead Nanopure unit. The stock solution was diluted with ultra-pure water to produce 400 mL solutions of

concentration  $1 \times 10^{-2}$ ,  $1 \times 10^{-3}$ ,  $1 \times 10^{-4}$ ,  $1 \times 10^{-5}$ ,  $1 \times 10^{-6}$ ,  $1 \times 10^{-7}$ ,  $1 \times 10^{-8}$  M. The solutions were placed into a sonic water bath (VWR Ultrasonic Cleaner USC – T) for 10 minutes. A solution of API (0.002 M) and each surfactant concentration was prepared in a 10 mL volumetric flask. The resulting solution was then placed into a sonic water bath for 10 minutes. The solution of surfactant was then loaded onto the column which was kept at 31 °C by a column oven (this temperature was chosen as it exceeded the temperature variation within the lab allowing for a consistent temperature for reactions year-round.) (Jones Chromatography model 7950 column chiller) for 20 minutes (using an Agilent Binary Pump G1312A) and the UV spectrophotometer (PerSeptive Biosystems UVIS – 205 Absorbance Detector) was set to the lambda max for each API, using the values from **Table 3**. The API/surfactant solution was then injected using a 10 µL syringe. After a peak was observed a cleaning solution consisting of 75 % acetonitrile and 25 % ultra-pure water was used as the mobile phase for 15 minutes, following this 100 % ultra-pure water was then used for a further 5 minutes.

## **2.3 UV Methodology**

### **2.3.1 UV Absorption of Surfactants**

Solutions of Tween 20, Tween 20 HP, Tween 20 SR, Tween 80, Tween 80 HP, Tween 80 SR, Etocas 35, Croduret 40, Crodasol HS HP, SDS and Brij 35 at concentrations  $1 \times 10^{-2}$ ,  $1 \times 10^{-3}$ ,  $1 \times 10^{-4}$ ,  $1 \times 10^{-5}$ ,  $1 \times 10^{-6}$ ,  $1 \times 10^{-7}$  and  $1 \times 10^{-8}$  M were prepared. The solutions were analysed using a WinCary UV machine and the UV detector was zeroed using ultra-pure water. A full scan of each surfactant, at each concentration from 200 – 800 nm was completed at 25 °C.

### **2.3.2 Measuring the effect of Surfactants on the Lambda max of APIs**

Solutions of Tween 20, Tween 80, Etocas 35, Croduret 40, Crodasol HS HP, SDS and Brij 35 at  $1 \times 10^{-4}$  M were prepared. 0.1 mg/mL solutions of acetaminophen, benzamide and 4-hydroxybenzamide were prepared via serial dilution using the solutions of surfactants previously prepared. The solutions were analysed using a WinCary UV machine the UV detector was zeroed using each surfactant solution. A full scan of each API/surfactant combination from 200 – 400 nm was completed at 25 °C.

## 2.4 CMC determination using ITC Methodology

Solutions of each purity of Tween 20 and Tween 80, in addition to solutions of Etocas 35, Croduret 40 and Crodasol HS HP were prepared by diluting concentrated surfactant in ultra-pure water. Each solution was then loaded into the Microcal™ isothermal titration calorimetric unit syringe and injected (1 initial injection of 4  $\mu$ L followed by 15 injections of 16  $\mu$ L) into a sample cell containing ultra-pure water, with 1200 seconds between injections, linked to a Microcal™ MCS observer. All experiments were performed to a minimum of duplicate, maintained at 304 K, stirred at 307 rpm and data was analysed using OriginPro® software. The CMC for each experiment was deemed to be the inflection point calculated using the 2<sup>nd</sup> derivative of the profile obtained.

## 2.5 Maximum Solubility Methodology

A stock solution of 25 mg/mL for each active in methanol was prepared, from this the following dilutions were made using the relevant mobile phase (50:50 methanol and water for acetaminophen, 80:20 10 mmol phosphate buffer pH 7 and acetonitrile for benzamide and 4-hydroxybenzamide) 10 mg/mL, 5 mg/mL, 1 mg/mL, 0.5 mg/mL, 0.1 mg/mL, 0.05 mg/mL and 0.01 mg/mL) These were then run on an Agilent 1260 Infinity II HPLC using an Eclipse XDB-C18 50 mm column at a flow rate of 1 mL/min at 30 °C at the UV wavelength shown for each active in **Table 3**.

200 mL solutions of  $2 \times 10^{-2}$  M of Tween 20, HP Tween 20, SR Tween 20, Tween 80, HP Tween 80, SR Tween 80, Etocas 35, Croduret 40, Crodasol HS HP, SDS and Brij 35 were prepared. Following this, 10 mL solutions of  $1 \times 10^{-2}$ ,  $1 \times 10^{-3}$ ,  $1 \times 10^{-4}$ ,  $1 \times 10^{-5}$ ,  $1 \times 10^{-6}$ ,  $1 \times 10^{-7}$ ,  $1 \times 10^{-8}$  M were prepared by serial dilution. Next 1 mL of each concentration was placed into a centrifuge tube and an excess of API was added. The samples were then placed onto a rotating wheel for 48 hours. The samples were then centrifuged, and the resulting solution placed into a filter centrifuge tube, the samples were then centrifuged for a second time. After this the samples were diluted by a factor of 4 with the relevant mobile phase (50:50 methanol and water for acetaminophen, 80:20 10 mmol phosphate buffer and

acetonitrile for benzamide and 4-hydroxybenzamide). These were then run on an Agilent 1260 Infinity II HPLC using an Eclipse XDB-C18 50 mm column at a flow rate of 1 mL/min with the previously stated mobile phase for each API at 30 °C at the UV wavelength shown for each active in **Table 3**.

### **3. Micellar Liquid Chromatography**

The effect of both concentration and surfactant purity upon retention times in MLC were investigated using Tween 20, HP Tween 20, SR Tween 20, Tween 80, HP Tween 80, SR Tween 80, Etocas 35, Croduret 40, Crodasol HS HP, SDS and Brij 35 with acetaminophen, benzamide, 4-hydroxybenzamide and hydrocortisone. This section contains work that was published prior to submission of my thesis.<sup>88</sup>

#### **3.1 Method Optimisation**

Results from initial experiments had a high degree of standard deviation, as calculated from values obtained from 3 repeats (the mean of the 3 results was calculated, then the mean was subtracted from each repeat and the result squared. The mean of the 3 squared differences was calculated and the square root of that value was taken to be the standard deviation.) this was hypothesised to be caused by interference from retained API on the modified stationary phase. This resulted in less free sites on the modified stationary phase for the next experiment, essentially presenting a different modified stationary phase each time, which would account for the disparity between results. In order to overcome this, three new methods were developed, aimed at reducing the interference caused by API retained on the column. Two of the methods involved the use of acetonitrile in the mobile phase at 30 % and 5 % by volume as this has been reported in literature as an often used cosolvent.<sup>35</sup> The final method involved cleaning the column in-between injections with a cleaning solution of 25 % ultra-pure water and 75 % acetonitrile by volume for 10 minutes, followed by 100 % ultra-pure water for 2 minutes.

*Each of the methods were completed using 0.002 M of 4-hydroxybenzamide as a model compound and using Tween 20, Tween 80, Etocas 35, Croduret 40 and Crodasol HS HP as the mobile phases with the specified amount of acetonitrile for each method respectively **Figure 12**, **Figure 13** and*

Figure 14 are the results for each of the three methods.

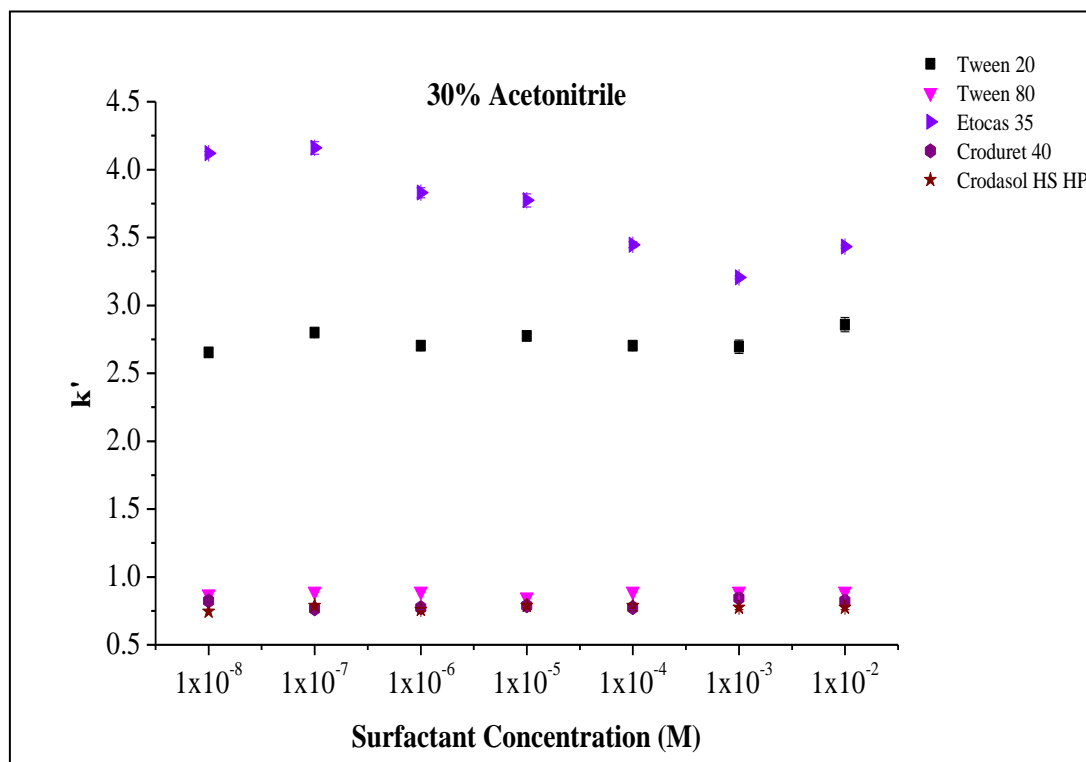
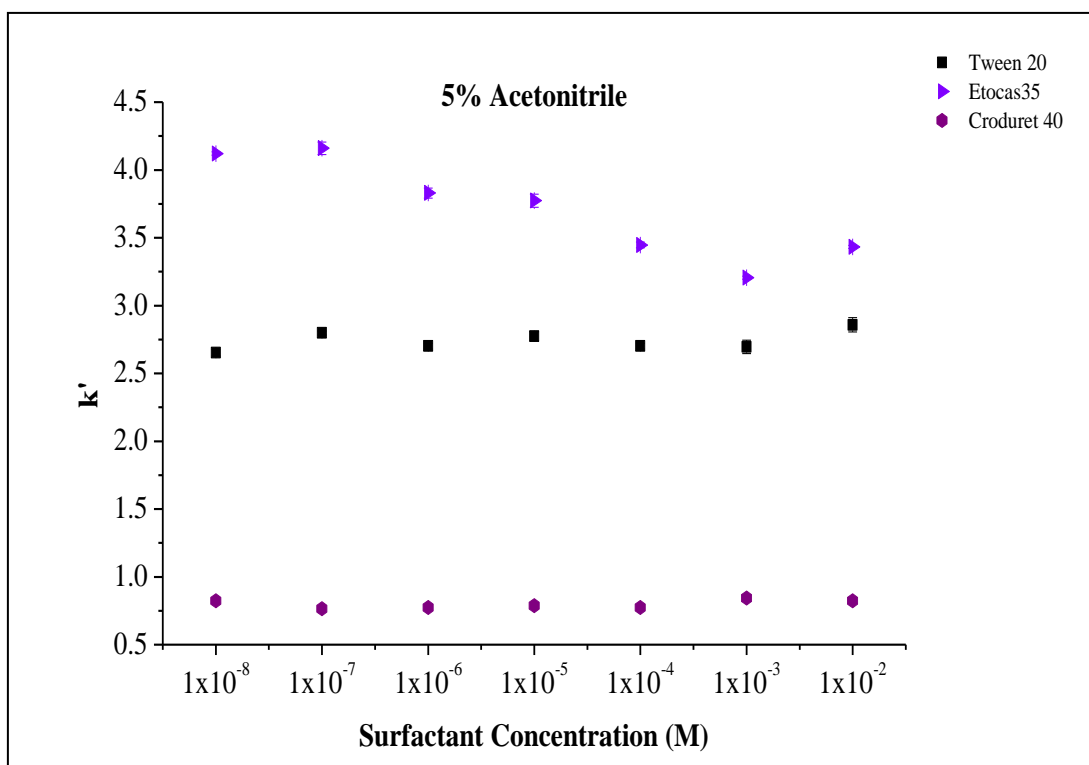
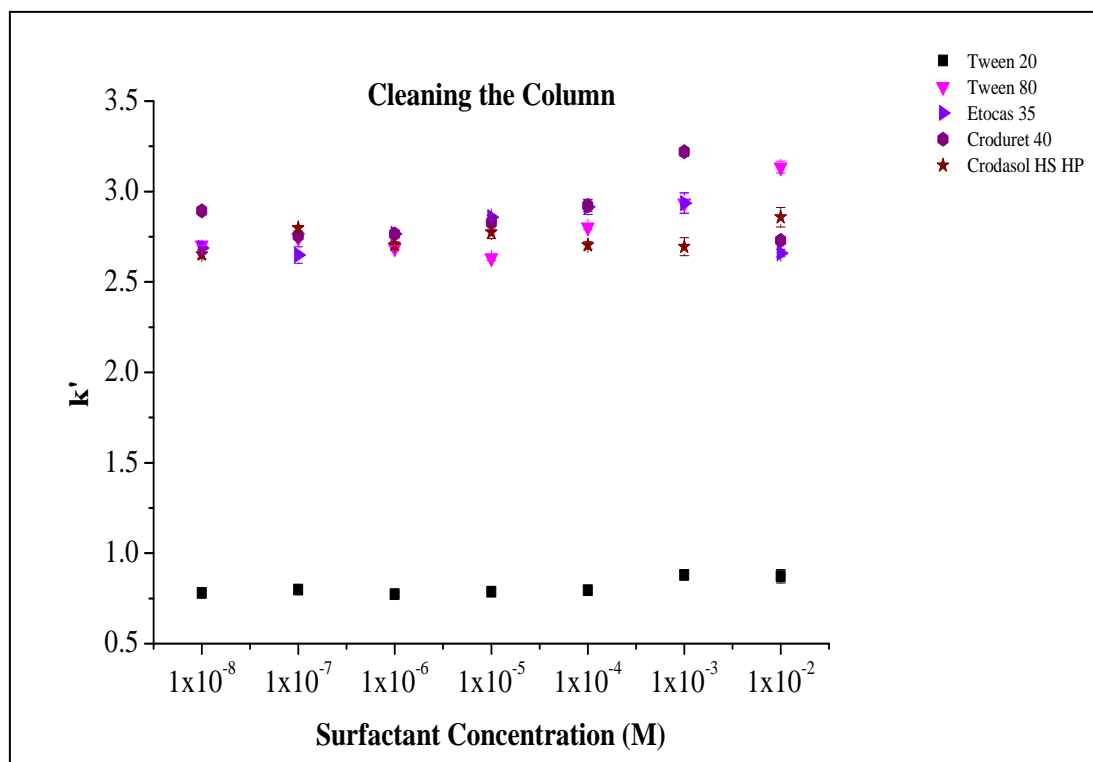


Figure 12. MLC with 4-hydroxybenzamide using a mobile phase consisting of 30 % acetonitrile with 70 % Tween 20, Tween 80, Etocas 35, Croduret 40 and Crodasol HS HP by volume. Error bars were calculated using the standard deviation from 3 repeats.



**Figure 13.** MLC with 4-hydroxybenzamide using a mobile phase consisting of 5 % acetonitrile with 95 % Tween 20 by volume, Tween 20, Etocas 35 and Croduret 40. Error bars were calculated using the standard deviation from 3 repeats.



**Figure 14.** MLC with 4-hydroxybenzamide, where the column was cleaned between each experiment and the mobile phase was Tween 20, Tween 80, Etocas 35, Croduret 40 and Crodasol HS HP. Error bars were calculated using the standard deviation from 3 repeats.

The method involving the use of 30 % v/v produced data with no change in  $k'$  values with increasing surfactant concentration with all of the surfactants apart from Etocas 35, suggesting that the API was interacting with the acetonitrile preferentially over the surfactant. As this study is investigating how surfactant concentration impacts  $k'$  values it was decided that this method wouldn't be appropriate for this study. However, it did significantly reduce the retention time as shown by the reduction in  $k'$  values, this is consistent with the results found in literature when the addition of a second solvent to the mobile phase decreased retention time as stated by Ruiz-Ángel.<sup>35</sup> Whilst the reduction in retention time would increase the rate at which experiments could be carried out, the lack of change in  $k'$  values with increasing surfactant concentration made this method unsuitable.

The second method completed involved the use of 5 % v/v acetonitrile in the mobile phase. This method reduced the amount of standard deviation present in the results (within 5%) but was incompatible with Tween 80 and Crodasol HS HP due to the low consistency of the results produced. As these surfactants were crucial for the project this method wasn't selected.

The final method produced results with a reduced standard deviation, when compared with the method used prior to the optimisation. As previously hypothesised, if the column wasn't cleaned in-between each experiment, then a different modified stationary phase would be presented to each injection. Removing all of the surfactant and any remaining API from the column, and then loading it for an equal amount of time, allowed for a near identical modified stationary phase to be presented to each injection. This led to the reduction in standard deviation observed when this method was used. Subsequent MLC work (Sections 3.3 – 3.6) presented in this report incorporated this adapted methodology.

## **3.2 Column Selection**

At the beginning of this study a cyano-propyl column (Waters Spherisorb 5.0  $\mu\text{m}$  CNRP, 80 Å, 4.6 mm x 150 mm) was used, this was because the method initially used required it. However, this produced

results with low precision, which was theorised to be caused by the weak interactions between the non-ionic surfactants and the charged surface of the column. The weak interactions were theorised to produce a non-uniform modified stationary phase, and therefore different conditions for each experiment, explaining the low precision.

Following this a C18 column (Spherisorb ODSB cartridge, 80 Å, 5 µm, 4.6 mm x 150 mm) was used, this provided a column surface that was more favourable for non-ionic surfactants, resulting in hydrophobic interactions. This allowed for a more uniform modification of the stationary phase and therefore more precise results.

The C18 column was not used for the experiments with hydrocortisone because of the long retention times produced (in excess of 1 hour at surfactant concentrations of  $1 \times 10^{-4}$  M) because of the comparative hydrophobicity of the API. In order to reduce the retention time, a shorter C8 column (Waters Spherisorb 5.0 µm, 80 Å, 4.6 mm x 50 mm) was chosen. A shorter column reduced the distance that the API had to traverse, as well as allowing an increased flow rate of 3.0 mL/min because of the reduction in system pressure. A C8 column was chosen instead of a C18 because of the reduction in hydrophobic interactions produced by the shorter carbon chain, causing a reduction in column interactions, which would also result in a reduction in retention time. As expected, this resulted in a reduction in retention time, however, retention times were still outside of acceptable limits at a surfactant concentration of  $1 \times 10^{-4}$  M.

As further reducing the length of the column wasn't possible, a reduction in carbon chain length was opted for instead leading to the decision to use a C1 column (Waters Spherisorb 5.0 µm, 80 Å, 4.6 mm x 50 mm). This resulted in acceptable retention times for all concentrations of surfactants used.

### **3.3 MLC with Acetaminophen**

MLC with acetaminophen using: Tween 20, HP Tween 20, SR Tween 20, Tween 80, HP Tween 80, SR Tween 80, Etocas 35, Croduret 40, Crodasol HS HP, SDS and Brij 35 as the mobile phase at



concentrations:  $1 \times 10^{-2}$ ,  $1 \times 10^{-3}$ ,  $1 \times 10^{-4}$ ,  $1 \times 10^{-5}$ ,  $1 \times 10^{-6}$ ,  $1 \times 10^{-7}$ ,  $1 \times 10^{-8}$  M was completed. The results from the experiments are displayed in **Figure 15** and summarised **Table 4**.

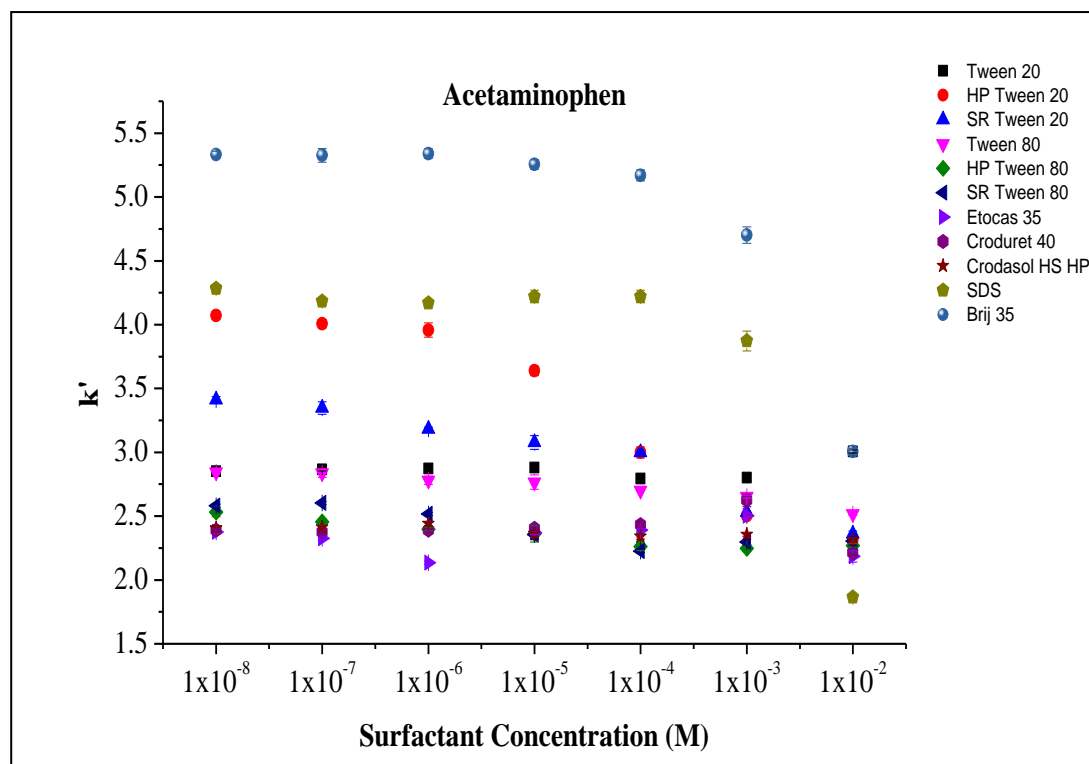


**Figure 15.** MLC with acetaminophen using: Tween 20, HP Tween 20, SR Tween 20, Tween 80, HP Tween 80, SR Tween 80, Etocas 35, Croduret 40, Crodasol HS HP, SDS and Brij 35 as the mobile phase at concentrations:  $1 \times 10^{-2}$ ,  $1 \times 10^{-3}$ ,  $1 \times 10^{-4}$ ,  $1 \times 10^{-5}$ ,  $1 \times 10^{-6}$ ,  $1 \times 10^{-7}$ ,  $1 \times 10^{-8}$  M. Error bars were calculated using the standard deviation from 3 repeats.

The CMC for Croduret 40, Crodasol HS HP and Etocas 35 hasn't been reliably characterised prior to this study. However, the CMCs for polysorbate 20 and polysorbate 80 have been reported with several different values spanning a range of 0.002 - 0.975 mM and 0.011 – 0.574 mM respectively, across a temperature range of 25 °C – 45 °C as shown in **Table 1**. SDS (6.80 mM<sup>89</sup>) and Brij 35 (0.06 mM<sup>90</sup>) have also been characterised. As previously mentioned in Section 1.2 non-ionic surfactants generally have lower CMC values, therefore, using the CMC values for polysorbates 20 and 80 instead of SDS and Brij 35 as a guide, the concentration range for the experiment was set with 3 concentrations below and 3 above the CMC values. It was theorised that the unknown CMC values should fall somewhere within the concentration range used because of its broadness. The hypothesis was that at a concentration below the CMC there wouldn't be any micelles present, therefore, the mobile phase wouldn't exhibit

the properties associated with standard MLC, in that below the CMC a change in retention time wouldn't be observed. After the CMC threshold was exceeded a change in retention time would then be seen such as a decrease of 20 %, as the second equilibrium would be introduced, and further increases in surfactant concentration would result in a greater effect on retention time caused by the increasing number of micelles. Polysorbate 20 was studied at 3 purities, standard, high purity and super refined the results of which are shown in **Figure 16**.

**Table 4.** The average  $k'$  values of acetaminophen with Tween 20, HP Tween 20, SR Tween 20, Tween 80, HP Tween 80, SR Tween 80, Etocas 3, Croduret 40, Crodasol HS HP, SDS and Brij 35 at  $1 \times 10^{-2}$  and  $1 \times 10^{-8}$  M.

Surfactant	Average $k'$ at $1 \times 10^{-8}$ M	Average $k'$ at $1 \times 10^{-2}$ M	Change in average $k'$
Tween 20	2.85	3.00	+ 0.15
HP Tween 20	4.07	2.31	- 1.76
SR Tween 20	3.41	2.36	- 1.05
Tween 80	2.84	2.51	- 0.33
HP Tween 80	2.53	2.27	- 0.26
SR Tween 80	2.58	2.30	- 0.28
Etocas 35	2.37	2.18	- 0.19
Croduret 40	2.39	2.21	- 0.18
Crodasol HS HP	2.40	2.31	- 0.09
SDS	4.28	1.86	- 2.42
Brij 35	5.33	3.00	- 2.33

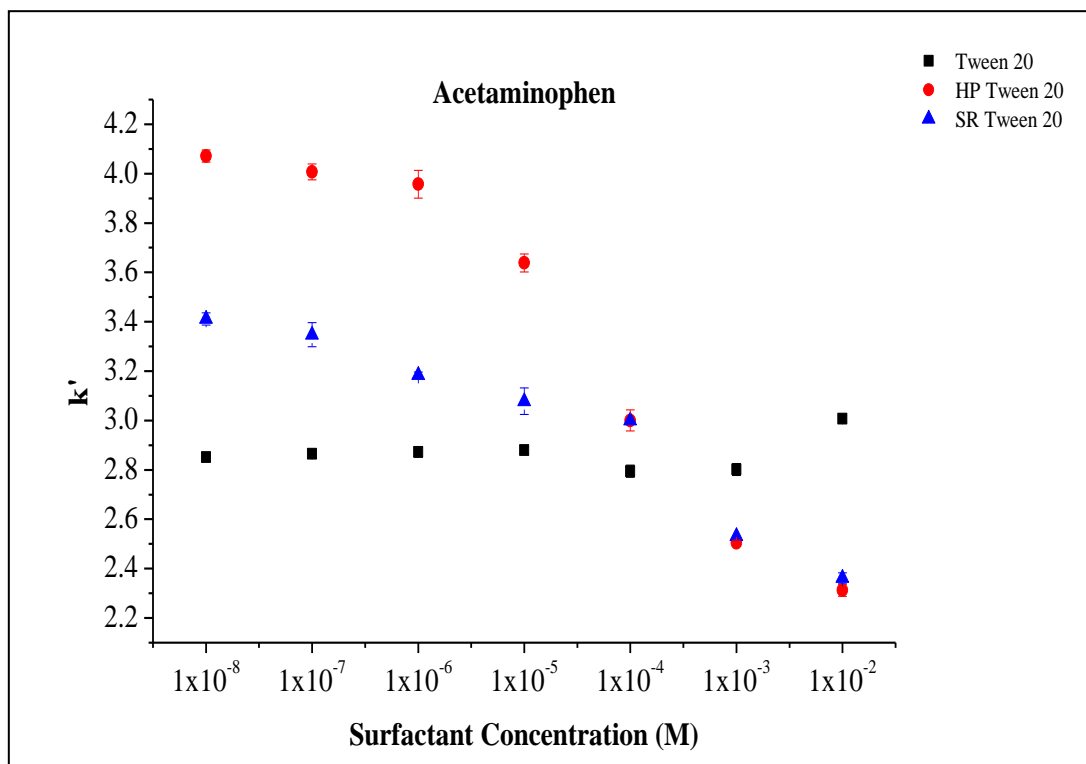


**Figure 16.** MLC with acetaminophen using: Tween 20, HP Tween 20 and SR Tween 20, as the mobile phase at concentrations:  $1 \times 10^{-2}$ ,  $1 \times 10^{-3}$ ,  $1 \times 10^{-4}$ ,  $1 \times 10^{-5}$ ,  $1 \times 10^{-6}$ ,  $1 \times 10^{-7}$ ,  $1 \times 10^{-8}$  M. Error bars were calculated using the standard deviation from 3 repeats.

Tween 20 exhibited little overall change in  $k'$ , as shown in **Table 4** and presented with a comparatively flat graph as shown in **Figure 16**. However, the other purity grades of polysorbate 20 showed reductions in  $k'$  values and the graphs followed the expected trend, with a relatively flat section followed by a significant change, in this case a decrease in  $k'$  values. SR Tween 20 had the biggest decrease in  $k'$  values occur between  $1 \times 10^{-5} - 1 \times 10^{-4}$  M which is encompassed by the range of literature values shown in **Table 1** (0.002 – 0.975 mM). Whereas HP Tween 20's biggest decrease occurred between  $1 \times 10^{-5} - 1 \times 10^{-4}$  M, with another big decrease occurring between  $1 \times 10^{-4} - 1 \times 10^{-3}$  M. It is worth noting that both HP and SR had very similar final  $k'$  values, within 0.05, of each other and that they both outperformed Tween 20 in terms of final and overall reduction in  $k'$  values. Polysorbate 80 was studied at 3 purities, standard, high purity and super refined the results of which are shown in **Figure 17**.

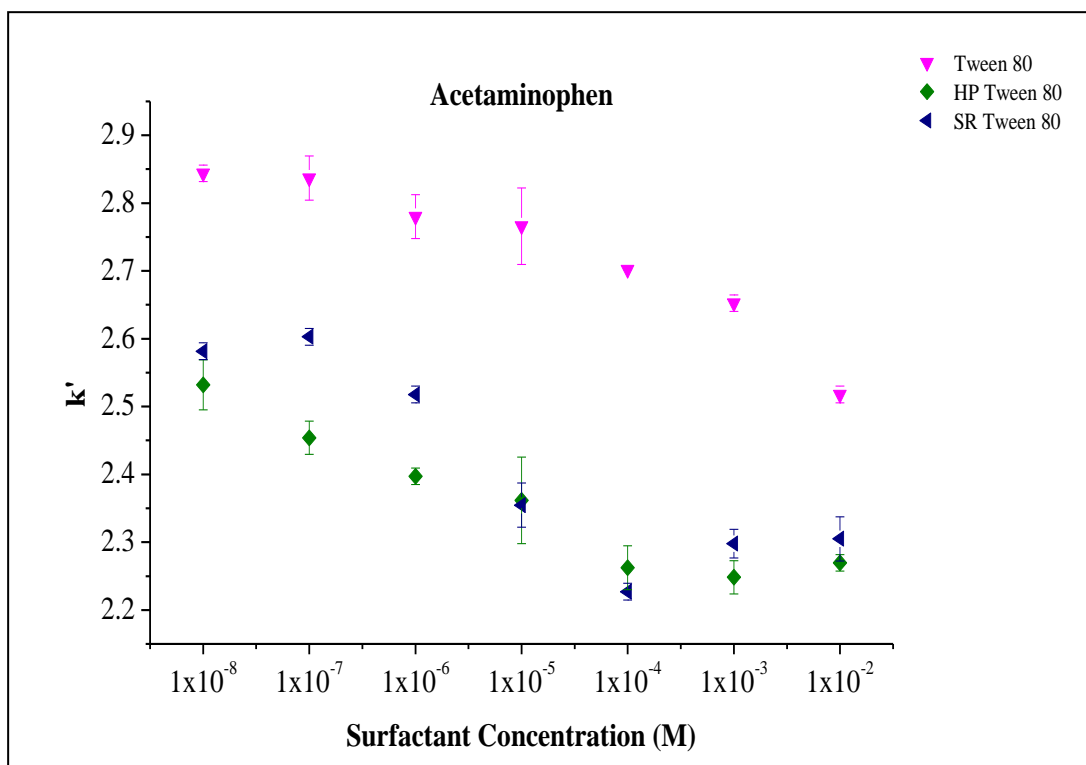


**Figure 17.** MLC with acetaminophen using: Tween 80, HP Tween 80 and SR Tween 80, as the mobile phase at concentrations:  $1 \times 10^{-2}$ ,  $1 \times 10^{-3}$ ,  $1 \times 10^{-4}$ ,  $1 \times 10^{-5}$ ,  $1 \times 10^{-6}$ ,  $1 \times 10^{-7}$ ,  $1 \times 10^{-8}$  M. Error bars were calculated using the standard deviation from 3 repeats.

All three grades of polysorbate 80 showed slight overall reductions in  $k'$  with increasing concentration (- 0.33 for standard Tween 80, - 0.26 for HP Tween 80 and - 0.28 for SR Tween 80) as shown in **Table 4** and **Figure 17**, with Tween 80 exhibiting a gradual decrease across all concentrations. However, if assuming the upper limits on the error bars it could be inferred that it presents as a flat graph until  $1 \times 10^{-5}$  M, where afterwards a decrease in  $k'$  values is observed. The HP and SR grades of polysorbate 80 follow the same trend of a decrease in  $k'$  values until  $1 \times 10^{-4}$  M, after which they exhibit a negligible increase (0.005 for HP Tween 80 and 0.080 for SR Tween 80), which could be interpreted as a flattening of the graph. It is worth noting that the change point in all three graphs (assuming the upper limits of the error bars for standard grade Tween 80) occurs between  $1 \times 10^{-5}$  –  $1 \times 10^{-3}$  M, which is within the range of the literature CMC values reported in **Table 1** for polysorbate 80 (0.011 – 0.574 mM). Similarly, as with the results for polysorbate 20, the HP and SR grades of Tween 80 have a very close endpoint, within 0.03 of each other. In addition to this, whilst they failed to outperform the standard grade in terms of overall  $k'$  reduction, the final  $k'$  value for both was lower than that of the standard grade.

Etocas 35, Croduret 40 and Crodasol HS HP exhibited a slight decrease in  $k'$  values overall (- 0.19, - 0.18 and - 0.09 respectively), as shown in **Table 4** and **Figure 15**. All three presented flat graphs with no obvious change point from which to infer an estimation of the CMC.

Both SDS and Brij 35 had large overall decreases in  $k'$  values (- 2.42 and - 2.33 respectively) when compared with the other surfactants as shown in **Table 4****Error! Reference source not found.** and **Figure 15**. The largest decrease in  $k'$  values occurred between  $1 \times 10^{-3}$  and  $1 \times 10^{-2}$  M for both surfactants, as previously shown in **Table 2**, is close to the CMC values for SDS (6.80 mM<sup>89</sup>). Whilst the CMC value for SDS is slightly higher than the concentration range used for this experiment, it has been reported by Waters et al. that the CMC of SDS in the presence of acetaminophen decreases with increasing temperature.<sup>85</sup> The experiment was conducted at 31 °C and the literature value for the CMC of SDS is recorded at 25 °C, this increased temperature could explain why the decrease in  $k'$  values happened at a concentration range lower than that of the reported CMC.

MLC with a variety of compounds was carried out by Kulikov using a solution of SDS as the mobile phase, it was reported that because of paracetamol's hydrophilicity increasing the concentration of the mobile phase resulted in the retention time barely altering.<sup>91</sup> Unfortunately Kulikov doesn't state what the maximum concentration of SDS used was. However, as it is unlikely that he would have selected concentrations below the CMC, like this study has, it is fair to assume that the concentrations were equal to or greater than the CMC. The results in **Figure 15** clearly show a staggered decrease in  $k'$  values across the range of  $1 \times 10^{-4}$  –  $1 \times 10^{-2}$  M for SDS. Therefore, it can also be assumed that the concentrations used were in excess of the CMC, as previously stated, Kulikov noted that there wasn't a marked difference in retention time with increasing SDS concentration.

### 3.4 MLC with Benzamide

MLC with benzamide using: Tween 20, HP Tween 20, SR Tween 20, Tween 80, HP Tween 80, SR Tween 80, Etocas 35, Croduret 40, Crodasol HS HP, SDS and Brij 35 as the mobile phase at concentrations:  $1 \times 10^{-2}$ ,  $1 \times 10^{-3}$ ,  $1 \times 10^{-4}$ ,  $1 \times 10^{-5}$ ,  $1 \times 10^{-6}$ ,  $1 \times 10^{-7}$ ,  $1 \times 10^{-8}$  M was completed. The results from the experiments are displayed in **Figure 18** and summarised in **Table 5**.

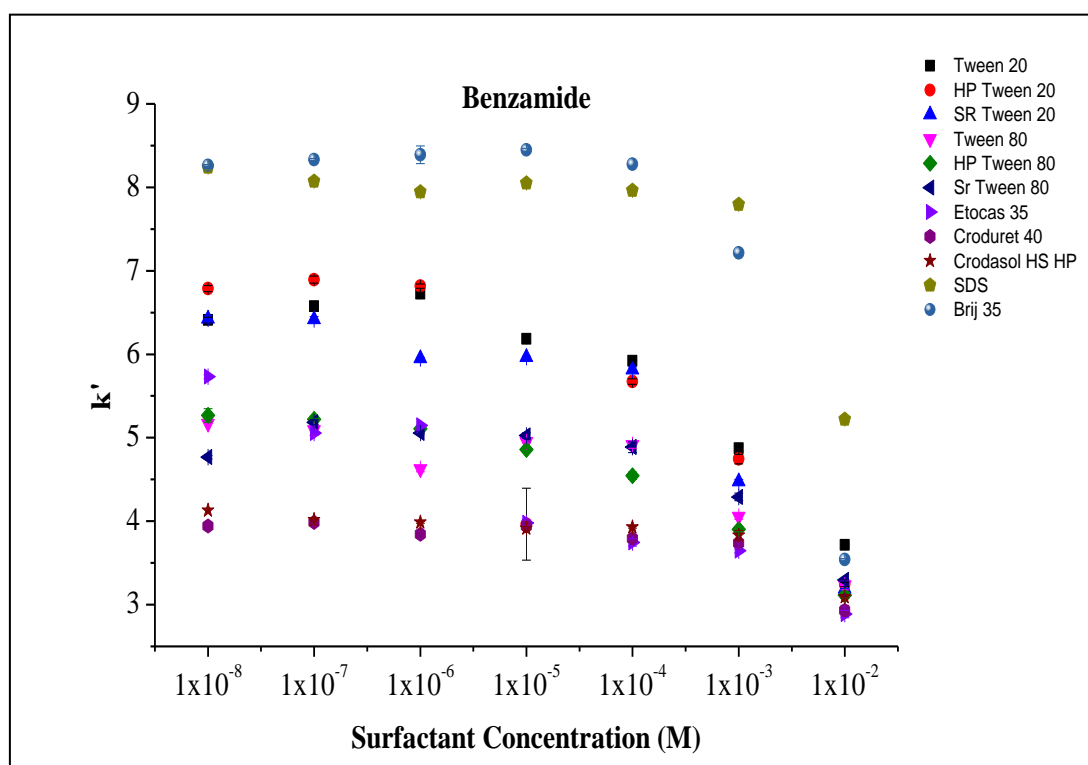


**Figure 18.** MLC with benzamide using: Tween 20, SR Tween 20, Tween 80, Etocas 35, Croduret 40, Crodasol HS HP, SDS and Brij 35 as the mobile phase at concentrations:  $1 \times 10^{-2}$ ,  $1 \times 10^{-3}$ ,  $1 \times 10^{-4}$ ,  $1 \times 10^{-5}$ ,  $1 \times 10^{-6}$ ,  $1 \times 10^{-7}$ ,  $1 \times 10^{-8}$  M. Error bars were calculated using the standard deviation from 3 repeats.

**Table 5.** The average  $k'$  values of benzamide with Tween 20, HP Tween 20, SR Tween 20, Tween 80, HP Tween 80, SR Tween 80, Etocas 3, Croduret 40, Crodasol HS HP, SDS and Brij 35 at  $1 \times 10^{-2}$  and  $1 \times 10^{-8}$  M.

Surfactant	Average $k'$ at $1 \times 10^{-8}$ M	Average $k'$ at $1 \times 10^{-2}$ M	Change in average $k'$
Tween 20	6.41	3.71	- 2.70
HP Tween 20	6.78	3.24	- 3.54
SR Tween 20	6.42	3.19	- 3.23
Tween 80	5.17	3.23	- 1.94
HP Tween 80	5.26	3.11	- 2.15
SR Tween 80	4.76	3.29	- 1.47
Etocas 35	5.70	2.88	- 2.82
Croduret 40	3.94	2.92	- 1.02
Crodasol HS HP	4.12	3.09	- 1.03
SDS	8.24	5.21	- 3.03
Brij 35	8.26	3.53	- 4.73

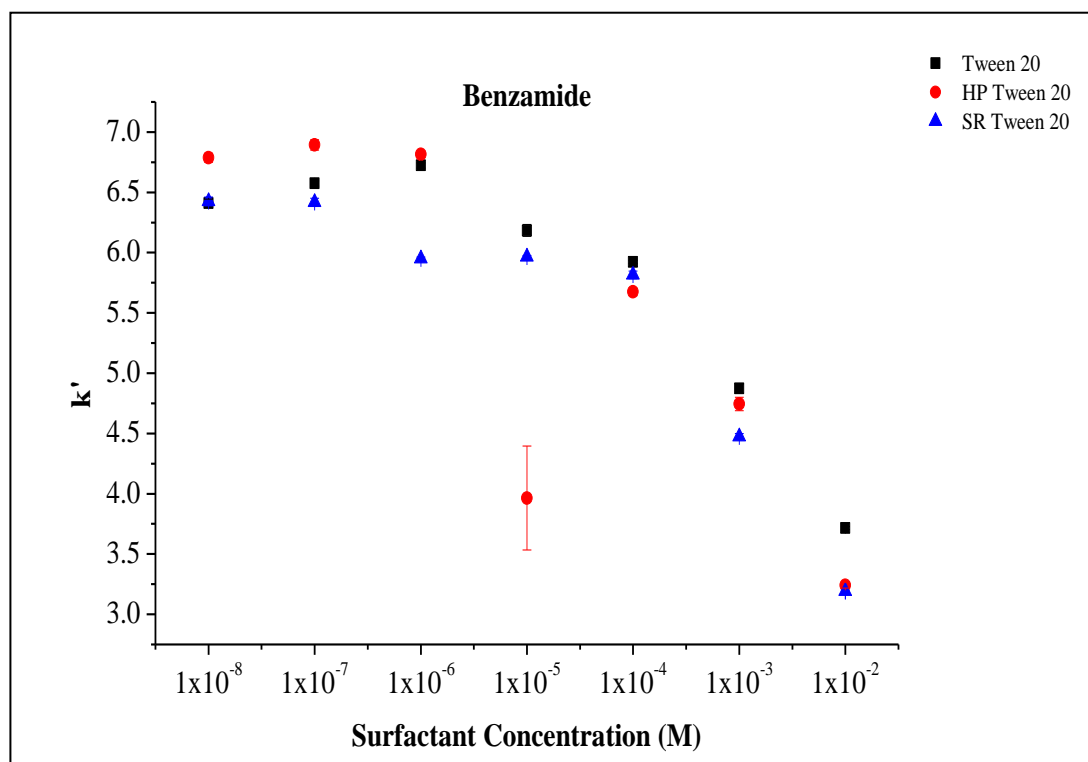


**Figure 19.** MLC with benzamide using: Tween 20, HP Tween 20 and SR Tween 20, as the mobile phase at concentrations:  $1 \times 10^{-2}$ ,  $1 \times 10^{-3}$ ,  $1 \times 10^{-4}$ ,  $1 \times 10^{-5}$ ,  $1 \times 10^{-6}$ ,  $1 \times 10^{-7}$ ,  $1 \times 10^{-8}$  M. Error bars were calculated using the standard deviation from 3 repeats.

Polysorbate 20 was studied at 3 purities, standard, high purity and super refined the results of which are shown in **Figure 19**. When compared to the results of MLC with acetaminophen, it can be said that increasing polysorbate 20 concentration had a greater effect on  $k'$  values as shown in **Figure 19** and **Table 5**. Similarly, to the results with acetaminophen, the biggest change in  $k'$  values for each grade of Tween 20 occurred between  $1 \times 10^{-4}$  and  $1 \times 10^{-3}$  M, which, as previously stated is encompassed by the range of CMC values shown in **Table 1** for polysorbate 20 (0.002 – 0.975 mM). Conversely, unlike with acetaminophen, Tween 20 did produce a change in  $k'$  values with increasing concentration. The graphs for each purity grade present with a slight decrease, until the aforementioned concentrations, after which a steep decrease in  $k'$  values were observed. Both HP and SR grades of Tween 20 outperformed Tween 20 in terms of overall  $k'$  reduction (- 2.70 for Tween 20, - 3.54 for HP Tween 20 and - 3.23 for SR Tween 20) as well as final  $k'$  value (3.71 for Tween 20, 3.24 for HP Tween 20 and 3.19 for SR Tween 20). Similarly, to the results with acetaminophen as shown in **Table 4** the values for each were close, with each of the purities of polysorbate 20 being within 0.05 of each other's final  $k'$  value and within 0.11 of each other's overall reduction in  $k'$  values. Polysorbate 80 was studied at 3 purities, standard, high purity and super refined, as with all grades of polysorbate 20, all of the grades of polysorbate 80 produced a greater overall reduction in  $k'$  values with benzamide than with acetaminophen as shown in **Figure 20** and **Table 5**



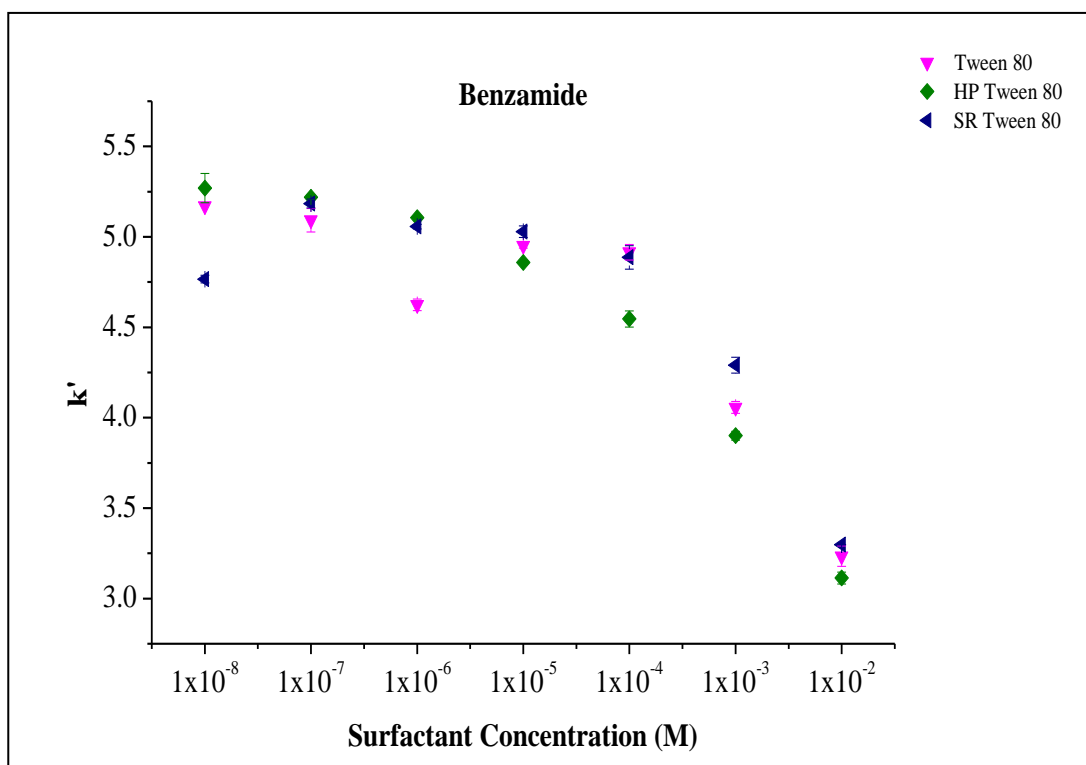


**Figure 20.** MLC with benzamide using: Tween 80, HP Tween 80 and SR Tween 80, as the mobile phase at concentrations:  $1 \times 10^{-2}$ ,  $1 \times 10^{-3}$ ,  $1 \times 10^{-4}$ ,  $1 \times 10^{-5}$ ,  $1 \times 10^{-6}$ ,  $1 \times 10^{-7}$ ,  $1 \times 10^{-8}$  M. Error bars were calculated using the standard deviation from 3 repeats.

All three purities produced graphs that were initially relatively flat or with little change in  $k'$  values until  $1 \times 10^{-4}$  M, where afterwards a sharp decrease in  $k'$  values were observed. Similarly, to the results with polysorbate 20, the range of reported CMC's for polysorbate 80 as shown in **Table 1** (0.011 – 0.574 mM) encompasses the concentration at which the sharp decrease is observed. The final  $k'$  values for each purity grade (3.23 for Tween 80, 3.11 for HP Tween 80 and 3.29 for SR Tween 80) were close, within 0.18 of each other. Whilst HP Tween 80 slightly outperformed Tween 80 in terms of overall change in  $k'$  values (- 1.94 for Tween 80 and - 2.15 for HP Tween 80), Tween 80 did perform better than SR Tween 80 (- 1.47 for SR Tween 80). This is markedly different to the results with acetaminophen, where the HP and SR grades noticeably outperformed Tween 80 on both fronts.

Etocas 35 presented with a constant decrease in  $k'$  values with increasing concentration and displayed a greater decrease in overall  $k'$  value (- 2.82) than was observed with acetaminophen, as shown in **Figure 18** and **Table 5**. The biggest decrease in  $k'$  values occurred between  $1 \times 10^{-6}$  and  $1 \times 10^{-5}$  M,

however, unlike the graphs with the Tween 20 and 80, there isn't a relatively flat section superseding the decrease.

Croduret 40 and Crodasol HSHP produced similar graphs, with a relatively flat section until  $1 \times 10^{-3}$  M after which a sharp decrease in  $k'$  values was observed as show in **Figure 18** and **Table 5**. They both had close final  $k'$  values (2.92 for Croduret 40 and 3.09 for Crodasol HS HP) which were greater than that which was observed with acetaminophen, and close overall changes in  $k'$  values (- 1.02 for Croduret 40 and -1.03 Crodasol HSHP). As previously mentioned, unlike the results with Etocas 35, they both had relatively flat sections before the sharp decrease in  $k'$  values. Whilst the concentration at which sharp decreases in  $k'$  values roughly align with the CMC for Tween 20, Tween 80, SDS and Brij 35, it cannot be said with confidence that this is where the CMC for Croduret 40 and Crodasol HS HP lies, without further supporting evidence.

SDS and Brij 35 produced similar graphs, as shown in **Figure 18**, to the results with acetaminophen, in regard to the comparatively flat section until  $1 \times 10^{-3}$  M after which the  $k'$  values sharply decrease. As with the other surfactants, the overall change in  $k'$  values were greater with benzamide (- 3.03 for SDS and - 4.73 for Brij 35) as shown in **Table 5**. The largest decrease in  $k'$  values occurred between  $1 \times 10^{-3}$  and  $1 \times 10^{-2}$  M, which as previously mentioned is close to the CMC for SDS.

### **3.5 MLC with 4-Hydroxybenzamide**

MLC with 4-hydroxybenzamide using: Tween 20, HP Tween 20, SR Tween 20, Tween 80, HP Tween 80, SR Tween 80, Etocas 35, Croduret 40, Crodasol HS HP, SDS and Brij 35 as the mobile phase at concentrations:  $1 \times 10^{-2}$ ,  $1 \times 10^{-3}$ ,  $1 \times 10^{-4}$ ,  $1 \times 10^{-5}$ ,  $1 \times 10^{-6}$ ,  $1 \times 10^{-7}$ ,  $1 \times 10^{-8}$  M was completed. The results from the experiments are displayed in **Figure 21** and summarised in **Table 6**.

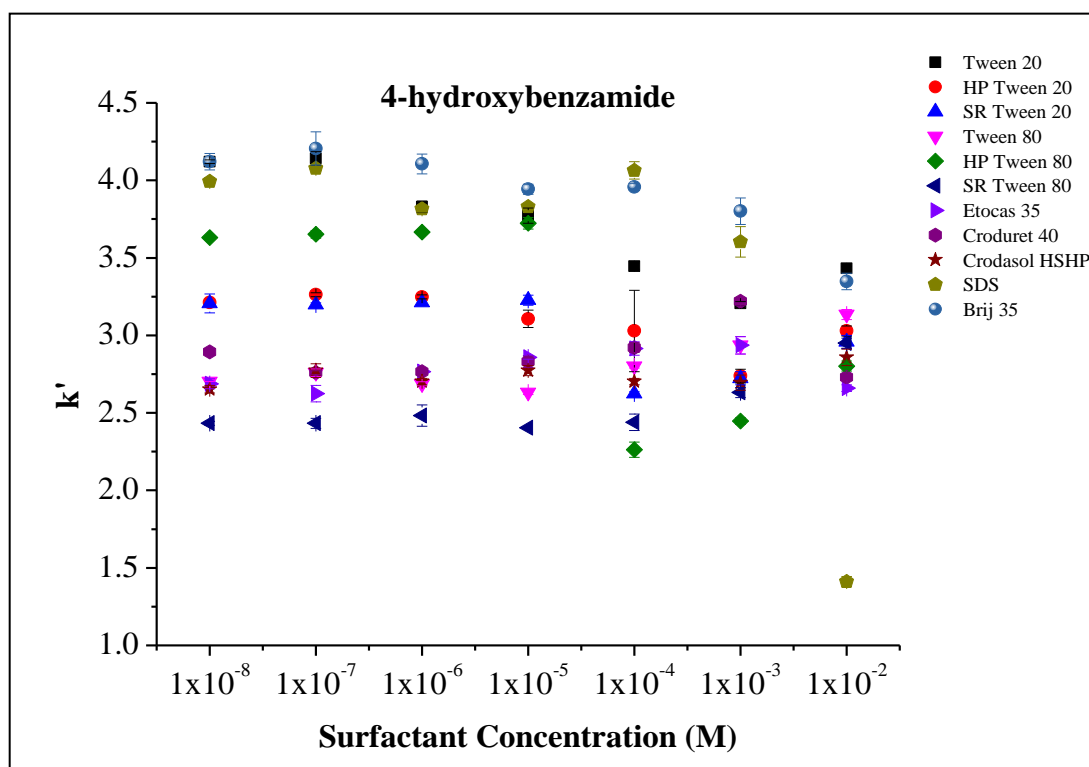


**Figure 21.** MLC with 4-hydroxybenzamide using: Tween 20, HP Tween 20, SR Tween 20, Tween 80, HP Tween 80, SR Tween 80, Etocas 35, Croduret 40, Crodasol HS HP, SDS and Brij 35 as the mobile phase at concentrations:  $1 \times 10^{-2}$ ,  $1 \times 10^{-3}$ ,  $1 \times 10^{-4}$ ,  $1 \times 10^{-5}$ ,  $1 \times 10^{-6}$ ,  $1 \times 10^{-7}$ ,  $1 \times 10^{-8}$  M. Error bars were calculated using the standard deviation from 3 repeats.

**Table 6.** The average  $k'$  values of 4-hydroxybenzamide with Tween 20, HP Tween 20, SR Tween 20, Tween 80, HP Tween 80, SR Tween 80, Etocas 3, Croduret 40, Crodasol HS HP, SDS and Brij 35 at  $1 \times 10^{-2}$  and  $1 \times 10^{-8}$  M.

Surfactant	Average $k'$ at $1 \times 10^{-8}$ M	Average $k'$ at $1 \times 10^{-2}$ M	Change in average $k'$
Tween 20	4.12	3.43	- 0.69
HP Tween 20	3.21	3.02	- 0.19
SR Tween 20	3.20	2.95	- 0.25
Tween 80	2.70	3.13	+ 0.43
HP Tween 80	3.63	2.80	- 0.83
SR Tween 80	2.43	2.95	+ 0.52
Etocas 35	2.68	2.65	- 0.03
Croduret 40	2.89	2.73	- 0.16
Crodasol HS HP	2.89	2.73	- 0.16
SDS	3.99	1.41	- 2.58
Brij 35	4.12	3.34	- 0.78

Polysorbate 20 was studied at 3 purities, standard, high purity and super refined, the higher purity grades of Tween 20, HP and SR, presented with similar graphs, as shown in **Figure 22** in that they both feature a relatively flat section until  $1 \times 10^{-5}$  M, after which a steep decrease is observed. However, unlike the results with acetaminophen and benzamide, the decrease does not continue, instead a gradual increase, nearly equal to the initial steep decrease observed between  $1 \times 10^{-5}$  and  $1 \times 10^{-4}$  M is observed between  $1 \times 10^{-4}$  and  $1 \times 10^{-2}$  M. The initial decrease is observed across concentrations where the CMC for polysorbate 20 has been reported as shown in **Table 1** (0.002 – 0.975 mM).

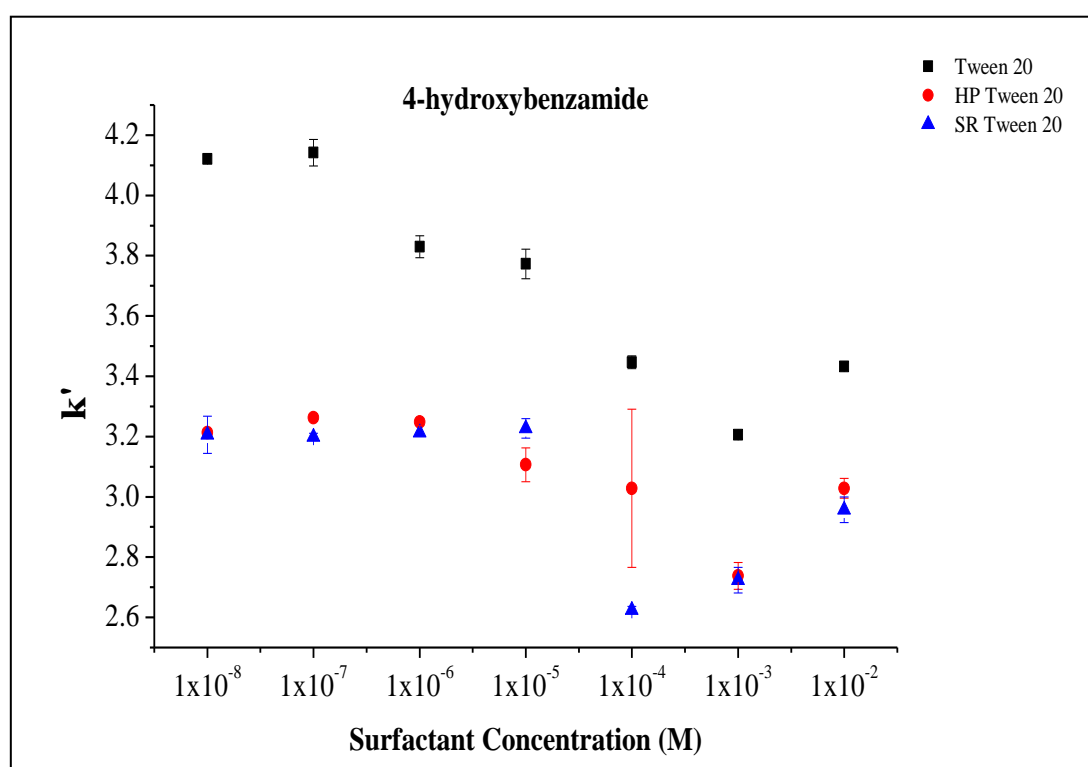


**Figure 22.** MLC with 4-hydroxybenzamide using: Tween 20, HP Tween 20 and SR Tween 20, as the mobile phase at concentrations:  $1 \times 10^{-2}$ ,  $1 \times 10^{-3}$ ,  $1 \times 10^{-4}$ ,  $1 \times 10^{-5}$ ,  $1 \times 10^{-6}$ ,  $1 \times 10^{-7}$ ,  $1 \times 10^{-8}$  M. Error bars were calculated using the standard deviation from 3 repeats.

The graph in **Figure 22** differs to both **Figure 16** and **Figure 19** in that it features both a decrease and then an increase in  $k'$  values with increasing surfactant concentration. Using the partition coefficients  $P_{WM}$ ,  $P_{MS}$  and  $P_{WS}$  and the resulting equilibria between the bulk solvent, micellar-pseudo and modified stationary phase as described by Ruiz-Ángel et al a plausible explanation can be provided.<sup>35</sup> As previously mentioned, the profiles within the graph can be seen to consist of three stages; a relatively flat section ( $1 \times 10^{-8}$  –  $1 \times 10^{-5}$  M) followed by a sharp decrease ( $1 \times 10^{-5}$  –  $1 \times 10^{-4}$  M) and finally a

section where  $k'$  values increase ( $1 \times 10^{-4} - 1 \times 10^{-2}$  M). When considering the theoretical discussion presented in Section 1.41,  $P_{WM}$  is the partition coefficient for the API between the bulk solvent and the micellar-pseudo phase,  $P_{WS}$  is the partition coefficient for the API between the bulk solvent and the modified stationary phase and  $P_{MS}$  is the partition coefficient for the API between the modified stationary phase and the micellar-pseudo phase as a result of direct transfer. The extent of transfer within this final stage is only significant with hydrophobic APIs and can be considered negligible otherwise; a diagram of this is shown in **Figure 23**.

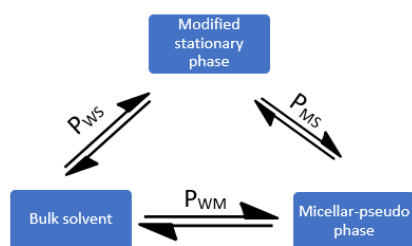


**Figure 23.** The equilibria that exists between the modified stationary phase, bulk solvent and micellar-pseudo phase.

$k'$  values are a reflection of the amount of time the API spends on the modified stationary phase, a comparatively higher  $k'$  value means that the API spends more time on the modified stationary phase than that with a lower  $k'$  value. Prior to the CMC the system can be considered to only have 2 phases, the bulk solvent and the modified stationary phase, this is because prior to the CMC micelles will not form and therefore, a micellar-pseudo phase does not exist. This means that the system remains unchanged even though surfactant concentration is increasing and therefore the partition of the API between the bulk solvent and the modified stationary phase remains constant, explaining the relatively flat section of the graph between  $1 \times 10^{-8}$  and  $1 \times 10^{-5}$  M.

It is important to remember than in this system the bulk solvent is water, and 4-hydroxybenzamide is a hydrophilic drug with a Log P of 0.33 (value obtained from PubChem), this means the equilibria resemble the system shown in **Figure 24** as direct transfer is negligible.

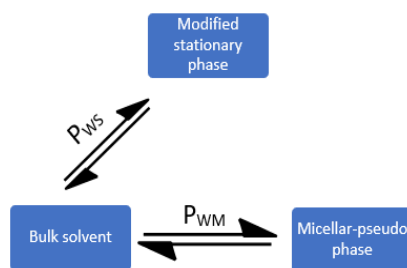


**Figure 24.** The equilibria that exists between the modified stationary phase, bulk solvent and micellar-pseudo phase for hydrophilic APIs in MLC.

After the CMC is reached and the micellar-pseudo phase is introduced the API has access to another phase that it can partition into, reducing the amount of time that the API spends partitioned on the modified stationary phase, this as previously mentioned would result in a reduction of  $k'$  values and could explain the reduction observed between  $1 \times 10^{-5}$  and  $1 \times 10^{-4}$  M (the sharp decrease in **Figure 22**). However, due to the API being relatively hydrophilic in nature, it will preferentially partition into the bulk solvent over the micellar-pseudo phase. Further increasing the concentration of the surfactant results in the equilibrium between the micellar-pseudo phase and the bulk solvent shifting towards the bulk solvent because of the hydrophilic nature of the API. As the API can only interact with the modified stationary phase via partitioning between the bulk solvent and the modified stationary phase, shifting  $P_{WM}$  in favour of the bulk solvent has the knock-on effect of the API partitioning onto the modified stationary phase to a greater degree than would have occurred at the previous, lower concentration of surfactant. This would account for the increase in  $k'$  values observed between  $1 \times 10^{-4}$  and  $1 \times 10^{-2}$  M. Whilst this is a possible explanation for the three distinct profiles seen within this graph, it doesn't take into account other factors such as steric hinderance and size that will also contribute to dictating the observed  $k'$  values. This may explain why the other surfactant/API combinations tend to present with differing profiles within the graphs to that seen in **Figure 22**. In general, the remaining API/surfactant combinations display comparatively flat profiles and/or reductions in  $k'$  as surfactant concentration increases. Using the same theoretical approach in these cases implies the API is initially partitioned between the bulk solvent and the modified stationary phase as suggested above, and then above the

CMC is partitioned into the micellar-pseudo phase, and with increasing concentration of surfactant partitioned to a greater extent in that phase, explaining the reduction in  $k'$  values

Tween 20 presented as a gradual decrease in  $k'$  values until  $1 \times 10^{-3}$  M, after which an increase, like that which was observed with the HP and SR grades, was observed.

The use of overall change in  $k'$  values as well as final  $k'$  as shown in **Table 6** isn't an effective way to compare the effect of surfactant concentration on values for polysorbate 20. This is because of the change to a somewhat parabolic shape towards the higher concentrations used which can't be described in terms of initial and final  $k'$  values, unlike the constant decrease in  $k'$  values observed with acetaminophen and benzamide as shown in **Figure 15** and **Figure 18**.

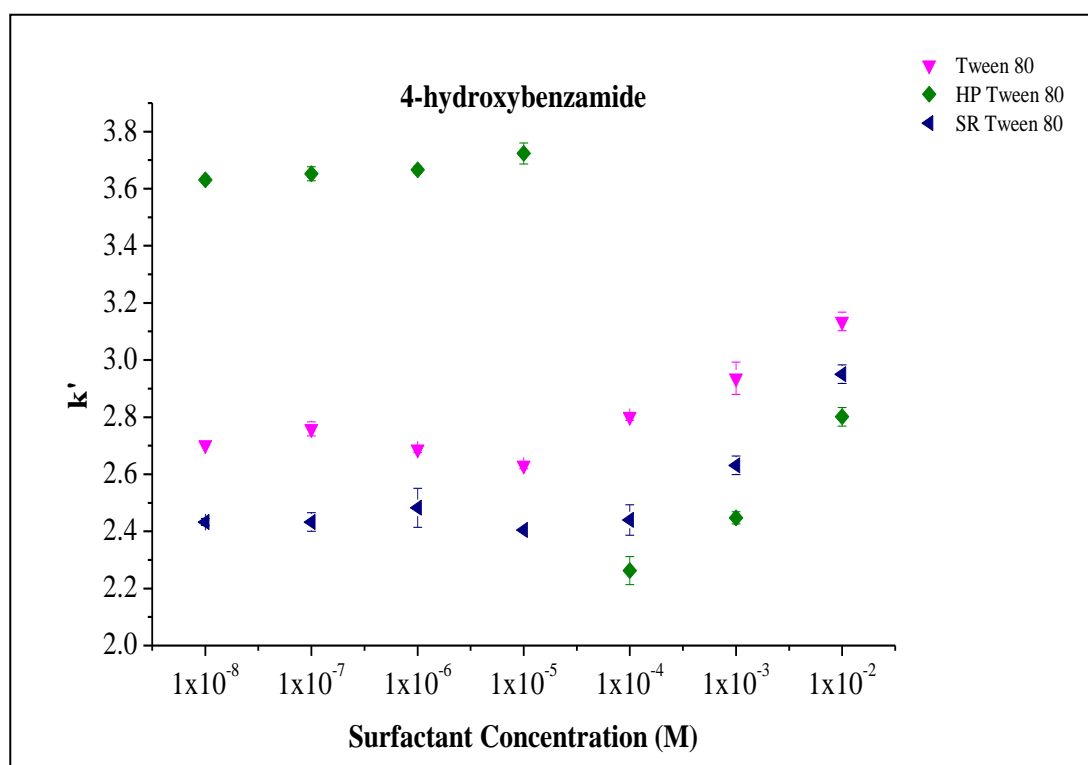


**Figure 25.** MLC with 4-hydroxybenzamide using: Tween 80, HP Tween 80 and SR Tween 80, as the mobile phase at concentrations:  $1 \times 10^{-2}$ ,  $1 \times 10^{-3}$ ,  $1 \times 10^{-4}$ ,  $1 \times 10^{-5}$ ,  $1 \times 10^{-6}$ ,  $1 \times 10^{-7}$ ,  $1 \times 10^{-8}$  M. Error bars were calculated using the standard deviation from 3 repeats.

Polysorbate 80 was studied at 3 purities, standard, high purity and super refined, Tween 80 and SR Tween 80 as shown in **Figure 25** and display similar trends as shown in **Figure 22**, with a flat section

until  $1 \times 10^{-5}$  M, after which an increase in  $k'$  values are observed. The previous explanation for the increase in  $k'$  values from the results with polysorbate 20 applies here as well, as the range of reported CMCs as shown in **Table 1** (0.22 – 0.574 mM) encompasses the point at which the increase starts. However, unlike the results with polysorbate 20 there isn't an initial decrease in  $k'$  values, suggesting that direct transfer is happening between the micellar-pseudo phase and the modified stationary phase, explaining the increase in  $k'$  values.

HP Tween 80 displays similar trends to polysorbate 20, in that it has a relatively flat section until  $1 \times 10^{-5}$  –  $1 \times 10^{-4}$  M after which a sharp decrease in  $k'$  values are observed, following this the  $k'$  values increase with increasing surfactant concentration. The explanation for the results of polysorbate 20 using partition equilibria can also be applied here.

Similarly to the results from polysorbate 20, the shape of the graph of HP Tween 80 means that overall change in  $k'$  values can't be used to get a true comparison between surfactants because of the change to a somewhat parabolic shape towards the higher concentrations. However, as both Tween 80 and SR Tween 80 feature a flat section followed by an increase, this method can be used as there is a steady increase in  $k'$  values across the concentrations and a lack of the aforementioned parabolic shape that the graph tends to with the higher concentrations of surfactant. Hence, the overall change for both Tween 80 and SR Tween 80 were similar with an overall change in  $k'$  values of + 0.43 and + 0.52, with a final  $k'$  of 3.13 and 2.95 respectively.

Etocas 35, Croduret 40 and Crodasol HS HP presented with relatively flat graphs as shown in **Figure 21**, unlike the results with polysorbate 20 and 80, no significant increase or decrease in  $k'$  values were observed across any of the concentrations used. Whilst a slight overall decrease in  $k'$  values as shown in **Table 6** (- 0.03 for Etocas 35, - 0.16 for Croduret 40 and -0.16 for Crodasol HS HP) was observed the difference is negligible.



SDS, as shown in **Figure 21**, presented with a relatively flat section until  $1 \times 10^{-3}$  M after which a sharp decrease in  $k'$  was observed, this sharp decrease correlates with the CMC of SDS ( $6.80 \text{ mM}^{89}$ ). SDS had the greatest overall change in  $k'$  values as shown in **Table 6** (- 2.58), as the other surfactants used in this study were non-ionic nature, a possible explanation for SDS's large reduction in overall  $k'$  could be due to its anionic nature. Further testing with other anionic surfactants would be required to further validate this theory.

Brij 35 as shown in **Figure 21**, presented with a slight decrease across  $1 \times 10^{-8} - 1 \times 10^{-3}$  M followed by a sharp decrease between  $1 \times 10^{-3} - 1 \times 10^{-2}$  M. It had an overall change in  $k'$  value of  $- 0.78$  as shown in **Table 6**.

### **3.6 MLC with Hydrocortisone**

MLC with hydrocortisone using: Tween 20, HP Tween 20, SR Tween 20, Tween 80, HP Tween 80, SR Tween 80, Etocas 35, Croduret 40, Crodasol HS HP, SDS and Brij 35 as the mobile phase at concentrations:  $1 \times 10^{-2}$ ,  $1 \times 10^{-3}$ ,  $1 \times 10^{-4}$ ,  $1 \times 10^{-5}$ ,  $1 \times 10^{-6}$ ,  $1 \times 10^{-7}$ ,  $1 \times 10^{-8}$  M was completed. The results from the experiments are displayed in **Figure 26** and summarised in **Table 7**.

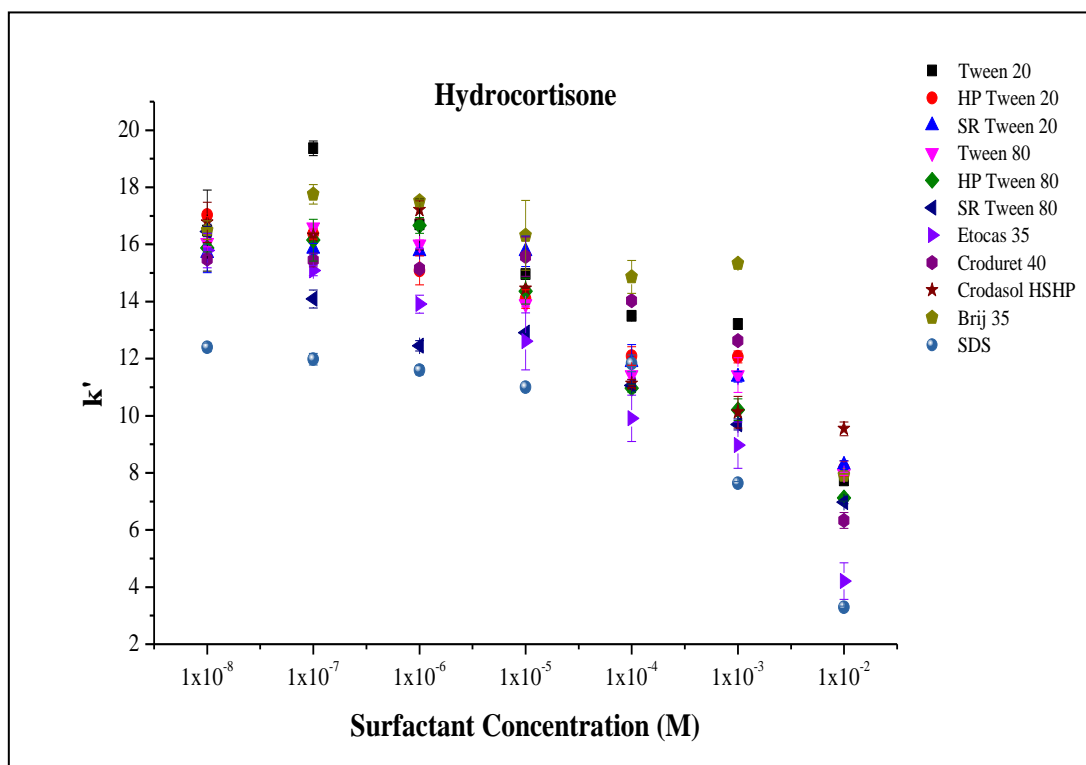


**Figure 26.** MLC with 4-hydroxybenzamide using: Tween 20, HP Tween 20, SR Tween 20, Tween 80, HP Tween 80, SR Tween 80, Etocas 35, Croduret 40, Crodasol HS HP, SDS and Brij 35 as the mobile phase at concentrations:  $1 \times 10^{-2}$ ,  $1 \times 10^{-3}$ ,  $1 \times 10^{-4}$ ,  $1 \times 10^{-5}$ ,  $1 \times 10^{-6}$ ,  $1 \times 10^{-7}$ ,  $1 \times 10^{-8}$  M. Error bars were calculated using the standard deviation from 3 repeats.

**Table 7.** The average  $k'$  values of hydrocortisone with Tween 20, HP Tween 20, SR Tween 20, Tween 80, HP Tween 80, SR Tween 80, Etocas 3, Croduret 40, Crodasol HS HP, SDS and Brij 35 at  $1 \times 10^{-2}$  and  $1 \times 10^{-8}$  M.

Surfactant	Average $k'$ at $1 \times 10^{-8}$ M	Average $k'$ at $1 \times 10^{-2}$ M	Change in average $k'$
Tween 20	16.5	7.7	- 8.8
HP Tween 20	17.0	8.2	- 8.9
SR Tween 20	15.7	8.3	- 7.4
Tween 80	16.1	8.0	- 8.1
HP Tween 80	15.9	7.1	- 8.8
SR Tween 80	16.5	7.0	- 9.5
Etocas 35	15.8	4.2	- 11.6
Croduret 40	15.5	6.3	- 9.2
Crodasol HS HP	16.8	9.5	- 7.3
SDS	12.4	3.3	-9.1
Brij 35	16.5	7.9	- 8.6

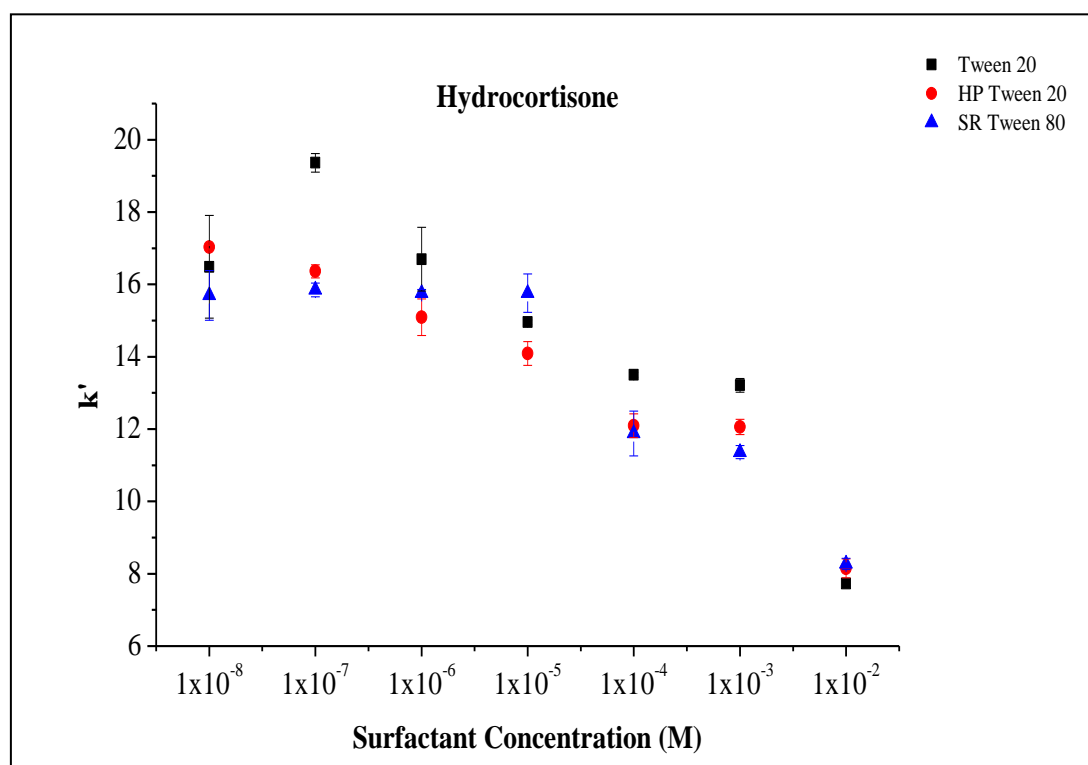


**Figure 27.** MLC with hydrocortisone using: Tween 20, HP Tween 20 and SR Tween 20, as the mobile phase at concentrations:  $1 \times 10^{-2}$ ,  $1 \times 10^{-3}$ ,  $1 \times 10^{-4}$ ,  $1 \times 10^{-5}$ ,  $1 \times 10^{-6}$ ,  $1 \times 10^{-7}$ ,  $1 \times 10^{-8}$  M. Error bars were calculated using the standard deviation from 3 repeats.

Polysorbate 20 was studied at 3 purities, standard, high purity and super refined, a decrease in overall  $k'$  values with increasing surfactant concentration was observed for all purity grades of polysorbate 20 as shown in **Figure 27**. The greatest decrease for each purity grades occurred between  $1 \times 10^{-3}$  and  $1 \times 10^{-2}$  and the second biggest decrease occurred between  $1 \times 10^{-5}$  and  $1 \times 10^{-4}$  M. Prior to these concentrations the graphs presented with a slight decrease in  $k'$  values with increasing surfactant concentration. As previously mentioned, the decrease between  $1 \times 10^{-5}$  and  $1 \times 10^{-4}$  M is within the range of reported values for the CMC of polysorbate 20 as shown in **Table 1** (0.002 – 0.975 mM), which after exceeding, would result in the partitioning of the API into the micellar-pseudo phase and spending less time on the modified stationary phase. This could explain the greater decrease in  $k'$  values observed compared to the decreases in  $k'$  values with increasing surfactant concentration.

Tween 20 and HP Tween 20 exhibited similar decreases in overall  $k'$  values as shown in **Table 7** (- 8.8 and - 8.9 respectively), however, Tween 20 has a lower final  $k'$  value of 7.7 compared with HP Tween 20's final  $k'$  value of 8.2. SR Tween 20 had an overall change in  $k'$  values of - 7.4, and a final  $k'$  value of 8.3 which is close to HP Tween 20's value of 8.3. Each grade of polysorbate 20 exhibited the largest decrease in overall  $k'$  values with hydrocortisone when compared to the overall decreases seen with the other API's in this study.

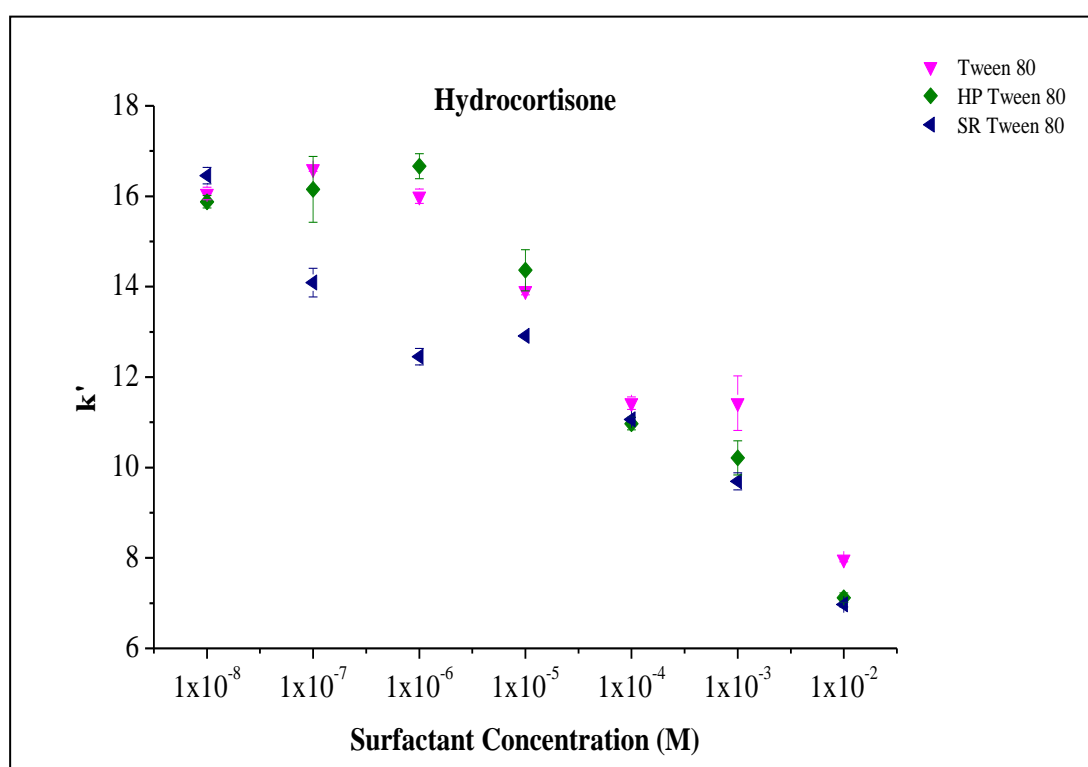


**Figure 28.** MLC with hydrocortisone using: Tween 80, HP Tween 80 and SR Tween 80, as the mobile phase at concentrations:  $1 \times 10^{-2}$ ,  $1 \times 10^{-3}$ ,  $1 \times 10^{-4}$ ,  $1 \times 10^{-5}$ ,  $1 \times 10^{-6}$ ,  $1 \times 10^{-7}$ ,  $1 \times 10^{-8}$  M. Error bars were calculated using the standard deviation from 3 repeats.

Polysorbate 80 was studied at 3 purities, standard, high purity and super refined, as with polysorbate 20, a decrease with increasing surfactant concentration was observed with all purity grades of polysorbate 80, as shown in **Figure 28**. Tween 80 and HP Tween 80 feature relatively flat sections until  $1 \times 10^{-6}$  M, after which a steady decrease in  $k'$  values with increasing surfactant concentration is observed.  $1 \times 10^{-5}$  M is within the range of reported values for the CMC of polysorbate 80 as shown in **Table 1** (0.011 – 0.574 mM).

SR Tween 80 exhibited a decrease with increasing surfactant concentration between  $1 \times 10^{-8}$  -  $1 \times 10^{-6}$  M, followed by a relatively flat section between  $1 \times 10^{-6}$  –  $1 \times 10^{-5}$  M, after which a decrease in  $k'$  values with each subsequent surfactant concentration was observed.

As shown in **Table 7**, SR Tween 80 had the greatest decrease in overall  $k'$  values (- 9.5), when compared to Tween 80 (- 8.1) and HP Tween 80 (- 8.8). Both HP and SR Tween 80 had close final  $k'$  values, 7.1 and 7.0 respectively, however Tween 80 had a markedly higher final  $k'$  value of 8.0. As with polysorbate 20, all the grades of polysorbate 80 had the greatest decrease in overall  $k'$  values with hydrocortisone, when compared to the other APIs in this study. This could be because of the hydrophobic nature of the API compared to the other APIs used, resulting in the API interacting with the micellar-pseudo phase to a greater degree.

Etocas 35 had the greatest decrease in overall  $k'$  values (- 11.6), as shown in **Table 7**, as well as the lowest final  $k'$  value (4.2), when compared to the other surfactants in this study. As shown in **Figure 26**, a decrease with increasing surfactant concentration is observed across all concentrations of Etocas 35, with the biggest decrease occurring between  $1 \times 10^{-3}$  and  $1 \times 10^{-2}$  M.

The graph of the results of Croduret 40, as shown in **Figure 26**, featured a relatively flat section between  $1 \times 10^{-8}$  –  $1 \times 10^{-5}$  M, after which a slight decrease was observed between  $1 \times 10^{-5}$  and  $1 \times 10^{-3}$  M. Following this, a sharp decrease occurred between  $1 \times 10^{-3}$  and  $1 \times 10^{-2}$  M. Croduret 40 had an overall change in  $k'$  values of - 9.2 and a final  $k'$  value of 6.3. As with the other surfactants, the results with hydrocortisone produced the largest overall decrease in  $k'$  values, when compared with the other APIs in this study.

Crodasol HS HP presented with a graph as shown in **Figure 26** containing a relatively flat section between  $1 \times 10^{-8}$  and  $1 \times 10^{-6}$  M, followed by a sharp decrease until  $1 \times 10^{-4}$  M, after which the decreases in  $k'$  values taper off. Crodasol HS HP had an overall reduction of 7.3 in  $k'$  values as well as a final  $k'$

value of 9.5 as shown in **Table 7**. As with the other surfactants in this study, this was the largest overall change observed with this surfactant compared to the results with the other APIs in this study.

Brij 35 had an overall reduction in  $k'$  values of 8.6 and had a final  $k'$  value of 7.9 as shown in **Table 7**. As with the other surfactants in this study, hydrocortisone produced the greatest reduction in  $k'$  values with Brij 35 when compared to the other actives in this study. The graph for Brij 35 as seen in **Figure 26**, initially has a flat section between  $1 \times 10^{-8}$  and  $1 \times 10^{-6}$  M, after which a slight decrease is observed until  $1 \times 10^{-3}$  M. Following this a sharp decrease is observed.

SDS had an overall reduction in  $k'$  values of 9.1 and a final  $k'$  value of 3.3 as shown in **Table 7**. Similarly, to the other surfactants in this study, hydrocortisone produced the greatest reduction in  $k'$  values, when compared to the other actives in this study. The graph for SDS as seen in **Figure 26**, presents with a gradual decrease in  $k'$  values from  $1 \times 10^{-8}$  M –  $1 \times 10^{-5}$  M, after which a slight increase is seen between  $1 \times 10^{-5}$  M and  $1 \times 10^{-4}$  M. Following this is a steep decrease in  $k'$  until the final concentration.

### **3.7 MLC Discussion**

A summary of the changes in  $k'$  for all scenarios is displayed in **Table 8**, followed by Log P and pKa values in **Table 9**

**Table 8.** The ranked overall change in  $k'$  values for each surfactant with each API used in this study. The ranking order is green (the greatest reduction) yellow, orange and red (smallest reduction).

Surfactant	Acetaminophen	Benzamide	4-hydroxybenzamide	Hydrocortisone
Tween 20	0.15	-2.7	-0.69	-8.8
HP Tween 20	-1.76	-3.54	-0.19	-8.9
SR Tween 20	-1.05	-3.23	-0.25	-7.4
Tween 80	-0.33	-1.94	0.43	-8.1
HP Tween 80	-0.26	-2.15	-0.83	-8.8
SR Tween 80	-0.28	-1.47	0.52	-9.5
Etocas 35	-0.19	-2.82	-0.03	-11.6
Croduret 40	-0.18	-1.02	-0.16	-9.2
Crodasol HS HP	-0.09	-1.03	-0.16	-7.3
SDS	-2.42	-3.03	-2.58	-9.1
Brij 35	-2.33	-4.73	-0.78	-8.6

**Table 9.** Ranked Log P and pKa values for the APIs used in this study. The ranking order is green (greatest value), yellow, orange and red (lowest value). Log P and pKa values obtained from PubChem.<sup>87</sup>

API	Log P	pKa
Acetaminophen	0.46	9.4
Benzamide	0.64	13
4-hydroxybenzamide	0.33	8.6
Hydrocortisone	1.61	13.8

When comparing **Table 8** and **Table 9** it becomes apparent that there are some similarities, namely that the greatest reduction in overall  $k'$  values coincides with the API with the greatest Log P and pKa value (hydrocortisone). The same can be said for the second greatest (benzamide), with the results for 3<sup>rd</sup> and 4<sup>th</sup> evenly distributed between the two remaining APIs (4-hydroxybenzamide and acetaminophen) and could be reflective of their closeness in values. APIs that have a high Log P value can be said to be more hydrophobic than those with lower Log P values, which could explain the trend observed with the MLC results. The greater the hydrophobicity of an API the greater the interactions between itself and the stationary phase, this results in a high  $k'$  as the partition equilibrium is greatly in favour of the modified stationary phase, compared to API's with a lower Log P value. Once the CMC threshold is crossed and the second partition equilibrium is introduced the  $k'$  values significantly decrease as the

equilibrium shifts in favour of the mobile phase. As drugs with a lower Log P value have an equilibrium that is initially more in favour of the mobile phase, compared to the those with a high Log P value, the effect is less, represented by the lower reduction in k' values.

It is also worth noting that the purity had a notable impact of k' values, with the SR and HP grades reducing the overall k' values by a greater amount than the standard grade. In addition to that the final k' values were also lower, suggesting the higher purity grade surfactants interact more strongly with the API than the standard grade. As previously mentioned in Section 1.2, the higher purity grade surfactants have less impurities, this would result in less interactions with non-micellar entities within the system, theoretically increasing the interactions that the API would have with the surfactant. However, it is also worth noting that the fatty acid composition of the polysorbates isn't uniform across purity grades and that these differences account for the better performance of the surfactants in terms of k' values.

The Pharmacopeial specifications for the fatty acid composition of polysorbate 20 and 80 are shown in **Table 10**. It is important to note that there aren't any specific values for the fatty acid chain composition, and that instead they are all reported as range.

**Table 10.** The fatty acid composition of polysorbate 20 and polysorbate 80 the values of which are obtained from the USP – NF<sup>92</sup>.

Fatty Acid	Polysorbate 20 Composition percentage	Polysorbate 80 composition percentage
Caproic acid	< 1.0	-
Caprylic acid	< 10.0	-
Capric acid	< 10.0	-
Lauric acid	40.0 – 60.0	-
Myristic acid	14.0 – 25.0	< 5.0
Palmitic acid	7.0 – 15.0	< 16.0
Palmitoelic acid	-	< 8.0
Steric acid	-	< 6.0
Oleic acid	<11.0	> 58.0
Linolenic acid	-	<4.0
Linoleic acid	-	<18.0

As was previously mentioned the composition of fatty acid chains across purity grades is different, this results in differences in performance. Owusu Apenten et al reports that the CMC of a surfactant is



related to the number of oxyethylene units in the surfactant head region, with more oxyethylene units resulting in an increase in the CMC of a surfactant, whilst increasing the length and size of the lipophilic tail region leads to a decrease in CMC value.<sup>93</sup> As each of the fatty acid chains have different sizes, some will result in the surfactant having a longer tail region and therefore a lower CMC. A difference in composition across multiple fatty acids, as is the case between purities, would result in different CMCs and therefore different surfactant-API interactions. Further experiments on how specific fatty acid compositions affect MLC would be required to prove this. This would be done by taking surfactant batches with known fatty-acid compositions and seeing how those differences impact retention times in MLC.

It is also important to consider the structure of each surfactant and the impact that this can have on interactions with APIs. Structurally Tween 20 and Tween 80 are very similar, however Tween 80 has a carbon-carbon double bond present in one of its chains, which will reduce its flexibility in terms of rotation and therefore provide a degree of steric hinderance that is not present in Tween 20. The same can be said for both Etocas 35 and Croduret 40, where Etocas 35 has a carbon-carbon double bond on each of its chains and Croduret 40 does not. The steric hindrance caused by the carbon-carbon double bonds will have an impact and is only one of several factors such as Log P and hydrophobicity that dictate where each of the APIs position themselves within the micelle. Crodasol HS HP, SDS and Brij 35 are all single chain surfactants, however, Crodasol HS HP has a greater chain length and will therefore have greater hydrophobic interactions, resulting in stronger interactions with the stationary phase and therefore longer retention times.

Rukhadze investigated how altering the concentration of Tween 80 in the mobile phase between 0.75 - 4 % affected retention time. Rukhadze also used a C<sub>18</sub> column, creating the same modified stationary phase that was present in experiments involving Tween 80 as the mobile phase. It was found that increasing the concentration of Tween 80 from 0.75 % - 1.5 % w/v reduced the retention factor for all 8 of the APIs tested whereas increasing it to 4 % increased retention time in some cases.<sup>94</sup> The highest concentration of Tween 80 used in the experiments with acetaminophen, benzamide and 4-

hydroxybenzamide was  $1 \times 10^{-2}$  M (1.39 % w/v). A similar reduction in retention time was observed for both acetaminophen and benzamide at 1.39 % w/v, but conversely an increase was exhibited with 4-hydroxybenzamide.

SDS is widely used in MLC and has been consistently reported to reduce retention time with increasing concentration in the mobile phase. Hadjmohammadi stated that increasing the concentration of SDS from 0.07 M to 0.09 M reduced the retention time of the 14 APIs that were tested.<sup>95</sup> For this study a C18 column was also used, producing the same modified stationary phase that would have been present in the experiments with acetaminophen, benzamide and 4-hydroxybenzamide when SDS was used as the mobile phase. In a paper on the separation optimisation of APIs in honey, Hadjmohammadi reported that increasing the SDS concentration from 0.07 M to 0.13 M reduced the retention time of all of the APIs tested, a C18 column was also used in this study.<sup>96</sup> Safa reported that increasing the concentration of SDS from 0.01 M to 0.09 M reduced the retention time for each of the 6 halogenated phenols analysed, a C18 column was also used in this study.<sup>97</sup> Their findings aligned with results obtained in this study from MLC with acetaminophen, benzamide and 4-hydroxybenzamide, where increasing the concentration of SDS resulted in an increase in retention time.

Peris-Garcia examined how increasing the concentration of Brij 35 from 0.01 M – 0.05 M affected retention times for 6 APIs, a C18 column was also used for this. It was shown for each of the APIs that increasing concentration resulted in a decrease of retention time.<sup>98</sup> The same was found by Mutelet where a concentration range of 0.05 M – 0.1 M was used.<sup>99</sup> These results align with the results presented here using MLC with acetaminophen, benzamide and 4-hydroxybenzamide and Brij 35 as the mobile phase, where increasing surfactant concentration resulted in a decrease in retention time.

### **3.8 pH Testing**

It was hypothesised that differences in retention time were caused by variations in the pH of the surfactants over the range of concentrations studied, thus approaching the pKa of the APIs. To resolve

this issue pH testing of each surfactant at each concentration was conducted using a pH probe at 31 °C, as displayed in **Table 11**.

**Table 11.** pH values for Tween 20, HP Tween 20, SR Tween 20, Tween 80, HP Tween 80, SR Tween 80, Etocas 35, Croduret 40, Crodasol HS HP, SDS and Brij 35 at concentrations:  $1 \times 10^{-2}$ ,  $1 \times 10^{-3}$ ,  $1 \times 10^{-4}$ ,  $1 \times 10^{-5}$ ,  $1 \times 10^{-6}$ ,  $1 \times 10^{-7}$ ,  $1 \times 10^{-8}$  M

Surfactant	$1 \times 10^{-2}$	$1 \times 10^{-3}$	$1 \times 10^{-4}$	$1 \times 10^{-5}$	$1 \times 10^{-6}$	$1 \times 10^{-7}$	$1 \times 10^{-8}$
<b>Tween 20</b>	4.5	5.0	5.2	5.3	5.0	5.0	5.0
<b>HP Tween 20</b>	4.9	5.3	4.6	5	4.9	4.9	4.9
<b>SR Tween 20</b>	5.2	5.2	5.3	5.3	5.3	5.1	5.2
<b>Tween 80</b>	5.9	5.8	5.5	5.4	5.4	5.3	5.2
<b>HP Tween 80</b>	4.2	4.5	5	5	5.2	5.3	5.3
<b>SR Tween 80</b>	5.4	5.5	5.1	5.4	5.4	5.4	5.4
<b>Etocas 35</b>	5.9	5.6	5.4	5.2	5.2	5.3	5.2
<b>Croduret 40</b>	5.8	5.4	5.6	5.4	5.4	5.4	5.2
<b>Crodasol HS HP</b>	5.5	5.3	5.4	5.4	5.3	5.2	5.2
<b>Brij 35</b>	5.4	5.4	5.5	5.3	5.3	5.4	5.3
<b>SDS</b>	5.8	5.5	5.5	5.5	5.3	5.5	5.6

When compared with the pKa values listed in **Table 3** it was clear that differences in pH couldn't be the direct cause of changes in retention time observed and therefore, the results were a consequence of micellisation events.

The effect of different concentrations of Tween 20, HP Tween 20, SR Tween 20, Tween 80, HP Tween 80, SR Tween 80, Etocas 35, Croduret 40, Crodasol HS HP, SDS, Brij 35 as the mobile phase in MLC with acetaminophen, benzamide, 4-hydroxybenzamide and hydrocortisone were analysed. It was found that the CMC of polysorbate 20, polysorbate 80, SDS and Brij 35 paired closely with the change point of the resulting graphs. The Log P of an API also impacted significantly on how increasing concentration of surfactant effected k' values, with a lower Log P incurring a significant change in k' values, as exhibited by hydrocortisone.

## 4. Solubility Enhancement

In order to better understand the impact that surfactant concentration has on the APIs used in this study, the solubility of each API across a range of surfactant concentrations was measured using HPLC. This will allow for a greater understanding of the impact surfactant concentration and surfactant purity has on the solubility of acetaminophen, benzamide, 4-hydroxybenzamide and hydrocortisone. This section contains work that was published prior to submission of my thesis.<sup>88</sup>

### 4.1 Calibrations

Prior to analysing the four model compounds in the presence of surfactants, a calibration plot was established for each compound. Calibration graphs for acetaminophen, benzamide, 4-hydroxybenzamide and hydrocortisone were completed using the methodology presented in Section 2.5 and the resulting graphs are shown in **Figure 29**, **Figure 30**, **Figure 31** and **Figure 32** respectively.

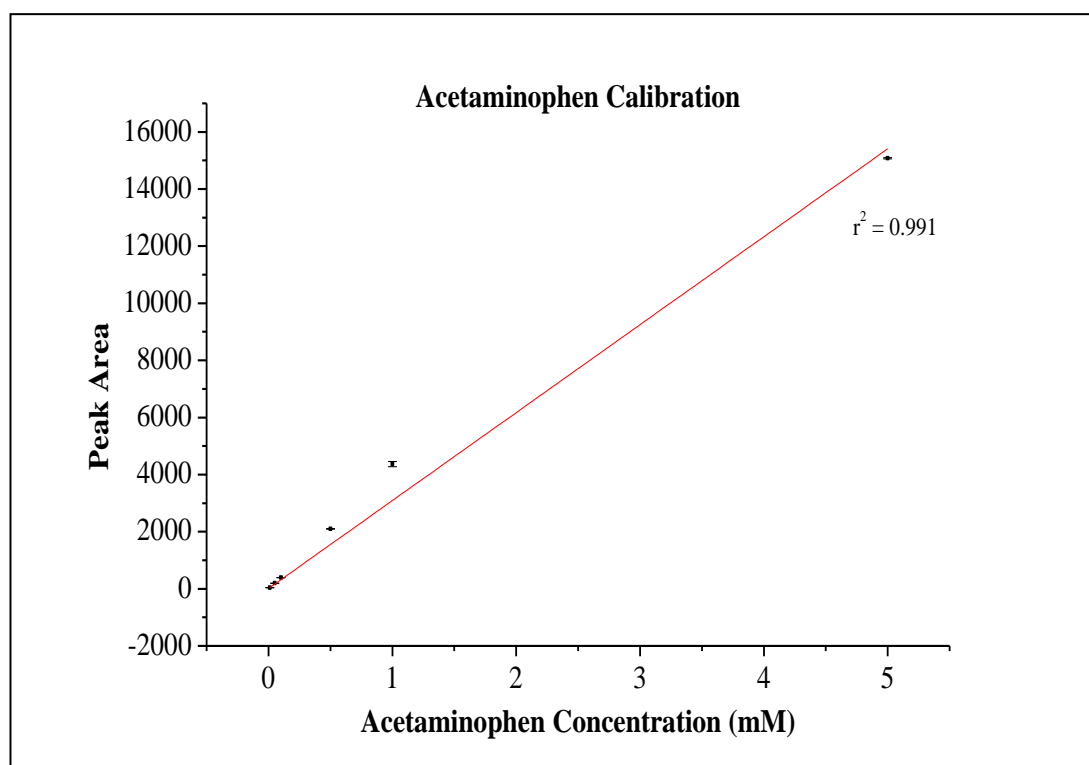


**Figure 29.** Acetaminophen calibration graph with an  $r^2$  value of 0.991.

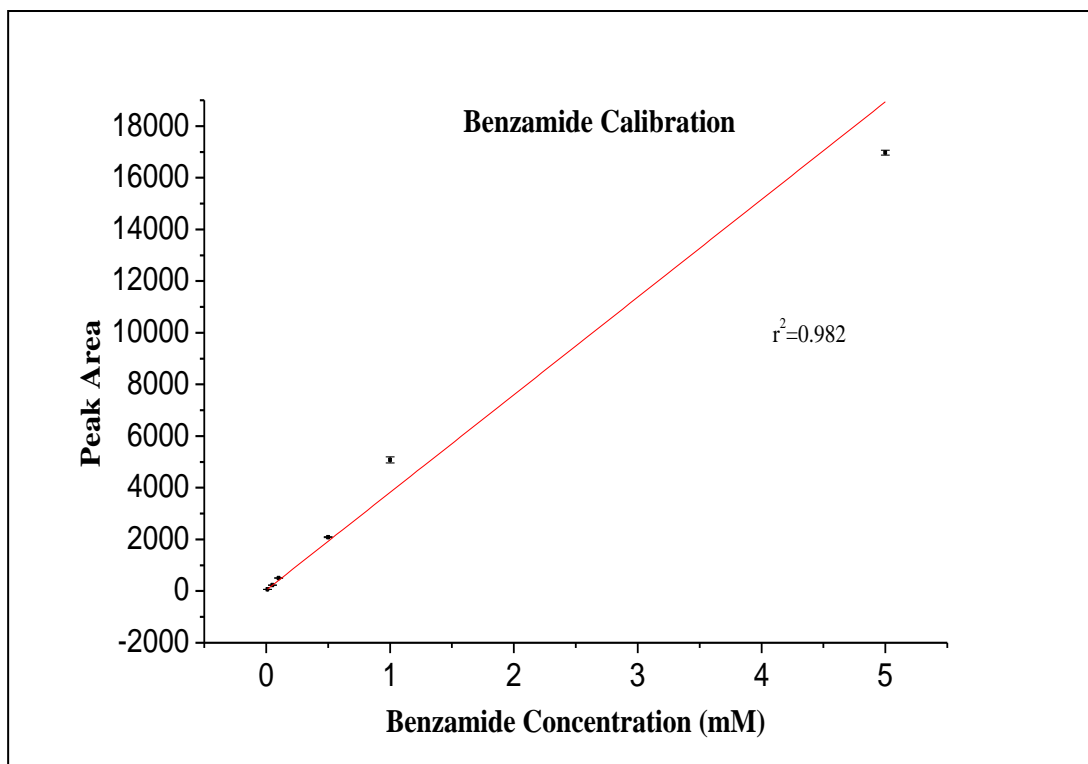


Figure 30. Benzamide calibration graph with an  $r^2$  value of 0.982.

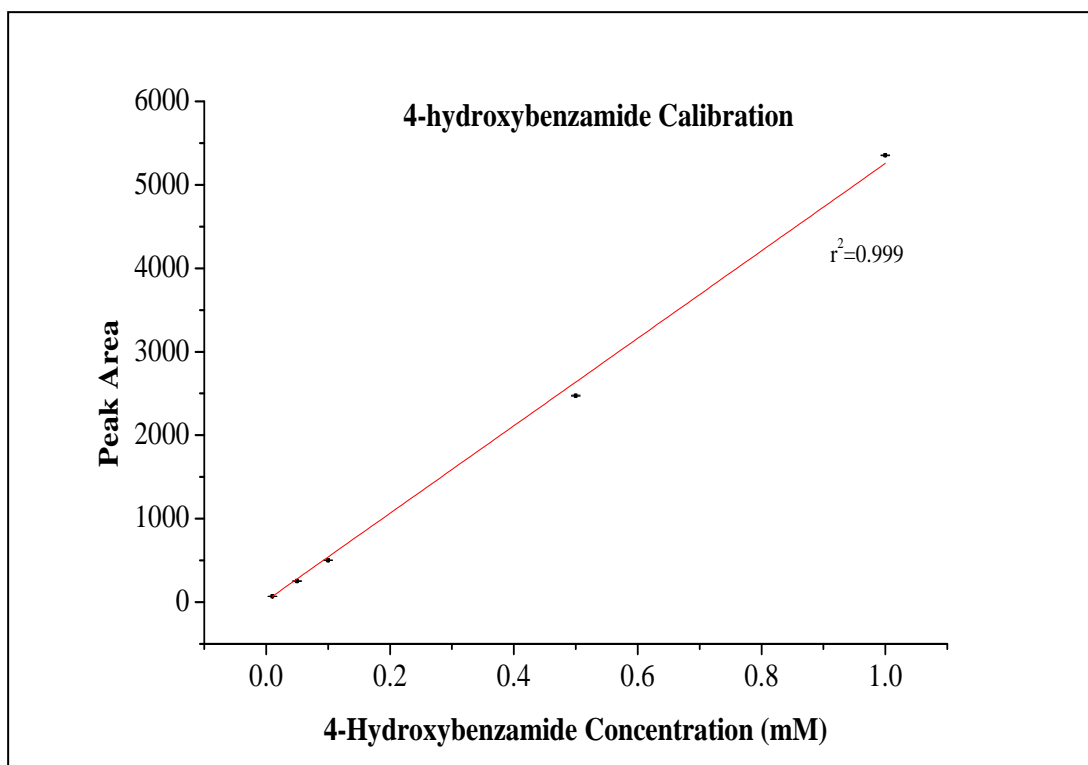
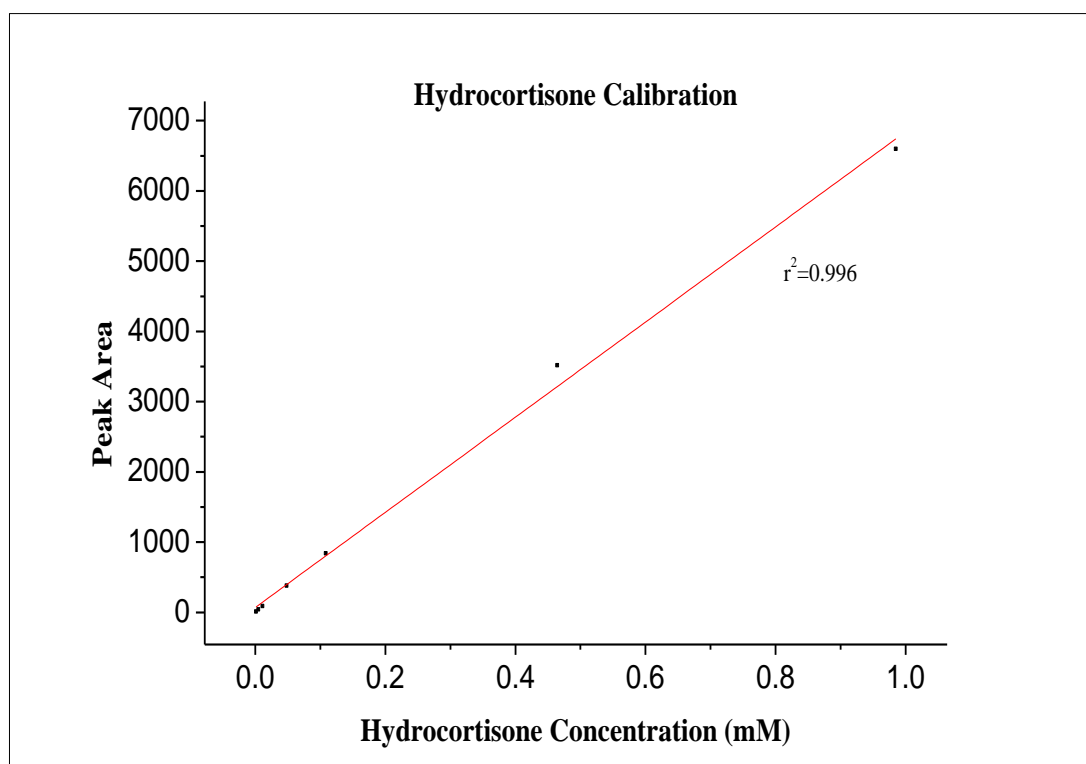


Figure 31. 4-hydroxybenzamide calibration graph with an  $r^2$  value of 0.999.



**Figure 32.** Hydrocortisone calibration graph with an  $r^2$  value of 0.996.

The concentration of APIs used for the calibration graphs were chosen because of earlier solubility trials, where the solubilities were calculated to be between 0.01 – 0.1 mM. This appeared to result in a leverage affect where higher concentrations did not align with lower ones and resulted in a line of best fit that was that did not intersect all of the data points. In future experiments, more concentrations will be used for calibrations at intervals of 0.1 mM, with the aim of reducing the leverage affect caused by the higher concentrations.

## 4.2 Solubility of Acetaminophen

The determination of the solubility of acetaminophen in Tween 20, HP Tween 20, SR Tween 20, Tween 80, HP Tween 80, SR Tween 80, Etocas 35, Croduret 40, Crodasol HS HP, SDS and Brij 35 was completed using the method detailed in Section 2.5. A graph displaying the results is presented in **Error! Reference source not found.** and the improvement in solubility compared with the aqueous experimental value (15.1 mg/mL) is shown in **Table 12.**

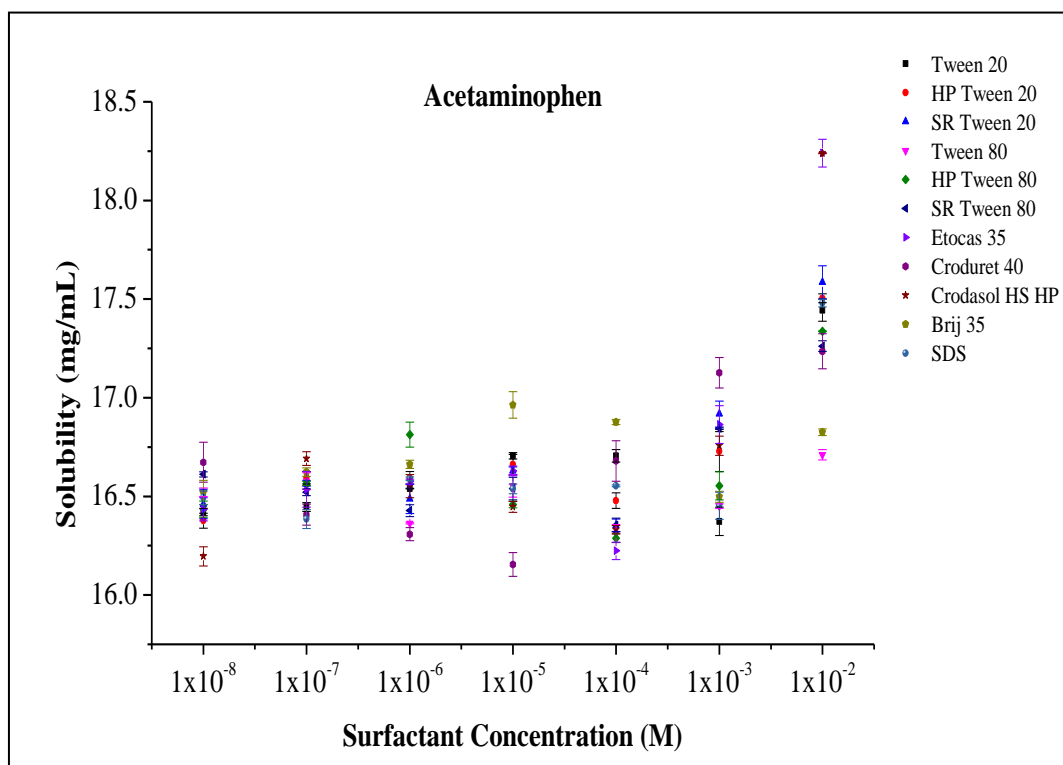


**Figure 35.** Solubility determination of acetaminophen in the presence of Tween 20, HP Tween 20, SR Tween 20, Tween 80, HP Tween 80, SR Tween 80, Etocas 35, Croduret 40, Crodasol HS HP, SDS, Brij 35 at surfactant concentrations of  $1 \times 10^{-2}$ ,  $1 \times 10^{-3}$ ,  $1 \times 10^{-4}$ ,  $1 \times 10^{-5}$ ,  $1 \times 10^{-6}$ ,  $1 \times 10^{-7}$  and  $1 \times 10^{-8}$  M<sup>8</sup> at 31°C. Error bars were calculated using the standard deviation from 3 repeats.

**Table 12.** Solubility of acetaminophen in Tween 20, HP Tween 20, SR Tween 20, Tween 80, HP Tween 80, SR Tween 80, Etocas 35, Croduret 40, Crodasol HS HP, SDS and Brij 35 at  $1 \times 10^{-2}$  M.

Surfactant	Solubility (mg/mL)	Solubility improvement compared with Aq (mg/mL)
No Surfactant	15.1	n/a
Tween 20	17.4	+ 2.3
HP Tween 20	17.5	+ 2.4
SR Tween 20	17.6	+ 2.5
Tween 80	16.7	+ 1.6
HP Tween 80	17.3	+ 2.2
SR Tween 80	17.3	+ 2.2
Etocas 35	18.2	+ 3.1
Croduret 40	17.2	+ 2.1
Crodasol HS HP	18.2	+ 3.1
SDS	17.5	+ 2.4
Brij 35	16.8	+ 1.7

An improvement in solubility was recorded for all surfactants, with the greatest improvement occurring at the highest concentration of surfactant solution. **Error! Reference source not found.** shows a clear general trend of increasing solubility with increasing surfactant concentration, with the greatest increases happening after  $1 \times 10^{-4}$  M, which could indicate a CMC threshold. This would align with the results in Section 3, where after the CMC was reached, a large change in  $k'$  values occurred. An increase in the maximum solubility of acetaminophen in the presence of non-ionic surfactant was also reported by Hamza et al, who recorded an increase in solubility of 5-7 fold when using a mixture of non-ionic surfactants.<sup>100</sup> This increase is significantly greater than what was observed in **Table 12**, and was the result of the optimisation of several surfactants blends, designed around enhancing solubility.

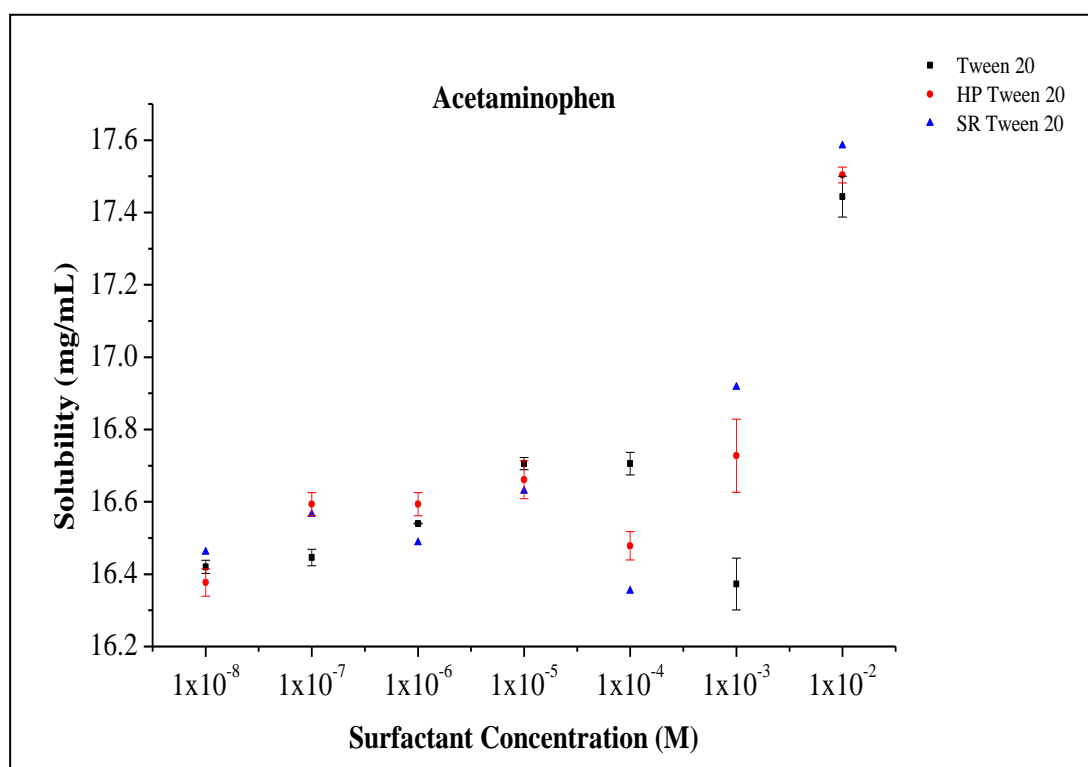


**Figure 33.** Solubility determination of acetaminophen in the presence of Tween 20, HP Tween 20, SR Tween 20, at surfactant concentrations of  $1 \times 10^{-2}$ ,  $1 \times 10^{-3}$ ,  $1 \times 10^{-4}$ ,  $1 \times 10^{-5}$ ,  $1 \times 10^{-6}$ ,  $1 \times 10^{-7}$  and  $1 \times 10^{-8}$  M<sup>8</sup> at 31°C. Error bars were calculated using the standard deviation from 3 repeats.



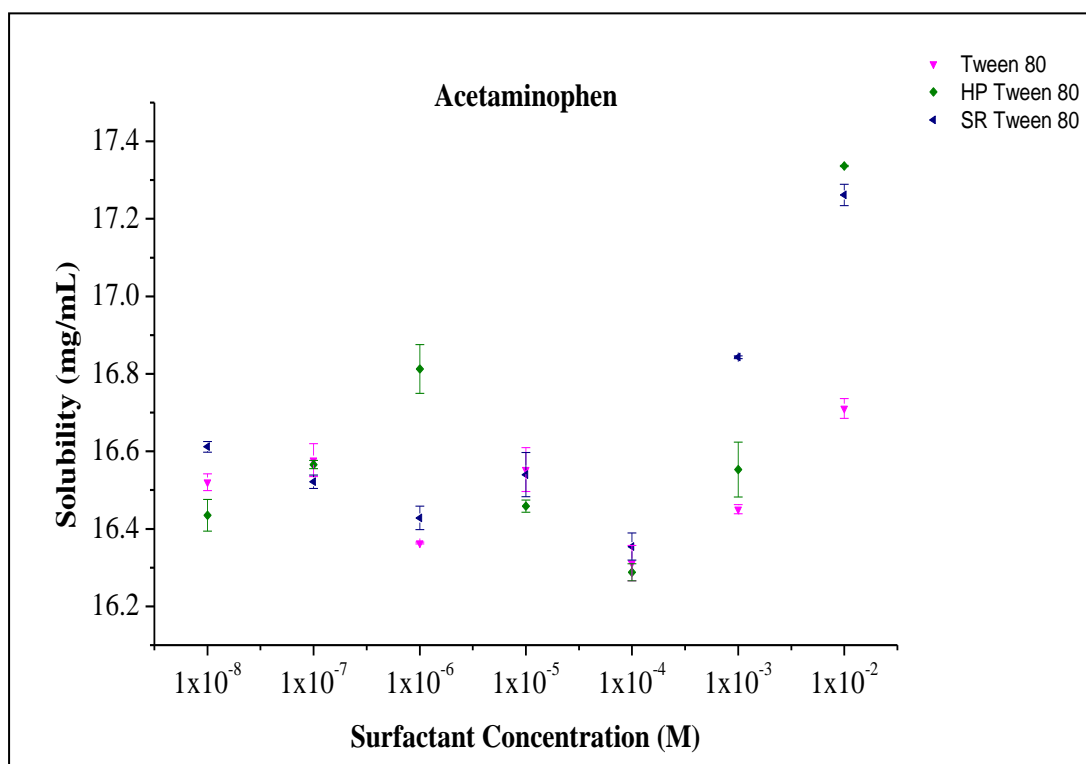


**Figure 34.** Solubility determination of acetaminophen in the presence of Tween 80, HP Tween 80, SR Tween 80, at surfactant concentrations of  $1 \times 10^{-2}$ ,  $1 \times 10^{-3}$ ,  $1 \times 10^{-4}$ ,  $1 \times 10^{-5}$ ,  $1 \times 10^{-6}$ ,  $1 \times 10^{-7}$  and  $1 \times 10^{-8}$  M<sup>8</sup> at 31°C. Error bars were calculated using the standard deviation from 3 repeats.

For two of the surfactants considered a range of purities was analysed. Data specifically for the two scenarios are presented in **Figure 33** for polysorbate 20 and **Figure 34** for polysorbate 80. **Figure 33** and **Figure 34** indicate that higher purity grade polysorbates outperform the standard grade in terms of solubility enhancement. As previously discussed in the introduction, the higher purity grades of polysorbates 20 and 80 contain a lower moisture content, in addition to lower levels of impurities such as peroxides as well as a slightly different composition of fatty-acid chains. These lower levels of impurities and differences in composition help to increase the solubilisation of the API in the micellar phase resulting in the greater solubility enhancement observed.

Alongside experimental solubilisation data it was possible to further consider each drug using a more theoretical approach. As the CMC for polysorbate 20, polysorbate 80, Etocas 35, Croduret 40, Crodasol HS HP, SDS and Brij 35 is known the molar solubilisation capacity ( $\chi$ ), micelle-water partition coefficient (P) and the molar micelle-water partition coefficient ( $P_M$ ) for each can be calculated using

**Equation 11, Equation 12, Equation 14** as shown by Rangel-Yagui et al and the derived values are shown in **Table 13**.<sup>39</sup>

**Table 13.** The derived values of the molar solubilisation capacity ( $\chi$ ), micelle-water partition coefficient (P) and the molar micelle-water partition coefficient ( $P_M$ ) for acetaminophen with Tween 20, HP Tween 20, SR Tween 20, Tween 80, HP Tween 80, SR Tween 80, Etocas 35, Croduret 40, Crodasol HS HP, SDS and Brij 35. Where  $S_{Tot}$  is the total amount of acetaminophen solubilised,  $S_w$  is the water solubility of acetaminophen (value determined experimentally),  $C_{Surf}$  is the surfactant concentration and CMC is the critical micelle concentration (using the derived values for Tween 20, HP Tween 20, SR Tween 20, Tween 80 HP Tween 80, SR Tween 80, Etocas 35, Croduret 40 and Crodasol HS HP from Section 6).

Surfactant	$S_{Tot}$ (M)	$S_w$ (M)	$C_{Surf}$ (M)	CMC (mM)	$\chi$	P	$P_M$
Tween 20	0.115	0.100	0.10	0.675	1.632	0.152	16.323
HP Tween 20	0.116	0.100	0.010	0.208	1.621	0.159	16.228
SR Tween 20	0.116	0.100	0.010	0.358	1.702	0.164	17.028
Tween 80	0.111	0.100	0.010	0.627	1.136	0.107	11.368
HP Tween 80	0.115	0.100	0.010	0.546	1.581	0.150	15.823
SR Tween 80	0.114	0.100	0.010	0.627	1.525	0.143	15.252
Etocas 35	0.121	0.100	0.010	0.447	2.174	0.208	21.758
Croduret 40	0.114	0.100	0.010	0.425	1.472	0.141	14.726
Crodasol HS HP	0.121	0.100	0.010	0.425	2.169	0.208	21.708
SDS	0.116	0.100	0.010	8.200 <sup>89</sup>	8.747	0.158	86.846
Brij 35	0.111	0.100	0.010	0.090 <sup>90</sup>	1.148	0.114	11.493

The values in **Table 13** mirror the results in **Table 12**, which is to be expected given the origins of the values used. However, it is interesting to note that Etocas 35 and Crodasol HS HP have the greatest P value yet was outperformed by SDS in terms of  $\chi$  value. This is interesting as it is suggested by Rangel-Yagui et al that the lower the CMC of a surfactant the greater the solubilising ability of it, therefore it could be expected that a surfactant with a CMC an order of magnitude lower than another would outperform it, which wasn't what was observed in the results.<sup>39</sup> This suggests that there are other, significant factors that contribute to the solubilising ability of a surfactant such as charge or stereochemical factors.

### 4.3 Solubility of Benzamide

The determination of the maximum solubility of benzamide in Tween 20, HP Tween 20, SR Tween 20, Tween 80, HP Tween 80, SR Tween 80, Etocas 35, Croduret 40, Crodasol HS HP, SDS and Brij 35 was completed using the method detailed in Section 2.5. A graph showing the results are presented in

**Figure 35** and the improvement in solubility compared with the aqueous experimental value (14.3 mg/mL) is shown in

**Table 14.**

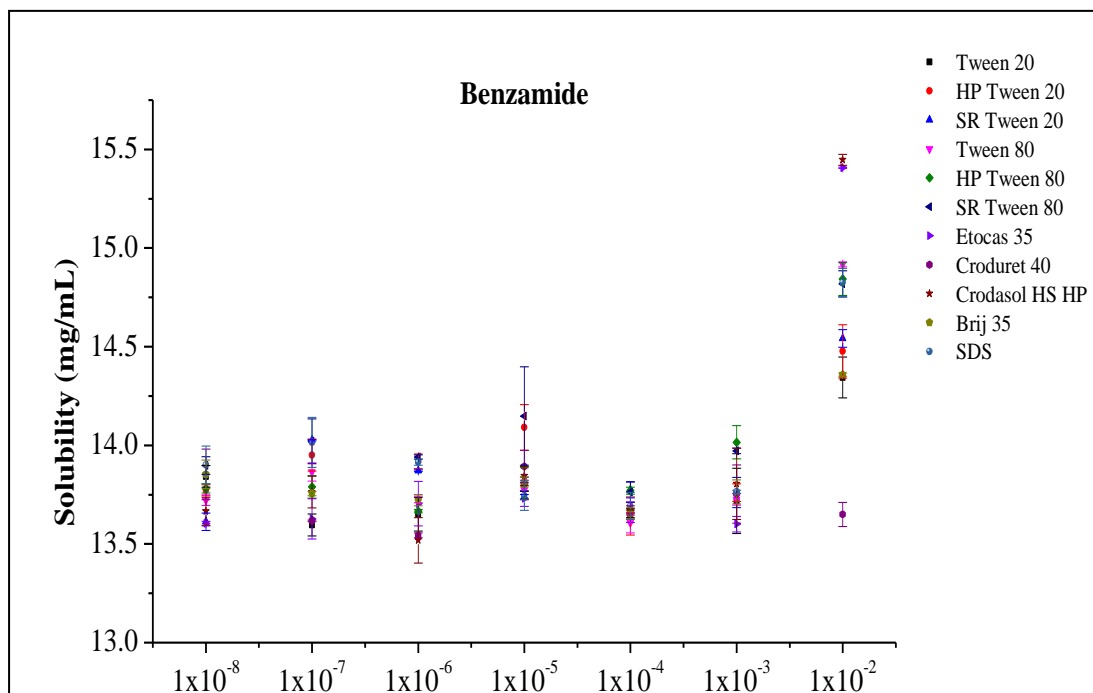


**Figure 35.** Solubility determination of benzamide in the presence of Tween 20, HP Tween 20, SR Tween 20, Tween 80, HP Tween 80, SR Tween 80, Etocas 35, Croduret 40, Crodasol HS HP, SDS, Brij 35 at surfactant concentrations of  $1 \times 10^{-2}$ ,  $1 \times 10^{-3}$ ,  $1 \times 10^{-4}$ ,  $1 \times 10^{-5}$ ,  $1 \times 10^{-6}$ ,  $1 \times 10^{-7}$  and  $1 \times 10^{-8}$  M<sup>8</sup> at 31°C. Error bars were calculated using the standard deviation

**Table 14.** Solubility of benzamide in Tween 20, HP Tween 20, SR Tween 20, Tween 80, HP Tween 80, SR Tween 80, Etocas 35, Croduret 40, Crodasol HS HP, SDS and Brij 35 at  $1 \times 10^{-2}$  M.

Surfactant	Solubility (mg/mL)	Solubility improvement compared to Aq (mg/mL)
No Surfactant	14.3	n/a
Tween 20	14.3	± 0.0
HP Tween 20	14.5	± 0.2
SR Tween 20	14.5	± 0.2
Tween 80	14.9	± 0.6
HP Tween 80	14.8	± 0.5
SR Tween 80	14.8	± 0.5
Etocas 35	15.4	± 1.1
Croduret 40	13.6	- 0.7
Crodasol HS HP	15.4	± 1.1
SDS	14.8	± 0.5
Brij 35	14.4	± 0.1

The solubility enhancement observed for benzamide is very slight and less than half of that which was observed for acetaminophen. This is similar to the comparison between acetaminophen and benzamide in Section 3 when analysed via MLC. In Section 3, acetaminophen gave a more noticeable difference in retention time as surfactant concentration increased, whereas benzamide produced a flatter graph with a small change being shown. It is worth noting that Croduret 40 produced a decrease in solubility at  $1 \times 10^{-2}$  M, however, the error bars (which are calculated as the standard deviation for 3 repeats) for the result are within the aqueous solubility values (14.3 mg/mL). Therefore, it is more reasonable to assume that no increase was observed instead of a decrease in solubility. The greatest increase in solubility was produced by both Etocas 35 and Crodasol HS HP with an increase of 1.1 mg/mL.

Focusing on the solubility enhancement regarding surfactant purity, **Figure 37** and **Figure 36** display the results of the different grades of polysorbate 20 and polysorbate 80.

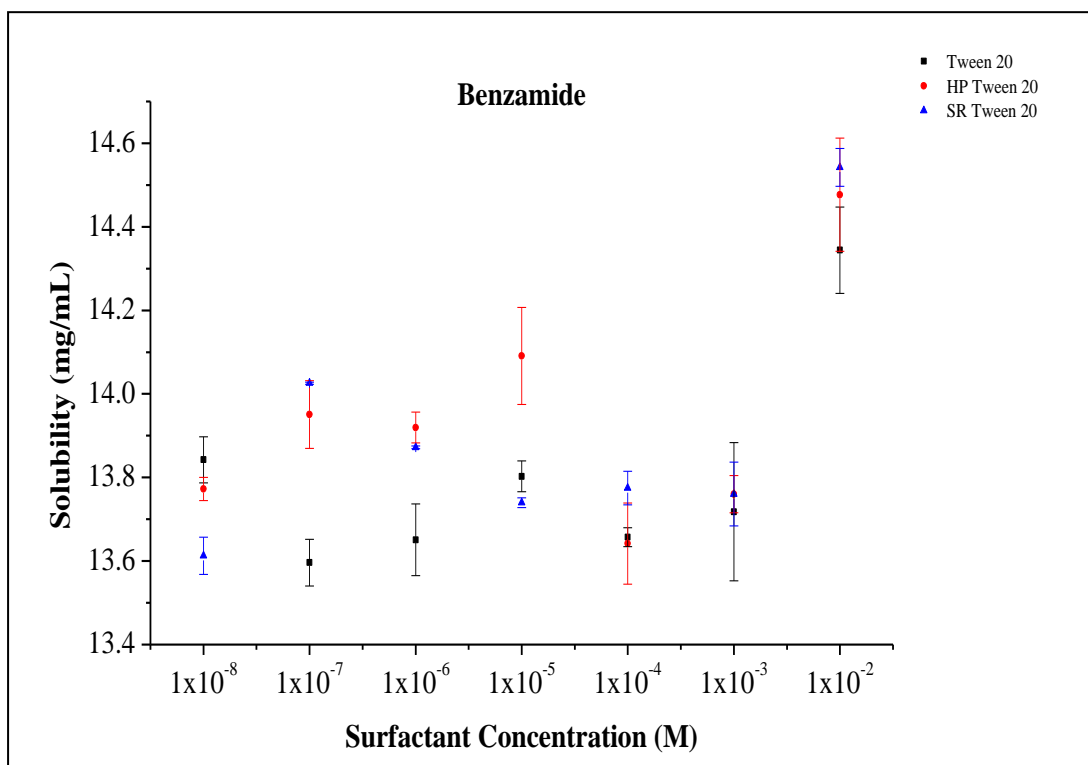


**Figure 37.** Solubility determination of benzamide in the presence of Tween 20, HP Tween 20, SR Tween 20, at surfactant concentrations of  $1 \times 10^{-2}$ ,  $1 \times 10^{-3}$ ,  $1 \times 10^{-4}$ ,  $1 \times 10^{-5}$ ,  $1 \times 10^{-6}$ ,  $1 \times 10^{-7}$  and  $1 \times 10^{-8}$  M<sup>8</sup> at 31°C. Error bars were calculated using the standard deviation from 3 repeats.

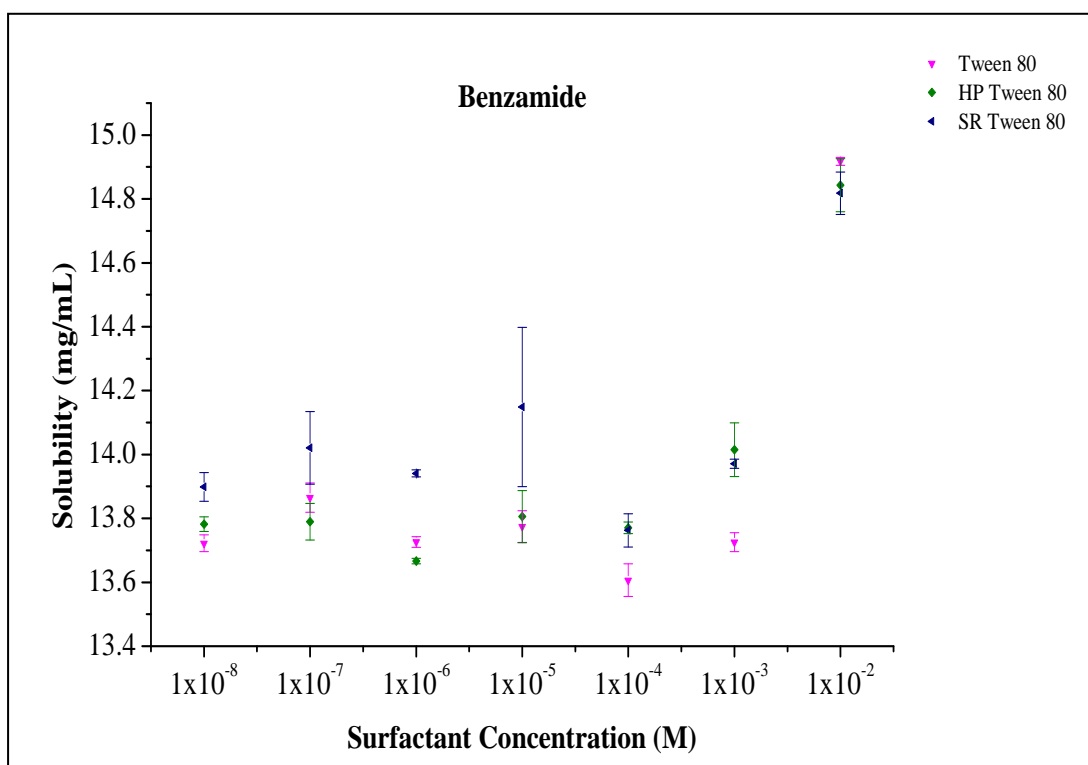


**Figure 36.** Solubility determination of benzamide in the presence of Tween 80, HP Tween 80, SR Tween 80, at surfactant concentrations of  $1 \times 10^{-2}$ ,  $1 \times 10^{-3}$ ,  $1 \times 10^{-4}$ ,  $1 \times 10^{-5}$ ,  $1 \times 10^{-6}$ ,  $1 \times 10^{-7}$  and  $1 \times 10^{-8}$  M<sup>8</sup> at 31°C. Error bars were calculated using the standard deviation from 3 repeats.

As expected, the higher purity grades of Tween 20, i.e. SR and HP, outperformed the standard grade with an improvement of 0.2 mg/mL for both SR and HP. However, the standard grade of Tween 80 outperforms both the SR and HP grade with an improvement of 0.6 mg/mL for the standard grade and an improvement of 0.5 mg/mL for both the SR and HP grades. It should be considered, given the close grouping of the results and overlapping error bars that the differences between them are slight enough to be negligible. It is interesting to note that polysorbate 20 outperformed polysorbate 80 in terms of  $k'$  reduction in MLC in Section 3.4, suggesting that benzamide interacts more strongly with polysorbate 20 than 80. However, as seen in

**Table 14**, polysorbate 20 produced the greater increase in solubility. This would suggest that the interactions that results in an increase in solubility are different to those which resulted in a decrease in  $k'$  values in MLC, and likely the result of structural differences between the polysorbates, namely the alkene bond which features in the tail groups of polysorbate 80, which aren't present in polysorbate 20.

Using the derived maximum solubility values, in conjunction with other properties allows for calculation of the molar solubilisation value ( $\chi$ ), micelle-water partition coefficient (P) and the molar micelle-water partition coefficient ( $P_M$ ) using the equations shown in Section 4.2. The derived values are shown in **Table 15**. Similarly, to the results with acetaminophen in Section 4.2, Etocas 35 has a higher P value but lower  $\chi$  value than SDS, providing further evidence that factors other than CMC influence the solubilisation ability of surfactants.

Surfactant	Solubility (mg/mL)	Solubility improvement compared to Aq (mg/mL)
No Surfactant	14.3	n/a
Tween 20	14.3	+ 0.0
HP Tween 20	14.5	+ 0.2
SR Tween 20	14.5	+ 0.2
Tween 80	14.9	+ 0.6
HP Tween 80	14.8	+ 0.5
SR Tween 80	14.8	+ 0.5
Etocas 35	15.4	+ 1.1
Croduret 40	13.6	- 0.7
Crodasol HS HP	15.4	+ 1.1
SDS	14.8	+ 0.5
Brij 35	14.4	+ 0.1

**Table 15.** The derived values of the molar solubilisation capacity ( $\chi$ ), micelle-water partition coefficient (P) and the molar micelle-water partition coefficient ( $P_M$ ) for benzamide with Tween 20, HP Tween 20, SR Tween 20, Tween 80, HP Tween 80, SR Tween 80, Etocas 35, Croduret 40, Crodasol HS HP, SDS and Brij 35. Where  $S_{Tot}$  is the total amount of acetaminophen solubilised,  $S_w$  is the water solubility of benzamide (value determined experimentally),  $C_{Surf}$  is the surfactant concentration and CMC is the critical micelle concentration (using the derived values for Tween 20, HP Tween 20, SR Tween 20, Tween 80, HP Tween 80, SR Tween 80, Etocas 35, Croduret 40 and Crodasol HS HP from Section 6).

Surfactant	$S_{Tot}$ (M)	$S_w$ (M)	$C_{Surf}$ (M)	CMC (mM)	$\chi$	P	$P_M$
Tween 20	0.118	0.118	0.010	0.675	0.035	0.003	0.300
HP Tween 20	0.122	0.118	0.010	0.208	0.388	0.032	3.284
SR Tween 20	0.120	0.118	0.010	0.358	0.205	0.017	1.740
Tween 80	0.123	0.118	0.010	0.627	0.537	0.043	4.548
HP Tween 80	0.123	0.118	0.010	0.546	0.472	0.038	3.992
SR Tween 80	0.122	0.118	0.010	0.627	0.449	0.036	3.803
Etocas 35	0.127	0.118	0.010	0.447	0.959	0.078	8.122
Croduret 40	0.113	0.118	0.010	0.425	-0.560	-0.045	-4.745
Crodasol HS HP	0.128	0.118	0.010	0.425	0.991	0.080	8.395
SDS	0.122	0.118	0.010	8.200 <sup>89</sup>	2.385	0.036	20.036
Brij 35	0.119	0.118	0.010	0.090 <sup>90</sup>	0.050	0.004	0.423

This is the first study to consider enhancing the solubility of benzamide using surfactants therefore it was not possible to compare the enhancements observed here with published values. However, comparing the enhancements observed for this drug with the previously considered acetaminophen reinforces the belief that surfactants can enhance the solubility of benzamide to an appreciable extent.

#### 4.4 Solubility of 4-Hydroxybenzamide

The determination of the solubility of 4-hydroxybenzamide in Tween 20, HP Tween 20, SR Tween 20, Tween 80, HP Tween 80, SR Tween 80, Etocas 35, Croduret 40, Crodasol HS HP, SDS and Brij 35 was completed using the method detailed in Section 2.5. A graph displaying the results are presented in **Figure 38** and the improvement in solubility compared with the aqueous experimental value (9.3 mg/mL) is shown in **Table 16**.

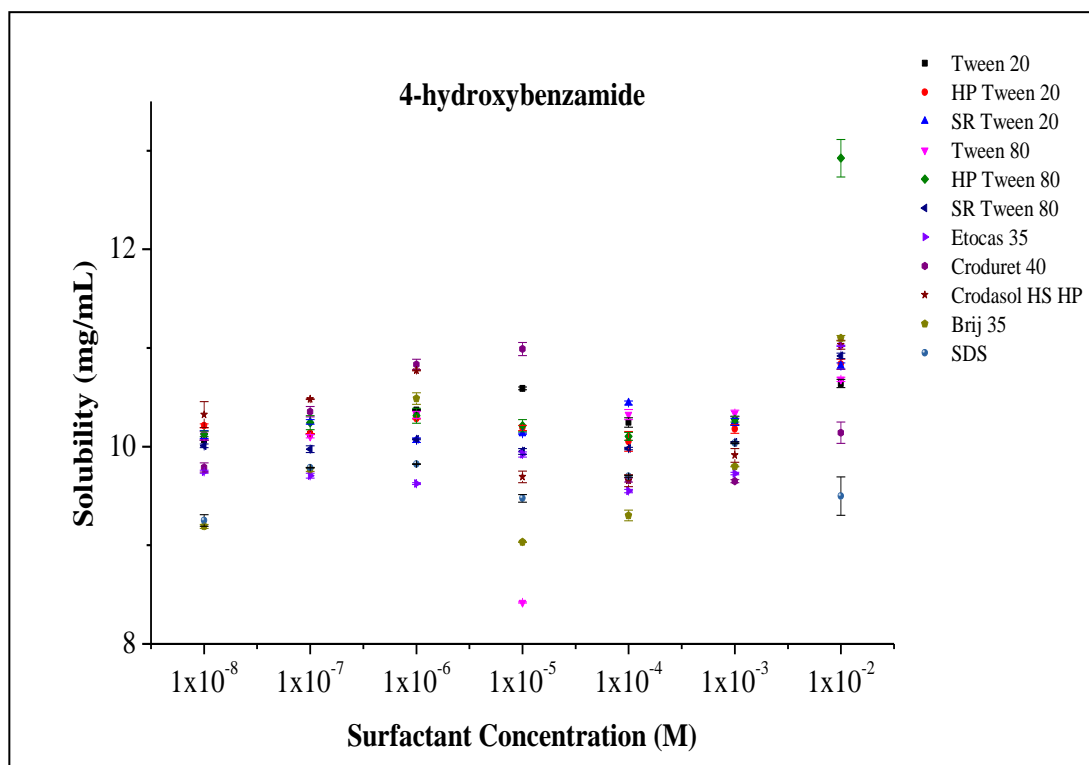


**Figure 38.** Solubility determination of 4-hydroxybenzamide in the presence of Tween 20, HP Tween 20, SR Tween 20, Tween 80, HP Tween 80, SR Tween 80, Etocas 35, Croduret 40, Crodasol HS HP, SDS, Brij 35 at surfactant concentrations of  $1 \times 10^{-2}$ ,  $1 \times 10^{-3}$ ,  $1 \times 10^{-4}$ ,  $1 \times 10^{-5}$ ,  $1 \times 10^{-6}$ ,  $1 \times 10^{-7}$  and  $1 \times 10^{-8}$  M<sup>8</sup> at 31°C. Error bars were calculated using the standard deviation from 3 repeats.

**Table 16.** The solubility of 4-hydroxybenzamide in Tween 20, HP Tween 20, SR Tween 20, Tween 80, HP Tween 80, SR Tween 80, Etocas 35, Croduret 40, Crodasol HS HP, SDS and Brij 35 at  $1 \times 10^{-2}$  M.

Surfactant	Solubility (mg/mL)	Solubility improvement compared to Aq (mg/mL)
No Surfactant	9.3	n/a
Tween 20	10.6	+ 1.3
HP Tween 20	10.8	+ 1.5
SR Tween 20	10.8	+ 1.5
Tween 80	10.7	+ 1.4
HP Tween 80	12.9	+ 3.6
SR Tween 80	10.9	+ 1.6
Etocas 35	11.0	+ 1.7
Croduret 40	10.1	+ 0.8
Crodasol HS HP	11.0	+ 1.7
SDS	9.5	+ 0.2
Brij 35	11.1	+ 1.8



As with the other APIs in Sections 4.2 and 4.3, a clear trend was observed with solubility increasing with surfactant concentration as seen in **Figure 38**. Whilst the increase in solubility isn't as much as was recorded with acetaminophen, it is a greater improvement than that which was seen with benzamide. The greatest increase in solubility was produced by HP Tween 80 with an improvement of 3.6 mg/mL, followed by Brij 35 with an increase of 1.8 mg/mL, then Etocas 35 and Crodasol HS HP with an improvement of 1.7 mg/mL. As with the other APIs, Etocas 35 is within the top 3 surfactants when ranked by solubility improvement. However, unlike the previous results SDS produced the least amount of solubility improvement with an increase of 0.2 mg/mL, with the second lowest from Croduret 40 with an increase of 0.8 mg/mL. Unlike the other surfactants used, SDS is an anionic surfactant and given that the results with the other surfactants, which are non-ionic in nature are similar to the results with the other API's, it can be assumed that this must be having a negative impact on its ability to enhance the solubility of 4-hydroxybenzamide. Further work with compounds structurally similar to 4-hydroxybenzamide and SDS and other anionic surfactants could be completed to confirm this.

Focusing on surfactant purity, **Figure 39** and **Figure 40** considers three purities of Tween 20 and Tween 80 respectively.

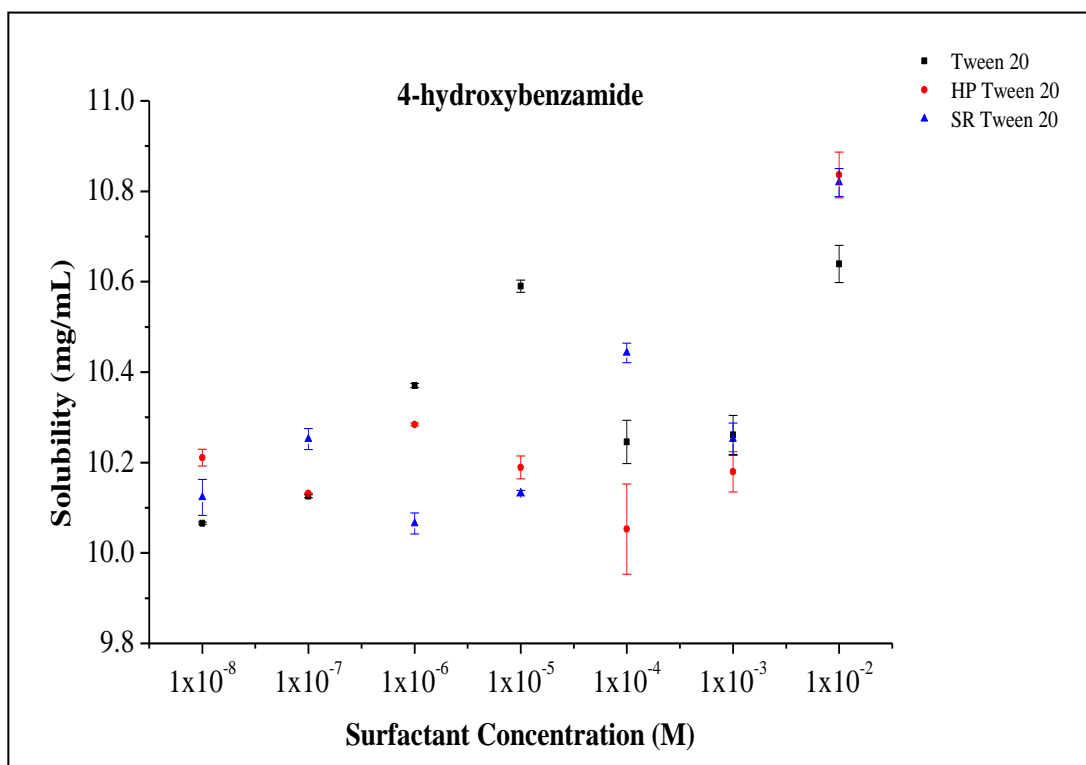


**Figure 40.** The results of the maximum solubility determination of 4-hydroxybenzamide in the presence of Tween 20, HP Tween 20, SR Tween 20, at surfactant concentrations of  $1 \times 10^{-2}$ ,  $1 \times 10^{-3}$ ,  $1 \times 10^{-4}$ ,  $1 \times 10^{-5}$ ,  $1 \times 10^{-6}$ ,  $1 \times 10^{-7}$  and  $1 \times 10^{-8}$  M<sup>8</sup> at 31°C. Error bars were calculated using the standard deviation from 3 repeats.

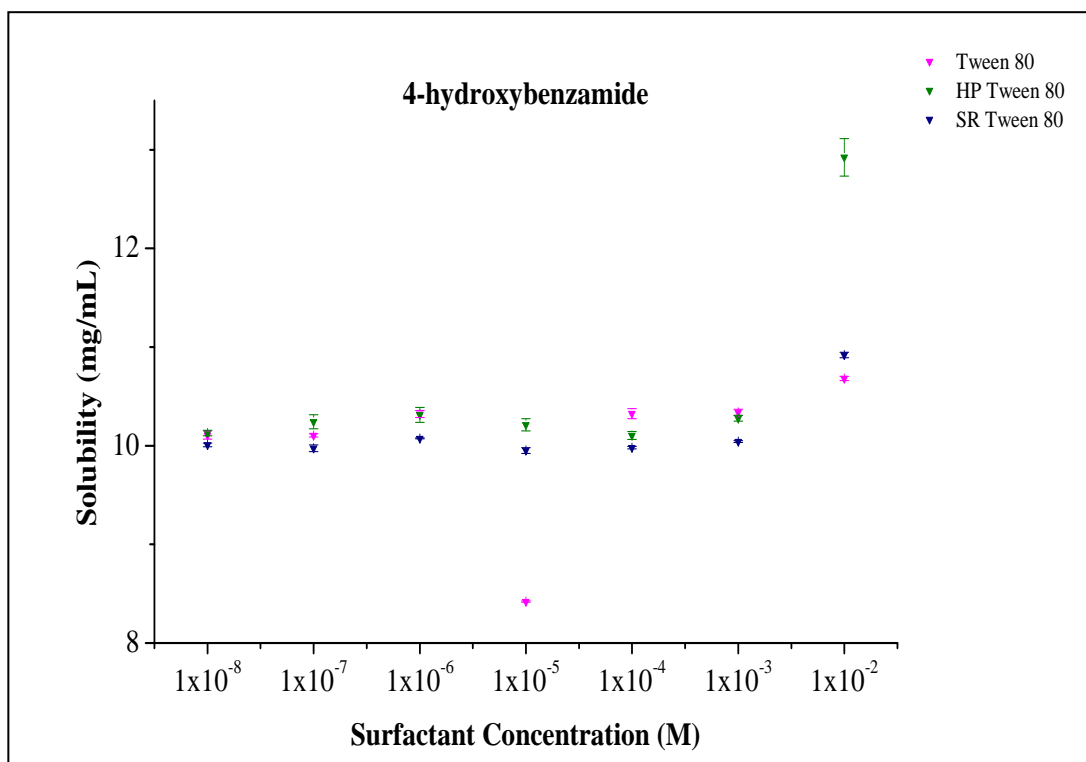


**Figure 39.** The results of the maximum solubility determination of 4-hydroxybenzamide in the presence of Tween 80, HP Tween 80, SR Tween 80, at surfactant concentrations of  $1 \times 10^{-2}$ ,  $1 \times 10^{-3}$ ,  $1 \times 10^{-4}$ ,  $1 \times 10^{-5}$ ,  $1 \times 10^{-6}$ ,  $1 \times 10^{-7}$  and  $1 \times 10^{-8}$  M<sup>8</sup> at 31°C. Error bars were calculated using the standard deviation from 3 repeats.

The higher purity grades of Tween 20 outperformed the standard grade of Tween 20, with HP and SR Tween 20 producing an improvement of 1.5 mg/mL and standard grade Tween 20 with an increase of 1.3 mg/mL compared with aqueous solubility. Similarly, for **Figure 39**, the higher purity grades of Tween 80 outperformed the standard grade. The standard grade Tween 80 produced an improvement of 1.4 mg/mL compared with aqueous solubility, followed by SR Tween 80 with 1.6 mg/mL and then HP Tween 80 with an improvement of 3.6 mg/mL. Similar to the results observed with benzamide in Section 4.4, polysorbate 80 produces a greater solubility increase than polysorbate 20. As was previously suggested, this is likely to be caused by the structural differences that exist between them.

Using the derived maximum solubility values, in conjunction with other properties allows for the calculation of the molar solubilisation value ( $\chi$ ), micelle-water partition coefficient (P) and the molar micelle-water partition coefficient ( $P_M$ ) using the equations shown in Section 4.2. The derived values are shown in **Table 17**. As expected, the results mirror the results from **Table 16**, with HP Tween 80 producing the greatest  $\chi$ , P and  $P_M$  values.

**Table 17.** The derived values of the molar solubilisation capacity ( $\chi$ ), micelle-water partition coefficient (P) and the molar micelle-water partition coefficient ( $P_M$ ) for 4-hydroxybenzamide with Tween 20, HP Tween 20, SR Tween 20, Tween 80, HP Tween 80, SR Tween 80, Etocas 35, Croduret 40, Crodasol HS HP, SDS and Brij 35. Where  $S_{Tot}$  is the total amount of acetaminophen solubilised,  $S_w$  is the water solubility of 4-hydroxybenzamide (value determined experimentally),  $C_{Surf}$  is the surfactant concentration and CMC is the critical micelle concentration (using the derived values for Tween 20, HP Tween 20, SR Tween 20, Tween 80 HP Tween 80, SR Tween 80, Etocas 35, Croduret 40 and Crodasol HS HP from Section 6).

Surfactant	$S_{Tot}$ (M)	$S_w$ (M)	$C_{Surf}$ (M)	CMC (mM)	$\chi$	P	$P_M$
Tween 20	0.079	0.068	0.010	0.675	1.173	0.161	17.285
HP Tween 20	0.079	0.068	0.010	0.208	1.117	0.161	16.468
SR Tween 20	0.079	0.068	0.010	0.358	1.134	0.161	16.722
Tween 80	0.078	0.068	0.010	0.627	1.089	0.151	16.051
HP Tween 80	0.094	0.068	0.010	0.546	2.777	0.387	40.923
SR Tween 80	0.080	0.068	1.010	0.627	0.012	0.174	0.172
Etocas 35	0.080	0.068	0.010	0.447	1.298	0.183	19.126
Croduret 40	0.074	0.068	0.010	0.425	0.609	0.086	8.980
Crodasol HS HP	0.080	0.068	4.010	0.425	0.003	0.186	0.046
SDS	0.069	0.068	0.010	8.200 <sup>89</sup>	0.810	0.022	11.849
Brij 35	0.081	0.068	0.010	0.090 <sup>90</sup>	1.324	0.194	19.529

This is the first study to consider solubility enhancement of 4-hydroxybenzamide thus cannot be compared with published data. However, the values recorded in this study fit well with those seen for the previously considered compounds as shown in **Table 18**.

**Table 18.** The literature and experimental solubility values for the aqueous solubility of acetaminophen, benzamide and hydrocortisone. The literature values are taken from PubChem<sup>101</sup> and are recorded at 25 °C, the experimental values were recorded at 31 °C.

API	Experimental Solubility (mg/mL)	Literature Solubility (mg/mL)
Acetaminophen	15.10	14.0
Benzamide	14.30	13.5
Hydrocortisone	0.28	0.3

#### 4.5 Solubility of Hydrocortisone

The determination of the solubility of hydrocortisone in Tween 20, HP Tween 20, SR Tween 20, Tween 80, HP Tween 80 and SR Tween 80 was completed using the method detailed in Section 2.5. Graphs showing the results are presented in **Figure 42** and **Figure 41**. The improvement in solubility compared to the aqueous experimental value (0.28 mg/mL) is shown in **Table 19**.

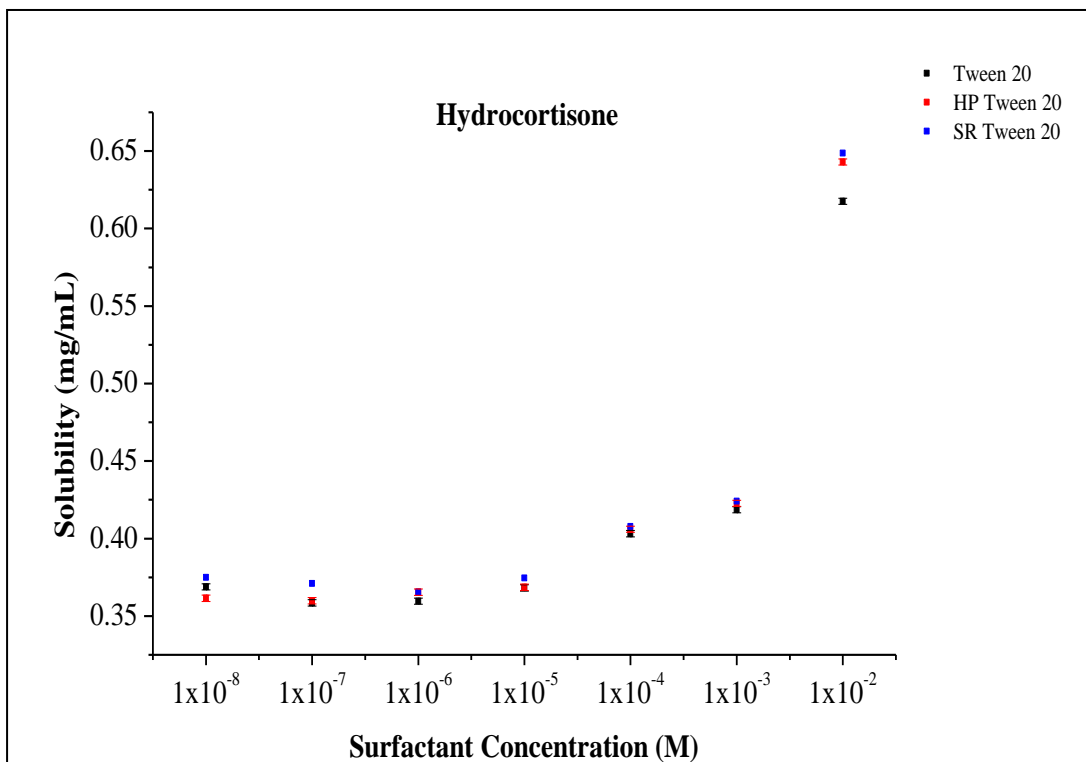


**Figure 42.** Solubility determination of hydrocortisone in the presence of Tween 20, HP Tween 20, SR Tween 20, at surfactant concentrations of  $1 \times 10^{-2}$ ,  $1 \times 10^{-3}$ ,  $1 \times 10^{-4}$ ,  $1 \times 10^{-5}$ ,  $1 \times 10^{-6}$ ,  $1 \times 10^{-7}$  and  $1 \times 10^{-8}$  M<sup>8</sup> at 31°C. Error bars were calculated using the standard deviation from 3 repeats.

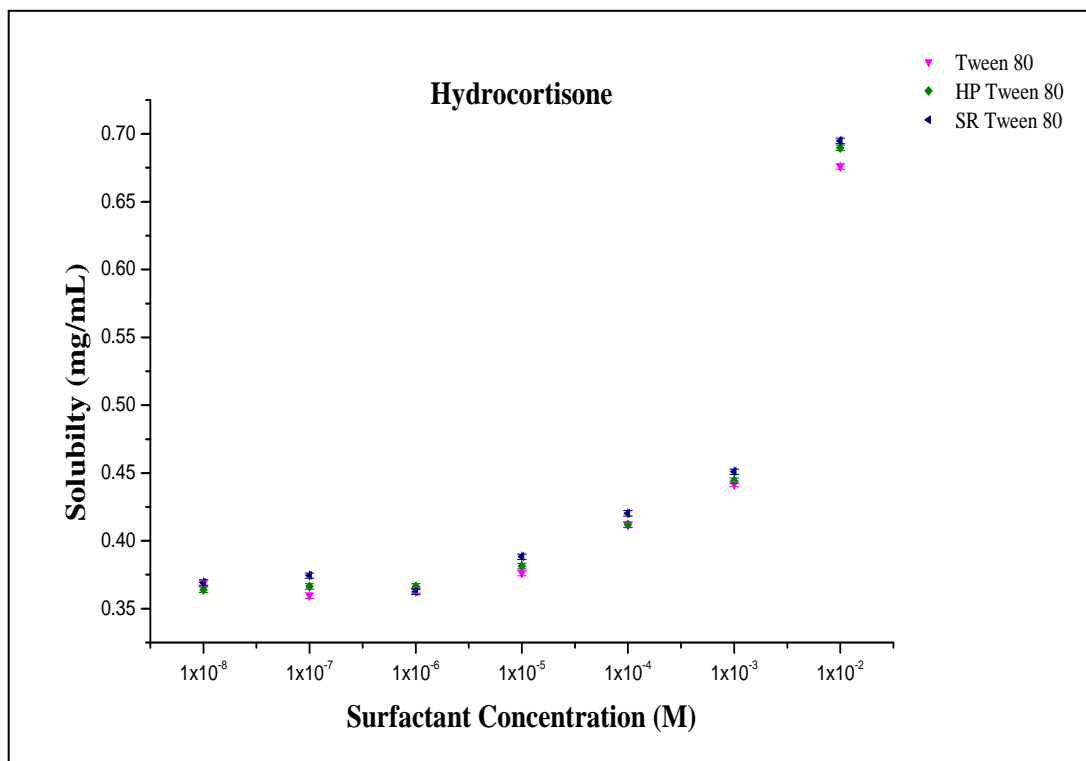


**Figure 41.** Solubility determination of hydrocortisone in the presence of Tween 20, HP Tween 20, SR Tween 20, at surfactant concentrations of  $1 \times 10^{-2}$ ,  $1 \times 10^{-3}$ ,  $1 \times 10^{-4}$ ,  $1 \times 10^{-5}$ ,  $1 \times 10^{-6}$ ,  $1 \times 10^{-7}$  and  $1 \times 10^{-8}$  M<sup>8</sup> at 31°C. Error bars were calculated using the standard deviation from 3 repeats.

**Table 19.** The solubility of hydrocortisone in Tween 20, HP Tween 20, SR Tween 20, Tween 80, HP Tween 80, SR Tween 80 at  $1 \times 10^{-2}$  M.

Surfactant	Solubility (mg/mL)	Solubility improvement compared to Aq (mg/mL)
No Surfactant	0.28	n/a
Tween 20	0.62	+ 0.34
HP Tween 20	0.64	+ 0.36
SR Tween 20	0.65	+ 0.37
Tween 80	0.67	+ 0.39
HP Tween 80	0.69	+ 0.41
SR Tween 80	0.69	+ 0.41

Unfortunately, because of time constraints placed upon the project, only a limited number of surfactants could be tested with hydrocortisone. It was decided that the results of the different purities of polysorbates and how they affected solubility enhancement would produce results of greater importance with regards to the project.

As with the other APIs, a general trend was observed with increasing surfactant concentration resulting in an increase in the solubility of hydrocortisone. Whilst the solubility improvements are smaller than that which was seen with acetaminophen and 4-hydroxybenzamide when compared using increase in mg/mL, it has the greatest improvement when compared using percentage increase, with each of the surfactants resulting in an increase of more than double the aqueous solubility.

SR Tween 20 had an improvement of 0.37 mg/mL, followed by HP Tween 20 with an improvement of 0.36 mg/mL and then standard grade Tween 20 with 0.34 mg/mL. The higher purity grades of Tween 20 outperformed the standard grade of Tween 20, similar to the result with the other APIs. The greatest increase in solubility was caused by SR and HP Tween 80 with an increase of 0.41 mg/mL, followed by standard grade Tween 80 with an increase of 0.39 mg/mL. As was seen with the other APIs, the higher purity grades of Tween 80 outperformed that standard grade, in terms of solubility improvement. As with the other APIs tested, polysorbate 80 outperformed polysorbate 20 in terms of solubility

enhancement. As was previously discussed this is likely because of the structural differences between them.

Whilst the increases in solubility in terms of mg/mL is small compared to results of benzamide in Section 4.3, when looking at them in terms of percentage increase they are significantly greater (1.4 - 3.5 % increase with benzamide compared to 121.1 – 146.4 % increase with hydrocortisone). This is likely because of the greater hydrophobicity that hydrocortisone possesses in comparison to benzamide, making the impact of a surfactant much greater.

Similar to the results presented in this study, B W Barry et al, also found that the solubility of hydrocortisone increased when in the presence of non-ionic surfactants. It was also found that an increase in surfactant chain length resulted in a greater increase in solubility, aligning with these results, where Tween 80 resulted in a greater improvement to solubility than Tween 20.<sup>102</sup>

Using the derived maximum solubility values, in conjunction with other properties allows for the calculation of the molar solubilisation value ( $\chi$ ), micelle-water partition coefficient (P) and the molar micelle-water partition coefficient ( $P_M$ ) using the equations shown in Section 4.2. The derived values are shown in **Table 20**. As expected, the results mirror the results from **Table 19**, with SR Tween 80 producing the greatest  $\chi$ , P and  $P_M$  values.

**Table 20.** The derived values of the molar solubilisation capacity ( $\chi$ ), micelle-water partition coefficient (P) and the molar micelle-water partition coefficient ( $P_M$ ) for hydrocortisone with Tween 20, HP Tween 20, SR Tween 20, Tween 80, HP Tween 80 and SR Tween 80. Where  $S_{Tot}$  is the total amount of acetaminophen solubilised,  $S_w$  is the water solubility of hydrocortisone (value determined experimentally),  $C_{Surf}$  is the surfactant concentration and CMC is the critical micelle concentration (using the derived values for Tween 20, HP Tween 20, SR Tween 20, Tween 80, HP Tween 80 and SR Tween 80 from Section 6).

Surfactant	$S_{Tot}$ (M)	$S_w$ (M)	$C_{Surf}$ (M)	CMC (mM)	$\chi$	P	$P_M$
Tween 20	0.002	0.001	0.010	0.675	0.101	1.214	130.130
HP Tween 20	0.002	0.001	0.010	0.208	0.101	1.286	131.275
SR Tween 20	0.002	0.001	0.010	0.358	0.106	1.321	137.000
Tween 80	0.002	0.001	0.010	0.627	0.115	1.393	148.510
HP Tween 80	0.002	0.001	0.010	0.546	0.120	1.464	154.801
SR Tween 80	0.002	0.001	0.010	0.627	0.121	1.464	156.126

## 4.6 Solubility Discussion

Each of the 4 APIs in this study exhibited an improvement in solubility with each surfactant, with the exceptions of standard grade Tween 20 and Croduret 40 with benzamide as shown in Section 4.3. Whilst the greatest improvement in solubility of an API for every surfactant in terms of increase in mg/mL was exhibited by acetaminophen, the greatest percentage increase in solubility was with hydrocortisone. This is of interest as the greatest reduction in  $k'$  values in Section 3 was also with hydrocortisone. However, the rest of the results do not align with the results in Section 3, as benzamide had the lowest percentage increase in solubility when tested with each of the surfactants, but the second greatest reduction in  $k'$  values. It is therefore difficult to link an increase in solubility with a reduction in  $k'$  values.

When comparing other characterisation data that aligned with the results in Section 3.7 such as pKa and Log P it becomes apparent that these factors, whilst certainly important in understanding the interactions between API and surfactant, are not the only contributing factor to the solubility enhancement in the presence of surfactants. Otherwise a repetition of the results seen in Section 3.7 would have been observed, with hydrocortisone producing the greatest solubility improvement, followed by benzamide, then acetaminophen and 4-hydroxybenzamide with close values.

**Table 21.** A table showing the graded solubility improvement of acetaminophen (A), benzamide (B), 4-hydroxybenzamide (4) and hydrocortisone (H) in terms of increase in mg/mL and percentage increase with Tween 20, HP Tween 20, SR Tween 20, Tween 80, HP Tween 80 and SR Tween 80 at a concentration of  $1 \times 10^{-2}$  M. Where green is the greatest improvement, followed by yellow, then orange then red.

Surfactant	A Solubility improvement (mg/mL)	B Solubility improvement (mg/mL)	4 Solubility Improvement (mg/mL)	H Solubility Improvement (mg/mL)	A Solubility improvement (% increase)	B Solubility improvement (% increase)	4 Solubility Improvement (% increase)	H Solubility Improvement (% Increase)
Tween 20	2.3	0	1.3	0.34	15.2	0	14	121.4
HP Tween 20	2.4	0.2	1.5	0.36	15.9	1.4	16.1	128.6
SR Tween 20	2.5	0.2	1.5	0.37	16.6	1.4	16.1	132.1
Tween 80	1.6	0.6	1.4	0.39	10.6	4.2	15.1	139.3
HP Tween 80	2.2	0.5	3.6	0.41	14.6	3.5	38.7	146.4
SR Tween 80	2.2	0.5	1.6	0.41	14.6	3.5	17.2	146.4



**Table 22.** A table showing the graded solubility improvement of acetaminophen (A), benzamide (B), 4-hydroxybenzamide (4) and hydrocortisone (H) in terms of increase in mg/mL and percentage increase with Etocas 35, Croduret 40, Crodasol HS HP, SDS and Brij 35 at a concentration of  $1 \times 10^{-2}$  M. Where green is the greatest improvement, followed by yellow, then orange then red.

Surfactant	A Solubility improvement (mg/mL)	B Solubility improvement (mg/mL)	4 Solubility Improvement (mg/mL)	H Solubility Improvement (mg/mL)	A Solubility improvement (% increase)	B Solubility improvement (% increase)	4 Solubility Improvement (% increase)	H Solubility Improvement (% Increase)
Etocas 35	3.1	1.1	1.7	-	20.5	7.7	18.3	-
Croduret 40	2.1	-0.7	0.8	-	13.9	-4.9	8.6	-
Crodasol HS HP	3.1	1.1	1.7	-	20.5	7.7	18.3	-
SDS	2.4	0.5	0.2	-	15.9	3.5	2.2	-
Brij 35	1.7	0.1	1.8	-	11.3	0.7	19.4	-

Using a t-test for paired two sample means with a significance level of 0.05 it was found that Tween 20 and HP Tween 20 had a significant difference with a p value of 0.058. Tween 20 and SR Tween 20 were found to be similar with a p value of 0.034, HP Tween 20 and SR Tween 20 were also found to be similar with a p value of 0.34. Tween 80 and HP Tween 80, Tween 80 and SR Tween 80 and HP Tween 80 and SR Tween 80 were all found to be similar with p values of 0.29, 0.32 and 0.39 respectively.

From these results it becomes apparent that each of the surfactants used in this study increase solubility to a degree, and that the purity of the surfactant can have a significant impact upon this, with the higher purity grades of polysorbate 20 and 80 resulting in greater increases when compared to their standard grade counter parts.

## 5. UV

### 5.1 Surfactants

Chromatograms obtained from the loading phase in MLC unexpectedly indicated that some of surfactants displayed a UV absorbance. This was hypothesised to be because of the presence of impurities or degradation products, normally the result of hydrolysis of the ester group. Full scan chromatograms from 200 – 800 nm were obtained for Tween 20, Tween 80, Etocas 35, Croduret 40, Crodasol HS HP, SDS and Brij 35 at concentrations:  $1 \times 10^{-2}$ ,  $1 \times 10^{-3}$ ,  $1 \times 10^{-4}$ ,  $1 \times 10^{-5}$ ,  $1 \times 10^{-6}$ ,  $1 \times 10^{-7}$ ,  $1 \times 10^{-8}$  M.

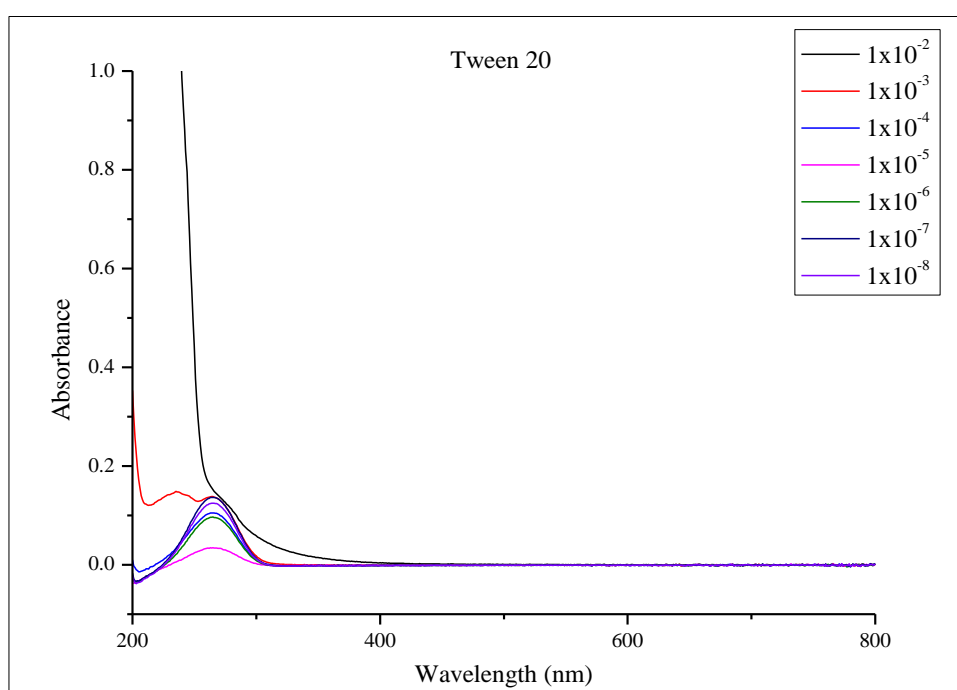


**Figure 43.** The chromatogram of a full scan of Tween 20 at concentrations:  $1 \times 10^{-2}$ ,  $1 \times 10^{-3}$ ,  $1 \times 10^{-4}$ ,  $1 \times 10^{-5}$ ,  $1 \times 10^{-6}$ ,  $1 \times 10^{-7}$ ,  $1 \times 10^{-8}$  M at 200 – 800 nm.

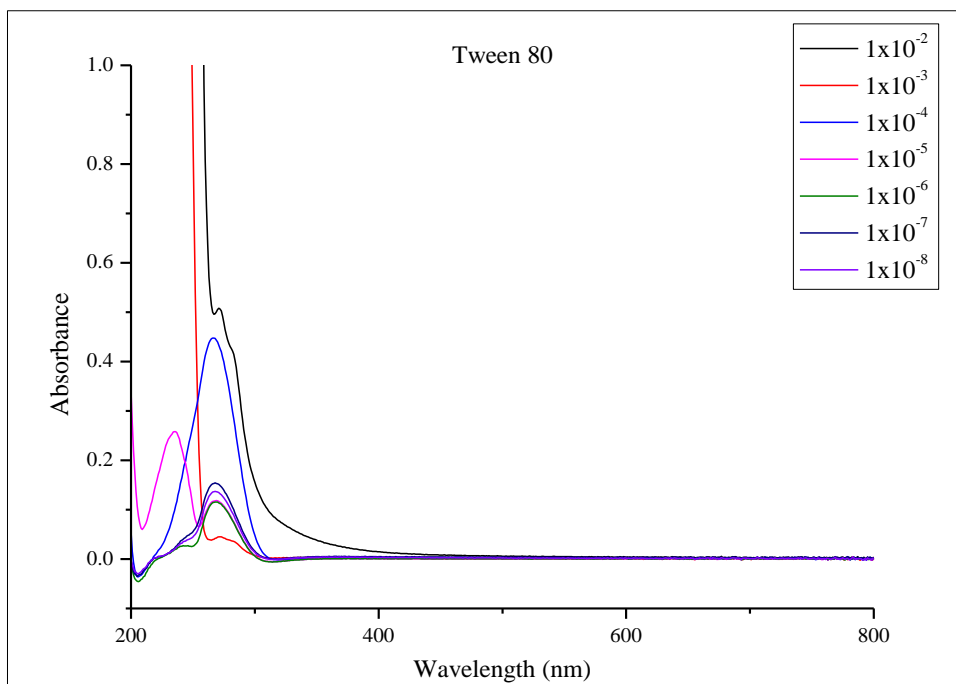


**Figure 44.** The chromatogram of a full scan of Tween 80 at concentrations:  $1 \times 10^{-2}$ ,  $1 \times 10^{-3}$ ,  $1 \times 10^{-4}$ ,  $1 \times 10^{-5}$ ,  $1 \times 10^{-6}$ ,  $1 \times 10^{-7}$ ,  $1 \times 10^{-8}$  M at 200 – 800 nm.

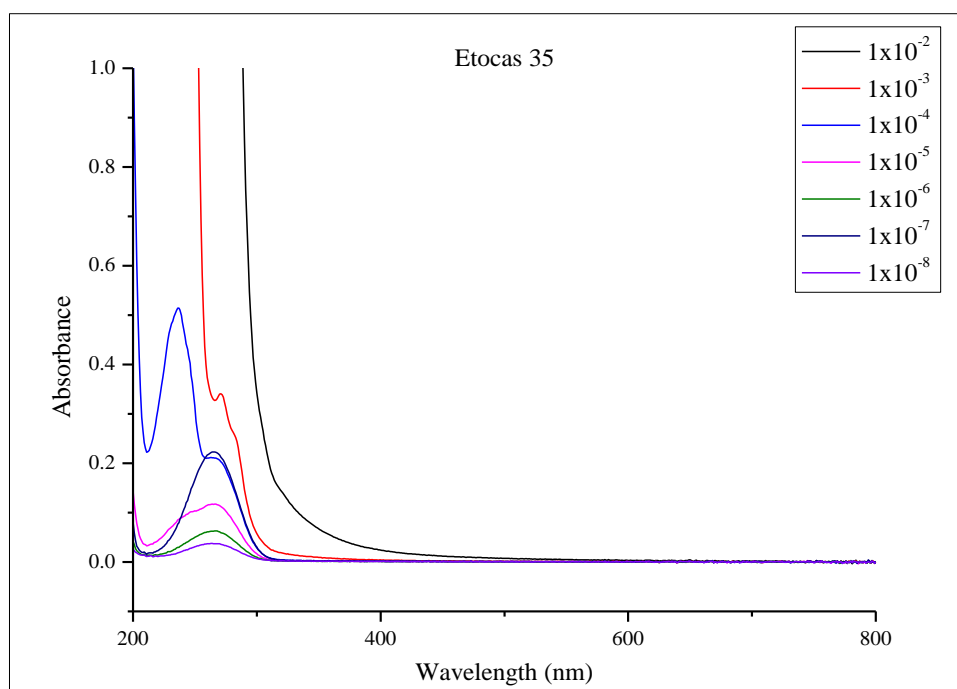


**Figure 45.** The chromatogram of a full scan of Etocas 35 at concentrations:  $1 \times 10^{-2}$ ,  $1 \times 10^{-3}$ ,  $1 \times 10^{-4}$ ,  $1 \times 10^{-5}$ ,  $1 \times 10^{-6}$ ,  $1 \times 10^{-7}$ ,  $1 \times 10^{-8}$  M at 200 – 800 nm.

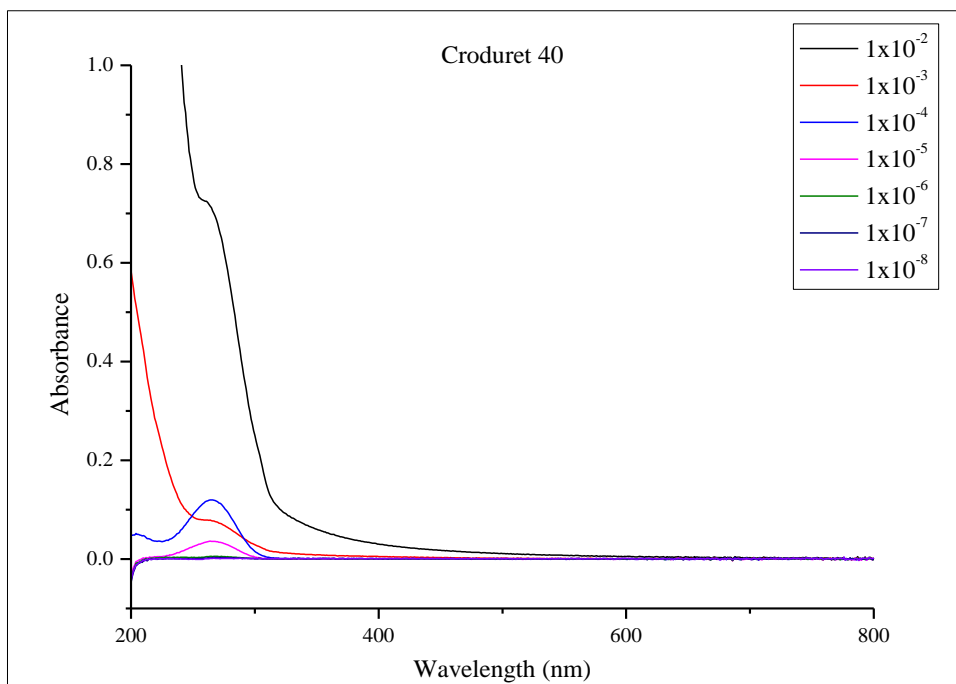


**Figure 46.** The chromatogram of a full scan of Croduret 40 at concentrations:  $1 \times 10^{-2}$ ,  $1 \times 10^{-3}$ ,  $1 \times 10^{-4}$ ,  $1 \times 10^{-5}$ ,  $1 \times 10^{-6}$ ,  $1 \times 10^{-7}$ ,  $1 \times 10^{-8}$  M at 200 – 800 nm.

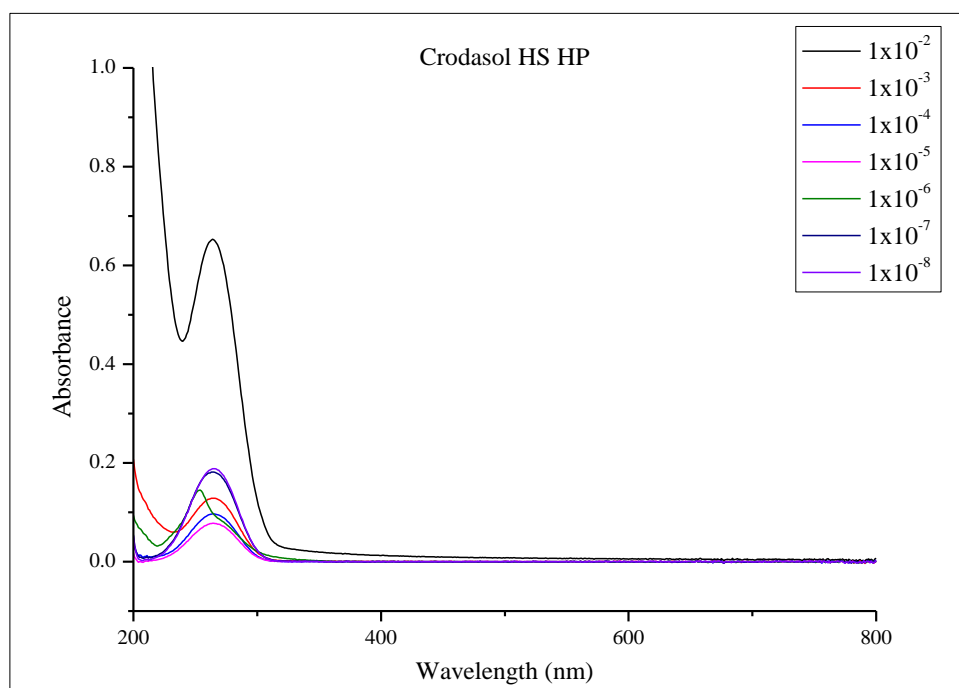


**Figure 47.** The chromatogram of a full scan of Crodasol HS HP at concentrations:  $1 \times 10^{-2}$ ,  $1 \times 10^{-3}$ ,  $1 \times 10^{-4}$ ,  $1 \times 10^{-5}$ ,  $1 \times 10^{-6}$ ,  $1 \times 10^{-7}$ ,  $1 \times 10^{-8}$  M at 200 – 800 nm.

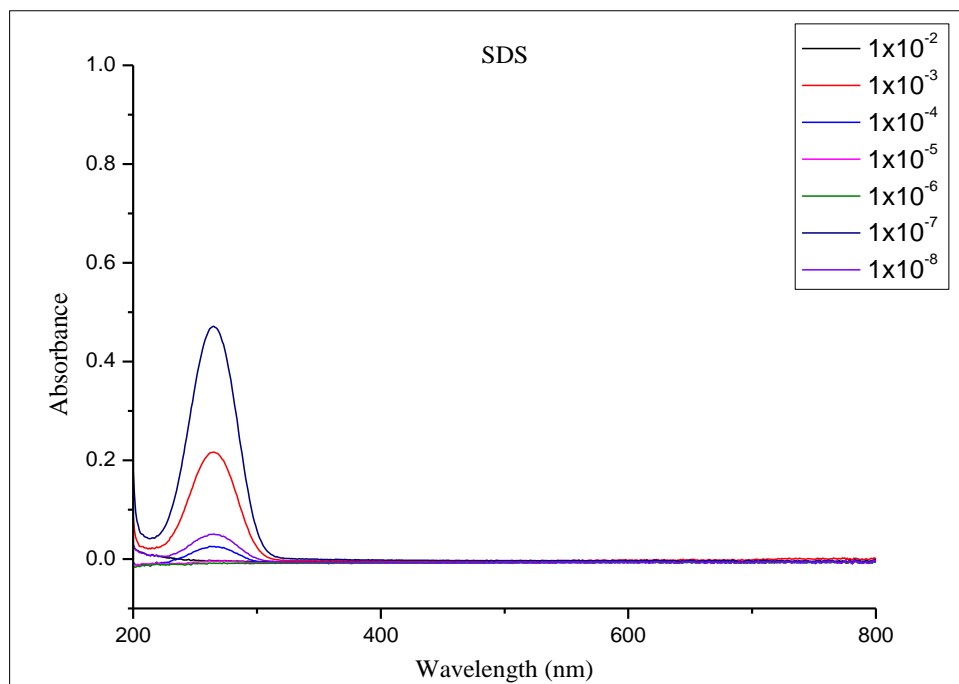


**Figure 48.** The chromatogram of a full scan of SDS at concentrations:  $1 \times 10^{-2}$ ,  $1 \times 10^{-3}$ ,  $1 \times 10^{-4}$ ,  $1 \times 10^{-5}$ ,  $1 \times 10^{-6}$ ,  $1 \times 10^{-7}$ ,  $1 \times 10^{-8}$  M at 200 – 800 nm.

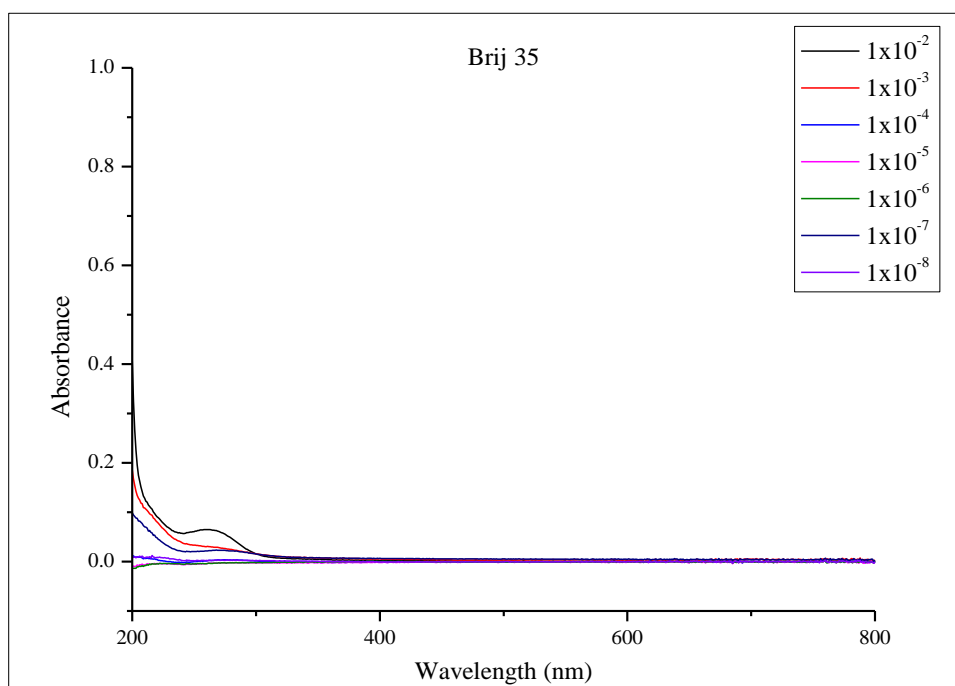


**Figure 49.** The chromatogram of a full scan of Brij 35 at concentrations:  $1 \times 10^{-2}$ ,  $1 \times 10^{-3}$ ,  $1 \times 10^{-4}$ ,  $1 \times 10^{-5}$ ,  $1 \times 10^{-6}$ ,  $1 \times 10^{-7}$ ,  $1 \times 10^{-8}$  M at 200 – 800 nm.

All of the surfactants displayed a significant presence at  $1 \times 10^{-2}$  M which decreased with decreasing surfactant concentration. The UV absorption at higher surfactant concentration makes them unsuitable

for use with low solubility APIs where the corresponding API signal was indistinguishable from the surfactant UV signal.

Tween 20 absorption was also reported by Calabrese who measured the UV absorption at concentrations of  $1 \times 10^{-2} \text{ M} - 2 \times 10^{-6} \text{ M}$ .<sup>103</sup> The decrease in absorption reported by Calabrese was mirrored in the Tween 20 data with the largest decrease in absorption occurring between  $1 \times 10^{-2} \text{ M}$  and  $1 \times 10^{-3} \text{ M}$ . SDS has also been observed to have a UV absorption by Gnanam, although Gnanam didn't investigate different concentrations, only using 0.05 M SDS.<sup>104</sup>

## **5.2 The effect of Surfactants on the Lambda max of APIs**

The effect of a surfactant on the lambda max of paracetamol, benzamide and 4-hydroxybenzamide was measured and the results shown in **Figure 50**, **Figure 51** and **Figure 52**. Solutions containing each API in  $1 \times 10^{-4} \text{ M}$  of Tween 20, Tween 80, Etocas 35, Croduret 40, Crodasol HS HP, SDS and Brij 35 were prepared and analysed between 200 – 400 nm.

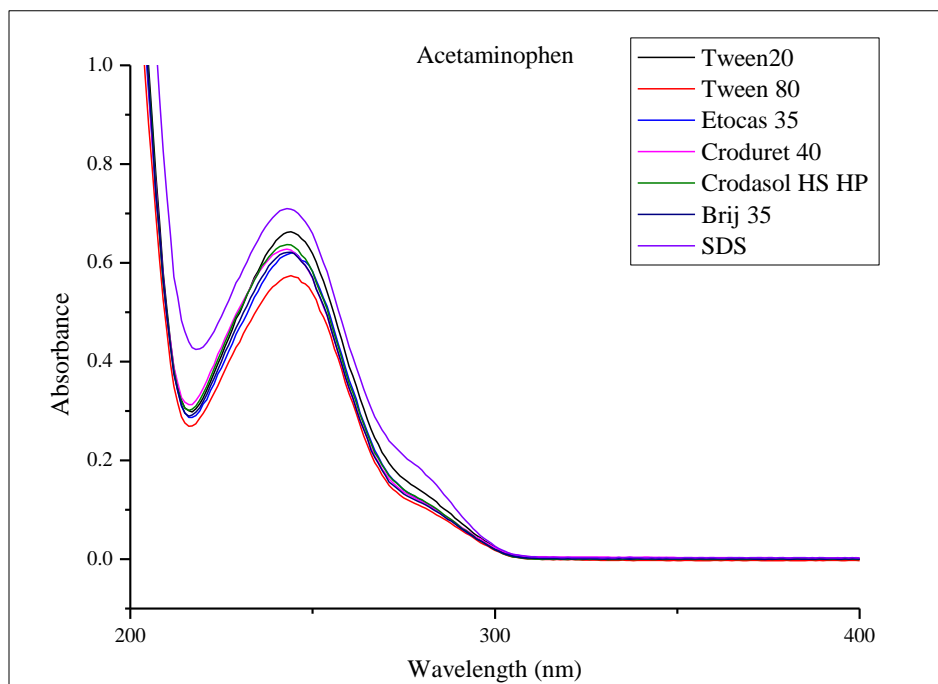


**Figure 50.** The chromatogram of a full scan of acetaminophen in  $1 \times 10^{-4}$  M of Tween 20, Tween 80, Etocas 35 Croduret 40, Crodasol HS HP, Brij 35 and SDS.

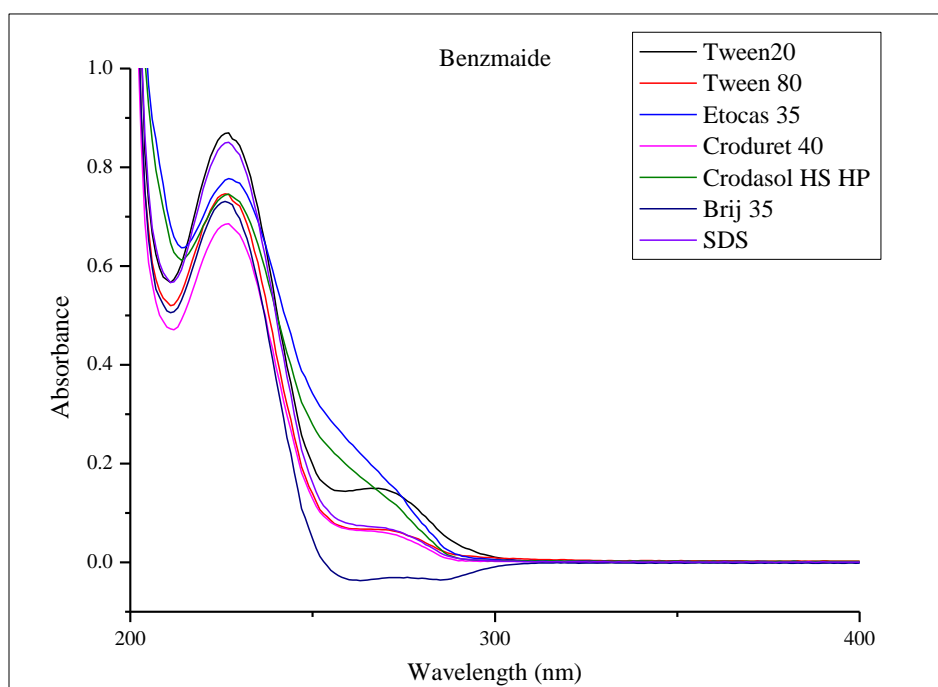


**Figure 51.** The chromatogram of a full scan of Benzamide in  $1 \times 10^{-4}$  M of Tween 20, Tween 80, Etocas 35 Croduret 40, Crodasol HS HP, Brij 35 and SDS.

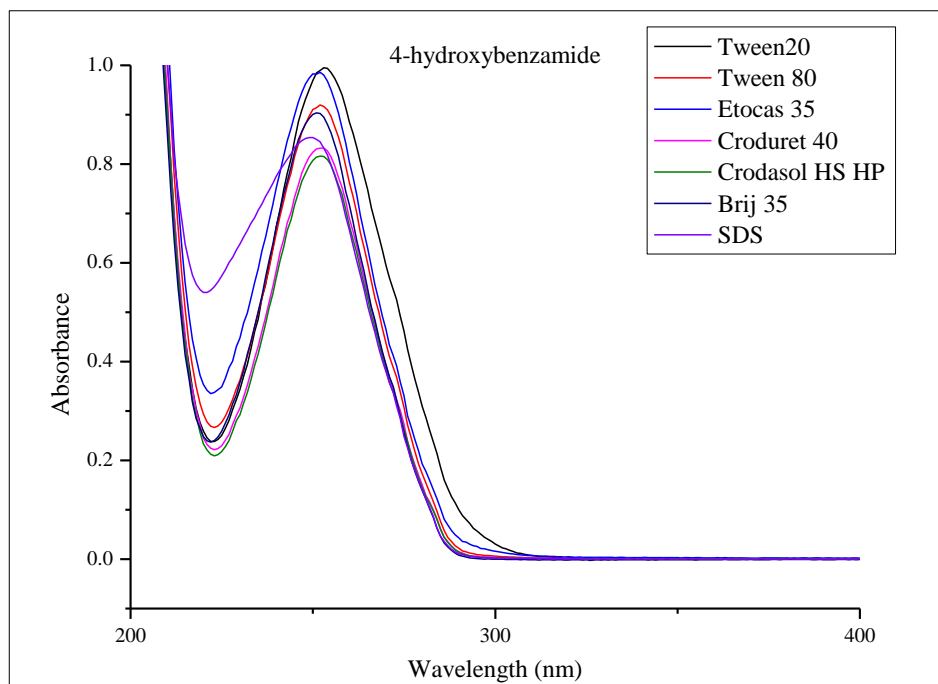


**Figure 52.** The chromatogram of a full scan of 4-hydroxybenzamide in  $1 \times 10^{-4}$  M of Tween 20, Tween 80, Etocas 35 Croduret 40, Crodasol HS HP, Brij 35 and SDS.

The lambda max for each surfactant API pairing is shown in **Table 23**.

**Table 23.** Lambda max values in nm for acetaminophen, benzamide and 4-hydroxybenzamide in ultra-pure water, and the following surfactants at  $1 \times 10^{-4}$  M: Tween 20, Tween 80, Etocas 35, Croduret 40, Crodasol HS HP, SDS and Brij 35

API	Ultra -pure Water	Tween 20	Tween 80	Etocas 35	Croduret 40	Crodasol HS HP	SDS	Brij 35
Acetaminophen	243	245	244	244	242	242	243	244
Benzamide	227	226	225	226	226	226	226	226
4-hydroxybenzamide	252	253	253	251	253	251	251	251

The values in **Table 23** display that the lambda max of each API exhibited a minor shift of +/- 1-2 nm in the presence of surfactant. This is similar to what has been reported by Dastidar, who found that 1 mM of Tween 20 resulted in a shift of -2 nm to the lambda max of diazepam. However, Dastidar also included 0.8 % (v/v) of propylene glycol, in addition to the use of a phosphate buffer solution (pH 7.4) in the solution.<sup>105</sup> Therefore, it cannot be agreed with certainty that the shift was only because of the presence of Tween 20. The effect of SDS on the lambda max of tris(2,2'-bipyridine) ruthenium (II) in



the presence of alumina was investigated by López who found that SDS increased the lambda max by 38 nm in 0.8 mM of SDS. However, López reports that this is because of SDS forming surface aggregates on the alumina, which affected the luminescence quenching of the compound, instead of being a direct result of micellisation.<sup>106</sup>

Finally, it was decided that no significant change in wavelength was observed in the presence of surfactants, based on the fact that the shift in absorption was approximately equal to the small variations recorded between samples.

## **6.ITC**

In Section 1.52 it was shown how ITC can be used to characterise the CMC of surfactants using the break point method as shown by Waters et al.<sup>84</sup> This method involves the injection of a surfactant into a reaction cell containing water, followed by analysis to calculate the point at which demicellisation ceases to occur; the CMC. This section discusses the use of this method to determine the CMC of Tween 20, HP Tween 20, SR Tween 20, Tween 80, HP Tween 80, SR Tween 80, Etocas 35, Croduret 40 and Crodasol HS HP.

### **6.1 CMC Determination of Tween 20**

#### **6.1.1 CMC Determination of Standard Grade Tween 20**

As discussed in Section 1.5, a solution of 0.0388 M HP Tween 20 was prepared, and subsequently analysed using ITC, as exemplified in **Figure 53**. **Figure 53** presents with an initial sharp decrease in peak size, after which, the peaks steadily decrease in size, until a near constant peak size is observed towards the end of the graph, signifying that demicellisation is no longer occurring and that the CMC has been reached.

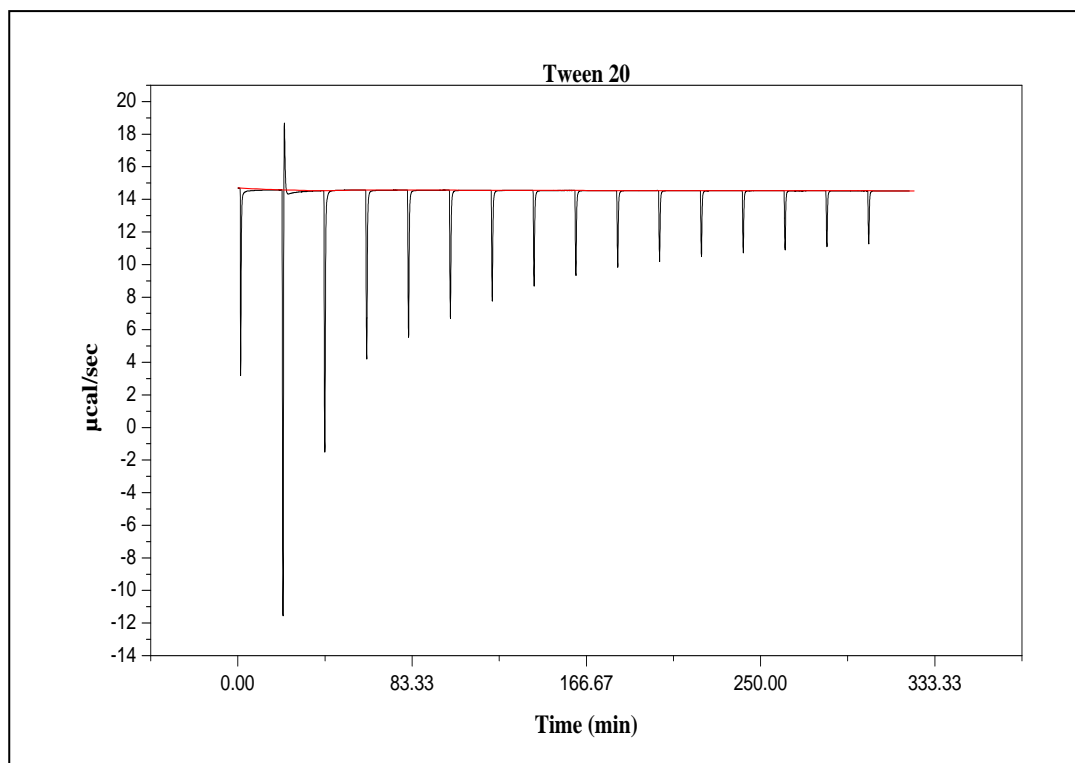


**Figure 53.** An example of a plot displaying  $\mu\text{cal/sec}$  with time (min) for the demicellisation of Tween 20.

Integrating each peak and converting the resulting values to kJoules/mol allowed for a plot of  $\Delta H$  with surfactant concentration as exemplified in **Figure 54**.

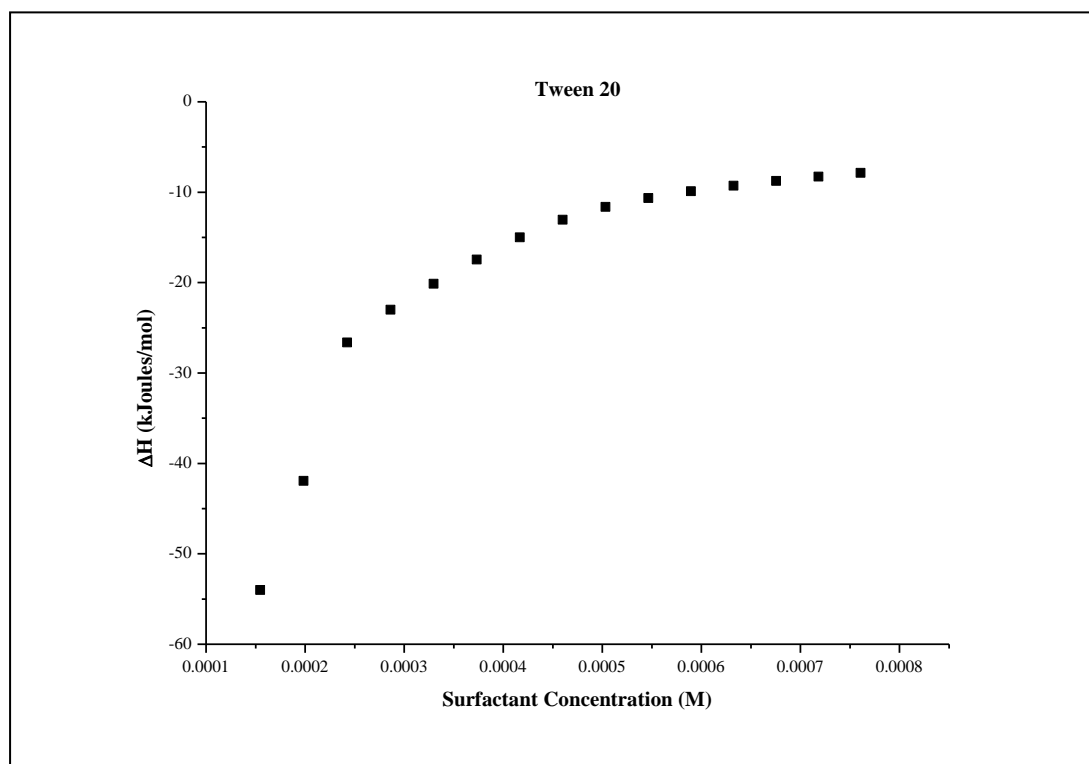


**Figure 54.** An example of a plot of  $\Delta H$  (kJoules/mol) with surfactant concentration (M) for Tween 20.

**Figure 54** doesn't present with a sigmoidal curve which has been observed with other surfactants when determining their CMC via ITC, as observed by Loh with C<sub>12</sub>TAB and sulfobetaine SB 3-12.<sup>82</sup> Instead, it presents with a sharp increase, that tapers into a gradual curve tending towards flat. The CMC was then determined by calculating the second derivative of  $\Delta H$  and subsequently plotting it with surfactant concentration as seen in **Figure 55**.

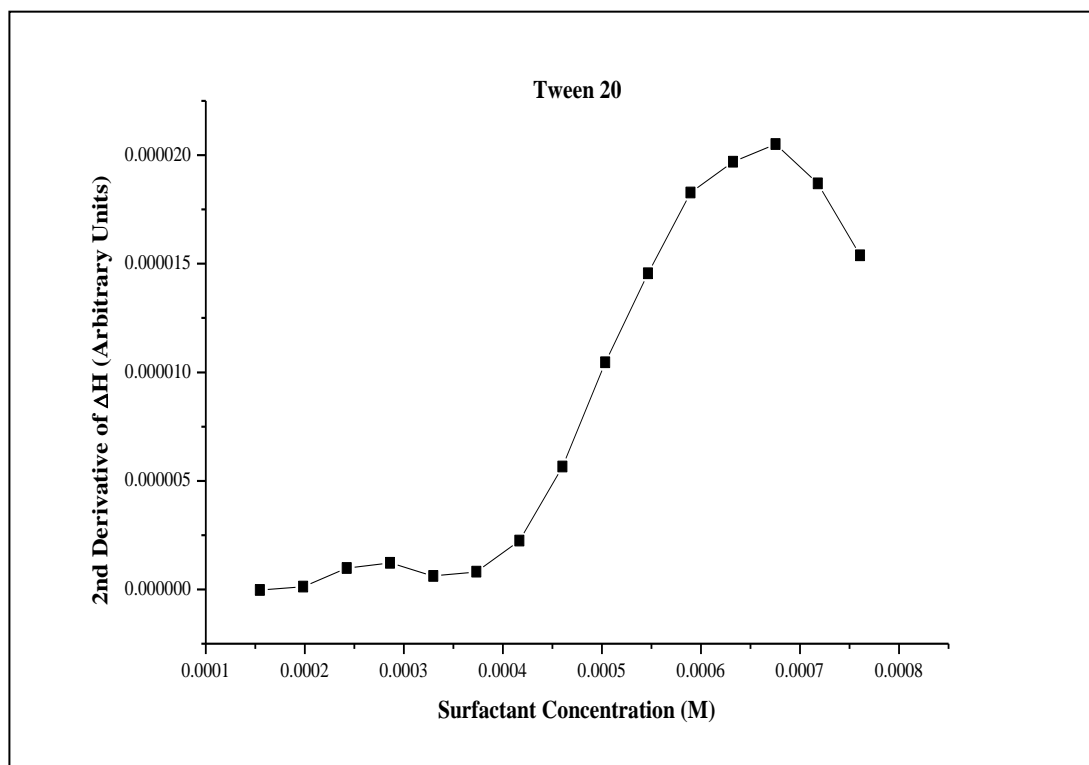


**Figure 55.** An example of a plot of the 2<sup>nd</sup> derivative of  $\Delta H$  (Arbitrary Units) with surfactant concentration (M) for Tween 20.

The break point in **Figure 55** is easy to determine and the CMC was derived to be 0.675 (+/- 0.0427) mM. This value falls within the literature values for the CMC of Tween 20 reported in **Table 1** (0.002 – 0.975 mM).

The accuracy of the literature values reported in **Table 1** is a debated topic as there are several different values reported for the CMC of Tween 20. Papers published by Mohajeri and Khoshnood both state that CMC decreases with increasing temperature for non-ionic surfactants.<sup>107 108</sup> Mohajeri states that the CMC of Tween 20 decreases with increasing temperature until 43 °C.<sup>107</sup> The increase in temperature decreases the hydrophilicity of the surfactant molecules as the probability of hydrogen bond formation

decreases with increasing temperature. This reduces the hydration of the hydrophilic oxyethylene group, which favours micellisation; causing micellisation to occur at lower concentrations.

Contradictory to this, Szymczyk reports that the CMC of Tween 20 increases with temperature, with the following reported CMC values: at 20 °C (0.115 mM), 25 °C (0.129 mM), 30 °C (0.144 mM), 35 °C (0.160 mM), 40 °C (0.178 mM) and 45 °C (0.200 mM).<sup>74</sup> As both arguments cannot be correct it calls into question the accuracy of the CMC's presented.

The CMCs reported at temperatures close to the temperature used for the ITC experiments in this study (31 °C) are as follows: 0.049 mM at 28 °C<sup>72</sup>, 0.144 mM at 30 °C<sup>74</sup>, 0.001 mM at 30 °C<sup>76</sup> and 0.942 mM at 30 °C.<sup>78</sup> This provides a broad range of values over 3 orders of magnitude and given the large differences between previously reported values, casts further doubt about the precision and accuracy of some of the CMCs presented in **Table 1**.

It is also important to note that a variety of techniques were used for these literature values such as fluoresce measurements in conjunction with different dyes and taking surface tension measurements, these differences in techniques and methods are the likely cause of the discrepancies in values.

### **6.1.2 CMC Determination of HP Tween 20**

As discussed in Section 2.4, a solution of 0.0159 M HP Tween 20 was prepared, and subsequently analysed using ITC, as exemplified in **Figure 57**. **Figure 57** presents with an initial steep drop off in peak size, followed by a more gradual reduction, similar to that which was observed for Tween 20 in **Figure 53**, which was expected as they remain largely the same surfactant.

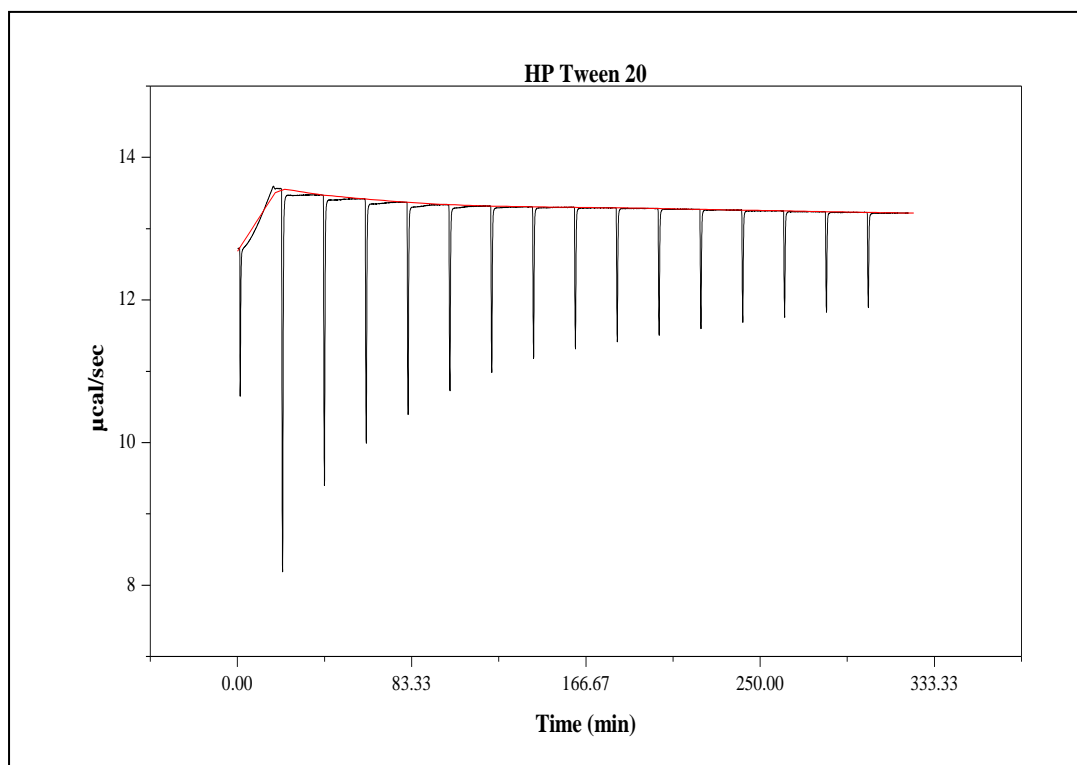


Figure 57. An example of a plot displaying  $\mu\text{cal/sec}$  with time (min) for the demicellisation of HP Tween 20.

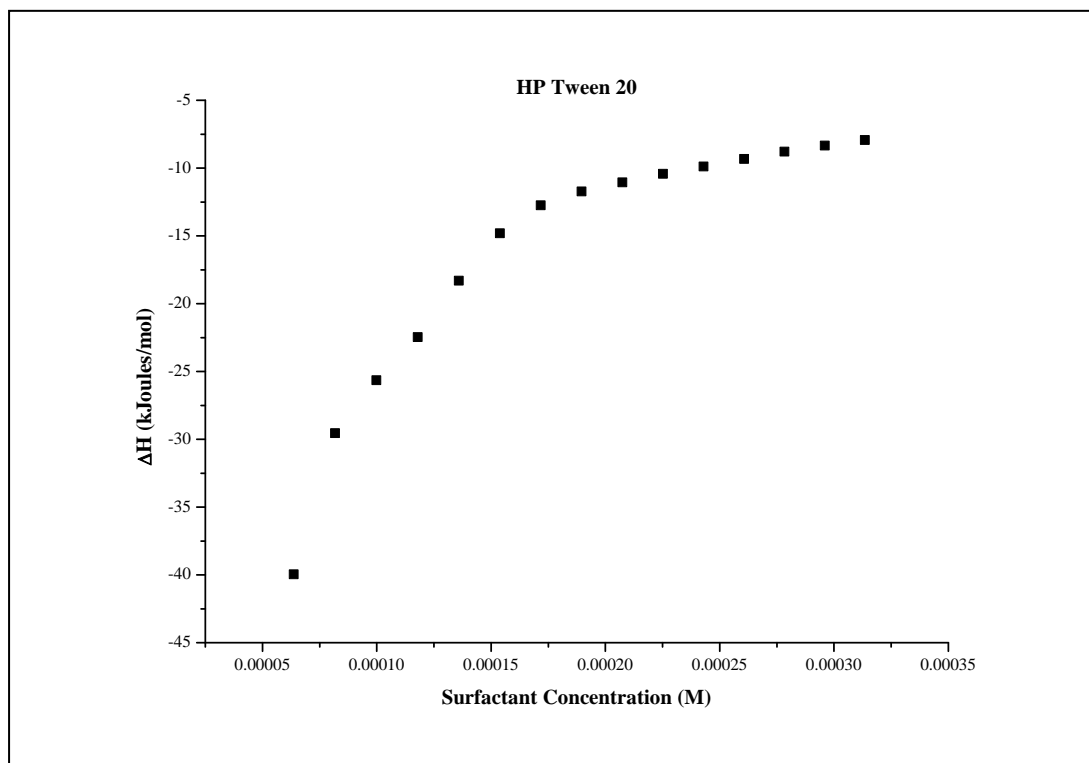
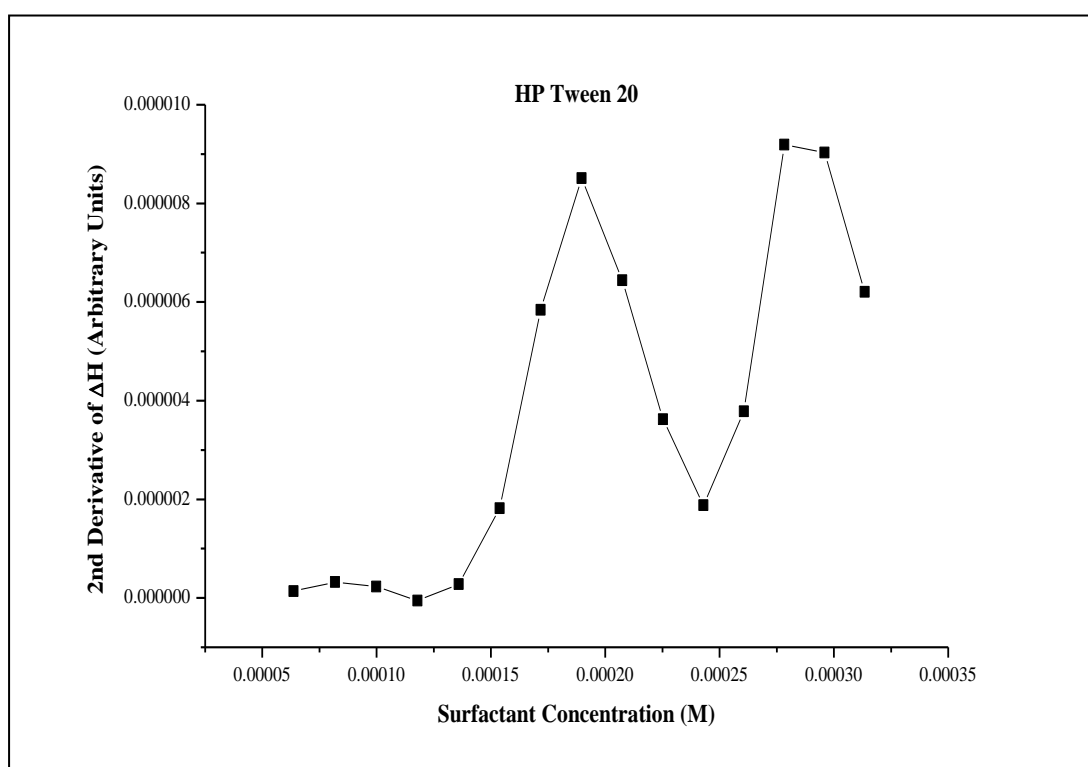


Figure 56. An example of a plot of  $\Delta H$  (kJoules/mol) with surfactant concentration (M) for HP Tween 20.

Integrating each peak and converting the resulting values to kJoules/mol allows for a plot of  $\Delta H$  with surfactant concentration as shown in **Figure 56**. The resulting graph doesn't present with the typical

sigmoidal shape that is commonly seen with other surfactants such as with SDS as reported by Waters et al.<sup>85</sup> Instead, it presents with a shape similar to that of Tween 20, as seen in **Figure 54**, with a sharp initial increase, followed by a gradual decrease that tapers into a gradual curve tending towards flat.

A plot of the 2<sup>nd</sup> derivative of  $\Delta H$  with surfactant concentration allowed for the visual realisation of the break point, which is taken to be the CMC, as shown in **Figure 58**. The break point is taken to be the greatest peak in the graph, as the smaller previous peaks are the result of pre-micellar events.<sup>109</sup> Using the average of the repeats for this experiment of the break points, the CMC for HP Tween 20 at 31°C was determined to be 0.243 (+/- 0.0179) mM. This falls within the range of literature values that was reported in **Table 1** (0.002 – 0.975 mM).



**Figure 58.** An example of a plot of the 2<sup>nd</sup> derivative of  $\Delta H$  (Arbitrary Units) with surfactant concentration (M) for HP Tween 20.

### 6.1.3 CMC Determination of SR Tween 20

As discussed in Section 2.4, a solution of 0.219 M SR Tween 20 was prepared, and subsequently analysed using ITC, as exemplified in **Figure 59**. The resulting graph shows the same initially steep

drop off in peak size followed by a more gradual reduction as seen in **Figure 53** and **Figure 57**, which is expected as they are all Tween 20 based surfactants.

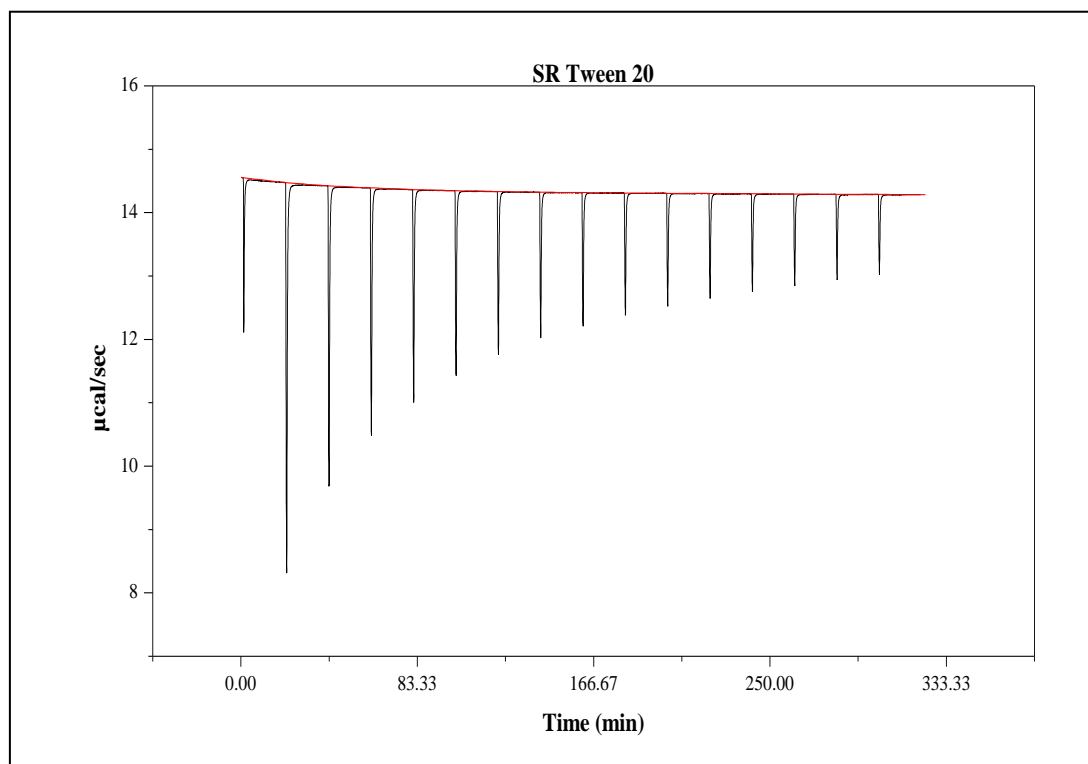


**Figure 59.** An example of a plot displaying  $\mu\text{cal/sec}$  against time (min) for the demicellisation of SR Tween 20.

Integrating each peak and converting the resulting values to kJoules/mol allowed for a plot of  $\Delta H$  with surfactant concentration as exemplified in **Figure 60**.

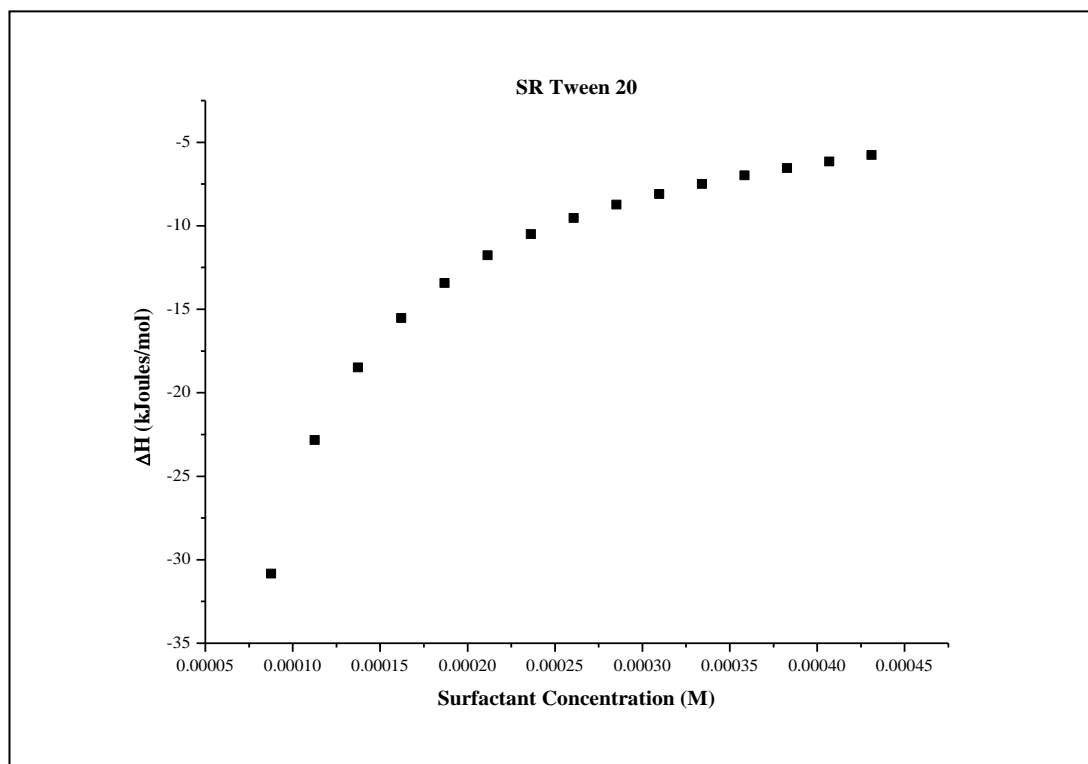


*Figure 60.* An example of a plot of  $\Delta H$  (kJoules/mol) with surfactant concentration (M) for SR Tween 20.

As with Tween 20 in **Figure 54** and HP Tween 20 in **Figure 56**, **Figure 60** presents with a non-sigmoidal shape with an initial steep curve that tapers off to a more gradual curve towards the end. The CMC was then determined by calculating the second derivative of  $\Delta H$  and subsequently plotting it with surfactant concentration as seen in **Figure 61**.



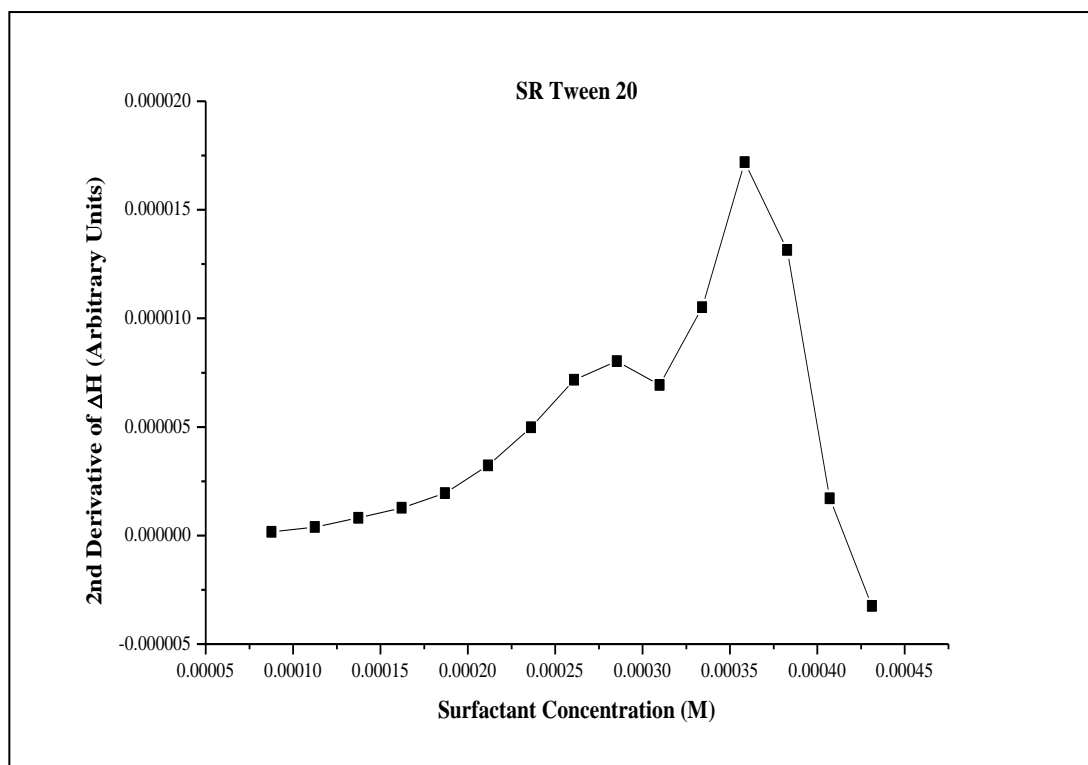


**Figure 61.** An example of a plot of the 2<sup>nd</sup> derivative of ΔH (Arbitrary Units) with surfactant concentration (M) for SR Tween 20.

The breakpoint in **Figure 61** is easy to ascertain and the resulting average CMC was calculated to be 0.358 (+/- 0.0248) mM. This value also falls within the literature values for the CMC of Tween 20 reported in **Table 1** (0.002 – 0.975 mM). The CMC value for SR Tween 20 is greater than that derived for HP Tween 20 (0.208 (+/- 0.0179) mM), but lower than the CMC derived for Tween 20 (0.0675 (+/- 0.00427) mM). The difference in values is unlikely to be caused by the presence of impurities, given their relatively small concentrations, instead it is more likely to be explained by considering the slightly different ratios of fatty acid chains that are present in each purity, due to differences in the manufacturing process as mentioned previously in Section 3.7.

## 6.2 CMC Determination of Tween 80

### 6.2.1 CMC Determination of Standard Grade Tween 80

As discussed in Section 2.4, a solution of 0.0339 M Tween 80 was prepared, and subsequently analysed using ITC, as exemplified in **Figure 62**. The graph presents with an initial slight decrease in peak size, followed by a steep drop off before levelling off to a near consistent peak size.

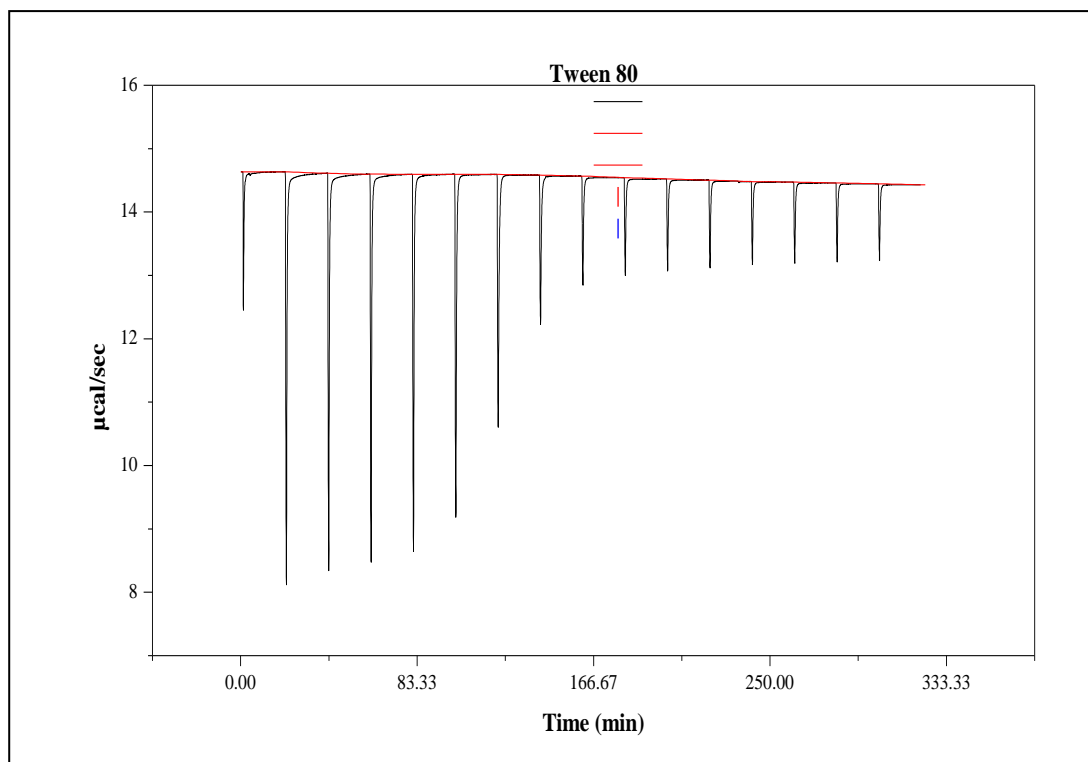


**Figure 62.** An example of a plot displaying  $\mu\text{cal/sec}$  against time (min) for the demicellisation of Tween 80.

Integrating each peak and converting the resulting values to kJoules/mol allowed for a plot of  $\Delta H$  with surfactant concentration as shown in **Figure 63**. **Figure 63** presents with a sigmoidal curve, which as previously mentioned, has been observed with other surfactants such as SDS and  $\text{C}_{12}\text{TAB}$ .<sup>84 82</sup>

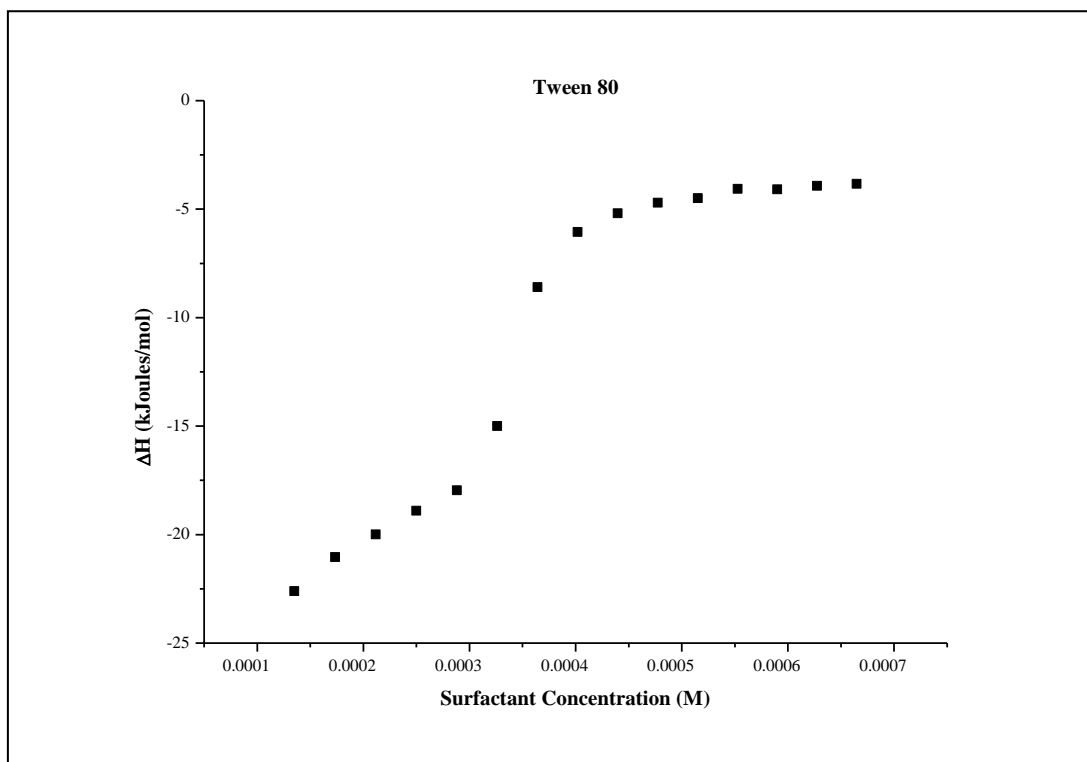


**Figure 63.** An example of a plot of  $\Delta H$  (kJoules/mol) with surfactant concentration (M) for Tween 80.

The CMC was then determined using the break point by calculating the second derivative of  $\Delta H$  and subsequently plotting it with surfactant concentration as seen in **Figure 64**.

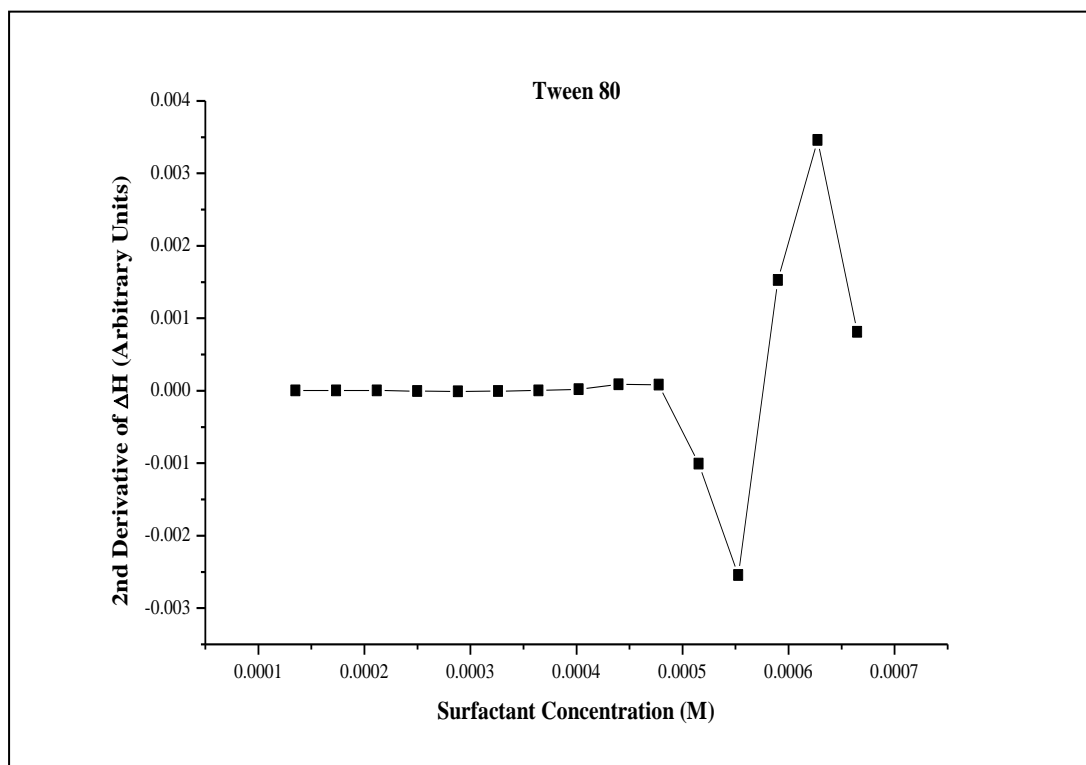


**Figure 64.** An example of a plot of the 2<sup>nd</sup> derivative of ΔH (Arbitrary Units) with surfactant concentration (M) for Tween 80.

The break point in **Figure 64**, in conjunction with repeat experiments, allowed for the calculation of the average CMC, which was determined to be 0.627 (+/- 0.0375) mM. This value slightly exceeds the range of literature values found in **Table 1** (0.011 – 0.574 mM), but as stated in Section 6.13, the accuracy of some of the literature values quoted is a topic of debate, and therefore exceeding the range of literature values doesn't invalidate the result. It is worth noting that taking the inflection point of the sigmoidal graph as the CMC, which is another method of interpreting the data to calculate the CMC would give a value of 0.35 mM which is closer to the literature value.

### 6.2.2 CMC Determination of HP Tween 80

As discussed in Section 2.4, a solution of 0.0335 M HP Tween 80 was prepared, and subsequently analysed using ITC, as exemplified in **Figure 65**, which presents a similar shape to the graph produced by Tween 80 in **Figure 62**. There is an initial slight decrease in peak size, followed by a steep decrease, which then tapers off until a near consistent peak size is observed.

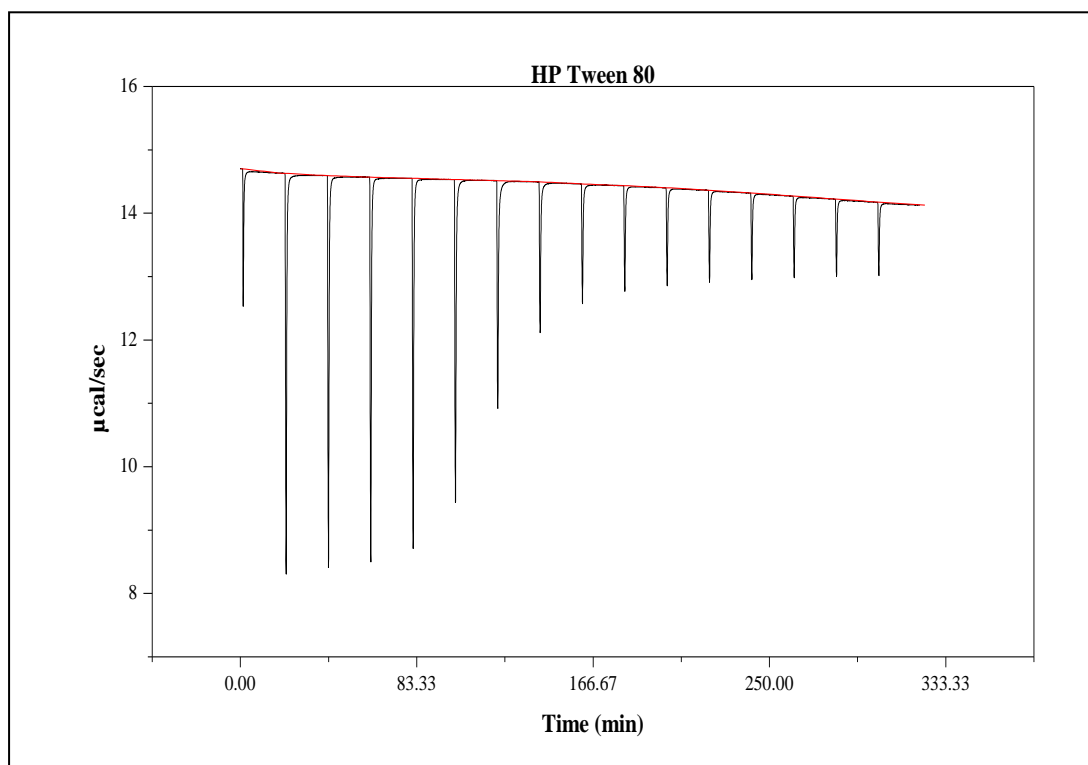


*Figure 65.* An example of a plot displaying  $\mu\text{cal/sec}$  against time (min) for the demicellisation of HP Tween 80.

By integrating the peaks and converting the resulting values to kJoules/mol a plot of  $\Delta H$  with surfactant concentration can be produced, as seen in **Figure 66**. **Figure 66** presents with a sigmoidal curve, which is expected as a sigmoidal curve was seen with Tween 80 in **Figure 63**.

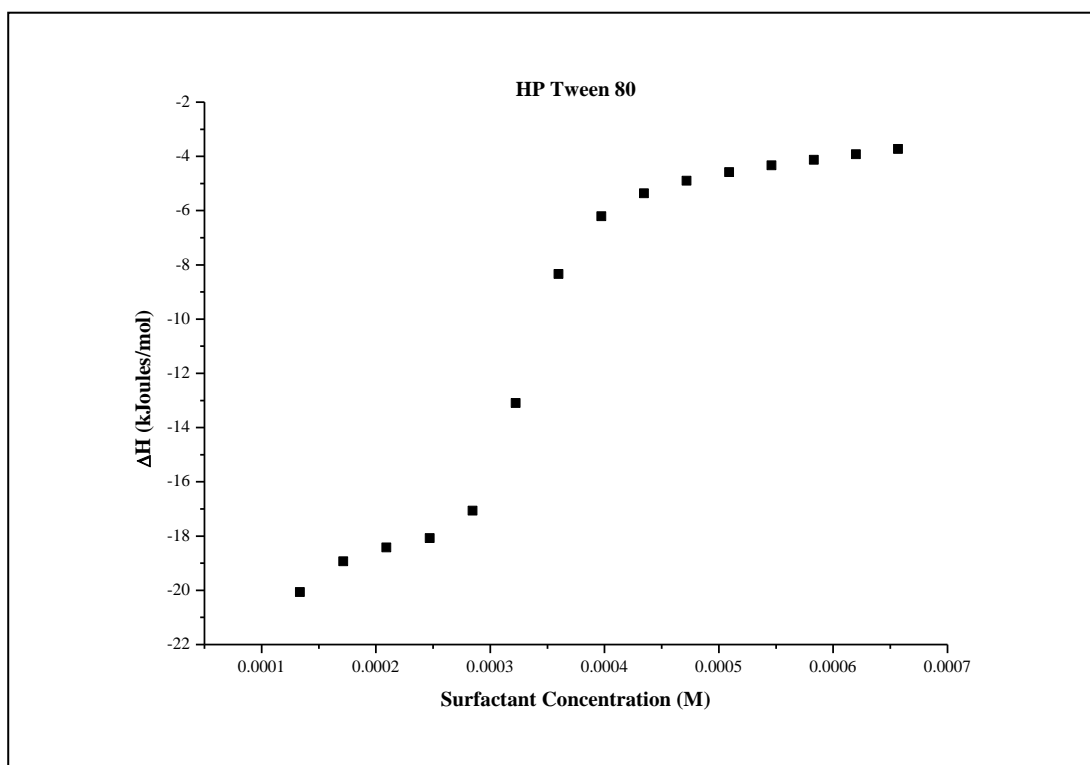


**Figure 66.** An example of a plot of  $\Delta H$  (kJoules/mol) with surfactant concentration (M) for HP Tween 80.

A plot of the 2<sup>nd</sup> derivative of  $\Delta H$  with surfactant concentration produced **Figure 67**. The break point is clear in this graph and in conjunction with other experiments allowed for calculation of the average CMC for HP Tween 80, which was determined to be 0.546 (+/- 0.0372) mM. This is within the range of literature CMCs for Tween 80 reported in **Table 1** (0.011 – 0.574 mM).

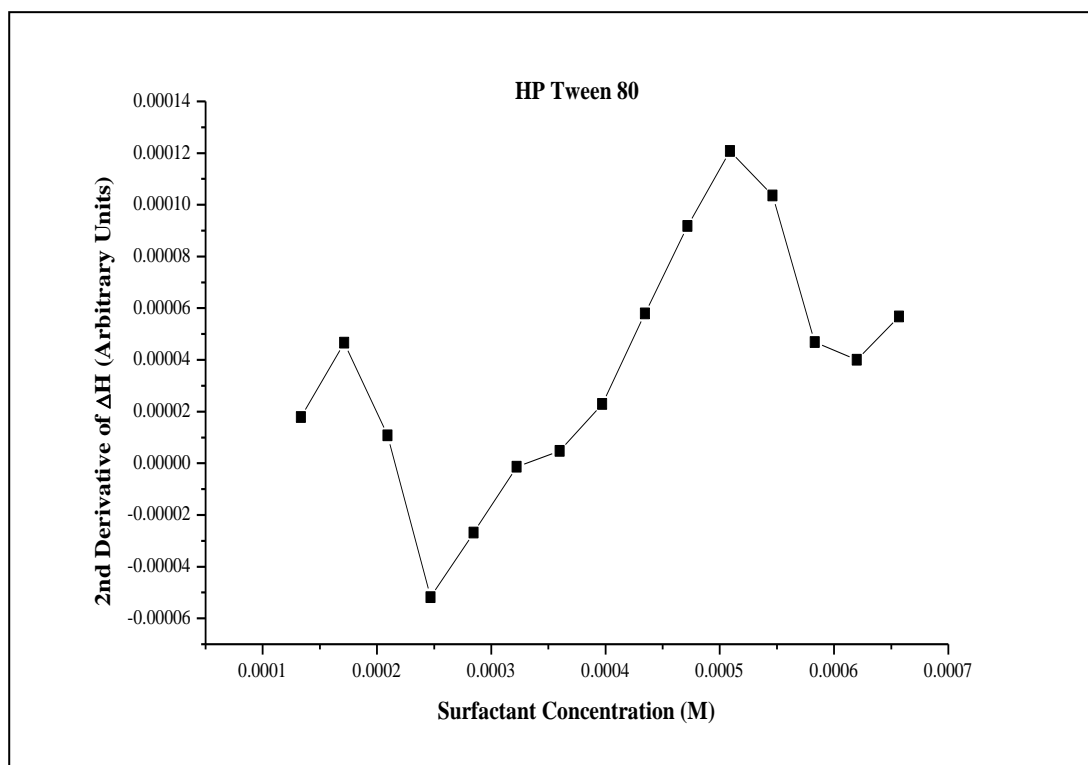


*Figure 67.* An example of a plot of the 2<sup>nd</sup> derivative of  $\Delta H$  (Arbitrary Units) with surfactant concentration (M) for HP Tween 80.

### 6.2.3 CMC Determination of SR Tween 80

As discussed in Section 2.4 a solution of 0.0360 M SR Tween 80 was prepared, and subsequently analysed using ITC, as exemplified in **Figure 68**.

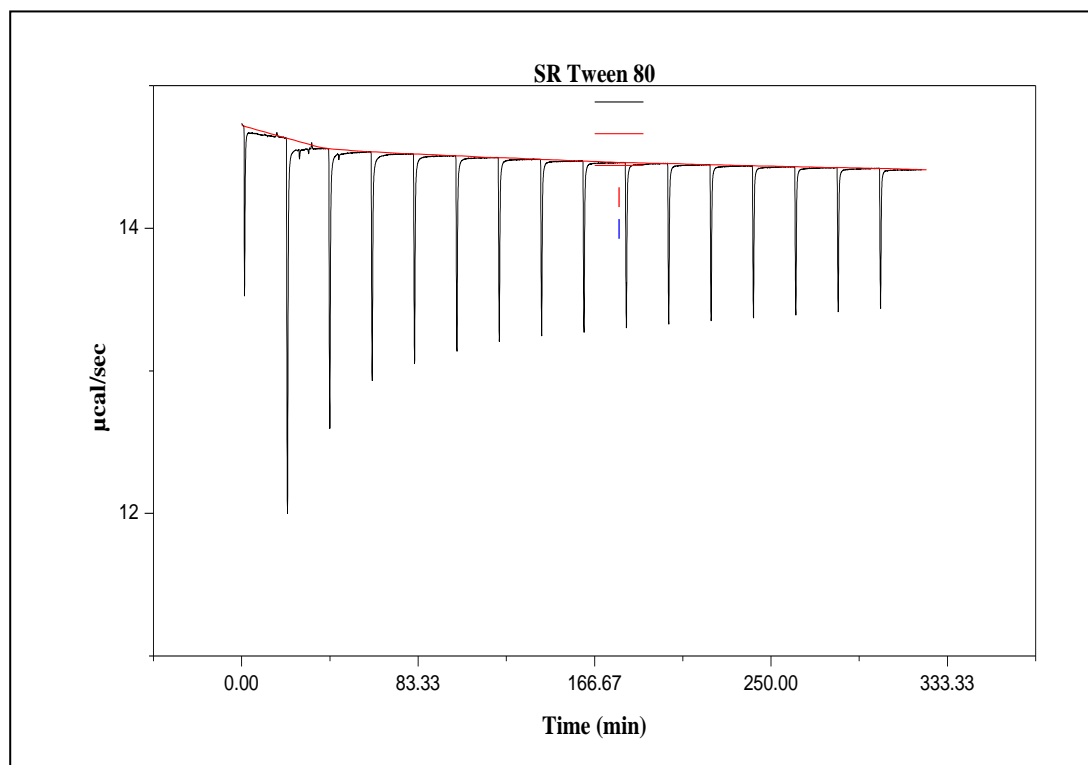


**Figure 68.** An example of a plot displaying  $\mu\text{cal/sec}$  against time (min) for the demicellisation of SR Tween 80.

**Figure 68** presents with an initial step decrease that quickly tapers to a more gradual decrease tending towards flat. This is dissimilar to the Tween 80 in **Figure 62** and HP Tween 80 in **Figure 65**, which both presented with an initial slight decrease in peak size, followed by a steep decrease, which then tapered off to a near consistent peak size. This difference is again reflected in **Figure 69** which is produced by integrating the peaks and converting the resulting values to kJoules/mol allowing for a plot of  $\Delta H$  with surfactant concentration, and is apparent in the lack of a sigmoidal curve, instead presenting in a similar fashion to polysorbate 20 as see in **Figure 54**, **Figure 56** and **Figure 60**. As mentioned previously, the different purities contain slightly different ratios of fatty acid chains that are present in each purity, due to differences in the manufacturing process, and it is likely this that is the cause of the different graph profiles.



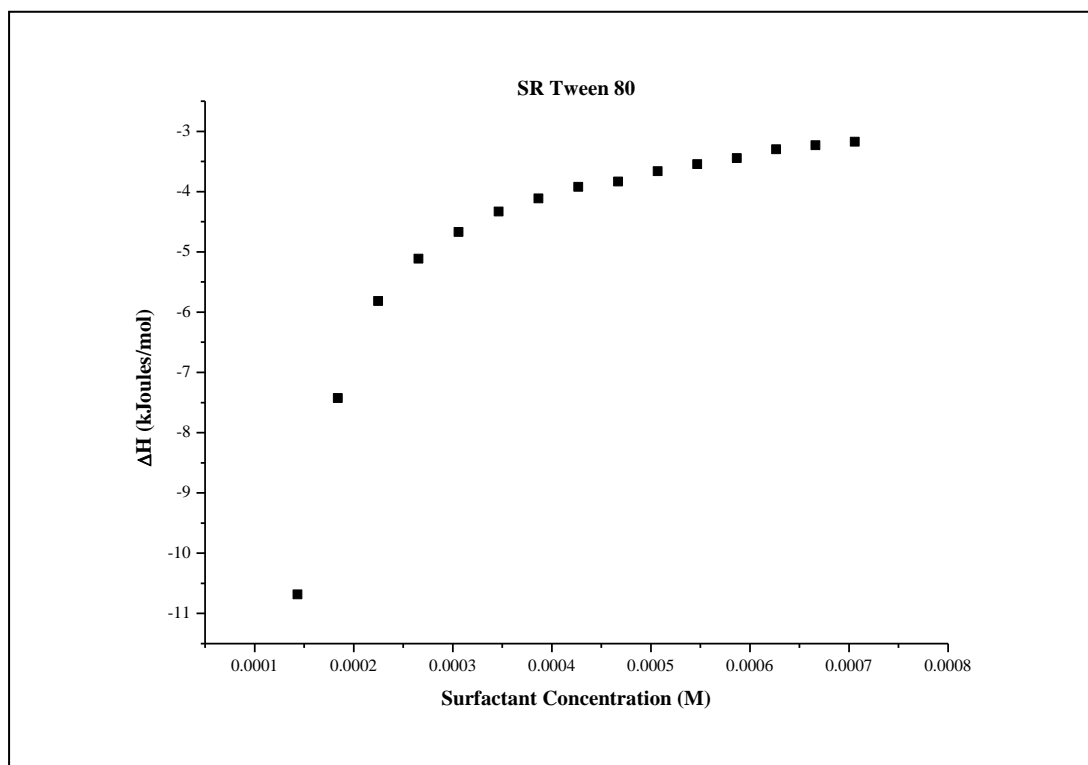


**Figure 69.** An example of a plot of  $\Delta H$  (kJoules/mol) with surfactant concentration (M) for HP Tween 80.

A plot of the 2<sup>nd</sup> derivative of  $\Delta H$  with surfactant concentration is displayed in **Figure 70**. The break point is clear in this graph and in conjunction with other experiments allowed for calculation of the average CMC for SR Tween 80, which was determined to be 0.627 (+/- 0.0396) mM. The CMC calculated for the SR grade of Tween 80 is the same as the one that was calculated for the standard grade Tween 80 and is only 0.071 mM greater than the value recorded for HP Tween 80 (0.546 mM), placing all 3 values within a tight grouping, within their error values (assuming the lowest possible value for SR Tween 80 and highest for HP Tween 80). This would suggest that the different purity grades of polysorbate 80 do not have significantly different CMC values, which is different to that which was observed in Section 6.1 with polysorbate 20. However, purity did have an impact on the profile of the  $\Delta H$  with surfactant concentration graphs, with a sigmoidal curve present for Tween 80 and HP Tween 80, but not with SR Tween 80. This different profile is likely to be caused by the difference in composition of the fatty acid chains within Tween 80 as a result of a different manufacturing process than that which is used for the other purities.

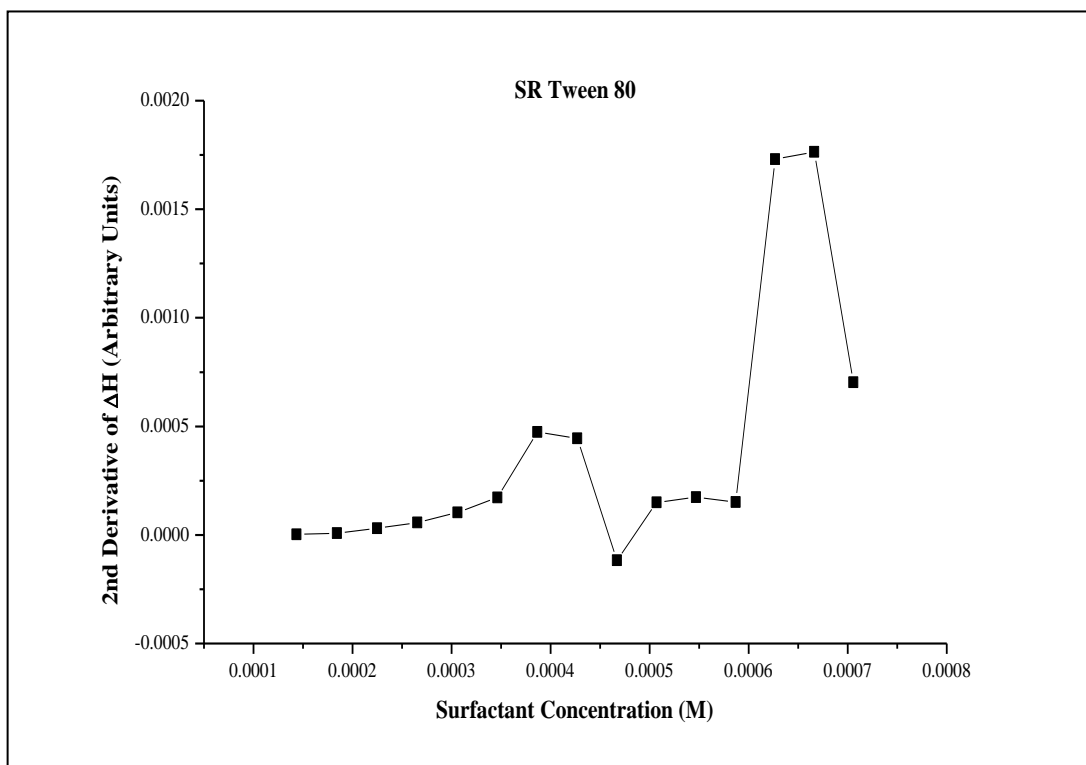


**Figure 70.** An example of a plot of the 2<sup>nd</sup> derivative of  $\Delta H$  (Arbitrary Units) with surfactant concentration (M) for SR Tween 80.

### 6.3 CMC Determination of Etocas 35

As discussed in Section 2.4 a solution of 0.0249 M Etocas 35 was prepared, and subsequently analysed using ITC, as exemplified in **Figure 71**. The graph presents with an initial steep drop off in peak size before a more gradual reduction, towards the end an almost consistent peak size was observed.

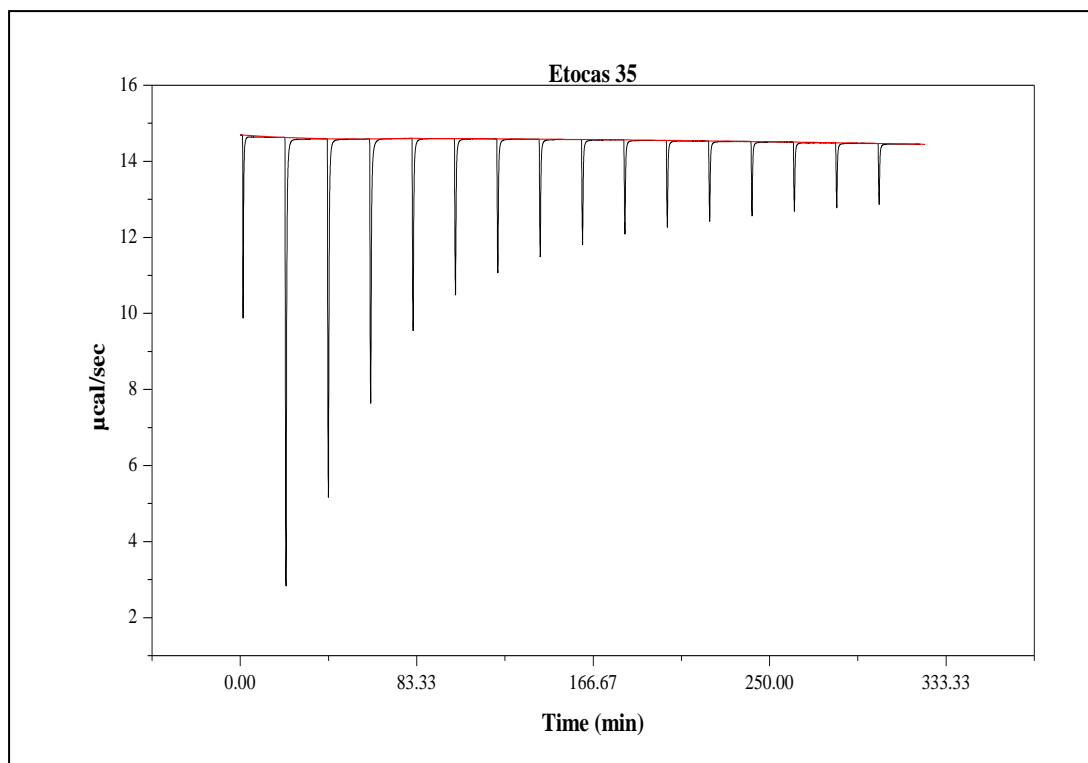


**Figure 71.** An example of a plot displaying  $\mu\text{cal/sec}$  against time (min) for the demicellisation of Etocas 35.

Integrating the peaks and converting the values to kJoules/mol and then plotting with surfactant concentration produced **Figure 72**. **Figure 72** doesn't present with a sigmoidal curve, and produced a similar shape to that observed with polysorbate 20 in **Figure 53**, **Figure 56** and **Figure 60**.

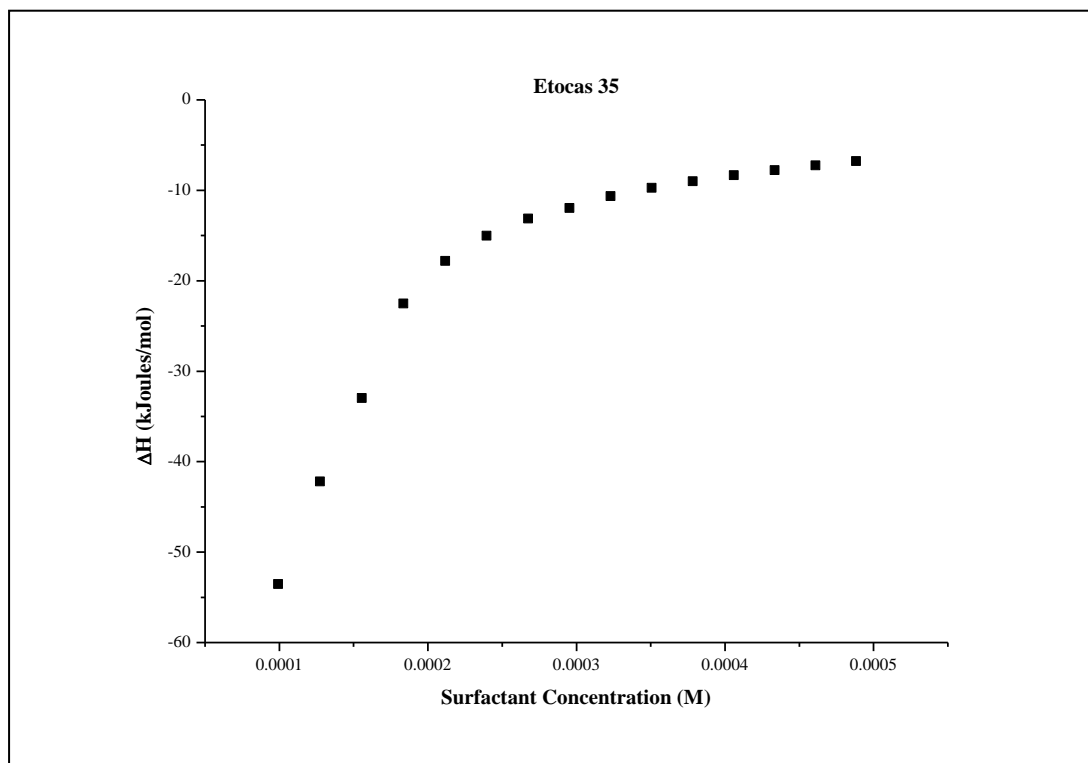


**Figure 72.** An example of a plot of  $\Delta H$  (kJoules/mol) with surfactant concentration (M) for Etocas 35.

A plot of the 2<sup>nd</sup> derivative of  $\Delta H$  with surfactant concentration allows for the calculation of the CMC via the breakpoint method and can be observed in **Figure 73**. The breakpoint was determined to be the second peak, as this was greater than the first one and they were within close proximity of each other. This value (when averaged with the other experiments) gave a CMC of 0.447 (+/- 0.0276) mM. This is the first time that the CMC of Etocas 35 has been derived, and therefore there isn't any literature to compare the value to, however it is within the same magnitude as the other non-ionic surfactants derived suggesting some level of accuracy.

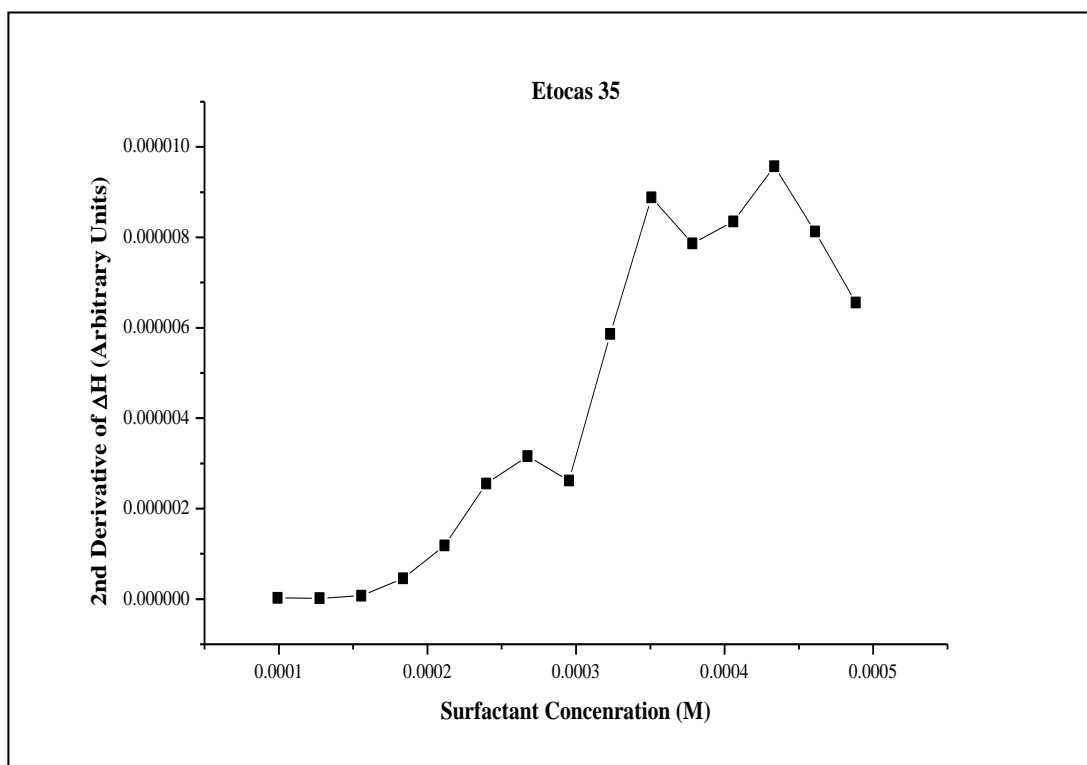


**Figure 73.** An example of a plot of the 2<sup>nd</sup> derivative of  $\Delta H$  (Arbitrary Units) with surfactant concentration (M) for Etocas 35.

#### 6.4 CMC Determination of Croduret 40

As discussed in Section 2.4, a solution of 0.0237 M Croduret 40 was prepared, and subsequently analysed using ITC, as exemplified in **Figure 74**. In **Figure 74** the peak size decreased in a more gradual manner than that which was observed with Etocas 35, before eventually reaching near consistent peak size, the overall shape of the graph is similar in shape to Tween 20.

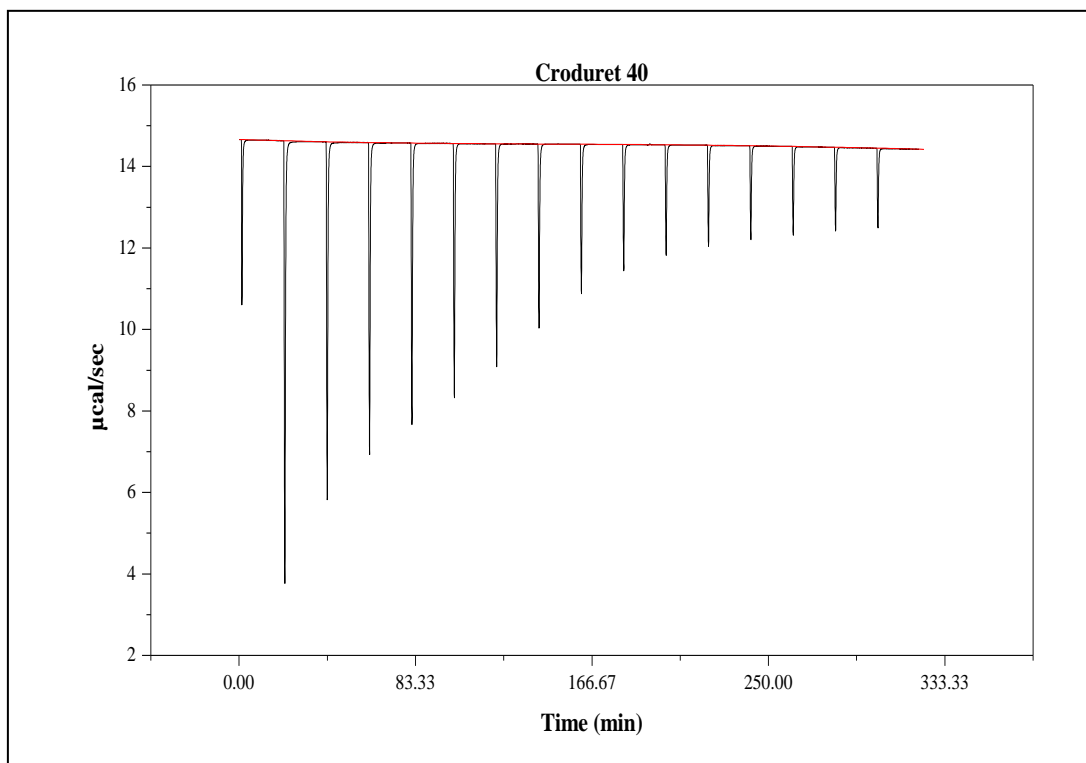


**Figure 74.** An example of a plot displaying  $\mu\text{cal/sec}$  against time (min) for the demicellisation of Croduret 40.

Integrating each of the peaks and converting the values to kJoules/mol allowed for a plot of  $\Delta H$  with surfactant concentration and can be seen in **Figure 75**. Similar to the other surfactants tested, apart from Tween 80 and HP Tween 80, the graph is non-sigmoidal in shape.

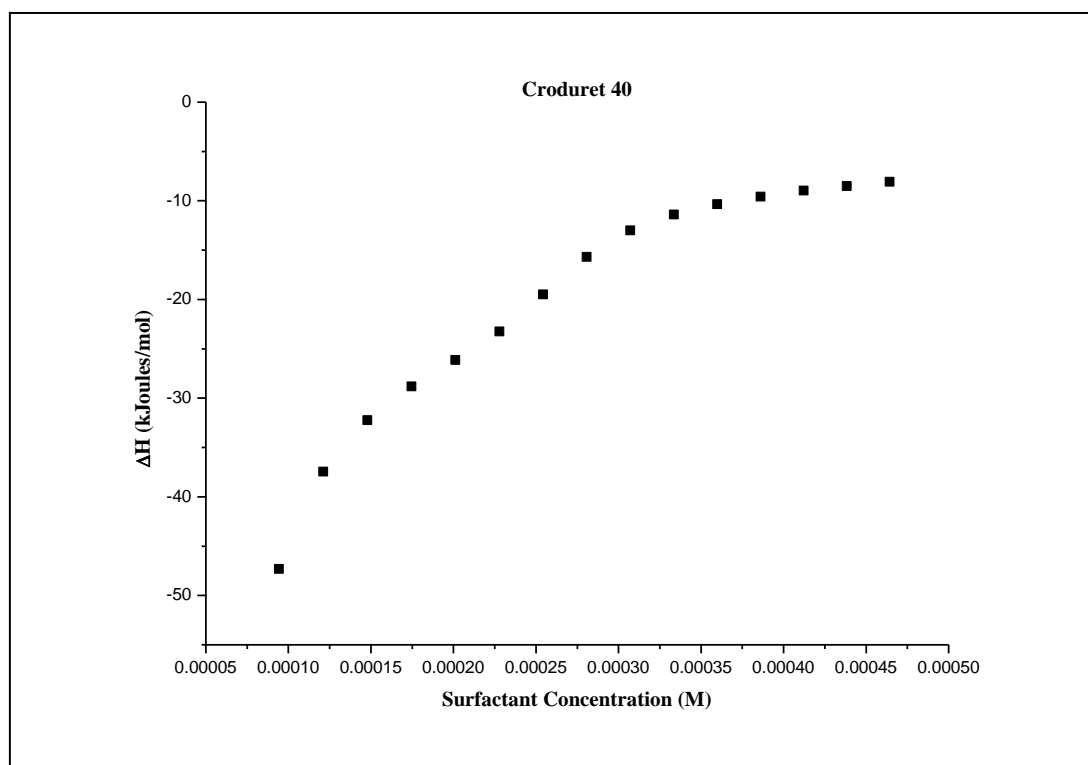


**Figure 75.** An example of a plot of  $\Delta H$  (kJoules/mol) with surfactant concentration (M) for Croduret 40.

Calculating the 2<sup>nd</sup> derivative of  $\Delta H$ , and plotting the resulting values with surfactant concentration allowed for the calculation of the CMC of Croduret 40, via the breakpoint method as can be seen in **Figure 76**. The breakpoint peak is clearly visible and when used in conjunction with the results from other experiments allowed for the calculation of the average CMC of Croduret 40, which was determined to be 0.425 (+/- 0.0262) mM. As with Etocas 35, there hasn't previously been an attempt to derive the CMC for Croduret 40, and thus there isn't any literature to compare the value against. However, Croduret 40 does share a similar molecular structure as seen in **Table 2** with Etocas 35 and therefore similar CMC values for the two surfactants would be expected and is seen here (0.425 (+/- 0.0262) mM for Croduret 40 and 0.447 (+/- 0.0276) mM for Etocas 35).

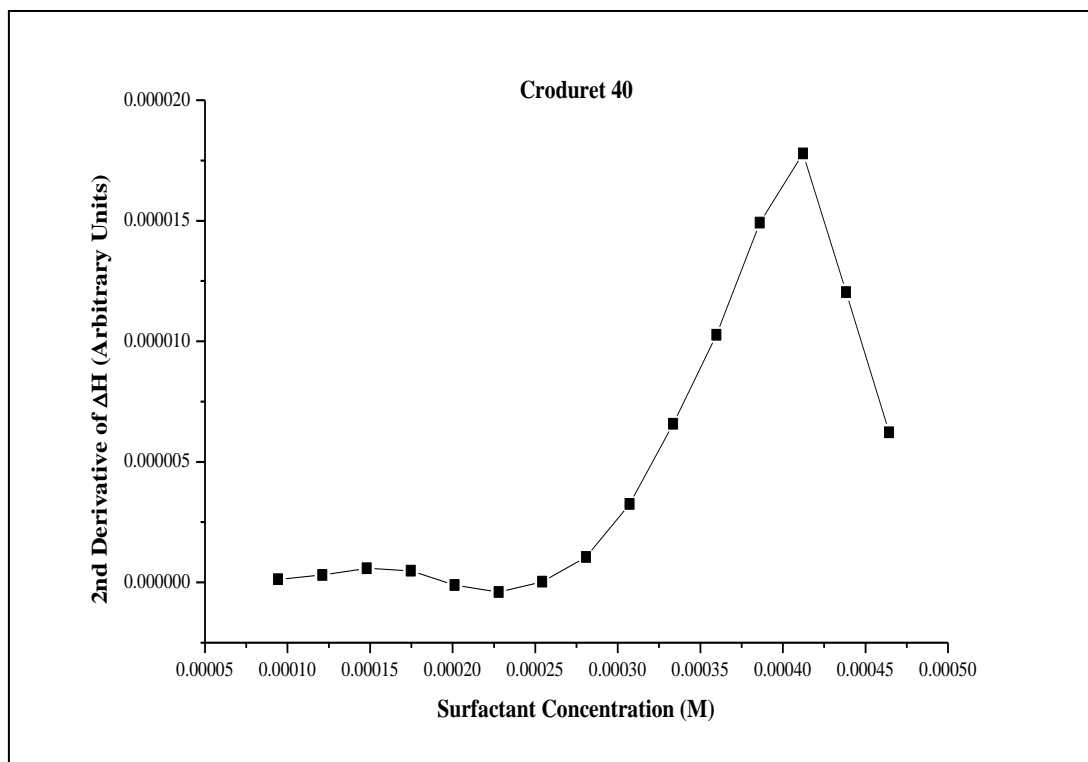


**Figure 76.** An example of a plot of the 2<sup>nd</sup> derivative of ΔH (Arbitrary Units) with surfactant concentration (M) for Croduret 40.

## 6.5 CMC Determination of Crodasol HS HP

As discussed in Section 2.4, a solution of 0.0418 M Crodasol HS HP 40 was prepared, and subsequently analysed using ITC, as exemplified in **Figure 77**. **Figure 77** presents with an initial gradual decrease in peak size, followed by a steeper decrease which then gradually tapers off to a near consistent peak size. This is similar to that which was seen with Tween 80 and HP Tween 80 in **Figure 62** and **Figure 65**.



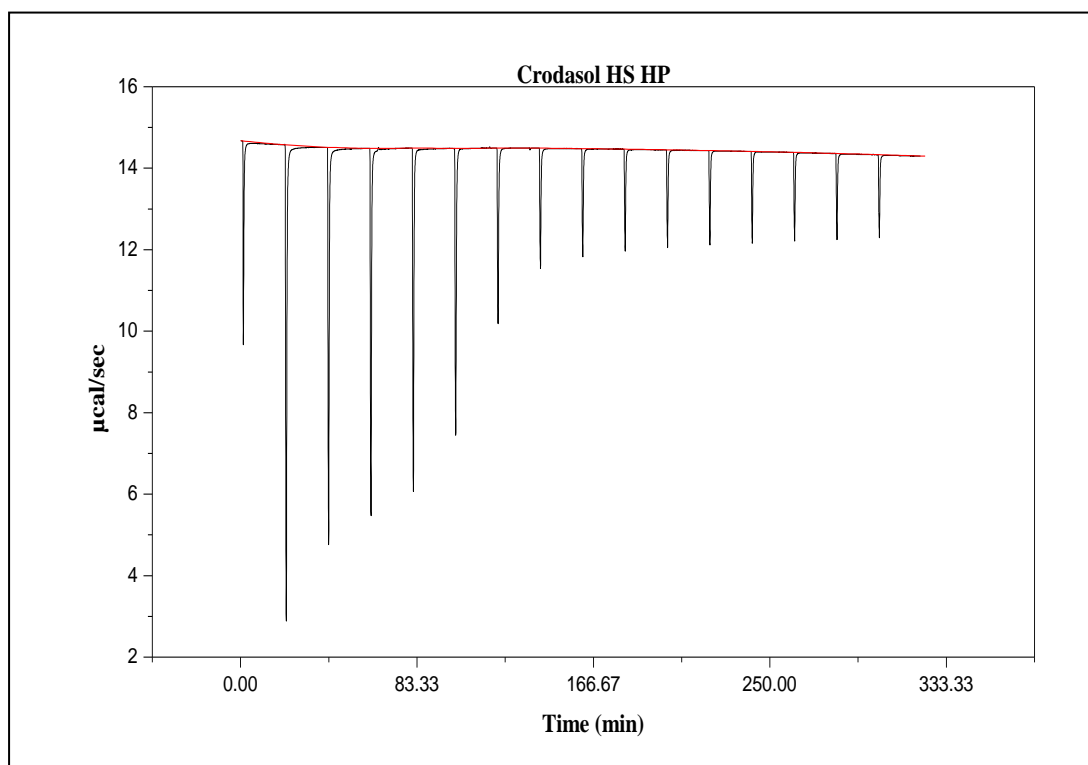


**Figure 77.** An example of a plot displaying  $\mu\text{cal/sec}$  against time (min) for the demicellisation of Crodasol HS HP.

Integrating the peaks in **Figure 77** and converting the values to kJoules/mol allows for a plot of  $\Delta H$  with surfactant concentration and can be seen in **Figure 78**. **Figure 78** presents with a sigmoidal shape, and is similar to that which was seen with Tween 80 and HP Tween 80 in **Figure 65** and **Figure 67**. There are no apparent structural similarities in Tween 80 and Crodasol HS HP that aren't present in the other surfactants tested that could account for the similarity between the graphs, suggesting that further testing of properties such as micelle size and shape would be needed before a link can be found.

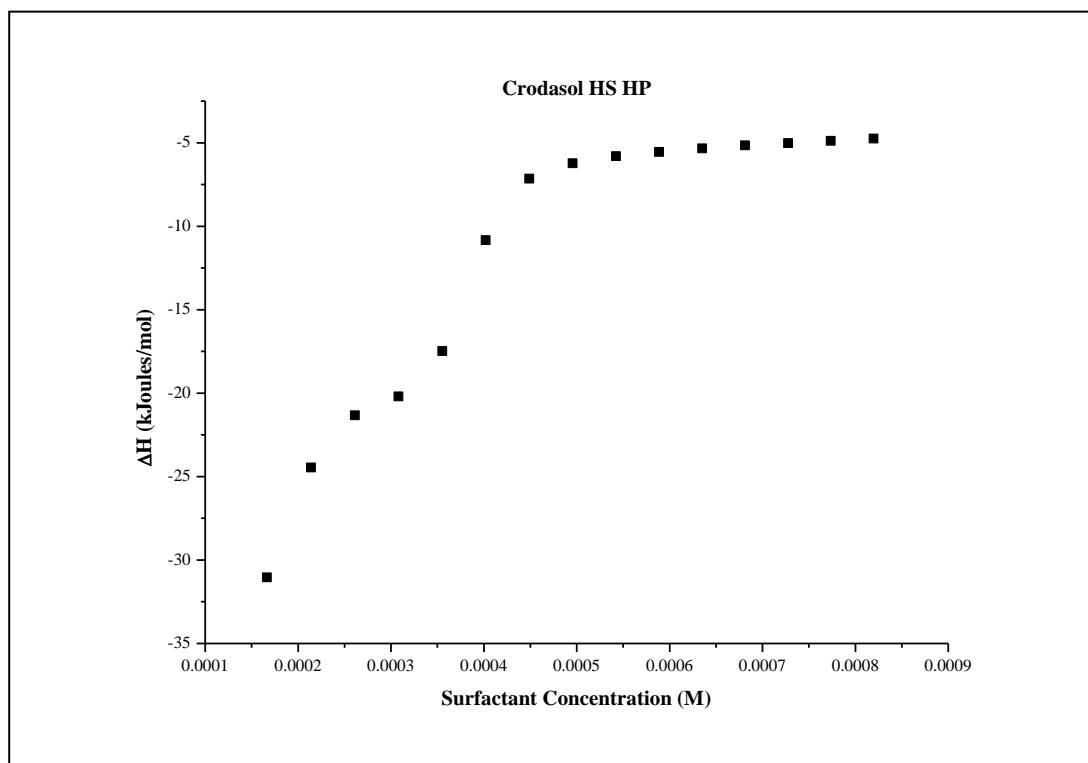


*Figure 78.* An example of a plot of  $\Delta H$  (kJoules/mol) with surfactant concentration (M) for Crodasol HS HP.

Calculating the 2<sup>nd</sup> derivative of  $\Delta H$  and plotting the resulting values with surfactant concentration allows for the calculation of the CMC of Crodasol HS HP, via the breakpoint method as can be seen in **Figure 79**. The breakpoint peak is clearly visible and when used in conjunction with the results from other experiments allowed for the calculation of the average CMC of Croduret 40, i.e. 0.728 (+/- 0.046) mM. As with Etocas 35 and Croduret 40, there are no literature values for the CMC of Crodasol HS HP to compare with. It is also not structurally similar to any of the other surfactants tested and cannot be compared in that manner either, however it is within the same order of magnitude as the other non-ionic surfactants suggesting a degree of accuracy.

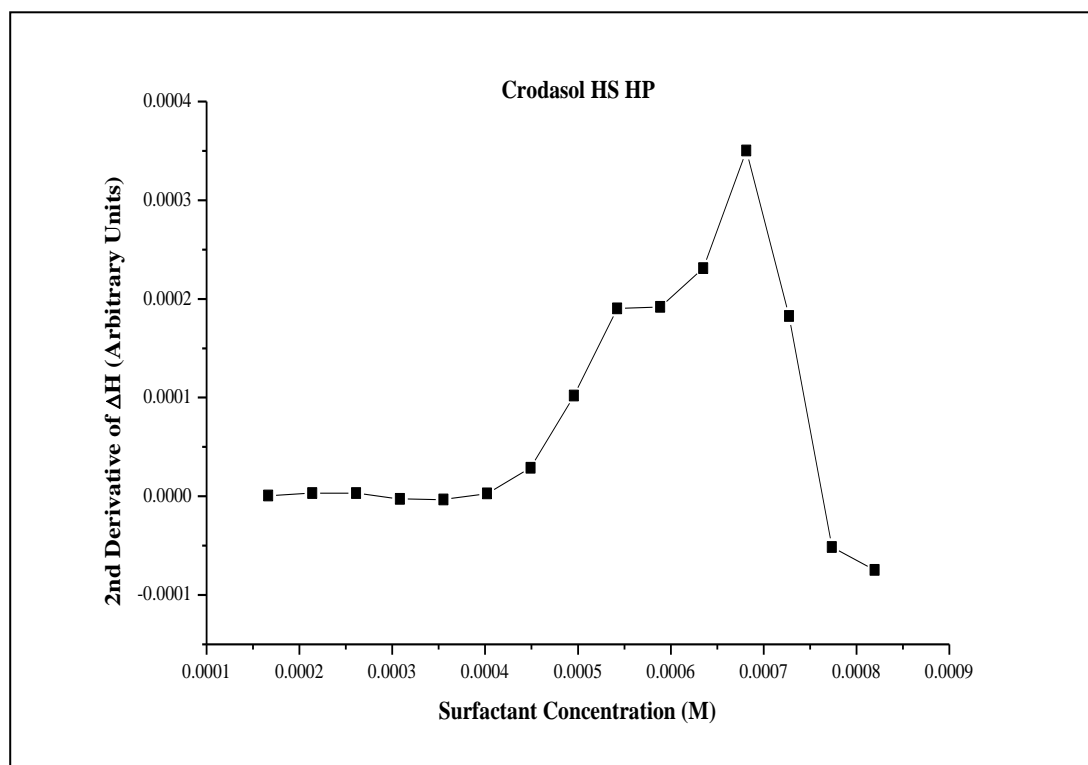


**Figure 79.** An example of a plot of the 2<sup>nd</sup> derivative of ΔH (Arbitrary Units) with surfactant concentration (M) for Crodasol HS HP.

## 6.6 ITC Discussion

Each of the surfactants supplied by Croda Ltd. had their CMC's derived and the values for each are shown in

**Table 24.** The lowest CMC derived was that of HP Tween 20 and the highest was that of Crodasol HS HP, however all surfactants have a CMC within the same order of magnitude.

**Table 24.** The derived average CMCs in mM via ITC of Tween 20, HP Tween 20, SR Tween 20, Tween 80, HP Tween 80, SR Tween 80, Etocas 35, Croduret 40 and Crodasol HS HP, the error values were determined to be the standard deviation calculated from 3 repeats.

Surfactant	Average CMC (mM)
Tween 20	0.675 +/- 0.0427
HP Tween 20	0.243 +/- 0.0179
SR Tween 20	0.358 +/- 0.0248
Tween 80	0.627 +/- 0.0375
HP Tween 80	0.546 +/- 0.0372
SR Tween 80	0.627 +/- 0.0396
Etocas 35	0.447 +/- 0.0276
Croduret 40	0.425 +/- 0.0262

As mentioned previously, the literature values for polysorbate 20 and 80 are varied and cover a large range, therefore the fact that some of the derived values don't fall within the literature range shouldn't discredit them, as there is a lack of agreement between the literature values. However, what is seen in each case where both polysorbate 20 and polysorbate 80 had their CMC derived in the same paper is that polysorbate 20 always had a greater CMC than polysorbate 80. This isn't seen in

**Table 24**, with only Tween 20 exceeding the CMC values for each of the polysorbate 80 purities; the HP and SR grades had a lower derived value. It is worth noting that none of the literature values mention using a higher purity grade of polysorbate 20, and it can therefore be assumed that only the standard grade was tested. The evidence above suggests that purity has an impact upon the CMC of polysorbate 20 and therefore, the fact that the derived values for the HP and SR purities are lower than the recorded values for each of the different purity grades of polysorbate 80, shouldn't result in the values being discredited as the impact of purity upon CMC hasn't been previously investigated.

Despite the fact that the purity of polysorbate 20 had a large impact on its CMC, the purity of polysorbate 80 didn't, with values within error limits. The purity of polysorbate 80 did affect the profile of the graphs of  $\Delta H$  with surfactant concentration, with a sigmoidal curve being present for Tween 80 and HP Tween 80 but not with SR Tween 80. These different graph profiles are likely to be caused by the difference in fatty acid chain composition that are caused by different manufacturing processes between the purities.

The CMC's for Etocas 35, Croduret 40 and Crodasol HS HP haven't previously been derived and literature values for each haven't been published. Therefore, it is difficult to be certain in the accuracy of each value, however, given that the values derived for polysorbate 20 and 80 are close to literature values and the same process was used for the remaining surfactants, a high level of accuracy can be assumed.

It is worth noting that there are different methods used to interpret ITC data to derive the CMC of surfactants, methods such as taking the inflection point as the CMC or using the first derivative are also used.<sup>82</sup> However, neither of these methods were successful when trying to interpret the data.

## 7. General Discussion

The aim of this project was to conduct research that would allow for a better understanding of the effect of surfactants on APIs. MLC in combination with ITC were used to investigate the impact of surfactant concentration and purity on retention times in MLC and solubility enhancement. In addition to this, the CMC of each of the surfactants was derived.

### 7.1 MLC

#### 7.1.1 Impact of Surfactant Concentration on Retention Time in MLC

The impact of surfactant concentration on retention time in MLC with acetaminophen, benzamide, 4-hydroxybenzamide and hydrocortisone using Tween 20, Tween 20 HP, SR Tween, Tween 80, HP Tween 80, SR Tween 80, Etocas 35, Croduret 40, Crodasol HS HP, SDS and Brij 35 as the mobile phase was investigated. It was found that prior to the CMC the change in retention time was minimal, however once the CMC had been reached a notable change could be observed in retention time with a general trend being apparent.

It was found that across the four APIs tested the non-ionic surfactants were outperformed in terms of  $k'$  reduction by their anionic (SDS) and cationic (Brij 35) counter parts. However, as only one anionic and cationic surfactant was tested, it isn't possible to state whether this is a characteristic of all anionic or cationic surfactants as SDS and Brij 35 could be outliers for each.

The greatest reduction in  $k'$  values for each surfactant was seen with hydrocortisone, followed by benzamide, and then either acetaminophen or 4-hydroxybenzamide. This was mirrored by **Table 9**, where the Log P and pKa of each of the APIs was ranked from greatest to smallest. This suggests that

APIs with both a high Log P and pKa value will result in a greater reduction in  $k'$  values with increasing concentration. APIs that have a high Log P value can be said to be more hydrophobic than those with lower Log P values, which could explain the trend observed with the MLC results. The greater the hydrophobicity of an API the greater the interactions between itself and the stationary phase, this results in a high  $k'$  as the partition equilibrium is greatly in favour of the modified stationary phase, compared to APIs with a lower Log P value. Once the CMC threshold is crossed and the second partition equilibrium is introduced the  $k'$  values significantly decrease as the equilibrium shifts in favour of the mobile phase. As drugs with a lower Log P value have an equilibrium that is initially more in favour of the mobile phase, compared to those with a high Log P value, the effect is less, represented by the lower reduction in  $k'$  values.

It is also important to consider the structure of each surfactant and the impact that this can have on interactions with APIs. Structurally Tween 20 and Tween 80 are very similar, however Tween 80 has a carbon-carbon double bond present in one of its chains, which will reduce its flexibility in terms of rotation and therefore provide a degree of steric hindrance that is not present in Tween 20. The same can be said for both Etocas 35 and Croduret 40, where Etocas 35 has a carbon-carbon double bond on each of its chains and Croduret 40 does not. The steric hindrance caused by the carbon-carbon double bonds will have an impact and is only one of several factors such as Log P and hydrophobicity that dictate where each of the APIs position themselves within the micelle. Crodasol HS HP, SDS and Brij 35 are all single chain surfactants, however, Crodasol HS HP has a greater chain length and will therefore have greater hydrophobic interactions, resulting in stronger interactions with the stationary phase and therefore longer retention times.

### **7.1.2 Impact of Surfactant Purity on Retention Time in MLC**

Both of the polysorbates studied have the HP purity grade resulting in the greatest reduction in  $k'$  values overall. What is interesting is the SR grade of both also ranked the lowest for each, however, it is important to remember that the reduction in  $k'$  values isn't necessarily related to MLC performance. It

is just a comparison on how surfactant concentration affects retention time. It is possible for a surfactant to have a low reduction in  $k'$  values across the concentrations tested but still have the lowest retention time, this was observed as the SR and HP purities outperformed the standard grade in terms of lowest retention time. It is likely a combination of the lack of purities present in the HP and SR grades (when compared to the standard grade), and difference in the composition of the fatty acid chains that result in the HP and SR grades interacting more strongly with the APIs, and therefore producing a lower retention time.

## **7.2 Solubility Enhancement**

### **7.2.1 The Impact of Surfactants on API Solubility**

It was found that for each of the surfactants tested that prior to the CMC little to no change was observed regarding solubility, however, after the CMC was exceeded the solubility of each of the API's tested increased apart from standard grade Tween 20 and Croduret 40 with benzamide.

Unlike the results with MLC, the anionic and cationic surfactants didn't outperform the non-ionic surfactants, with SDS and Brij 35 having results that place them in the middle of the surfactants tested in terms of solubility enhancement. However, as mentioned in Section 7.1.1, a greater number of anionic and cationic surfactants need to be tested before any conclusions can be drawn with regards to how surfactant category affects its ability to enhance solubility.

The greatest solubility enhancement across each of the API's tested was produced by Etocas 35 and Crodasol HS HP, which do not share structural similarities such as that which is seen between polysorbate 20 and 80 in terms of being identical apart from the presence of an alkene bond and the greater length of the carbon chains in polysorbate 80, this explains their close groupings in the rankings.

## **7.2.2 The Impact of Surfactant Purity on Solubility Enhancement of APIs**

It was found that the standard grade of polysorbate 20 and polysorbate 80 were outperformed by their higher purity grade counter parts regarding solubility enhancement. This is likely the result of a combination of the lack of purities present in the HP and SR grades (when compared to the standard grade), and differences in the composition of the fatty acid chains that result in stronger interactions between the higher purity grade surfactants and the APIs tested, leading to a greater solubility enhancement.

## **7.3 ITC**

### **7.3.1 CMC Determination**

The CMC of Tween 20, HP Tween 20, SR Tween 20, Tween 80, HP Tween 80, SR Tween 80, Etocas 35, Croduret 40 and Crodasol HS HP was determined using ITC.

It was found that purity of the surfactant had a significant impact on the CMC of polysorbate 20, with the standard grade having a notably higher CMC value than the HP or SR grades. This is likely caused by the difference in the composition of the fatty acid chains that exist across purities, with a higher percentage of longer fatty acid chains resulting in an increase in CMC. It was interesting to note that this wasn't the case with polysorbate 80, where each of the 3 purity grades had close CMC values. The values for polysorbate 20 and polysorbate 80 were higher than those that have previously been recorded in literature, however, given the broad range of values reported this shouldn't necessarily negate the accuracy of the values as there isn't agreement amongst the scientific community for published values.

Etocas 35, Croduret 40 and Crodasol HS HP hadn't previously had their CMCs derived and reported, therefore there isn't any literature to compare the values against. However, Croduret 40 does share a similar molecular structure with Etocas 35 and therefore similar CMC values for the two surfactants would be expected, as was seen.



## 7.4 Future Work

In the future, expanding the surfactants used to include other anionic surfactants such as ammonium lauryl sulfate, sodium laureth sulfate, sodium myreth sulfate, cationic surfactants such as cetrimonium bromide, cetlypyridinium chloride and benzalkonium chloride and zwitterionic surfactants such as lauryldimethylamine oxide and myristamine oxide would allow for a more complete study on how surfactant concentration affects the retention time and solubility for each category of surfactant. In addition to this, testing how Etocas 35, Croduret 40, Crodasol HS HP, SDS and Brij 35 affect the solubility of hydrocortisone and increasing the number of APIs to include other insoluble molecules such as glipizide and progesterone, as well as more readily soluble APIs such as caffeine, would allow for a more diverse data set and for a more thorough testing of the theory that greater Log P and pKa values result in a greater reduction in  $k'$  values with increasing surfactant concentration.

In the future CMC determinations in the presence of APIs such as those used in MLC previously (acetaminophen, benzamide, 4-hydroxybenzamide and hydrocortisone) should be undertaken, this would allow for a better understanding of surfactant-API interactions.

## 8. Conclusions

It was found that increasing the concentration of Tween 20, HP Tween 20, SR Tween 20, Tween 80, HP Tween 80, SR Tween 80, Etocas 35, Croduret 40, Crodasol HS HP, SDS and Brij 35 reduced the retention time of acetaminophen, benzamide, 4-hydroxybenzamide and hydrocortisone in MLC. It was also found that purity had a notable impact on this with the SR and HP grades outperforming the standard grades in terms of reduction in retention time.

The solubility enhancement of acetaminophen, benzamide, 4-hydroxybenzamide and hydrocortisone with Tween 20, HP Tween 20, SR Tween 20, Tween 80, HP Tween 80, SR Tween 80, Etocas 35, Croduret 40, Crodasol HS HP, SDS and Brij 35 was calculated and found that increasing the concentration of surfactant resulted in an increase in solubility for each of the APIs. The affect of

surfactant purity on solubility enhancement was also investigated, with SR and HP grades outperforming the grades of Tween 20 and Tween 80.

The CMC of Tween 20, HP Tween 20, SR Tween 20, Tween 80, HP Tween 80, SR Tween 80, Etocas 35, Croduret 40, Crodasol HS HP were also calculated using ITC.

In summary, this project has utilised a variety of analytical techniques to investigate the behaviour of non-ionic surfactants. The information acquired in this study has furthered the understanding of such systems and will be beneficial in the development of future formulations.

## 9. References

1. Solubility. 2016. 7 ed.: Oxford University Press.
2. Alsenz J, Kansy M. 2007. High throughput solubility measurement in drug discovery and development. *Advanced Drug Delivery Reviews*. 59(7):546-567.
3. Po HN, Senozan NM. 2001. The henderson-hasselbalch equation: Its history and limitations. *Journal of Chemical Education*. 78(11):1499.
4. Savjani KT, Gajjar AK, Savjani JK. 2012. Drug solubility: Importance and enhancement techniques. *ISRN Pharmaceutics*. 2012:10.
5. Vemula VR, Lagishetty V, Lingala S. 2010. Solubility enhancement techniques. *International journal of pharmaceutical sciences review and research*. 5(1):41-51.
6. Pereira DA, Williams JA. 2007. Origin and evolution of high throughput screening. *British Journal of Pharmacology*. 152(1):53-61.
7. Stuart M, Box K. 2005. Chasing equilibrium: Measuring the intrinsic solubility of weak acids and bases. *Analytical Chemistry*. 77(4):983-990.
8. Dokoumetzidis A, Papadopoulou V, Macheras P. 2006. Analysis of dissolution data using modified versions of noyes-whitney equation and the weibull function.
9. Black S, Muller F. 2010. On the effect of temperature on aqueous solubility of organic solids. *Organic Process Research & Development*. 14(3):661-665.
10. Sun J, Wang F, Sui Y, She Z, Zhai W, Wang C, Deng Y. 2012. Effect of particle size on solubility, dissolution rate, and oral bioavailability: Evaluation using coenzyme q(10) as naked nanocrystals. *International Journal of Nanomedicine*. 7:5733-5744.
11. Völgyi G, Baka E, J Box K, Comer J, Krisztina T-N. 2010. Study of ph-dependent solubility of organic bases. Revisit of henderson-hasselbalch relationship.
12. Higuchi T, Connors KA. 1965. Advances in analytical chemistry and instrumentation. *Advances in Analytical Chemistry and Instrumentation*. 117-212.
13. Jouyban A, Abolghassemi Fakhree MA. 2012. Experimental and computational methods pertaining to drug solubility.
14. Hankinson RW, Thompson D. 1965. Equilibria and solubility data for the methanol-water-1-nitropropane ternary liquid system. *Journal of Chemical & Engineering Data*. 10(1):18-19.
15. Yang Z-S, Zeng Z-X, Xue W-L, Zhang Y. 2008. Solubility of bis(benzoxazolyl-2-methyl) sulfide in different pure solvents and ethanol + water binary mixtures between (273.25 and 325.25) k. *Journal of Chemical & Engineering Data*. 53(11):2692-2695.
16. Hoelke B, Gieringer S, Arlt M, Saal C. 2009. Comparison of nephelometric, uv-spectroscopic, and hplc methods for high-throughput determination of aqueous drug solubility in microtiter plates. *Analytical Chemistry*. 81(8):3165-3172.
17. Pan L, Ho Q, Tsutsui K, Takahashi L. 2001. Comparison of chromatographic and spectroscopic methods used to rank compounds for aqueous solubility. *Journal of Pharmaceutical Sciences*. 90(4):521-529.
18. McDonnell G, Russell AD. 1999. Antiseptics and disinfectants: Activity, action, and resistance. *Clinical Microbiology Reviews*. 12(1):147-179.
19. Sekhon B. 2013. Surfactants: Pharmaceutical and medicinal aspects.
20. Kirkman R, Chantler E. 1993. Contraception and the prevention of sexually transmitted diseases. *Br Med Bull*. 49(1):171-181.
21. Boyd BJ, Bergström CAS, Vinarov Z, Kuentz M, Brouwers J, Augustijns P, Brandl M, Bernkop-Schnürch A, Shrestha N, Pr at V et al. 2019. Successful oral delivery of poorly

- water-soluble drugs both depends on the intraluminal behavior of drugs and of appropriate advanced drug delivery systems. *European Journal of Pharmaceutical Sciences*. 137:104967.
22. Vinarov Z, Gancheva G, Katev V, Tcholakova S. 2018. Albendazole solution formulation via vesicle-to-micelle transition of phospholipid-surfactant aggregates. *Drug Development and Industrial Pharmacy*. 44:1-32.
  23. Super refined polysorbate 20. 2019. [accessed]. [https://www.crodahealthcare.com/en-gb/products-and-applications/product-finder/product/1864/Super\\_1\\_Refined\\_1\\_Polysorbate\\_1\\_20](https://www.crodahealthcare.com/en-gb/products-and-applications/product-finder/product/1864/Super_1_Refined_1_Polysorbate_1_20).
  24. Rowe RC, Sheskey PJ, Owen SC, American Pharmacists A. 2006. *Handbook of pharmaceutical excipients*. London; Greyslake, IL; Washington, DC: Pharmaceutical Press ; American Pharmacists Association.
  25. Capra P, Musitelli G, Perugini P. 2017. Wetting and adhesion evaluation of cosmetic ingredients and products: Correlation of in vitro–in vivo contact angle measurements. *International Journal of Cosmetic Science*. 39(4):393-401.
  26. Food EPoFAaNSat. 2015. Scientific opinion on the re-evaluation of polyoxyethylene sorbitan monolaurate (e 432), polyoxyethylene sorbitan monooleate (e 433), polyoxyethylene sorbitan monopalmitate (e 434), polyoxyethylene sorbitan monostearate (e 435) and polyoxyethylene sorbitan tristearate (e 436) as food additives. *EFSA Journal*. 13(7):4152.
  27. Zhang R, Wang Y, Tan L, Zhang HY, Yang M. 2012. Analysis of polysorbate 80 and its related compounds by rp-hplc with elsd and ms detection. *Journal of Chromatographic Science*. 50(7):598-607.
  28. Orchard A, van Vuuren S. 2017. Commercial essential oils as potential antimicrobials to treat skin diseases. *Evidence-based complementary and alternative medicine : eCAM*. 2017:4517971-4517971.
  29. Rachmawati H, Novel MA, Ayu S, Berlian G, Tandrasasmita OM, Tjandrawinata RR, Anggadiredja K. 2017. The in vitro-in vivo safety confirmation of peg-40 hydrogenated castor oil as a surfactant for oral nanoemulsion formulation. *Scientia pharmaceutica*. 85(2):18.
  30. Bittner B, Mountfield RJ. 2002. Formulations and related activities for the oral administration of poorly water-soluble compounds in early discovery animal studies: An overview of frequently applied approaches. Part 2.
  31. Cui X, Mao S, Liu M, Yuan H, Du Y. 2008. Mechanism of surfactant micelle formation. *Langmuir*. 24(19):10771-10775.
  32. Moroi Y. 1992. *Micelles: Theoretical and applied aspects*. New York: Plenum Press.
  33. Shahzad Y. 2013. *Micellar chromatographic partition coefficients and their application in predicting skin permeability [Doctoral]*. University of Huddersfield.
  34. Xu J, Zhang Y, Chen H, Wang P, Xie Z, Yao Y, Yan Y, Zhang J. 2013. Effect of surfactant headgroups on the oil/water interface: An interfacial tension measurement and simulation study. *Journal of Molecular Structure*. 1052(Supplement C):50-56.
  35. Ruiz-Ángel MJ, Carda-Broch S, Torres-Lapasió JR, García-Álvarez-Coque MC. 2009. Retention mechanisms in micellar liquid chromatography. *Journal of Chromatography A*. 1216(10):1798-1814.
  36. Dai C, Du M, Zhao M, You Q, Guan B, Wang X, Liu P. 2013. Study of micelle formation by fluorocarbon surfactant n-(2-hydroxypropyl)perfluorooctane amide in aqueous solution. *The Journal of Physical Chemistry B*. 117(34):9922-9928.

37. Baloch MK, Hameed G, Bano A. 2002. Effect of electrolyte concentration and temperature on cmc of surfactants. *Journal of the Chemical Society of Pakistan*. 24(2):77-86.
38. Starov V, Zhdanov V, Kovalchuk NM. 2010. Kinetic models of micelles formation. *Colloids and Surfaces A: Physicochemical and Engineering Aspects*. 354(1):268-278.
39. Rangel-Yagui C, Pessoa A, Tavares L. 2005. Micellar solubilization of drugs. *Journal of pharmacy & pharmaceutical sciences : a publication of the Canadian Society for Pharmaceutical Sciences, Société canadienne des sciences pharmaceutiques*. 8:147-165.
40. Lee SC, Huh KM, Lee J, Cho YW, Galinsky RE, Park K. 2007. Hydrotropic polymeric micelles for enhanced paclitaxel solubility: In vitro and in vivo characterization. *Biomacromolecules*. 8(1):202-208.
41. Mirgorodskaya AB, Valeeva FG, Yackevich EI, Beschastnova TN, Zhukova NA, Zakharova LY, Sinyashin OG, Mamedov VA. 2014. Effect of surfactant micelles on solubility and spectral characteristics of 2,2'-bibenzimidazole. *Russian Chemical Bulletin*. 63(12):2681-2685.
42. Torchilin VP. 2001. Structure and design of polymeric surfactant-based drug delivery systems. *Journal of Controlled Release*. 73(2):137-172.
43. Ambrose RJ. 1989. *Surfactants and interfacial phenomena—second edition*, by Milton J. Rosen, John Wiley & Sons, Inc., New York, 1989, 431 pp. Price: \$49.95. *Journal of Polymer Science Part C: Polymer Letters*. 27(12):503-503.
44. Alvarez-Núñez FA, Yalkowsky SH. 2000. Relationship between polysorbate 80 solubilization descriptors and octanol–water partition coefficients of drugs. *International Journal of Pharmaceutics*. 200(2):217-222.
45. Lu Y, Zhang E, Yang J, Cao Z. 2018. Strategies to improve micelle stability for drug delivery. *Nano research*. 11(10):4985-4998.
46. Yokoyama M. 1992. Block copolymers as drug carriers. *Crit Rev Ther Drug Carrier Syst*. 9(3-4):213-248.
47. Bird IM. 1989. High performance liquid chromatography: Principles and clinical applications. *BMJ : British Medical Journal*. 299(6702):783-787.
48. Czaplicki S. 2013. Chromatography in bioactivity analysis of compounds. p. 99-122.
49. McMaster MC. 2007. *HPLC: A practical user's guide*. Hoboken, N.J: Wiley-Interscience.
50. Grushka E. 1974. Solute band spreading in liquid chromatography. Causes and importance. *Analytical Chemistry*. 46(6):510A-518a.
51. Kawczak P, Baczek T. 2012. Recent theoretical and practical applications of micellar liquid chromatography (mlc) in pharmaceutical and biomedical analysis. *Central European Journal of Chemistry*. 10:570-584.
52. Rambla-Alegre M. 2012. Basic principles of mlc. *Chromatography Research International*. 2012:6.
53. Fuchs O. Micellization, solubilization and microemulsions. *Colloid and polymer science*. 258(8):980-981.
54. Marina ML, Jiménez O, García MA, Vera S. 1996. Study of the separation selectivity of a group of benzene and naphthalene derivatives in micellar liquid chromatography. *Microchemical Journal*. 53(2):215-224.
55. Mithani SD, Bakatselou V, TenHoor CN, Dressman JB. 1996. Estimation of the increase in solubility of drugs as a function of bile salt concentration. *Pharmaceutical research*. 13(1):163.

56. Lu R, Sun J, Wang Y, Li H, Liu J, Fang L, He Z. 2009. Characterization of biopartitioning micellar chromatography system using monolithic column by linear solvation energy relationship and application to predict blood–brain barrier penetration. *Journal of Chromatography A*. 1216(27):5190-5198.
57. Waters LJ, Kasprzyk-Hordern B. 2010. Micellar chromatographic determination of partition coefficients and associated thermodynamic data for pharmaceutical compounds. *Journal of Thermal Analysis and Calorimetry*. 102(1):343-347.
58. De Vrieze M, Lynen F, Chen K, Szucs R, Sandra P. 2013. Predicting drug penetration across the blood–brain barrier: Comparison of micellar liquid chromatography and immobilized artificial membrane liquid chromatography. *Analytical and Bioanalytical Chemistry*. 405(18):6029-6041.
59. Waters LJ, Shahzad Y, Stephenson J. 2013. Modelling skin permeability with micellar liquid chromatography. *European Journal of Pharmaceutical Sciences*. 50(3):335-340.
60. Beltrán-Martín Navarro B, Peris-Vicente J, Carda-Broch S, Esteve-Romero J. 2014. Development and validation of a micellar liquid chromatography-based method to quantify melamine in swine kidney. *Food Control*. 46(Supplement C):168-173.
61. Waters LJ, Shokry DS, Parkes GMB. 2016. Predicting human intestinal absorption in the presence of bile salt with micellar liquid chromatography. *Biomedical Chromatography*. 30(10):1618-1624.
62. Richardson AE, McPherson SD, Fasciano JM, Pauls RE, Danielson ND. 2017. Micellar liquid chromatography of terephthalic acid impurities. *Journal of Chromatography A*. 1491(Supplement C):67-74.
63. Shokry DS, Waters LJ, Parkes GMB, Mitchell JC. 2018. Incorporating physiologically relevant mobile phases in micellar liquid chromatography for the prediction of human intestinal absorption. *Biomedical Chromatography*. 32(12):e4351.
64. Shokry DS, Waters LJ, Parkes GMB, Mitchell JC. 2019. Prediction of human intestinal absorption using micellar liquid chromatography with an aminopropyl stationary phase. *Biomedical Chromatography*. 0(0):e4515.
65. Ali Aa-kF, Danielson ND. 2020. Micellar and sub-micellar liquid chromatography of terephthalic acid contaminants using a c18 column coated with tween 20. *Analytica Chimica Acta*. 1105:214-223.
66. Ramezani AM, Ahmadi R, Absalan G. 2020. Designing a sustainable mobile phase composition for melamine monitoring in milk samples based on micellar liquid chromatography and natural deep eutectic solvent. *Journal of Chromatography A*. 1610:460563.
67. Duan X, Liu X, Dong Y, Duan T, Zhang J, He S, Yang F, Dong Y. 2020. A mixed micellar liquid chromatography with direct injection for rapid analysis of eight sulfonamides in milk. *Food Analytical Methods*.
68. Prasad Pawar R, Mishra P, Durgbanshi A, Bose D, Albiol-Chiva J, Peris-Vicente J, García-Ferrer D, Esteve-Romero J. 2020. Use of micellar liquid chromatography to determine mebendazole in dairy products and breeding waste from bovine animals. *Antibiotics*. 9(2).
69. Grolier J-PE, del Río JM. 2012. Isothermal titration calorimetry: A thermodynamic interpretation of measurements. *The Journal of Chemical Thermodynamics*. 55:193-202.

70. Olofsson G, Lund University L, Sweden, Loh W, University of Campinas C, Brazil. 2009. On the use of titration calorimetry to study the association of surfactants in aqueous solutions. *J Braz Chem Soc.* 20(4):577-593.
71. Patist A, Bhagwat SS, Penfield KW, Aikens P, Shah DO. 2000. On the measurement of critical micelle concentrations of pure and technical-grade nonionic surfactants. *Journal of Surfactants and Detergents.* 3(1):53-58.
72. Mittal KL. 1972. Determination of cmc of polysorbate 20 in aqueous solution by surface tension method. *Journal of Pharmaceutical Sciences.* 61(8):1334-1335.
73. Wan LSC, Lee PFS. 1974. Cmc of polysorbates. *Journal of Pharmaceutical Sciences.* 63(1):136-137.
74. Szymczyk K, Taraba A, Szaniawska M. 2019. Interactions of tween 20, 60 and 80 with dye molecules: Spectroscopic analysis. *Journal of Molecular Liquids.* 290:111227.
75. Ortiz-Tafoya MC, Tecante A. 2018. Physicochemical characterization of sodium stearyl lactylate (ssl), polyoxyethylene sorbitan monolaurate (tween 20) and κ-carrageenan. *Data in Brief.* 19:642-650.
76. Niño MRR, Patino JMR. 1998. Surface tension of bovine serum albumin and tween 20 at the air-aqueous interface. *Journal of the American Oil Chemists' Society.* 75(10):1241.
77. Mandal AB, Nair BU, Ramaswamy D. 1988. Determination of the critical micelle concentration of surfactants and the partition coefficient of an electrochemical probe by using cyclic voltammetry. *Langmuir.* 4(3):736-739.
78. Szymczyk K, Zdziennicka A, Jańczuk B. 2018. Adsorption and aggregation properties of some polysorbates at different temperatures. *Journal of Solution Chemistry.* 47(11):1824-1840.
79. Li H, Hu D, Liang F, Huang X, Zhu Q. Influence factors on the critical micelle concentration determination using pyrene as a probe and a simple method of preparing samples. *Royal Society Open Science.* 7(3):192092.
80. Šteflová J, Štefl M, Walz S, Knop M, Trapp O. 2016. Comprehensive study on critical micellar concentrations of sds in acetonitrile–water solvents. *ELECTROPHORESIS.* 37(10):1287-1295.
81. Bouchemal K, Agnely F, Koffi A, Ponchel G. 2009. A concise analysis of the effect of temperature and propanediol-1, 2 on pluronic f127 micellization using isothermal titration microcalorimetry. *Journal of Colloid and Interface Science.* 338(1):169-176.
82. Loh W, Brinatti C, Tam KC. 2016. Use of isothermal titration calorimetry to study surfactant aggregation in colloidal systems. *Biochimica et Biophysica Acta (BBA) - General Subjects.* 1860(5):999-1016.
83. Scholz N, Behnke T, Resch-Genger U. 2018. Determination of the critical micelle concentration of neutral and ionic surfactants with fluorometry, conductometry, and surface tension—a method comparison. *Journal of Fluorescence.* 28(1):465-476.
84. Waters LJ, Hussain T, Parkes GMB. 2012. Titration calorimetry of surfactant–drug interactions: Micelle formation and saturation studies. *The Journal of Chemical Thermodynamics.* 53:36-41.
85. Waters LJ, Hussain T, Parkes GMB. 2014. Thermodynamics of micellisation: Sodium dodecyl sulfate/sodium deoxycholate with polyethylene glycol and model drugs. *The Journal of Chemical Thermodynamics.* 77:77-81.
86. Wang Y, Wu H, Wang J, Lou P, Zhao Y, Bai G. 2019. Thermodynamics of self-aggregation of mixed cationic gemini/sodium deoxycholate surfactant systems in aqueous solution. *Journal of Thermal Analysis and Calorimetry.* 135(5):2903-2913.

87. Pubchem. 2020. [accessed].
88. Waters LJ, Smith OEP, Small W, Mellor S. 2020. Understanding polysorbate-compound interactions within the cmc region. *Journal of Chromatography A*. 1623:461212.
89. Wołowicz A, Staszak K. 2020. Study of surface properties of aqueous solutions of sodium dodecyl sulfate in the presence of hydrochloric acid and heavy metal ions. *Journal of Molecular Liquids*. 299:112170.
90. Hait S, Moulik S. 2001. Determination of critical micelle concentration (cmc) of nonionic surfactants by donor-acceptor interaction with iodine and correlation of cmc with hydrophile-lipophile balance and other parameters of the surfactants. *Journal of Surfactants and Detergents*. 4:303-309.
91. Kulikov AU, Verushkin AG. 2008. Simultaneous determination of paracetamol, caffeine, guaifenesin and preservatives in syrups by micellar lc. *Chromatographia*. 67(5):347-355.
92. Usp-nf. 2020. [accessed].
93. Owusu Apenten RK, Zhu Q-H. 1996. Interfacial parameters for selected spans and tweens at the hydrocarbon—water interface. *Food Hydrocolloids*. 10(1):27-30.
94. Rukhadze MD, Sebiskveradze MV, Akhalkatsi TG, Makharadze TG. 2006. Imitation of artificial membrane system via mobile phases with tween-80 and cholic acid in biopartitioning micellar chromatography. *Biomedical Chromatography*. 20(8):753-759.
95. Hadjmohammadi M, Salary M. 2013. Biopartitioning micellar chromatography with sodium dodecyl sulfate as a pseudo  $\alpha$ 1-acid glycoprotein to the prediction of protein–drug binding. *Journal of Chromatography B*. 912:50-55.
96. Hadjmohammadi MR, Nazari SSSJ. 2010. Separation optimization of quercetin, hesperetin and chrysin in honey by micellar liquid chromatography and experimental design. *Journal of Separation Science*. 33(20):3144-3151.
97. Safa F, Hadjmohammadi MR. 2005. Chemometric approach in optimization of micellar liquid chromatographic separation of some halogenated phenols. *Analytica Chimica Acta*. 540(1):121-126.
98. Peris-García E, Ortiz-Bolsico C, Baeza-Baeza JJ, García-Alvarez-Coque MC. 2015. Isocratic and gradient elution in micellar liquid chromatography with brij-35. *Journal of Separation Science*. 38(12):2059-2067.
99. Mutelet F, Rogalski M, Guermouche MH. 2003. Micellar liquid chromatography of polyaromatic hydrocarbons using anionic, cationic, and nonionic surfactants: Armstrong model, Iser interpretation. *Chromatographia*. 57(9):605-610.
100. Hamza YE, Paruta AN. 1985. Solubilization of paracetamol using non-ionic surfactants and co-solubilizers. *Drug Development and Industrial Pharmacy*. 11(1):187-206.
101. Kim S, Thiessen PA, Bolton EE, Chen J, Fu G, Gindulyte A, Han L, He J, He S, Shoemaker BA et al. 2016. Pubchem substance and compound databases. *Nucleic Acids Research*. 44(Database issue):D1202-D1213.
102. Barry BW, El Eini DI. 1976. Solubilization of hydrocortisone, dexamethasone, testosterone and progesterone by long-chain polyoxyethylene surfactants. *J Pharm Pharmacol*. 28(3):210-218.
103. Calabrese I, Merli M, Turco Liveri ML. 2015. Deconvolution procedure of the uv–vis spectra. A powerful tool for the estimation of the binding of a model drug to specific solubilisation loci of bio-compatible aqueous surfactant-forming micelle. *Spectrochimica Acta Part A: Molecular and Biomolecular Spectroscopy*. 142:150-158.



104. Selvaraj G, Rajendran V. 2013. Influence of various surfactants on size, morphology, and optical properties of ceo2 nanostructures via facile hydrothermal route.
105. Dastidar DG, Sa B. 2009. A comparative study of uv-spectrophotometry and first-order derivative uv-spectrophotometry methods for the estimation of diazepam in presence of tween-20 and propylene glycol. *AAPS PharmSciTech*. 10(4):1396-1400.
106. López S, Senz A, Gsponer HE. 2000. The effect of adsorbed sodium dodecylsulfate at the alumina–water interface on the luminescence quenching of tris(2,2'-bipyridine) ruthenium(ii) by nitrophenols. *Journal of Colloid and Interface Science*. 224(1):126-132.
107. Mohajeri E, Noudeh GD. 2012. Effect of temperature on the critical micelle concentration and micellization thermodynamic of nonionic surfactants: Polyoxyethylene sorbitan fatty acid esters. *E-Journal of Chemistry*. 9(4).
108. Khoshnood A, Lukanov B, Firoozabadi A. 2016. Temperature effect on micelle formation: Molecular thermodynamic model revisited. *Langmuir*. 32(9):2175-2183.
109. Hadgiivanova R, Diamant H. 2007. Premicellar aggregation of amphiphilic molecules. *The Journal of Physical Chemistry B*. 111(30):8854-8859.